Report LR-699

ALFIS

September 1992

A feasibility study under coordination of ir. M.P. Nieuwenhuizen

TU Delft
Delft University of Technology

Faculty of Aerospace Engineering

ALFIS

A feasibility study under coordination of ir. M.P. Nieuwenhuizen

ALFIS

ASTRONOMICAL LOW FREQUENCY INTERFEROMETRY SATELLITES

a feasibility study
under coordination of
ir. M.P. Nieuwenhuizen

September 1992

Faculty of Aerospace Engineering
Delft University of Technology

Editors: Richard Beenen, Wim Simons

Cover design: Tibor Muhar, Richard Beenen

This report is written with WordPerfect 5.1. The used letter-type is Courier 10 cpi. Most the illustrations are drawn using AutoCad 10 and Drawperfect 1.1.

The ALFIS-team would like to thank the following persons without whom we would not have been able to perform the study.

All at TU Delft, University of Leiden, Fokker Space and Systems, Estec, Astron, TNO-TPD and many others for your advises.

Mr Piersma, Mr McGillavry and the facility managers:
Gerard, Gerard, Ed, Kees, Hans and Jan.

Ask not what ALFIS can do for you,
ask what you can do for ALFIS!

THANKS!!

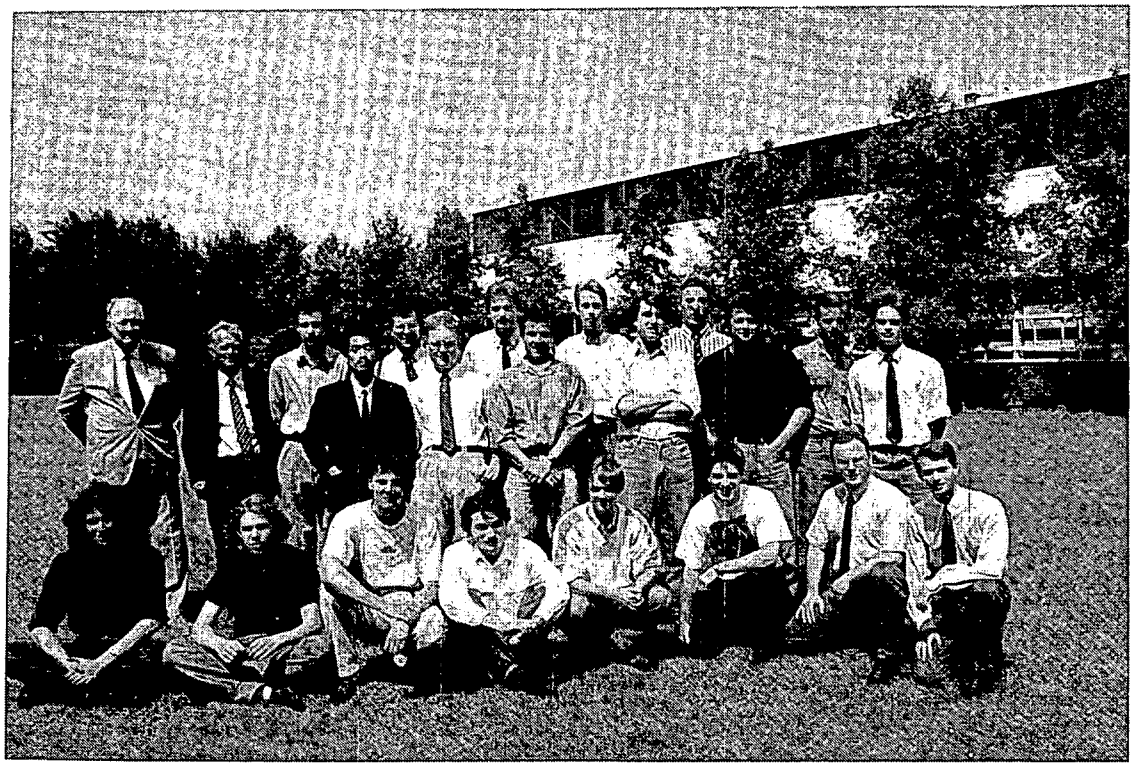

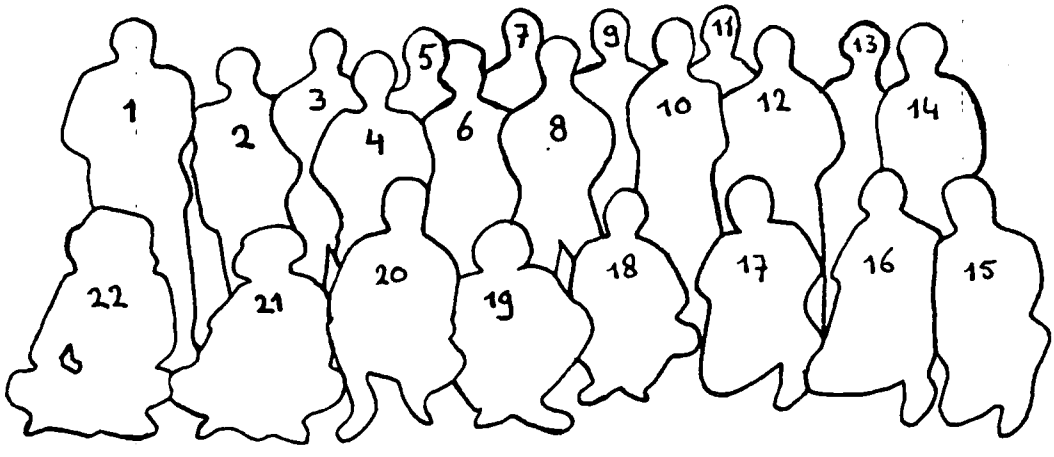

1. Ir. M. Nieuwenhuizen
2. Drs. R. Le Poole
3. Remco van Gelder
4. Kikik Yaranusa
5. Hermen Rehorst
6. Robert Meppelink
7. Gert-Jan van Rie
8. Wim Simons
9. Jan Athmer
10. Hans Wamsteker
11. Peter Wormgoor
12. Geo Meyerink
13. Anton Kramer
14. Geert Graafmans
15. Oscar van der Jagt
16. Tibor Muhar
17. Richard Beenen
18. Koen Matijsen
19. Floris Avezaat
20. Walter Schrauwen
21. Frank Wokke
22. Mischa de Brouwer

CONTENTS

ABBREVIATIONS

1. INTRODUCTION

ESA	European Space Agency
ESTEC	European Space Research and Technology Center
TNO	Nederlandse Organisatie voor Toegepast Natuurwetenschappelijk Onderzoek
TPD	Technisch Physische Dienst

2. SCIENTIFIC OBJECTIVES

COS-B	Cosmic Ray Satellite B
GTO	Geostationair Transfer Orbit
HII	ionized hydrogen
IRAS	Infra Red Astronomical Satellite
ISM	InterStellair Medium
NASA	National Aeronautics and Space Administration
LFSA	Low Frequency Space Array
RAE	Radio Astronomical Explorer

3. MISSION REQUIREMENTS AND PROJECT BASELINE

GTO	Geostationair Transfer Orbit

4. MANAGEMENT

OBC	On Board Computer
TTC	Telemetry and Telecommand

5. SYSTEM ENGINEERING

AC	Attitude Control
ASAP	Ariane Structure for Auxiliary Payloads
CAD	Computer Aided Design
CPU	Central Processing Unit
FSS	Fokker Space & Systems
GTO	Geostationairy Transfer Orbit
ISO	Infrared Space Observatory
LEO	Low Earth Orbit
NIVR	Nederlands Instituut voor Vliegtuigontwikkeling en Ruimtevaart
TTC	Telemetry and Telecommand
VAB	Van Allen Belts

6. LAUNCHER

ASAP	Ariane Structure for Auxiliary Payloads
CCD	Charge Coupled Device
CNES	Centre Nationale d'Etudes Spatiales
EPCU	Ensemble de Préparation Charge Utile (Payload Preparation Complex)
GTO	Geostationar Transfer Orbit

BPD	Italian Defence and Space Organisation
NASA	National Aeronautics and Space Administration

7. ORBIT

GTO	Geostationary Transfer Orbit
VAB	Van Allen Belts

8. CONFIGURATION

ASAP	Ariane Structure for Auxiliary Payloads
ESS	Earth Sun Sensor
PMAD	Power Managment and Distribution
OSR	Optical Solar Reflector
TTC	Telemetry and Telecommand

9. STRUCTURE

AC	Attitude Control
ASAP	Ariane Structure for Auxiliary Payloads
FEM	Finite Elements Method

10. PAYLOAD

ADC	Analogue to Digital Converter
AMP	Amplifier
BPF	Band Pass Filter
GS	GroundStation
HBR	High BitRate
LBR	Low Bitrate
LPF	Low Pass Filter
MPL	Multiplier
MPX	Multiplexer
MXR	Mixer
OBC	On Board Computer
PLL	Phase Locked Loop
PM	Phase Modulator
PRN	Pseudo Random Noise
TM	Telemetry
VCO	Voltage Controlled Oscillator

11. POWER SUPPLY

AEPS	ALFIS Electrical Power System
BOL	Begin Of Life
B2R	Bi-directional Battery Regulator
DC	Direct Current
DOD	Depth Of Discharge
GaAs	Gallium Arsenide
Ge	Germanium
EMC	ElectroMagnetic Compatibility
EMI	ElectroMagnetic Interference
EOL	End Of Life
NiCd	Nickel-Cadmium
NiH_2	Nickel-Hydrogen
PCU	Power Control Unit

PCDU	Power Conditioning and Distribution Unit
PMAD	Power Management And Distribution
Si	Silicon
S3R	Sequential Switching Shunt Regulator
VAB	Van Allen Belts

12. PROPULSION

APS	ALFIS Propulsion System
a.r.	apogee raised
AC	attitude control
AU	Accounting Unit
GTO	Geostationary Transfer Orbit
MMH	Mono Methyl Hydrazine
MON	Mixed Oxides of Nitrogen
OC	orbit control
p.r.	perigee raised
tankw.	tankwall

13. ATTITUDE CONTROL

AC	Attitude Control
CCD	Charge Coupled Device
ESS	Earth Sun Sensor
FOV	Field of View
IR	InfraRed
OBC	On Board Computer
QSS	Quadrant Sun Sensor

14. THERMAL CONTROL

OSR	Optical Solar Reflector
MLI	Multi Layer Insulation

15. TELEMETRY AND TELECOMMAND

A/D	Analogue/Digital
AM	Amplitude Modulation
BPF	Band Pass Filter
ESA	European Space Agency
FM	Frequency Modulation
HBR	High Bit Rate
LBR	Low Bit Rate
OBC	On Board Computer
PCM	Pulse Code Modulation
PM	Phase Modulation
PRE	Payload Ranging Equipment
PSK	Phase Shift Modulation
RF	Radio Frequency
TTC	Telemetry & Telecommand

16. ON BOARD COMPUTER

A/D	Analogue/Digital
D/A	Digital/Analogue
AC	Attitude Control

Amp.	Amplifier
CPU	Central Processing Unit
DIL	Dual In Line (type IC housing)
ESS	Earth Sun Sensor
ESA	European Space Agency
I/O	Input/Output
IC	Integrated Circuit
ISO	Infrared Space Observatory
MAM	Mathematical Attitude Model
MPX	Multiplexer
OBDH	On Board Data Handling
OBC	On Board Computer
PCB	Printed Circuit Board
PMAD	Power Management And Distribution
PROM	Programmable Read Only Memory
RAM	Random Access Memory
ROM	Read Only Memory
SMD	Surface Mounted Device
TTC	Telemetry & Telecommand

17. COSTS

AC	Attitude Control
KAU	Kilo Accounting Unit
NRC	Non Recurrent Costs
RC	Recurrent Costs
VDK	Vanderkerckhove

NOTATIONS

2. SCIENTIFIC OBJECTIVES

A	array aperture
B	magnetic field strength
N	number
N(E)	electron spectrum
R	radius
S	flux density
T	temperature
t	time
α	spectral index
β	power law index
γ	energy index of the cosmic ray
λ	wavelength
ν	frequency
σ	rms-error
τ	optical depth
Θ	source angular size

indices:

det	detectable sources
e	effective
O	solar
0	observing

6. LAUNCHER

ϕ	diameter

7. ORBIT

α	characteristic angle of visibility area
R_{vab}	radius to Van Allen Belts
R_e	radius of Earth

8. CONFIGURATION

r	radius of 'cheese' shape
R	maximum radius of tank

9. STRUCTURE

I_1, I_2, I_3	Principal coordinate system
x,y,z	Reference coordinate system

indices:

c.g.	center of gravity

11. POWER SUPPLY

A	area
C	capacity
E	energy
I	current
n	number
P	power
V	voltage
η	efficiency

indices:

b	battery
bdc	battery discharge
c	charge
c	cells
ca	available for charge
cn	need for charge
dc	discharge
e	eclipse peak
eoc	end of charge
eod	end of discharge
n	need
mc	middle of charge
md	middle of discharge
mp	maximum power point
l	load
oc	open circuit
p	equivalent generator
sc	short circuit
0	at 28°C, 1 AM0
0	regulated
5	from 5 hours discharge

12. PROPULSION

a	half long axis ellipisoide
a_{air}	acceleration due to air resistance
A	surface
AU	accountant unit
D_{tank}	tankdiameter
g	gravity acceleration
I_{sp}	specific impuls
M_{co}	construction mass
M_i, M^o	initial satelltie mass
M_p	propellant mass
$M_{x,y,z}$	moment x,y,z direction
P_{begin}	pressure tank at begin of life
P_{end}	pressure tank at end of life
P_{tank}	pressure tank

R	radius of earth
T	period of orbit
$T_{x,y,z}$	translation x,y,z direction
V	velocity
$V_{sat1,2}$	velocity satellite 1,2
V_0	initial velocity satellites
ΔV	velocity change
ΔV_a	velocity change to raise apogee
ΔV_p	velocity change to raise perigee
ΔV_{air}	change in velocity due to air resistance
ΔV_{tot}	total velocity change
Δt_{burn}	burntime change
μ	gravity parameter

13. ATTITUDE CONTROL

B_i	Earth magnetic induction
d_a	diameter Earth in degrees
i	inclination
I_{ii}	principal moment of inertia about the i-axis
M_i	magnetic dipole Earth in i-direction
M_{sat}	magnetic dipole parallel to the spin axis
r	distance to the center of the Earth
r_a	radius Earth
r_b	distance between the center of the Earth and the center of the satellite
T_m	
Ti_1	gravity gradient torque in i_1-direction
Tp_i	perturbation torque in i-direction
Δt	time between the pulse of the meridian slit and the skew slit pulse
β	the sun elevation angle
θ	drift angle in y-direction (rad)
θ_b	true anomaly
θ_s, ψ_s	angles of spin-axis in local orbital reference system
μ	gravitationparameter of the earth
ξ	angle between magnetic Earth axis and Earth rotation axis
ϕ	drift angle in x-direction (rad)
ω	spin rate
ω_0	angular rate of change of the position of the satellite orbit
Ω	right ascend of the ascending node

14. THERMAL CONTROL

A	contact area
B	Gebhart factor
C	coupling for conduction
F	viewfactor
I_a	albedo radiation
I_{a0}	reference albedo radiation
k	conduction coefficient

l	conduction distance
m	mass
P_{diss}	dissipated power
q	heat load
r	radius
R	reference radius
T	temperature
ε	emmission coefficient
ρ	reflectivity
σ	Stefan Boltzmann constant

15. TELEMETRY & TELECOMMAND

c	speed of light
D	antenna diameter of groundstation
f_c	carrier frequency
G_b	antenna gain
K	antenna factor
T_{noise}	systematic noise temperature
δ	elevation

1. INTRODUCTION

System engineering is an unavoidable and important activity for every project. An expert in a certain field does not need to be a system engineer but he has to know how his/her expertise fits into the whole system. This is certainly the case for space systems. There are many interfaces between the different sub-systems. Moreover the interfaces are important for the system. With respect to this phenomenon the space systems are even more complex than other projects. The best way to be able to get feeling for this complexity, is to be involved in a system feasibility study.

The Delft University of Technology offered the students the possibility to be involved in such a system concept study. Although there are still many shortcomings in the way this case study is organized and set-up, it has been proven to be an excellent way to learn the difficulties of a project start in a short time.

As coordinator of this study-element it was impossible to know the solution for every problem of all sub-systems.

Discussions with experts of the TU-Delft, Fokker Space & Systems, National Aerospace Laboratory, TNO-TPD and others, guided the project. In particular it proved to be of extreme importance that close contact with the scientists was guaranteed. The active role of drs. Le Poole was of great importance.

The chosen project was proposed by Dutch astronomers (University of Leiden) to ESA on a call for ideas for a small scientific mission. And ESA (Estec) has received this proposal with interest and had selected it as a possible candidate for such a small mission. The selection of a project which has the interest of the professional space community is certainly motivating the students of the University of Technology. The conceived system concept consists of two very small satellites for which the costs are estimated to be reasonable. The performance expected might hopefully encourage all those who are interested to continue this study. In order to bring forward all factors which are needed for the decision of a go or not go. The students and the coordinator have a dream, namely ***that they have made a beginning for the realization of a real project***.

M.P. Nieuwenhuizen.

2. SCIENTIFIC OBJECTIVES

2.1 INTRODUCTION

ALFIS, the Astronomical Low Frequency Interferometric Satellites, are directed towards imaging the entire sky at frequencies below 15 MHz, which are inaccessible from the ground due to ionospheric absorption and scattering. This frequency range covers the lowest energy region of the electromagnetic spectrum that is essentially unexplored by astronomy. This region, at ~10^6 Hz, is as far from centimeter radio wavelengths (~10^9 Hz) as centimeter radio phenomena are from infrared (~10^{12} Hz). Hence, the likelihood of discovering new processes and objects is great. An improvement in sensitivity to the few Jansky level and in resolution to the sub-minute-of-arc level will be as much of an advance for the field as was the UHURU satellite for x-ray astronomy or the IRAS for infrared astronomy.

Observing at frequencies as low as ~1 MHz extends astronomy to the lowest practicable physical limit for studying electromagnetic radiation from within our Galaxy. At still lower frequencies the diffuse interstellar ionized hydrogen gives a very high optical depth due to free-free absorption over relatively short path lengths (Alexander, et al. 1969). In order to work at such low frequencies, however, ionospheric disturbances dictate that observations must be taken from space.

The angular resolution of a telescope in radians is approximately equal to the observing wavelength divided by the diameter of the telescope aperture. To achieve useful resolutions (arcminutes) at the long wavelengths that ALFIS will operate, we are led to propose an interferometer, for which the resolution is determined by the baseline between the elements rather than the diameter of the individual elements. A previous proposal was submitted to NASA for a Low Frequency Space Array (LFSA) of interferometers consisting of four elements (Dennison et al 1985). Although ALFIS is less ambitious and cheaper than the LFSA, most of the scientific justification given in the LFSA proposal also applies to ALFIS and has been appropriately modified below.

2.2 THE ALFIS CONCEPT

The concept of ALFIS is summarized here and discussed in more detail in Section 2.4. The present instrumental concept is a single launch bus which places two free-flying spacecraft (array elements) into almost identical GTO (geostationary transfer orbit) type orbits with a small inclination between them to provide for baseline components at right angles to the

orbital plane. The orbital period is half a day to enhance compatibility with only one ground station. The two array elements are identical spinning spacecraft with three axis control capability for manoeuvering and orbit control, with a broad beam, wide bandwidth antennas and full polarization capability. Baselines between 1 km and 300 km in all directions will be achieved by having the two satellites in almost identical orbits. The baseline geometry will be known instantly to 500 m accuracy and later retrievable to 1m.

The receivers will observe at one or two simultaneous frequencies between 1 and 10 MHz with individual bandwidths of 25 or 50 kHz, controllable from the ground. The full signal received, after suitable digitization and the addition of monitor and control information, will be downlinked in real time to the ground for archiving, correlation, and analysis. Clock stability aboard each array element will allow for full array coherence to be maintained at all times. The twin antennas are modular in design and could be combined with further elements to increase the number of simultaneous baselines. After a (net) period of ~1 year of coherent integration with varying baseline lengths and orientations, a complete synthesis of the sky with high resolution and sensitivity at all 4 frequencies will be available.

The estimated capability of a two-element ALFIS is given in Table 2.1.

Freq. (MHz)	T_s (K)	t (sec)	A_e (m^2)	σ (Jy)	N_{det}	Appx. Resol.[a]
1.5	$3x10^7$	$7.5x10^6$	2400	100	300	~6′
4.4	$5x10^6$	$3.8x10^6$	1000	22	1250	~1′
13.1	$3x10^5$	$1.5x10^6$	400	7.5	1500	~0.3′

Table 2.1: ESTIMATED CAPABILITY

The maximum resolution is generally limited by the interstellar scattering (see Section 2.4.3 and Table 2.2)

T_s = Effective System Temperature (determined by galactic background)

A_e = Total Effective Array Aperture = 4 x effective aperture per antenna

σ = Rms Error (assuming full polarization, 50 kHz bandwidth per channel, and a sensitivity constant of 2)

N_{det} = Number of Detectable Sources (extrapolated from the Clark Lake survey; Viner and Erickson, 1975)

2.3 PREVIOUS WORK

The most extensive investigations at the very lowest frequencies have been carried out with the Radio Explorer (RAE) satellites 1 and 2, in Earth and lunar orbit, respectively (Weber, Alexander, and Stone, 1971; Alexander and Novaco, 1974). They were launched at different epochs and used as single survey antennas. Their travelling wave V-antennas yielded only steradian resolution.

Ground-based observations are normally confined to frequencies >10 MHz (during solar minimum), or >20 MHz (during solar maximum), and only under special conditions, at preferred locations does the ionosphere transmit radiation at frequencies as low as 2 to 5 MHz (Reber, 1968; Ellis and Hamilton, 1966). The Llanherne array in New Zealand has produced galactic surveys at 3.7 and 8 MHz, but with relatively low resolution (5.°6 at 3.7 MHz and 2.°6 at 8 MHz; Cane, 1975; Cane and Whitham, 1977). At 10 to 30 MHz and above, several ground-based surveys exist (e.g., Bridle and Purton, 1968; Hamilton and Haynes, 1968; Caswell, 1968; Viner and Erickson, 1975; Braude, et al., 1979) which will permit a connection of our results to earlier work and to higher frequency observations. However, all of this work has also been carried out at relatively low resolution.

We propose a concept which would significantly improve upon previous work and extend it to otherwise inaccessible low frequencies. For example, in comparison to the RAE program we expect to be able to obtain an increase in resolution by 3 orders of magnitude and in point source sensitivity by more than 2 orders.

2.4 SCIENTIFIC PROGRAMS

As an astrophysical observatory operating at very low frequencies, ALFIS will be a powerful tool for investigating a broad range of phenomena. Here we discuss some of the most important questions to be addressed.

2.4.1 Solar System Observations

Although the solar system is not envisaged as the most important area for ALFIS research, any deep survey of discrete

sources at low radio frequencies will of necessity reveal Jupiter and the Sun as the brightest radio emitters in the sky. ALFIS will, therefore, provide us with the opportunity of studying them and other solar system bodies with high resolution and provide considerable and heretofore unobtainable information regarding the structure of their emission regions, their plasma properties, and their emission mechanisms.

2.4.1.1 Sun

In the 1 to 10 MHz frequency range, the effective surface of the Sun ranges from 3 to 30 R_O. This is an interesting range of solar heights to observe. However, theoretical expectations indicate that such observations may be difficult since the quiet corona is a thermal source and since ray paths through the outer corona are refracted and reflected before they encounter much attenuation. Thus, the outer corona may act more like a reflector than an emitter and we might expect that most of the radiation from the corona will be reflected galactic background emission. However, since such an expectation is only based on theoretical predictions, it must be checked by observation, which heretofore has not been possible.

From the active corona, intense emission is to be expected at these low frequencies. For the longer lived emission centers, ALFIS will allow mapping of the propagation of electron streams through the corona (Type III emission) and propagation of coronal shock waves (Type II emission).

2.4.1.2 Jupiter

Extensive Earth-based and spacecraft-based observations have revealed the rich phenomenology of Jupiter's non-thermal emission (Carr, Desch, and Alexander, 1983). However, owing to disturbance by the ionosphere, no direct information exists on its location within the Jovian atmosphere. In a major review of the field, Goldstein and Goertz (1983) stress the importance of position determinations for theoretical understanding of the emission processes. Even very basic questions have yet to be answered. For example, from which hemisphere do the various emissions originate and is any of the emission associated with the jovian aurora or is it all driven by the satellite Io? The answers to these and other questions directly affect our understanding of physical processes taking place within Jupiter's magnetosphere. (Strongly dependent on frequency)

To date, emission locations have had to be inferred indirectly by assuming that the emission frequency is near the local electron cyclotron frequency and that emission is beamed from Io's magnetic flux tube. While these assumptions are

almost certainly valid for the so-called Io-B radio source, thereby locating its position to within a few arc-seconds (This fact will be helpful for providing a known phase calibration source for ALFIS), for the remaining jovian sources any one or all of these assumptions may be violated. Observations with ALFIS will alter this situation dramatically by providing the first accurate measurements of such source positions at these low frequencies.

2.4.2 The Galaxy

ALFIS will provide several unique diagnostics for studying our galaxy at low frequencies. These include studies of emission, absorption and scattering processes.

2.4.2.1 Diffuse Galactic Emission

Study of the distributed non-thermal background emission of the Milky Way is a rewarding task in all parts of the electromagnetic spectrum; different frequencies emphasize different physical processes. For example, the COS-B survey of γ-ray emission is sensitive to the interaction of cosmic rays with the ambient interstellar gas, the well known Palomar Sky Survey emphasizes stars and ionized hydrogen (HII) regions, and the IRAS survey enhances visibility of the relatively cold interstellar dust. Radio frequency studies (see, e.g., Haslam, et al., 1982 at 408 MHz; Wielebinski, Smith, and Cardenas, 1968 at 151 MHz; Milogradov-Turin and Smith, 1973 at 38 MHz; and Jones and Finlay, 1974 at 29.9 MHz) are known to be most sensitive to the relativistic electron component of cosmic rays and the distribution of interstellar magnetic fields. It has been shown, for example, that there is a good correlation between the energy spectrum of the cosmic ray electrons detected in the solar vicinity and the flux density spectrum of the non-thermal galactic radio background. Even here, however, there are problems in explaining the observed break in the cosmic ray electron energy spectrum near 3 GeV since neither attributing it to existing loss mechanisms nor ascribing it to the initial injection spectrum is completely satisfactory (see, e.g., Longair, 1981). Since this e^- energy break is equivalent to the observed break in the background radio spectrum at ~300 MHz, low frequency observations may be able to distinguish regions in the Galaxy with different spectral properties and provide clues to the relevant loss and injection mechanisms. Existing surveys do not have sufficient resolution or provide sufficient spectral range to do this.

By performing surveys at the low frequencies and high resolutions which will be possible with ALFIS, we will not only be able to define spectral indices below the 300 MHz break to high precision but also will be able to resolve and study the distribution of different components of the galactic

background. For example, it should be possible to test the theories on whether the loop-like features seen in the background are old remnants from nearby supernovae (Berkhuijsen, 1971) or loops of magnetic field and particles leaking out of the galactic plane (Parker, 1965) by measuring their spectral index values and distributions. Also, at low frequencies the non-thermal halo of the Milky Way will be prominent and it should be possible to measure its extent, relativistic particle density, and magnetic field strength for a better determination of the confinement mechanisms for cosmic ray e^- and p^+. It should also be kept in mind that at the low frequencies which we propose to observe, the lifetime of the synchrotron electrons is a significant fraction of the age of the universe (~3 x 10^9 years at 1 MHz) so that we will be studying distributions relatively unaltered by evolutionary effects.

Under the concept which we propose, ALFIS will be ideally suited to imaging the Galaxy at low frequencies. The brightness sensitivity of ALFIS is sufficient to study the galactic background at resolutions of ~1 degree at 1 MHz and <15 arcminutes at 13 MHz. Also, although most of the information on the galactic non-thermal background radiation will be obtained with baselines <25 km in length, larger antenna separations will still be needed for the study of small scale, higher brightness structures in the background and for the detailed study of individual radio sources.

2.4.2.2 Diffuse Galactic Free-Free Absorption

By observing a large number of extragalactic radio sources and determining their low frequency spectra as a function of galactic latitude and longitude, it should be possible to measure the changes due to absorption by the diffuse, interstellar gas in the Milky Way and thereby investigate its distribution. While near 1 MHz this interstellar absorption may affect survey results of the non-thermal background in the galactic plane, we expect that, by combining the survey results at the several frequencies available through ALFIS and the low resolution, higher frequency maps from the literature, the thermal absorption and non-thermal emission components of the Galaxy can be successfully separated. Then, models for a "warm" (T_e ~ 10^4 K) disk of ionized hydrogen embedded in a "hot" (T_e ~ 10^6 K) halo can be tested and a global picture of the free-free absorption obtained for comparison with existing higher frequency pulsar dispersion and Faraday polarization rotation measurements. These results will also be supplementary to the COS-B γ-ray measurements which are related to the local cosmic ray energy and interstellar gas density.

A complementary technique to studying the diffuse free-free absorption is to use nearby HII regions, which are optically thick at these low frequencies, to completely block the non-thermal background radiation from more distant parts of

the Galaxy. Then, any emissivity observed can be attributed solely to the synchrotron radiation arising between the observer and the HII region, yielding a measurement of local values of the cosmic ray e^- and magnetic field components. This technique has, so far, been successfully employed only in a small number of cases (Odegard, 1986) but it can be extended by the superior sensitivity and resolution of ALFIS to many more lines of sight.

2.4.2.3 Interstellar Scattering and Refraction

It is generally accepted that small scale (~10^9 cm) fluctuations in electron density in the interstellar medium can diffractively scatter radio waves from a background source (see, e.g., Dennison, et al., 1984). Less clear, yet of considerable importance, is the ability of somewhat larger irregularities (~10^{13} cm) to refractively focus and defocus radio waves. Such refractive scintillation has been proposed as the origin of some low-frequency variability observed in compact extragalactic sources (Shapirovskaya, 1978; Rickett, Coles, and Bourgois, 1984). It is likely that interstellar plasma irregularities occur on many spatial scales, and Rickett (1977) characterizes them by a power spectrum of the spatial wavenumber. Some major questions remain concerning interstellar scattering:

What is the correct form of the irregularity power spectrum, and what are the values of the power law index, β, and the inner and outer size scales?

Is the irregularity spectrum, and therefore the scattering, ever anisotropic?

How common are refractive distortions, and refractive scintillation?

What is the origin of the turbulence and how is it distributed throughout the Galaxy?

What is the relationship between the turbulence and the known phases of the interstellar medium (ISM)?

Because the scattering and refraction angles scale roughly as $\lambda^{2.2}$, these effects will be quite large at low frequencies, causing measurable angular broadening of many of the discrete sources in the all-sky surveys at 1.5, 4.4, and 10.1 MHz. Table 2.2 lists the range of scattering sizes expected for extra-galactic sources seen at high galactic latitudes ($|b| > 30°$).

With many broadening measurements spanning the full range of galactic latitudes and longitudes, it will be possible to map the distribution of scattering material in the Milky Way.

This distribution is expected to be complex with localized regions of heavy scattering concentrated in the galactic disk which is itself imbedded in a more uniform component distributed throughout the halo (Dennison, et al., 1984; Cordes, Weisberg, and Boriakoff, 1985). A detailed picture of the distribution of scattering material in the Galaxy should elucidate the nature of the scattering medium and its relationship to the phase structure of the ISM.

Frequency (MHz)	Scattering Diameter (arcsec)	Max. Useful Baselines (km)
1.5	300 - 1800	20 - 130
4.4	50 - 150	100 - 300
13.1	6 - 20	300 - 1000
26.3	1 - 3	1000 - 3000

Table 2.2: ESTIMATED SCATTERING DIAMETERS

A unique and closely related capability of ALFIS will be the possibility of estimating both $(\sigma N_3)^2 dl$ and $\sigma N_e^2 dl$ through the Galaxy toward extragalactic sources. The first integral, the square of the thermal electron density fluctuations integrated along the line of sight, is estimated from the apparent image size by assuming values for β and the wavenumber cutoffs. The second integral, the emission measure, is estimated from the very low frequency galactic absorption by assuming a value for the electron temperature. Comparing these values for many different paths through the Galaxy will provide important clues as to which component of the ISM causes the fluctuations. It will also provide an estimate of the fractional modulation of the ionized gas and will complement pulsar dispersion measures which, yielding $N_e dl$, tend to underestimate the effect of small, relatively dense regions on the scattering.

From the appearance of the broadened images, it will be possible to evaluate refractive effects. If present, refraction should produce a patchy or even multiple image (Goodman and Narayan, 1985) and would be evidence for quite large (0.01 - 1.0 pc) refracting structures in the ISM. On the other hand, if the broadening is dominated by diffraction, the images should appear smooth. A simple asymmetry such as an elliptical image, would result from an anisotropy in the irregularity spectrum and might be expected if particle motions are constrained by a magnetic field.

By extending scattering measurements to low frequencies, it will be possible to obtain important new information on the irregularity spectrum of the ISM by determining the exponent of the wavelength scaling law (related to β) and by searching

for an expected cutoff in the wavenumber spectrum at small scales (results in a transition to λ^2 scaling at some low frequency). Since no such cutoffs have yet been identified in the irregularity spectrum (Armstrong, Cordes, and Rickett, 1981), such a finding would be significant for understanding the physical properties of interstellar turbulence. (up to here only the last bit about interstellar scattering appears reasonably up to date, the rest seems badly historic)

2.4.2.4 Pulsars

One of the most important galactic objects for study by ALFIS will be pulsars. The spectra of most pulsars turn over in the 100 to 500 MHz range, but a few, interesting, fast pulsars have spectra which are very steep and flux densities which continue to increase down to the lowest observed frequency of 10 MHz. Two examples are the Crab pulsar (PSR0531+219; Bobeiko, et al., 1979) and the millisecond pulsar (PSR1937+214; Erickson and Mahoney, 1985). These pulsars are among the strongest sources in the sky at 10 MHz so that ALFIS observations may be able to discover other, similar objects. Also, to avoid radiating infinite power, the spectra of these pulsars must turn over at some frequency <10MHz and measurement of this turnover frequency can provide information on the spatial structure of the coherently radiation electrons in the pulsar's magnetosphere. (It is important to evaluate the number of pulsars to be detected in relatively short integration times, in order to estimate the potential for 'real time' calibration of ALFIS. This would significantly relax the mission requirements)

2.4.3 Extragalactic Radio Sources

Discrete extragalactic radio sources will be amongst the most important subjects for study by ALFIS. Since their discovery by Reber in the thirties, these objects have played a vital role in astrophysics and cosmology. There is considerable evidence that the radio radiation emitted by them is produced by the synchrotron process, namely electrons moving with relativistic speeds in a magnetic field. Discrete radio sources include the closest galaxies such as M 31 and the most distant known galaxies.

Because they are so luminous and often associated with galaxies that emit bright emission lines, radio sources have been among the most important cosmological probes. In particular, ultra-steep-spectrum radio sources with indices steeper than -1 are preferentially associated with the most distant galaxies. For example, 4C 41.17 the most distant galaxy at a redshift of 3.8 has an anomalously steep spectrum at frequencies to below 26 MHz.

Little is known about the properties of individual radio sources at low frequencies. However, the expected capability of the ALFIS is such that hundreds (see Table 2.1) of discrete sources can be detected and the brighter ones studied for such properties as integrated spectrum, surface brightness and spectral index distribution, and source counts ("log N - log S").

This is especially important since the relativistic electrons which ALFIS will detect are, in general, much older than those normally studied by radio astronomy. Thus, "fossil", steep spectrum sources which are not observable at higher frequencies may become available for study with an impact on theories for the evolution and lifetimes of radio sources and of the universe.

2.4.3.1 Spectra

Radio sources are generally characterized by a spectral index α which describes the change of flux density S with frequency as a power of the observing frequency ($S \propto^{-\alpha}$). However, it has long been known that the spectral index is a function of frequency $\alpha(\nu)$ and that the measurement of this frequency dependence is important for understanding the physics of the emission and absorption processes and the physical environment in the sources.

Determination of $\alpha(\nu)$ requires measurements of source flux densities at all frequencies, and, in particular, at low frequencies where a number of absorptive and emissive processes become prominent. At present, very little is known about source spectra at frequencies as low as 20 MHz and practically nothing has been measured for $\nu < 10$ MHz. It is thus an important parameter of ALFIS that it will have multifrequency capability to provide this information throughout this poorly explored range and to investigate the many possible emission and absorption processes involved.

2.4.3.1.1 Emission Processes

Enhanced emission from sources at the lowest frequencies and thereby enhanced numbers of individual sources available for study can be anticipated due to a number of phenomena.

A class of sources with spectral indices $\alpha > 1$ which are only detectable at low frequencies (see e.g., Baldwin and Scott, 1973). These display no peak in their spectra and apparently increase monotonically in flux density even at the lowest measured frequencies.

Some low frequency sources are large (~1 Mpc) and are associated with clusters of galaxies. Erickson, Matthews, and

Viner (1978) have shown that there is, in fact, a strong correlation between these steep spectrum clusters and x-ray emission from the intra-cluster gas. However, the physical connection remains unclear. Although the electrons seen at low frequencies can, in principle, scatter the universal 3° K background radiation to produce the observed x-ray emission through the inverse Compton process, the x-rays appear to be well described by thermal bremsstrahlung from a tenuous, hot (~10^6 K) gas distributed throughout the cluster. In order to investigate this further, better resolution and sensitivity measurements at low frequencies are needed. Hence, ALFIS can help define the spectrum and emission distribution in these clusters as well as to obtain better statistics on more clusters.

A possibly related question is the process by which central radio galaxies in some clusters "leak" their relativistic electrons into the intra-cluster medium to produce a cluster "halo" of megaparsec dimensions such as that seen in the Coma Cluster or Abell 2256 (Bridle et al. 1979). Hanisch and Erickson (1980) have shown that the apparent rate of relativistic particle propagation observed in clusters which are bright at low frequencies is several orders of magnitude greater than the Alfven speed and even exceeds the ion sound speed. These high propagation rates seem to rule out a diffusion process and are consistent with a constant velocity streaming of the particles. However, this is surprising since the intracluster medium is expected to be quite inhomogeneous and stirred by galaxy motions. Again, observations with higher resolution and sensitivity are needed to investigate both the statistics and the distribution of the effect.

2.4.3.1.2 Absorption Processes

Many radio synchrotron sources possess a spectrum whose intensity peaks at some intermediate frequency and declines both above and below that. For extended sources the frequency of peak flux density is usually quite low and in some cases this "turnover" is presumed to occur at frequencies below present observational limits. A decline at low frequencies is usually attributed to one of 3 absorption processes: external ionized hydrogen (HII) free-free absorption, internal free-free absorption and synchrotron self absorption. Additionally, while not strictly an absorption process, the Razin-Tsytovich effect can suppress low frequency emission. Since these processes have different and predictable frequency behaviors, accurate measurement of low frequency spectra can determine which is prominent.

If the absorbing medium is located between the source and the observer, external free-free absorption modifies the observed spectrum by the factor e^{-tau} while for an internal mixture of emitting and absorbing regions, the factor is

$(1-e^{-tau})$. Thus, for a simple case one can choose between mechanisms on the basis of the observed spectrum, calculate the optical depth tau, and estimate the integral electron density and temperature along the path through the absorbing medium. Although actual sources are likely to be complicated and require full modelling, this example illustrates that basic astrophysical information can be obtained from the accurate measurement of low frequency turnover spectra.

When the apparent brightness temperature of a source approaches the equivalent kinetic temperature of the relativistic electrons, part of the synchrotron emission is reabsorbed. In the approximation of an optically thick relativistic electron gas, the flux density below the turnover will be $S \propto B^{-0.5}\theta$ where θ is the source angular size, B is the magnetic field strength, and ν_0 is the observing frequency. Therefore, an observed decrease in the flux density below turnover indicates synchrotron self absorption and, if the source size is known, allows the estimation of the internal magnetic field strength.

These three processes, at least for simple models, therefore have distinctive signatures below the turnover frequency ν_0.

If the plasma density is sufficiently large so that the index of refraction of the medium must be taken into account, the synchrotron emission is no longer concentrated along the electron trajectories and the higher harmonics are suppressed. This "Razin-Tsytovich effect" cuts off the spectrum very sharply and is easily recognizable compared to absorption processes.

We may therefore anticipate that observations of peaked spectrum sources at low frequencies will provide important astrophysical information on thermal electron densities, temperatures, and distributions as well as on magnetic field strengths and relativistic particle densities and lifetimes.

2.4.3.1.3 Radio Source Evolution

A number of loss processes can affect the energy of relativistic electrons. These alter the observed spectrum in different ways. For example (Longair, 1981), if γ is the power law index of the cosmic ray electron energy spectrum $N(E) \propto E^{-\gamma}$ [N.B.: It can be shown that this cosmic ray energy index γ is related to the radio spectral index α by $\gamma = (2\alpha + 1)$.]

ionization losses dominate, $N(E) \propto E^{-(\gamma-1)}$; i.e., the observed spectral index α is flatter by 0.5;

bremsstrahlung or adiabatic losses dominate, $N(E) \propto E^{-\gamma}$; i.e., the spectral index α is unchanged

inverse Compton or synchrotron losses dominate, $N(E) \propto E^{-(\gamma+1)}$; i.e., the index α is steeper by 0.5.

Thus, if an estimate can be made of the dominant energy loss processes and magnetic field strengths, detection of breaks in the spectrum permits the determination of the approximate age of the relativistic electrons being observed.

Another possible source of spectral turnovers at low frequencies is the requirement that the acceleration mechanisms for relativistic electrons become inefficient at some low energy. Since the number of relativistic electrons increases very rapidly with decreasing energy ($\gamma \sim 2.5$), at some point this process must cease to avoid an infinite energy content for radio galaxies. Searches have been made (Erickson and Cronyn, 1965; Hamilton and Haynes, 1968; Roger, Bridle, and, Costain, 1973) but such a cutoff has never been clearly identified. To investigate this further, determination of spectra down to the lowest frequencies is required.

2.4.3.2 Morphological Studies

Numerous sources detectable with ALFIS will be resolved. Even though at low galactic latitudes and at the lowest observing frequency of 1.5 MHz interstellar scattering will place an effective limit on the maximum resolution available, ALFIS will generally be able to image brightness distributions to the <1′ resolution typical for source studies at centimeter wavelengths. At these 3 to 4 order of magnitude lower frequencies (i.e., over a similar frequency span as that from centimeter radio to optical!) diffuse synchrotron components have very high brightness temperatures and the detailed mapping of supernova remnants, normal galaxy disks, normal galaxy halos, radio galaxies and quasars, radio tails, component bridges, and distributed emission from clusters of galaxies to deeper levels and greater extensions will be possible. ALFIS will also be able to map spectral index distributions across extended objects to high accuracy (because of the large interval between these very low frequencies and existing high frequency maps) permitting searches for evolutionary effects in component motions and/or electron distributions such as Perley and Erickson (1979) have been able to do for giant radio galaxies and Winter, et al. (1980) have been able to do for the bridges in Cygnus A. Such information will help to identify relativistic electron injection, acceleration, diffusion, and evolution processes which are still only poorly understood. With high resolution at low frequencies, direct comparisons can also be made with other wavelength bands such as optical, x-ray, and γ-ray where surveys and individual source studies with comparable resolution exist.(Looks again badly outdated)

2.4.4 The Unusual and the Unexpected:

In this relatively unexplored frequency range, new processes and phenomena which we cannot now predict may be encountered, even in apparently well studied objects. For example, supernova remnants are thought to be reasonably well understood globally even though many details still remain elusive. Shell-type remnants appear to arise from shock waves expanding into and interacting with the interstellar medium and generating radio emission through Rayleigh-Taylor acceleration of relativistic electrons (see, e.g., Gull, 1973a,b). Therefore, a remnant like Cassiopeia A (SN~1670) is expected to decay slowly in flux density due to adiabatic energy losses (Shklovsky, 1968) and a decrease of roughly the proper magnitude has been observed at high frequencies (see, e.g., Baars, et al., 1977). However, this tidy picture may need to be modified. A series of observations by Erickson and Perley (1975) show that Cas A increased in flux density at 39 MHz at a rate of ~1.5% per year between 1967 and 1975. It remains unusual in that it appears to only occur at low frequencies. Confirmation and study in Cas A and possible detection in other objects and at still lower frequencies will be extremely interesting.

An exciting possibility is that ALFIS may be able to detect and study coherent radiation processes. There are valid physical reasons to anticipate that the smaller distance between individual radiating electrons measured in terms of the electromagnetic wavelength is likely to amplify collective radiative modes. In such a plasma, the ratio of stimulated emission to spontaneous emission can be very high. If an inverted energy level population can be established and is sufficiently long lived, there are numerous collective modes which can be excited by instabilities in the magnetoactive plasma. Enhanced radiation should be generated at critical frequencies such as the plasma and gyro resonances and, in an inhomogeneous medium or in the non-linear case, coupling between modes can occur to produce wave amplification. In fact, the occurrence of coherent emission at low frequencies appears to be the rule rather than the exception for solar system objects such as the Sun, the major planets, and the magnetosphere of the Earth. Since objects such as the Crab Nebula, Seyfert galaxies, and quasars typically have densities of $\sim 10^4$ to 10^5 cm^{-3} and magnetic fields <1 Gauss, we may anticipate an analogous situation leading to coherent plasma phenomena in the 1 to 3 MHz range.

Finally, we remark that serendipity has always played an important role in the development of astronomy and, while the possibility of new discoveries is not in itself sufficient justification for a program, large improvements in sensitivity and resolution over previous instruments and extensions of observations to new electromagnetic frequency domains certainly provide an environment which increases its likelihood.

3. MISSION REQUIREMENTS AND PROJECT BASELINE

3.1 MEASUREMENT PRINCIPLE

ALFIS being conceived as an interferometric all sky antenna with full polarization sensitivity requires that the instantaneous baseline be known to a small fraction of a wavelength.

3.1.1 Phase errors

A specification has been set at 1 m a posteriori knowledge, equivalent to 12 degrees of phase at an observing frequency of 10 MHz. For the same reason the electrical phase of the LO system, antennae and other electronics affecting the interferometer phase (downlink f.i.) is also specified to 1 m electrical, also in terms of stability (after known corrections) to allow proper calibration of the interferometer phase to this limit. A reasonable lack of correlation of the phase errors allowed within these limits during the total integration time should than allow the sidelobes of the synthesized antenna pattern to be kept around 1 percent or less.

3.1.2 Orbit

Filling of the X,Y,Z space for the interferometer baseline of the synthesized omnidirectional antenna requires rather minimal manoeuvering along the orbit, providing for slight a-synchronism at choice of the two satellites in their orbits up to about 300 km along their orbits.

3.1.3 Receivers

Even with the high brightness temperatures of the sky at these frequencies the low gain of the ferrite antennae requires the preamplifiers to have noise temperatures of around 100 K.

The additional complication of significant terrestrial interference requires them to be linear for at least 20 dB above the 'normal' sky signal. For this reason also the separate RF filters require rather steep edges.

3.1.4 Attitude

In order to retrieve the polarization from the correllator channels the instantaneous attitude must (a posteriori) be known to 1 degree accuracy.

3.2 PROJECT- BASELINE

The present project concept is as follows:

- The mission is to accomplish an interferometric all-sky survey at frequencies for which the ionosphere obstructs observation from the ground, i.e. 1 to 10 (15?) MHz. It will do so at a resolution which at the lowest frequencies will be matched to the angular sizes of sources set by interstellar scattering.

- Two small satellites in orbits with almost the same apsides in an orbit similar to a GTO, both with an orbital period of 12 hours but with different initial conditions. With the appropriate maneuvering of the satellites this allows for a (X,Y,Z) space of a size of some 300 km to be filled sufficiently to generate a 'nice' synthesized antenna pattern all over the sky.

- The satellites are to be equipped with an omnidirectional antenna system for full polarization (base line 3 orthogonal ferrite rods and coils)

- The satellites' 'dry mass' will be limited to 50 kg. They will be boxes that fit onto Ariane IV's 'passenger seats' (less than 50 cm on the side); they are to be equipped with a cold gas attitude control (3 axes) that will also be the propulsion system for the orbital maneuvers as well as the orbit control; they will operate in slow spinning mode; their attitude will be known to better than 1 degree (polarization), and their orbital position will (a posteriori) be known to 1 meter accuracy (U,V,W coordinates of baselines). The experiment will be operated only when the satellites are in view of the Westerbork Radio Telescope, and above the Van Allen Belts. This will provide for about 40% of real time for the true integration time, and a total net integration time of one year has been taken as target.

- The satellite will have a dual frequency phaselocked transponder system to provide for phasestable LO signal on board.

- The payload presently is specified to have 5 observing frequencies distributed (strategically?) between 1 and 15 MHz, and two bandwidths of 25 and 50 kHz, simultaneously operable for all three polarizations. Therefore the downlink bandwidth will be 150 kHz, at choice to be 3 * 50 or 6 * 25 kHz, the latter for dual frequency operation if required. The dynamic range of the mixers and amplifiers (and therefore unfortunately also for the downlink) will be such that the celestial signal will be passed on healthily for terrestrial interference up to 20 dB above the sky signal. Phasestability of the relevant components

is specified to be better than 1 m electrical length, and at present a temperature controlled compartment to 1 degree is foreseen to (possibly) be necessary. The payload (including LO transponder) mass is limited to about 10 kg, the volume to 6 liter and the power to 9 Watt (excluding downlink).

4. MANAGEMENT

4.1 INTRODUCTION

Management of a feasibility study for a small satellite, involves mainly planning and the coordination of 10 divisions, all of them working on their own subsystem or problem. So we're providing a time-schedule, regulations and overhead to support a dynamic corporation between all participants.

4.2 PROJECT ORGANIZATION

4.2.1 Group Division

The project we're dealing with, consists of 20 engineering students in their pre graduate study phase. The group is coordinated by ir. M.P. Nieuwenhuizen, space structures Professor at the faculty of Aerospace Engineering.

As in all development programs in aerospace engineering, everyone's a specialist in his own field of work, since there's no single person who can possibly know all. Mainly for this reason a project development team consists of several groups, all dealing with their own sub-system. In our case the students were able to choose a group matching their interest, instead of their proven experience.

We defined the following groups with its associated tasks:

Management:	*m*	Mischa de Brouwer	System engineering
		Remko van Gelder	Orbit definition
	m	Gert-Jan van Rie	Launcher choice
Payload:	*m*	Geert Graafmans	Design and calculus of
		Frank Wokke	the scientific payload
Structure:	*m*	Geo Meyerink	Design of S/C structu-
	m	Hermen Rehorst	re and defining confi-
	m	Hans Wamsteker	guration
	m	Kikik Yaranusa	
Power Supply:		Richard Beenen	Electrical power gene-
		Tibor Muhar	ration and distributi-
			on
Propulsion:	*m*	Anton Kramer	Design of propulsion
		Wim Simons	system

Att. Control:	*m*	Oscar van der Jagt	Calculus on satellite
	m	Peter Wormgoor	attitude
Computer:	*m*	Robert Meppelink	Choice of On Board Computer (OBC)
Telemetry & Telecommand:		Walter Schrauwen	Calculus on telemetry and telecommand
Thermal Control:		Jan Athmer Floris Avezaat Koen Matijsen	Providing an environment meeting all thermal requirements

m: members of the model committee, the other students took part of the report committee

The original tasks described changed during the project study. The reasons were the continuous change of configuration and new launcher and technologies (antennas) mentioned after the mid-term meeting april 1992. Computer and TTC used to be one group, but split up because of the lack of overlap between the systems. They have always been able to replace each other. (All groups consisted out of at least two students).

4.2.2 Organization

Making the twenty students to cooperate, appeared to be more difficult than we expected. One of the most important ways of communication, was the weekly meeting, which all participants were obliged to attend. Each group had to write a report before every meeting, in which they presented the latest developments and changes on their subject. One of the group-members had to present the report during the meeting, normally followed by severe discussions, meant to define a trade-off or to freeze a concept.

Another major communication facility, was the ALFIS control center, equipped with computer & printer, telephone, overhead projector, library and espresso machine. There were always some students working, and many times have experienced the advantages of solving related problems with other groups. The ALFIS room has been an important tool to motivate all participants and strengthen the group-spirit.

4.3 SUPPORTING COMMITTEES

4.3.1 Hardware Committee

The other student design studies in 1991 and 1990, used to make a model of the external configuration to show it the

faculty. This year we have tried making the model to be more useful to us. Because of its limited size we could make a 1:1 scale model. Its simple modular design allowed us to build solarpanels which are easy to disconnect, thus showing the internal configuration. All modules are shown as blackboxes. This helped us to understand the problems concerning the internal configuration better. We used mainly wood and paper for the ALFIS model.

4.3.2 Report Committee

The editors of this report did their work in their summer holidays, using an IBM PS/2 machine supplied with WP51, (US spellingchecker), Drawperfect and AutoCad. Their tasks were gathering the info from all groups, equalizing the layout, checking english grammar and spelling, printing a draft report, making all facts consistent and taking the whole to the publisher.

5. SYSTEM ENGINEERING

5.1 INTRODUCTION

The responsibility of making all subsystems fit together into one satellite is for the management. It seems to be the main task of system engineering. Furthermore some aspects like a design and development plan (closely related to the planning mentioned in chapter 5), qualification strategy, error management and operations have been studied.

The configuration has been defined by structure-members, they were relatively free to chose a suitable system of axes, as showed in figure 5.1. All groups (AC, propulsion) had to use it.

The mass-budget has weekly been updated by structure, the power-budget by the power-group. Both are presented in chapter 5.3.

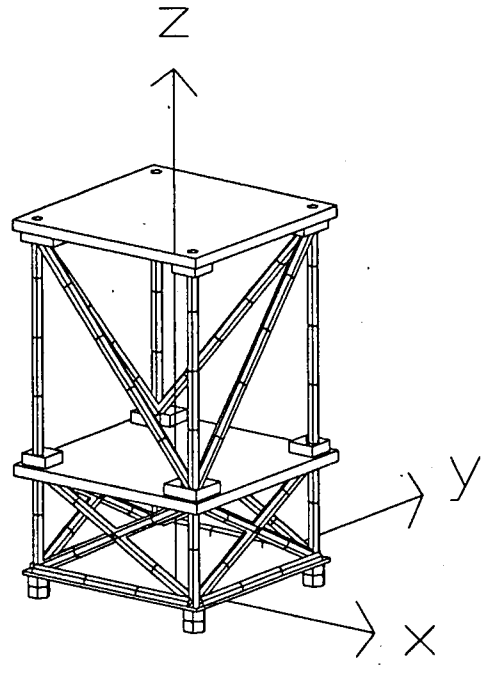

Figure 5.1: SYSTEM OF AXIS

5.2 SYSTEM REQUIREMENTS

System requirements have a major impact on the design of the spacecraft. They are obligatory for all subsystems to define their own requirements while the above mentioned mission requirements are the boundary constraints for this definition. We have obtained the following mission requirements:

Orbit:
- both satellites must be outside the Van Allen Belts (VAB) simultaneously for at least 40% of their orbital period
- it must be possible for at least 25% of time spent outside the VAB to have ground contact with both satellites

- in order to create an interferometric base-line, the absolute distance between both satellites must vary between 1 and 300 km.

These requirements leave a Geostationary Transfer Orbit (GTO) as most favorable (cheapest) orbit.

Launcher: - a very cheap launch can be given by a special Ariane 4 option, namely ASAP. Design constraints for ASAP payloads are:
  - total mass < 50 kg
  - dim. 450x450x450 mm (height negotiable)
  - stiffness: eigenfreqency > 50 Hz

According to these system requirements the options for attitude control enable us to choose between any type of stabilizing, including free tumbling.

5.3 MASS AND POWER BUDGETS

The mass budget given hereafter is specified in more detail in chapter 9, the power budget given is the 'operation'-mode, other modes and details are shown in chapter 11. These budgets make a contribution to a first impression of ALFIS.

ALFIS mass budget and power budget august 1992.

Subsystem	Mass (kg)	Power (W)
Payload	6.1	7.8
AC	2.2	2.0
Propulsion	11.0	1.0
Computer	4.2	5.5
TTC	2.8	6.5
Power	11.4	-
Thermal	1.5	1.5
Structure	5.9	-
Subtotal	45.1	24.3
10% margin	4.5	2.4
TOTAL	**49.6 kg**	**26.7 W**

5.4 SYSTEM ASPECTS

System engineering involves features like Planning, Design & Development, Qualification strategy, Testing of new technologies and the assembled satellites, Operations, Redundancy and Error management and Costs. Project cost will be discussed in a separate chapter. The other subjects in the chapters 5.5 to 5.8.

During our study, several principal trade-offs have been made, and some off them rejected and remade after a while.

Making the wrong choice isn't a big err, if only the mistake has been discovered soon enough. An example of a false decision is the stabilization as described in our midterm report. After very few discussions we decided a free-tumbling concept would suit our satellites best. The reasons we have chosen this were a.o. that it is not necessary to have a stabilized satellite to perform our mission. So when we would just let the satellite go, it would save us quite a lot of fuel needed for attitude control. But when the design continued, and the satellites grew smaller, there were certain facts that made a spin-stabilized satellite much lighter:

- a spinner requires a maximum of two low-mass sensors, while a free-tumbling satellite needs more and heavier sensors. Taking our mass and space limitations into account, this was the most important criterion.
- the structure of a spinner is simpler, e.g. looking at solarpanels, radiators, etc.
- spin-stabilization requires rotation on the highest axis of inertia, so the configuration would become more complex.

Wrong choices are inevitable when you have so little information, so normally you'll design several options simultaneously. Alas because of a lack of time and people, this was impossible for us.

5.5 PLANNING

As we were missing quite an amount of experience on planning, we decided to follow the planning as far as concerned our phase-A study.

Continuing the project after this study highly depends on politics and the future of FSS and NIVR aerospace-funds. We attempted to make a project-planning even with a lack of information about these aspects. The main driver has been the wish to design and launch the satellites within a few years. The long period between kick-off and operations of scientific missions is considered to be a great disadvantage for users of these missions. When operating from 1995 to 1998, we're also dealing with a minimal solar activity. This causes better results to be measured.

The planning as showed below is dependent on technology chosen in phase B. Therefore there are still some doubts on the time needed for subsystem tests and qualification.

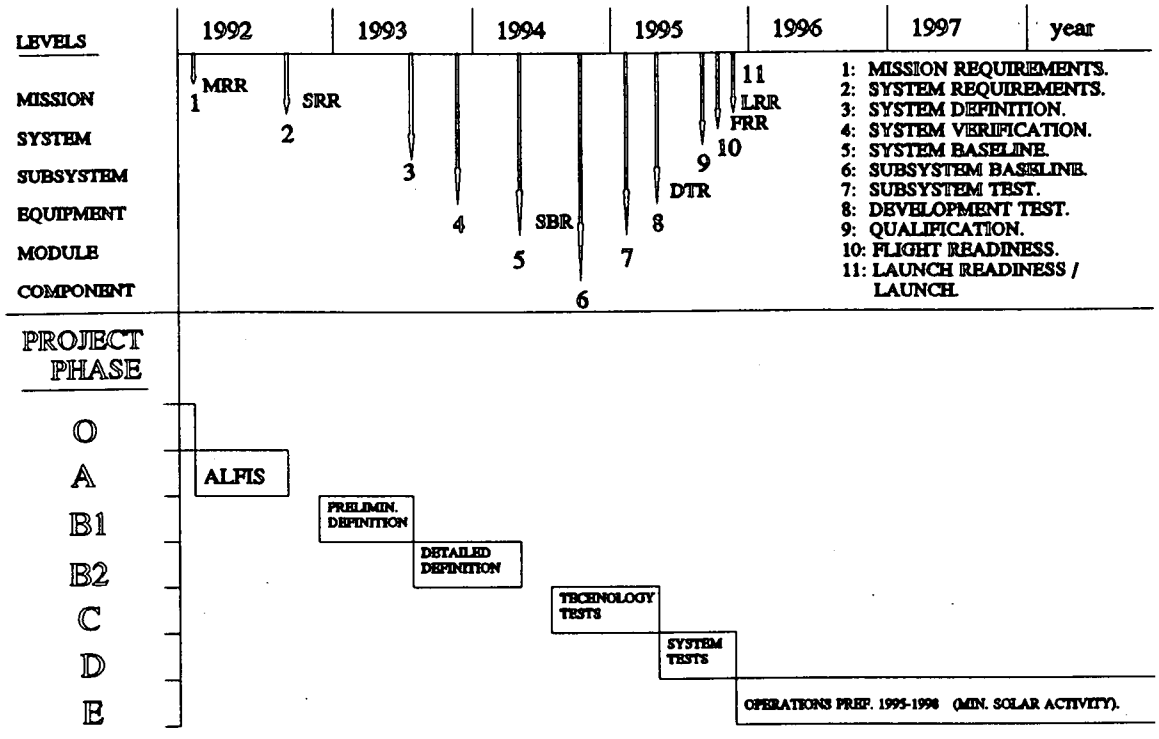

Figure 5.1: PROJECT PLANNING

5.6 DESIGN AND DEVELOPMENT PLAN

Looking at the planning, we can remark several important details. The projects time-schedule is very narrow, so several aspects of the development can be done less thorough than in usual projects.

The administration setup of the test procedure, consisting of two elements, is as follows:

- Test plan, describing what part is going to be tested, and why.
- Test procedure, i.e. the way the tests proceed and a list of required facilities.

The models used are a mock-up, to find out the best assembly sequence, and models needed for qualification. These are a structure model, to be sure the satellite can survive the different loads during the launch-phase, than a thermal model, to test the thermal control system on board the satellite, followed by an electrical model, that tests the interfaces between all components/subsystems (probably we're not able to build one thermal/electrical model, because of the extra thermometers that have to be assembled in the thermal model. These thermometers and their wiring might disturb

electrical system tests). Perhaps it is possible to use one of the satellites as a flight model to do a.o. electrical tests with.

The size of the satellites makes them easy to transport (by air for instance). Mechanical ground support equipment will be either available or easy to manufacture. We're thinking about computerized design systems (CAD), tools to assemble the satellite, containers for transportation of components, models and the final satellites to the launch base. Also electrical ground support equipment has to be designed in phase B.

5.7 OPERATIONS

One of the attempts to lower the cost of the project, is using two Dutch 25 m radio telescopes (each satellite its own groundstation) for radiocommunication. The telescopes used are two Westerbork radio-astronomy telescopes. To get access to them, our project has to be chosen from several astronomy projects. Let's stay optimistic about the chances of this. ALFIS has to take care for the scientists, development of the receiver and the tracking software. The last task may be expensive, because it's hard to get good programmers for this software. We don't need to be in Westerbork at all time; results will be stored on tape and tracking-software can be loaded once per week. Limitation of tracking speed only concerns for LEO.

5.8 REDUNDANCY AND ERROR MANAGEMENT

In general, we have chosen not to make all subsystems redundant. This would end in two much heavier and more expensive satellites. We believe it's easier to make a third (and if necessary fourth) satellite in case some major problems occur during launch or operation. Some components are redundant anyway for other reasons.

- The computer had to be on-the-shelf and radiation-proof. This resulted in only one available computer: the one used for ISO. It's discussed in chapter 16. The ISO computer consisted of two CPU's and is therefore redundant the way you buy it.

- Solar cell- or thruster-failure only cause less performance. The mission will not be lost if some part disfunctions.

- Payload, communication and active thermal control components are not redundant.

- Moving parts (release mechanism) are not redundant/fail safe.

- Both computer and other semiconductor parts (like interfaces) can be influenced by VAB-radiation.

Errors to be solved from the ground, mainly involve computer failure like memory-loss or CPU-jamming. There will always be a possibility to switch from one processor to the other, but we also have to consider ways of uploading memory-contents if necessary, and the possibility to reset the computer from the ground.

6. LAUNCHER

6.1 INTRODUCTION

In this chapter, a launcher trade-off and in sequence the launcher choice will be made. This turned out to be very difficult because of a lack of information. Nevertheless we succeeded in finding a suitable launcher.

The ALFIS-project consists out of 2 satellites, which will be placed in two almost identical orbits. This means that a dual launch is preferable. Besides the ALFIS is a scientific satellite, indicating a low budget and resulting in a low-cost-launch.

On the other hand we have to deal with constraints, which are determined by the launcher characteristics.

6.2 GENERAL CONSTRAINTS

In order to make the right choice, we have to take several constraints into account. In general, the two major constraints are:

- mass: depending on the performances of the launcher
- volume: defined by the fairing geometry.

Besides these general constraints, we have to deal with a third major constraint: low cost, because of the small financial scientists budget as mentioned above.

6.3 TRADE OFF

6.3.1 Possible Launchers

On the basis of these requirements and constraints, of which the availability of information formed the biggest obstacle, a few launchers are considered to make the trade-off. These launchers are:

- Pegasus Launch Vehicle:
  low cost and omni-inclination launch is possible
- Improved Scout II:
  low cost and orbital performances are good
- Ariane 4 (A.S.A.P. configuration)
  very low cost

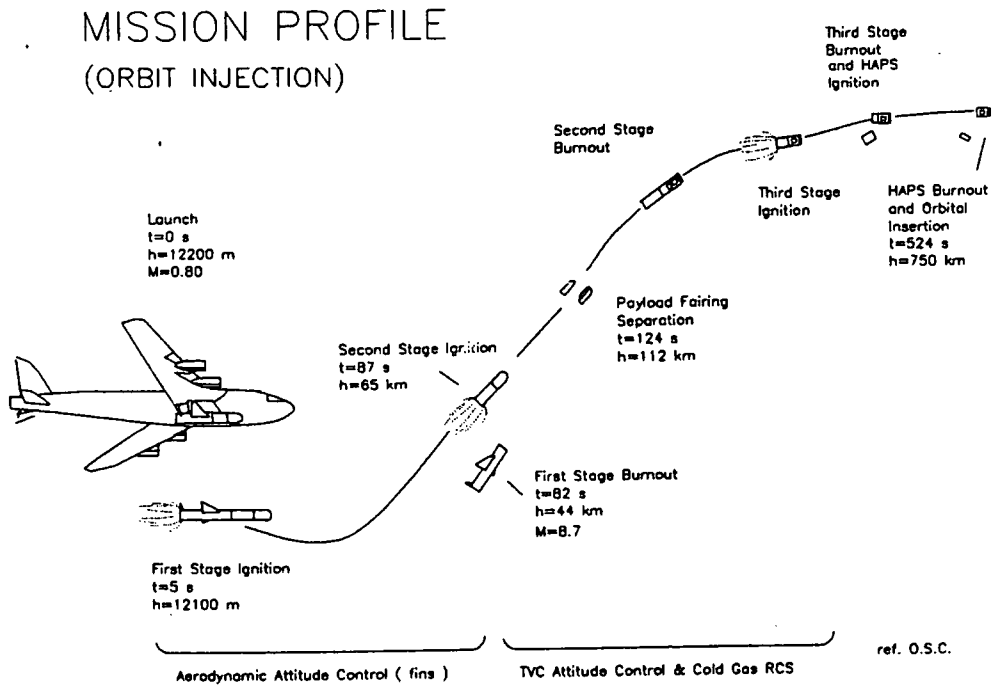

Figure 6.1: PEGASUS LAUNCHER SEQUENCE

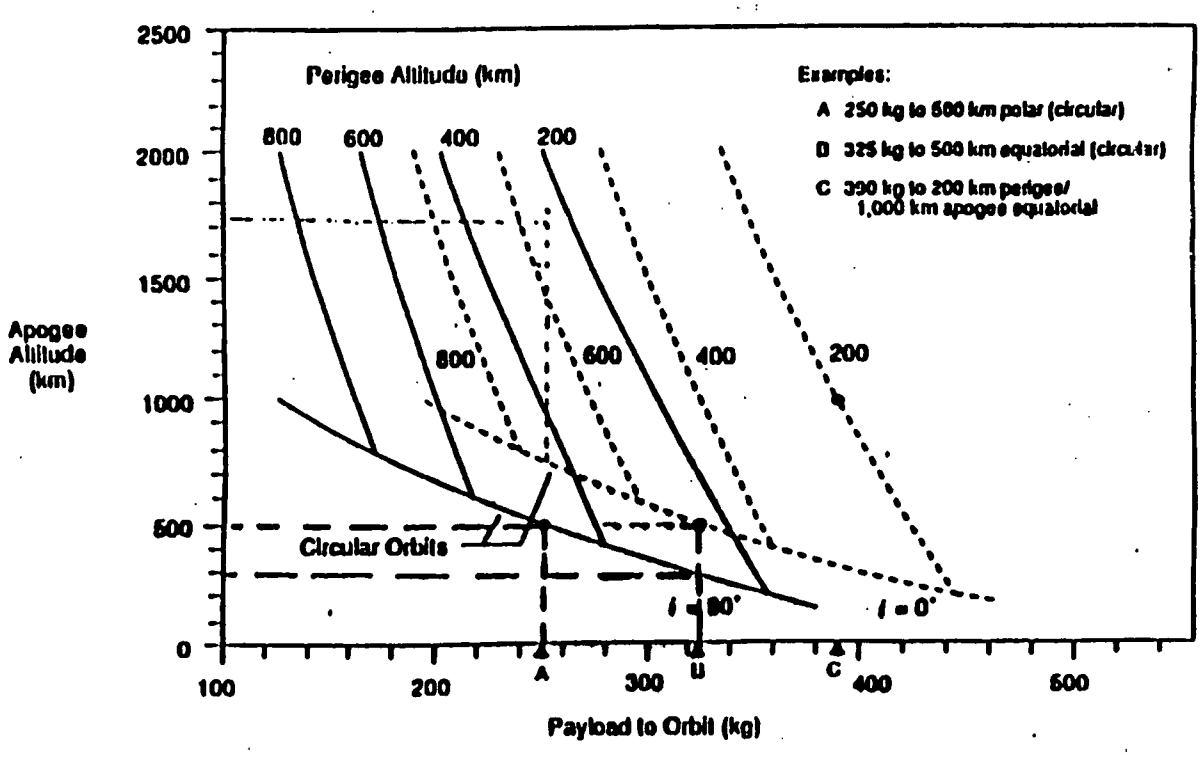

Figure 6.2: PEGASUS ORBITAL PERFORMANCES

6.3.2 Pegasus Launch Vehicle

The Pegasus is a three-stage winged launch vehicle, launched with a NASA B-52 aircraft (see figure 6.1). The main advantages are:

- low cost
- no weather constraints (The NB-52 can avoid bad weather)
- omni-inclination launch (The NB-52 can fly in any direction)

Despite these advantages the Pegasus is not a suitable launcher for our project, because of the orbital performances.

First of all, figure 6.2 doesn't show us the performances for an orbit with an apogee over 2000 km. Although we contact the Orbital Science Corporation, represented in Europe by Arianespace, we didn't get the required information for these orbital performances. It may be clear that injection in final orbit is out of the question.

Another solution is to raise the final orbit, deployed by the Pegasus, by using the satellites propulsion system. This leads to an enormous amount of required fuel and in sequence to an increase of mass. The latter forces us to look more to the right in the figure, which gives us a worse performance. So also this alternative is not hopeful.

6.3.3 Improved Scout II

The improved Scout II is a low-cost launch vehicle, developed by LTV-BPD. Despite the uncertain future of the improved Scout II, we looked at it in more detail. The configuration of the Improved Scout II is shown in figure 6.3.

The improved Scout II consists out of reliable components:

- four strap on boosters, success rate 100%
- fifth stage Mage 2 motor, success rate 100%

However the success rate of the launch vehicle is not known, because of the non-operational status.

In figure 6.4 is shown the orbital performances of the improved Scout II. We can conclude that these performances are better than those of the Pegasus, but an injection in final orbit is still impossible. Using the propulsion system, it is possible to raise the satellite to its final orbit. This will of course, as mentioned above, increase the total mass, but not in such an amount as with the Pegasus. This makes this option more realistic. But because of the uncertainty of the availability of the improved Scout II launch vehicle, we are forced to turn also this option down.

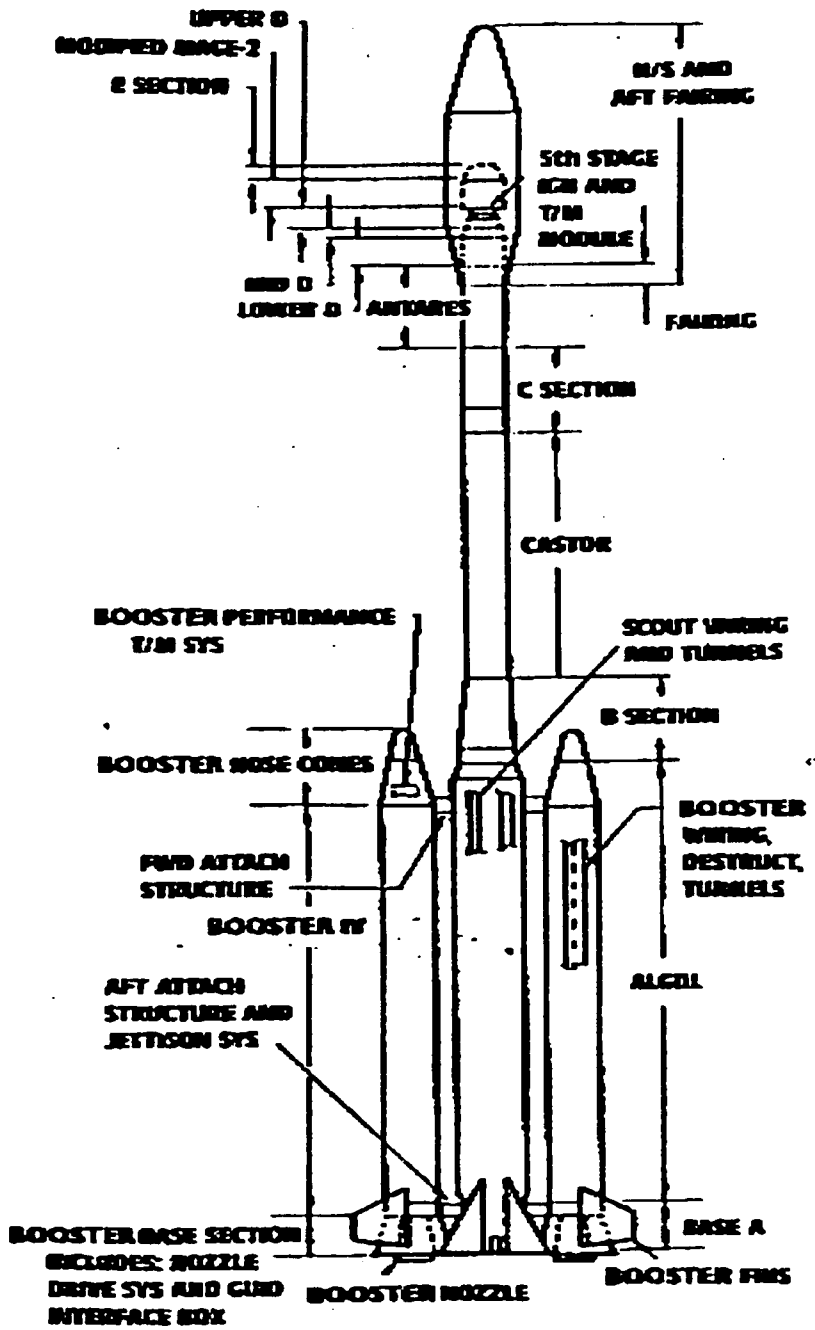

Figure 6.3: IMPROVED SCOUT II, 5TH STAGE MAGE 2 MOTOR

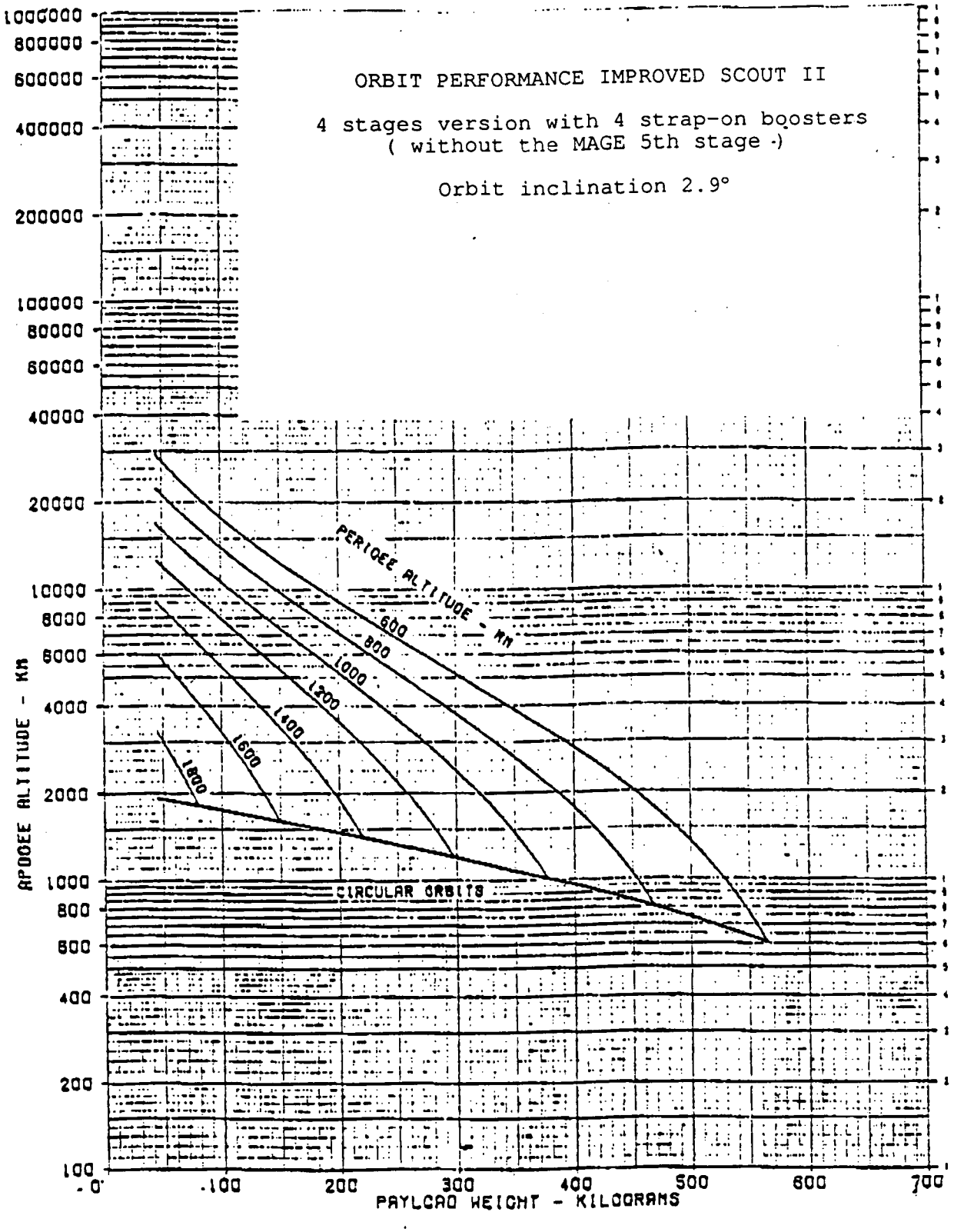

Figure 6.4: IMPROVED SCOUT II, ORBITAL PERFORMANCES

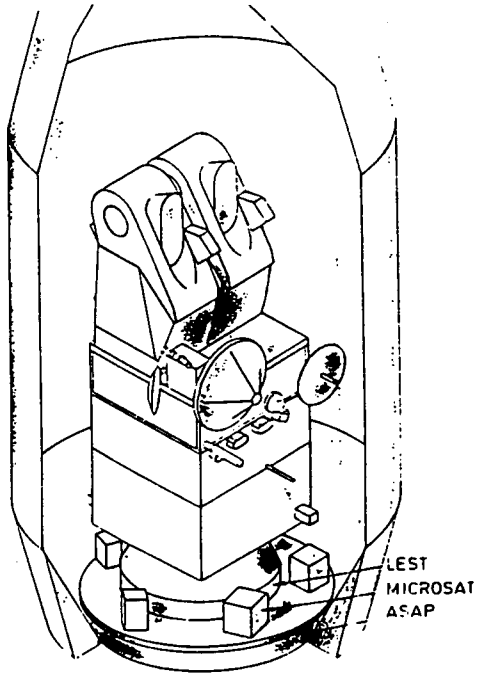

Figure 6.5: ARIANE 4, A.S.A.P. CONFIGURATION

6.3.4 A.S.A.P. Ariane 4 Configuration

The A.S.A.P. Ariane 4 configuration is a very low cost launch option, approx. 0.2 million US$. The satellite is placed on a circular platform beneath the main load in the Ariane 4 launcher (see figure 6.5). Ariane 4 brings the satellites in a GTO. Then the orbit will be raised to the final orbit, using the propulsion system. The extra required fuel is not that much to make it unrealistic.

Besides the low cost, this launch option is also very reliable.

6.3.5 Launcher Choice

Overlooking the three launch options, we can conclude that the A.S.A.P. launch configuration is the most suitable for our mission. First of all, it is a very low cost launch opportunity in comparison with the other two launchers. Besides, this option provides a dual launch which makes an accurate mutual orbit positioning possible.

The Pegasus is not suitable because of the orbital performances and the improved Scout II is not realistic.

6.4 ARIANE STRUCTURE FOR AUXILIARY PAYLOADS

6.4.1 A.S.A.P. Description

In order to provide launch opportunities to scientists, radio-amateurs, universities and other entities, ARIANESPACE has developed a structure called A.S.A.P., Ariane Structure for Auxiliary Payloads, to carry and deploy small satellites (see figure 6.5).

A.S.A.P. is a circular platform mounted externally to the 1920 mm bolted interface between the vehicle equipment bay inner cone and the main payload adaptor (see figure 6.6). This platform is a honeycomb structure faced with aluminum alloy skins. Twelve to fourteen rods stiffen the structure by linking the extremity of the plate to the third stage interface.

6.4.2 Design Data

The maximum mass of an auxiliary payload (including it's adaptation to A.S.A.P.) must be less or equal to 50 kg. The maximum aggregate mass is 200 kg.

The maximum dimensions for the payload with its adaptation to A.S.A.P. (to be provided by the costumer) is 450 mm x 450 mm for the basis (crossection) and 450 mm for the height. The latter may be higher at a particular flight.

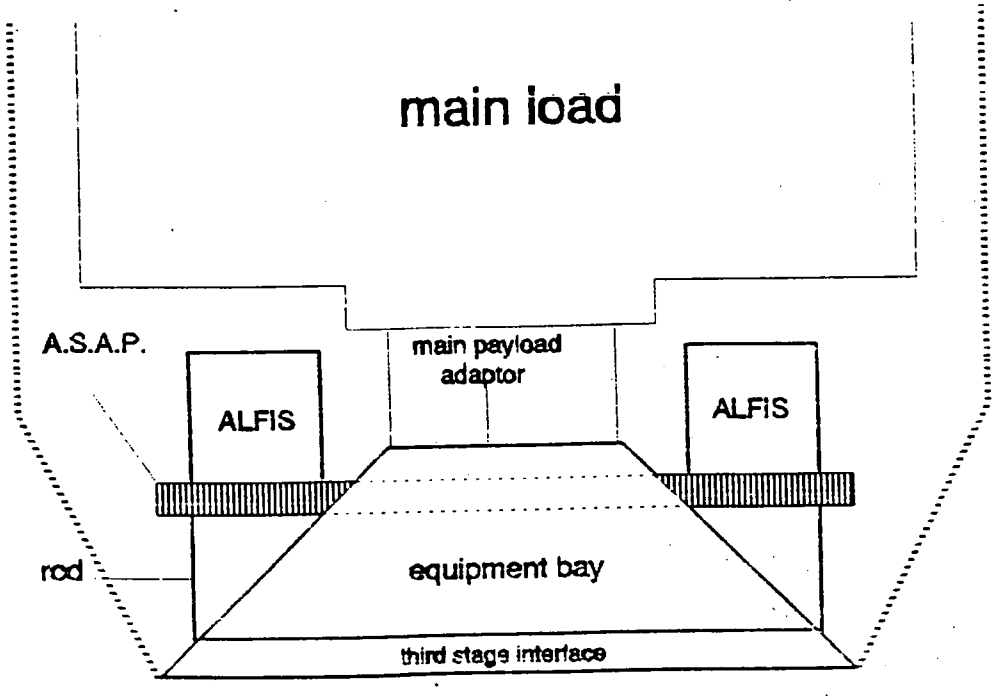

Figure 6.6: A.S.A.P. STRUCTURE

The adaptor, including separation system must be provided by the costumer. The separation system should induce a relative velocity at separation between 0.5 and 2 m/s.

The electrical circuit must be insulated.

To avoid dynamic coupling between the vehicle and the spacecraft the fundamental frequencies in the thrust and lateral axis must be resp. over 50 and 45 Hz.

6.4.3 Environmental Conditions

During the flight the auxiliary payload is subjected to static and dynamic loads induced by the launch vehicle. In the following we look at the different flight loads, applied to the spacecraft.

6.4.3.1 Steady State Acceleration

A typical longitudinal acceleration profile is given in appendix II.a, considering the lateral acceleration to be negligible and therefore ignored.

6.4.3.2 Dynamic Environment

- Low frequency longitudinal vibrations

The vibration level at the base of the payload is ≤ 1.25g from 5 to 100 Hz. This spectrum takes into account any sinusoidal or transient in the bandwidth.

- Low frequency lateral vibrations

The vibration level at the base of the payload is ≤ 0.8 g from 5 to 18 Hz and ≤ 0.6 g from 18 to 100 Hz.

- Random vibrations

The spectrum shown in Appendix II.b is applicable to all axes and refers to the ϕ 1920 mm bolted interface.

- Acoustic vibrations

Acoustic vibrations are generated by engine noise, buffeting and boundary-layer noise. It is maximum at lift-off and during the transonic phase. Outside these time periods, it is substantially lower (see Appendix II.c).

- Shocks:

The payload is subjected to shocks during separation of the fairing and during actual payload separation. The

shock experienced by the auxiliary payload at separation is produced by the separation system provided by the costumer. The acceptable shock spectrum must be lower than the one expressed in Appendix II.d.

6.4.4 Final Remarks and Launch Record

The main disadvantage of the Ariane 4 A.S.A.P. launch option is that one is dependent on the launch parameters of the main load. Generally speaking, the auxiliary payload will receive what is left available by the main mission and has no possibility to impose any change not accepted by Arianespace and its main customer. Hence, it follows that we have to make some final remarks.

6.4.4.1 Ground Constraints

- Dummy

The auxiliary payload which has been taken into account for the mission analysis of the flight will be used for the launch whatever its status is. If the auxiliary payload is not ready it will be launched as it is or a representative dummy (mass, center of gravity location) will be used. It is to be provided by the costumer.

- Launch site

A minimum area of 50 m^2 (to be shared with two other auxiliary payloads) will be allocated in the (payload preparation) EPCU building to the customer, allowing for integration and installation on A.S.A.P.. A maximum of 1 person is allowed during the final countdown in the launch center.

- Launch campaign

Real time operations will be depicted through dedicated operational documentation. The priority will be in any case given to the main passenger. The launch campaign duration is limited to 3 weeks from arrival of the auxiliary payload op to the integration on A.S.A.P. The auxiliary payload ground equipment and containers must be ready to leave the launch base within the 3 working days following the actual launch day. Aggregate will be ready to start the Arianespace combined operations at least 9 working days prior to the launch day.

6.4.4.2 Flight Constraints

The auxiliary payload is to be totally inert (no radio-transmission) during the countdown, the flight and up to 2

minutes or more after the separation, depending to a radio compatibility analysis carried on with the main passenger.

The attitude pointing at separation will be defined by Arianespace according to the mission analysis. The auxiliary payload has no means to impose a preferred orientation.

The separation will be provided in a 3 axis stabilized mode only.

6.4.4.3 Launch Record

11 nov. 1990 A.S.A.P. no. 1 AR. 40:
Heliosynchronous orbit with SPOT 2 mission-CNES.

Customer	Aux. payload	Mass	Mission
UOSAT/SST (UK)	UOSAT-D	45.5 Kg	Scientific experimentation. Store and forward digital communications.
	UOSAT-E	47.5 Kg	Scientific experimentation. Telecommunication and imaging demonstration.
AMSAT N.A. (USA)	MICROSAT A	12.1 Kg	Digital store and forward communications.
	MICROSAT B	12.1 Kg	Scientific educational and communications.
	MICROSAT C	14.3 Kg	Educational CCD earth imaging.
	MICROSAT D	12.1 Kg	Digital store and forward communications.

7. ORBIT

7.1 INTRODUCTION

During the project it became clear that the orbit-requirements weigh heavily on the missions. They suggest that there must be a close interaction between orbit control and the other subsystems. Defining an orbit that meets both orbit-requirements and available propulsion technology taking the mass budget of the ALFIS satellites into consideration, came only at the end of the project. In this chapter we will look at the orbit-aspects, especially at the interferometric base-line and the launch-window.

7.2 TRADE-OFF & ORBIT DEFINITION

The orbit-requirements suggest that we must look for a GTO. Making a simple calculus with elliptic orbit parameters pointed out that the first orbit-requirement would be exactly satisfied for a orbit with a 6.6 hr. orbital period, with a perigee height of 400 km. The second orbit-requirement suggests that we would like to see the apogee turn up above the groundstation. Because of orbit perturbations that sweep the orbit slower/faster around the Earth then the Earth rotates, the apogee would only turn up above the groundstation now and then. Taking an 8 hr. or a 12 hr. orbit would solve the problem. The 8 hr. orbit turns up every third orbit and the 12 hr. every second orbit. The 12 hr. orbit has a preference above the 8 hr. orbit because it spends more time outside the Van Allen Belts. The observing time for the 12 hr. orbit is more than 30% greater and will eventually contribute to low ground segment costs. But there is another constraint, taking the Ariane 4 as the launch vehicle, we would end up in a GTO with a perigee height of only 200 km. In order to get to a perigee height of 800 km, which is preferable because at a lower height the aerodynamical loads on the ALFIS satellites would not be acceptable, we decided to use the propulsion system as an apogee/perigee booster. The only question left open was whether the mass budget would allow this or not. It did, and so we have chosen the 12 hr. orbit.

	Orbit sat. #1	Orbit sat. #2
-Perigee height	800.00 km	Idem
-Apogee height	39694.34 km	"
-Orbital period	12.01 hrs	"
-Outside Van Allen Belts		
-Observation time[1)]	9.01 hrs	"
-Optical visibility	100.00 %	"
-Inclination[2)]	5.20 degr	"

	Orbit sat #1	Orbit sat #2
-Maximum eclipse[3)]	75.00 min	idem
-Initial conditions		
-Ascending knot	185 degr	182 degr
-Argument of perigee	270 degr	273 degr

1) Depending on whether the system is ready.
2) At the final presentation of the project Mr. Ambrosius (T.U. Delft) pointed out that the minimum inclination in a GTO with Ariane 4 is 7 degr.
3) Depending on initial conditions.

7.3 GROUNDTRACK AND VISIBILITY

Figure 7.1 shows the groundtrack for one of the ALFIS satellites. The solid drawn line indicates that the satellites are visible for the groundstation in Dwingeloo (Holland).

Because of orbit perturbations and the drift of the Greenwich meridian relative to the inertial x-axis, the apogee tends to drift away in longitude and latitude. By changing the orbital period slightly, by in- or decreasing the semi major axis, we are able to keep the apogee longitude fixed above the groundstation, this explains the extra .01 hr orbital period.

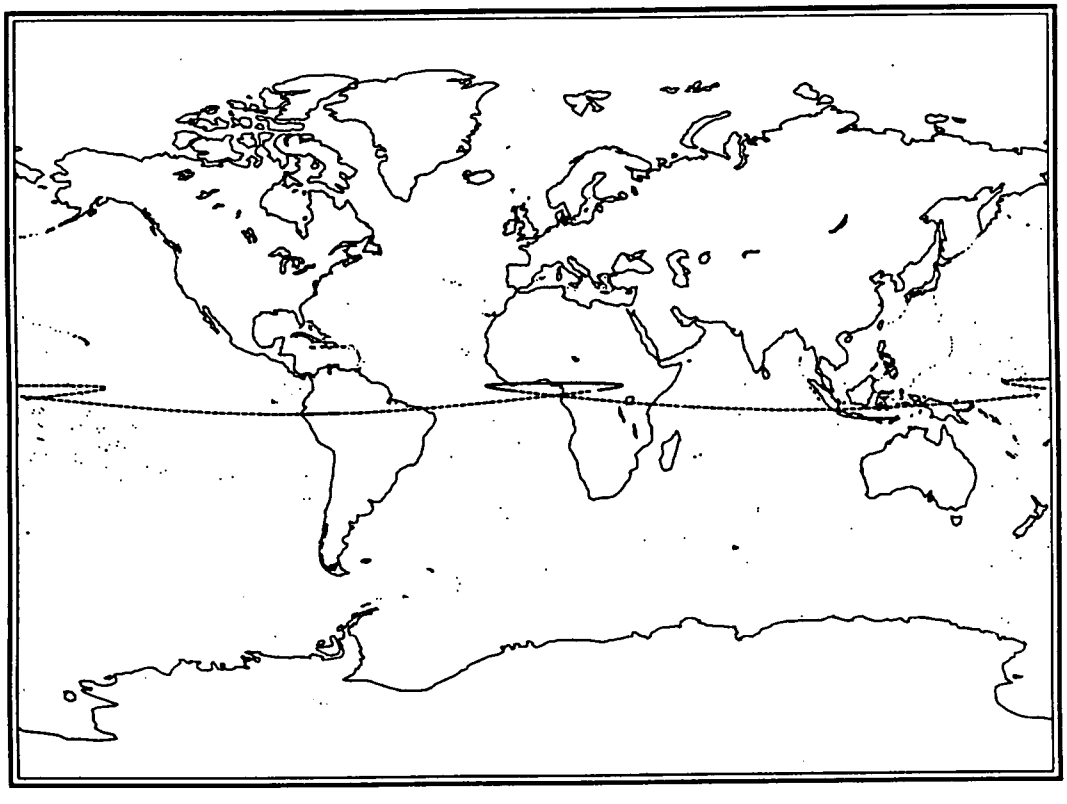

Figure 7.1: ONE DAY ALFIS GROUNDTRACK

As we can see in figure 7.2, the apogee latitude oscillates in time between 5.2 degrees North and South. This movement is unavoidable, but of no great concern.

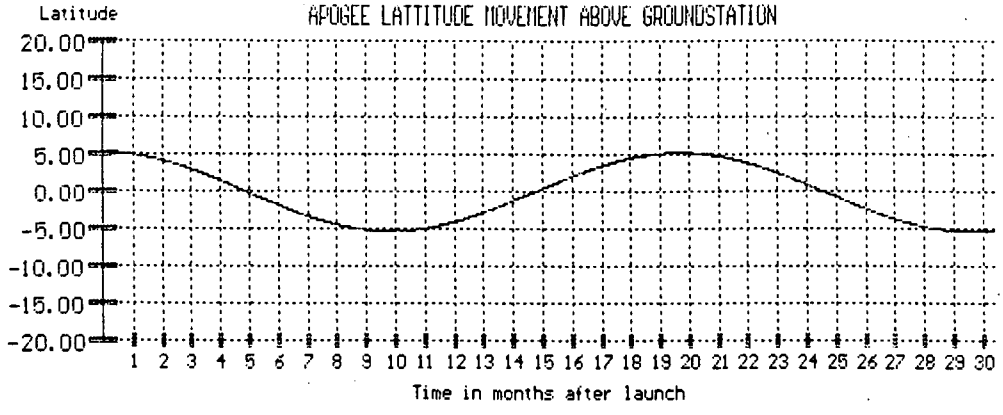

Figure 7.2: APOGEE LATTITUDE MOVEMENT

One mission-requirement is that observations are done only outside the Van Allen Belts. The Van Allen Belts are charged particles trapped in the Earth's magnetic field. They stretch out into space to a distance of approximately four times the radius of the Earth. When the satellites leave the Van Allen Belts they can see more than 80% of one side of the Earth. So when the apogee longitude point coincides with the groundstations longitude point, it must be possible for the satellites to see the ground station. We can prove this in the following way, figure 7.3 shows that the visibility area is characterized by α. If we know the value of α we are able to draw a circle with radius α in the groundtrack figure (figure 7.1) and check if the groundstation lies within the circle. If the groundstation lies close to the edge of the circle the groundstations elevation might be insufficient and the satellites would not be visible because of the horizon. In this case we have to speak of the optical visibility rather than the visibility.

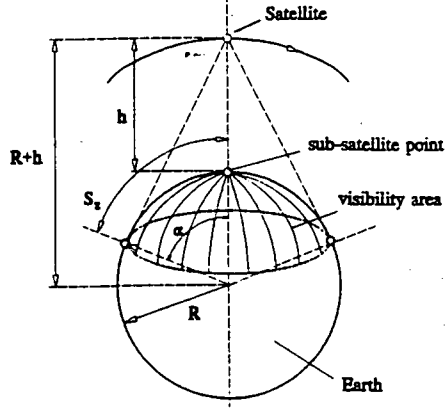

Figure 7.3: VISIBILITY AREA

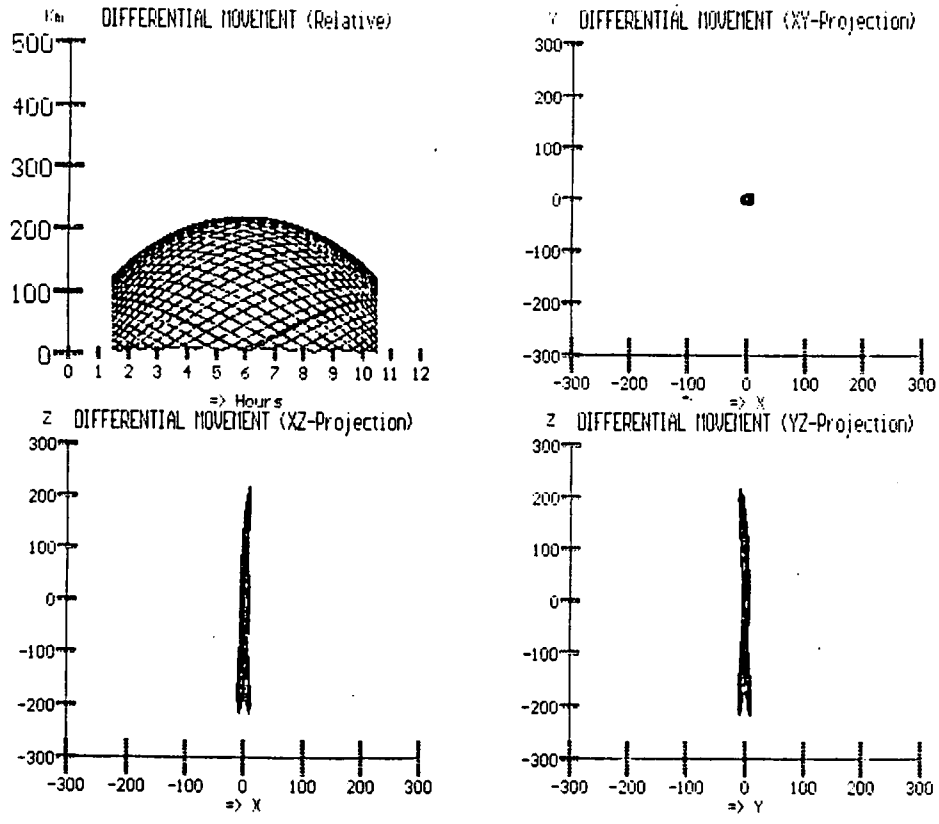

Figure 7.4: RADIAL AND TANGENTIAL FILLING

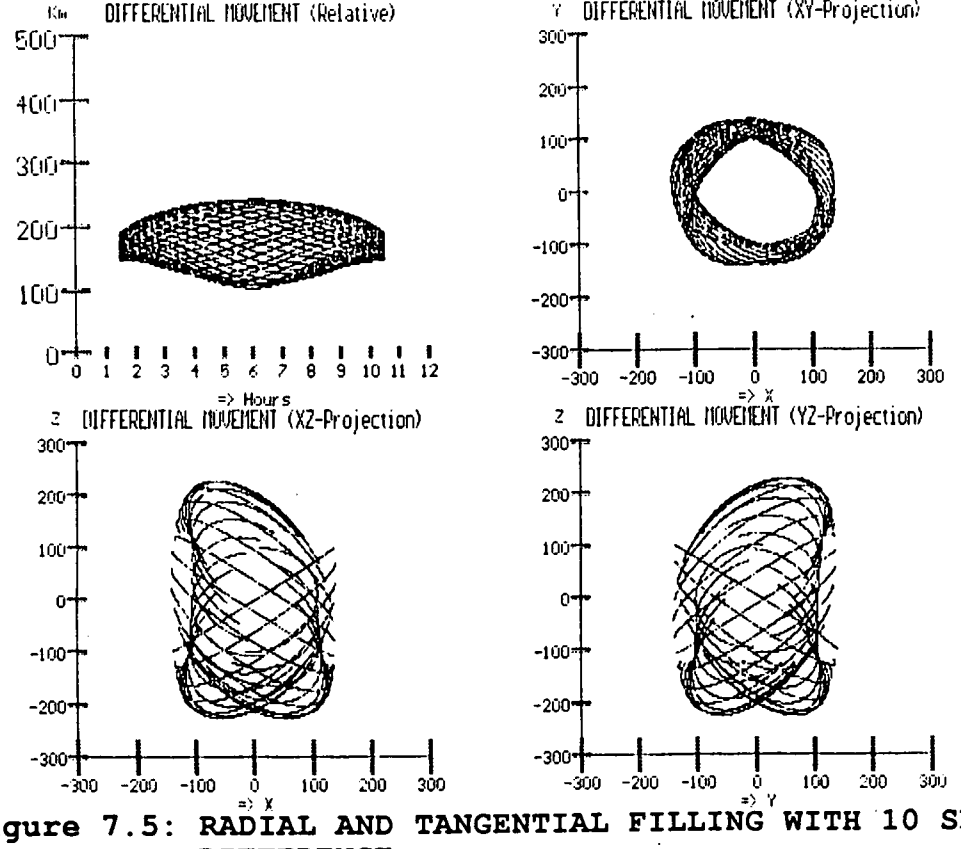

Figure 7.5: RADIAL AND TANGENTIAL FILLING WITH 10 SEC. TIME DIFFERENCE

Using Figure 7.3 we find for α:

$$R_{V.A.B.}=4\cdot R_e \Rightarrow \alpha=\arccos\left(\frac{R_e}{R_{V.A.B.}}\right)=\arccos(0.25)=75.52$$

Drawing a circle with a radius of 75.52 degrees at the moment the satellites leave the VAB suggests the optical visibility is 100%, the groundstation lies within the circle. As we shall see later in Chapter 15 Telemetry and Telecommand the groundstation elevation at this time is sufficient.

7.4 INTERFEROMETRIC BASELINE

The concept of ALFIS is to use two array elements (satellites) as a interferometer. To observe at all desired frequencies the relative distance between the two satellites must vary in absolute values between 1 and 300 km. An absolute value in distance between the two satellites is called a baseline. The third orbit-requirement suggests that observations must be done in all directions, so we must create a sphere filled with baselines in all directions.

At the start of the project it was suggested that we should look for identical orbits with different inclination. A difference in inclination means different orbit perturbations, the thought was that this difference would fill our sphere evolutionary. However after simulating this method it soon became clear that there was no combination that would fill the core of the sphere sufficiently without intervenience.

Another suggestion is to take two identical orbits with only a difference in initial conditions (ascending knot and argument of perigee), then by creating a time difference in orbit between the two satellites the problem would be solved.

The main difference between the two methods is that the last implies a low rate of interference, by giving one satellite a small boost along track with the propulsion system the time difference becomes bigger every orbit. When the time difference becomes too large (the absolute distance becomes larger than 300 km) we have to boost in opposite direction; the time difference becomes smaller. Two effects become clear. Firstly, the orbit perturbations take care of the tangential filling of the sphere. Secondly, the time difference takes care of the radial filling. This implies that we cannot enter our sphere at every point whenever we want to. But the orbit-requirement suggests that we want to see a distribution of baselines during the life time of the satellites.

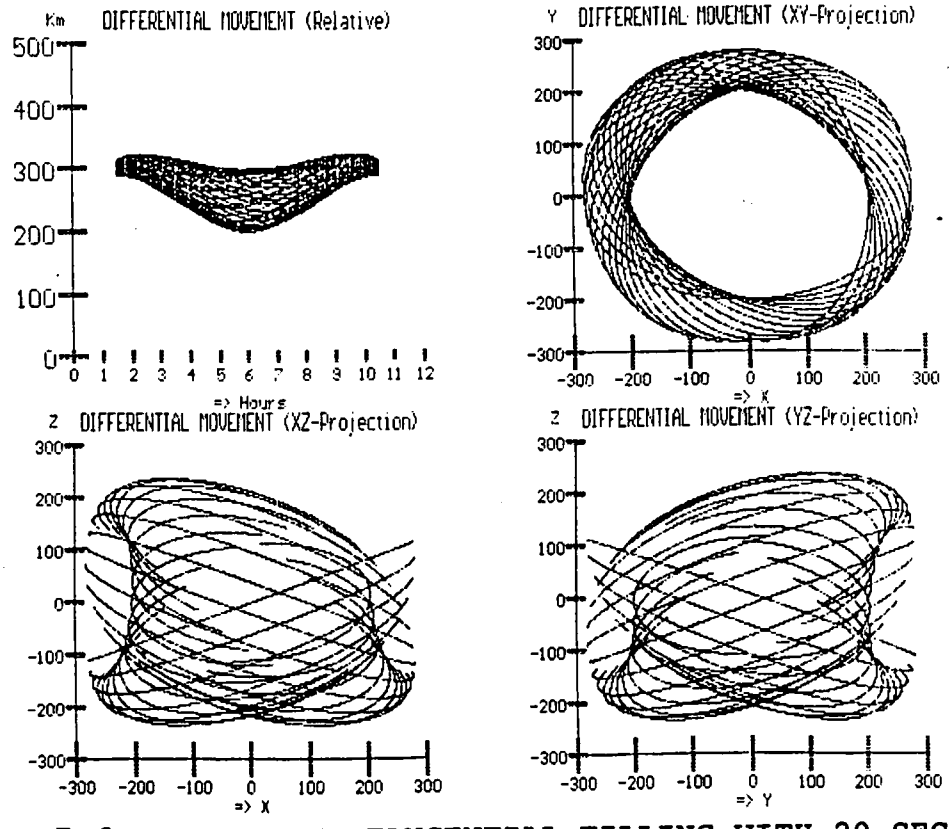

Figure 7.6: RADIAL AND TANGENTIAL FILLING WITH 20 SEC. TIME DIFFERENCE

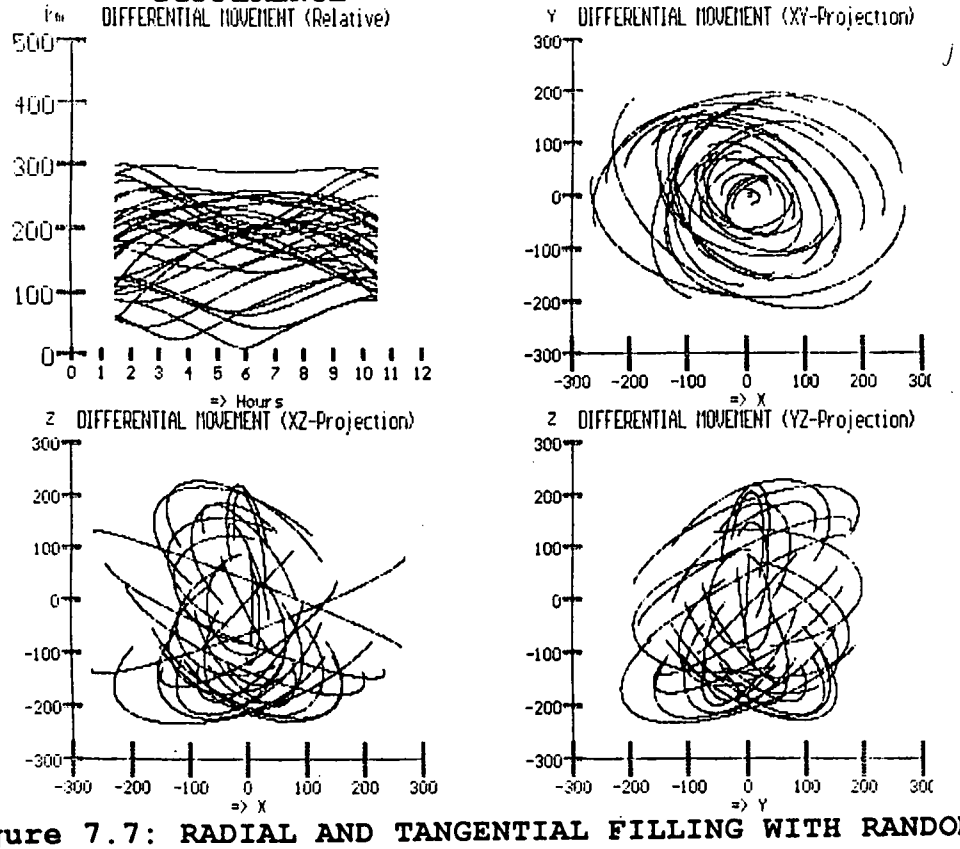

Figure 7.7: RADIAL AND TANGENTIAL FILLING WITH RANDOM TIME DIFFERENCE

This radial and tangential filling is visualized in figure 7.4: it shows the relative distance of the two satellites and the projection of these distances on the Earths inertial frame during a life time of two and a halve years sampled weekly with no time difference in orbit. It shows that the relative distance has its maximum far below 300 km and that these distances are mainly perpendicular to the orbit-plane (z-axis movement).

Figure 7.5 shows the situation with 10 seconds time difference. It is very clear that we go to the outside of the sphere, this is especially clear in the XY-plane. Also the relative distance becomes greater. It is as if we entered another layer of the sphere. Figure 7.6 shows the situation when the time difference is some 20 seconds and figure 7.7 shows the situation when we take random time differences during life time.

7.5 ECLIPSES & LAUNCH WINDOW

Every component in a satellite has allowable temperature ranges, exceeding these ranges means such a component will disfunction in some way. When a satellite goes into eclipse the temperature will fall and so we need a system to keep the satellite inside the allowable temperature ranges: the thermal control system. Although there are many ways to maintain a desired temperature, if the eclipse is too long it will cost power to maintain the temperature.

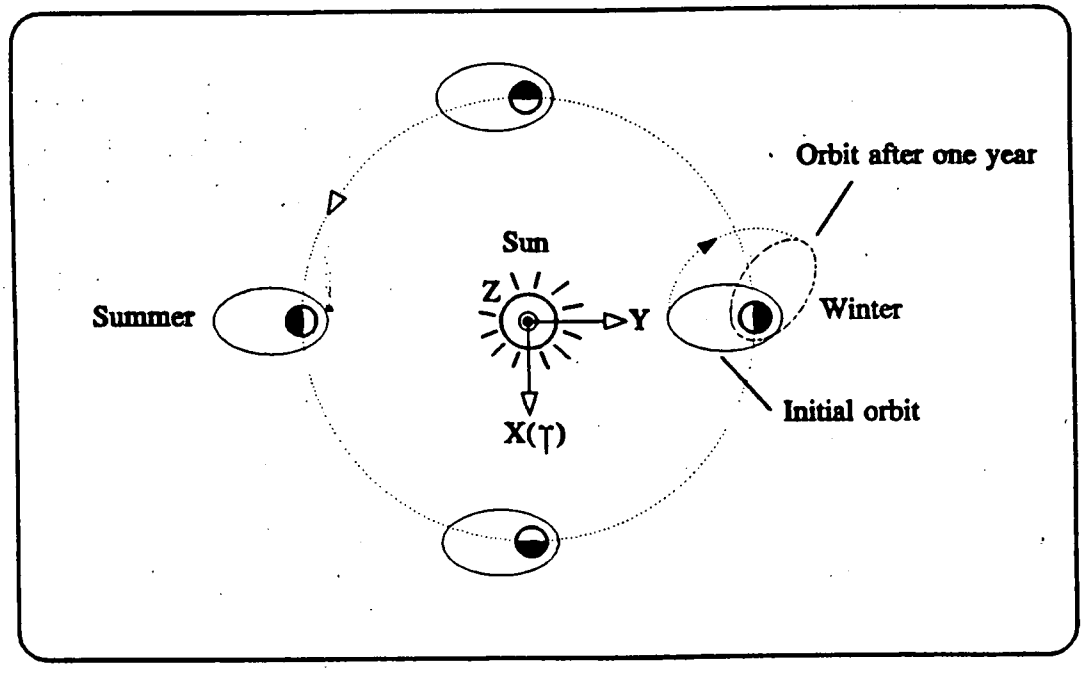

Figure 7.8: EFFECT OF PRECESSION OF THE EARTH

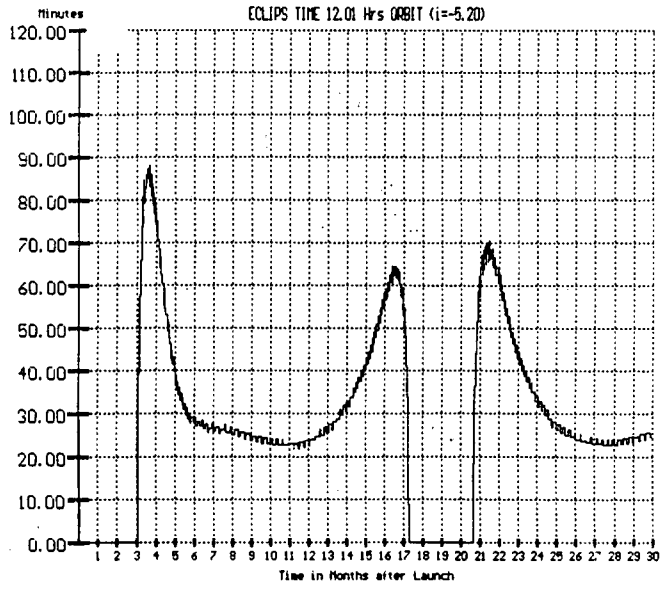

AUGUST

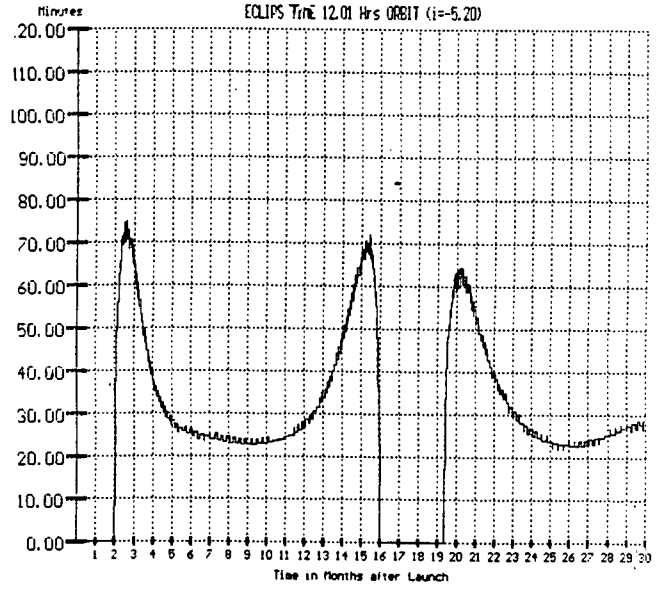

SEPTEMBER

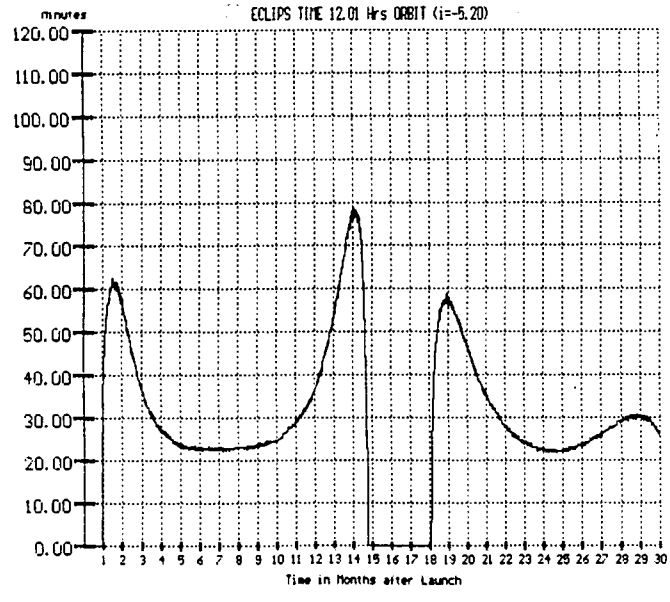

OCTOBER

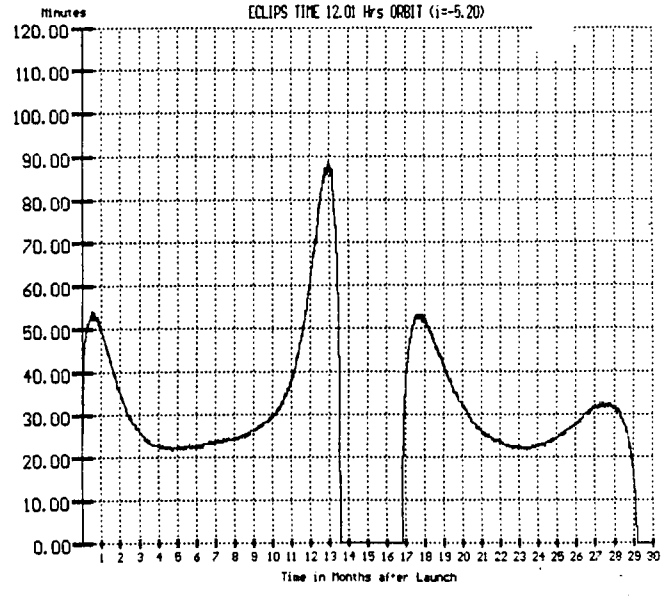

NOVEMBER

Figure 7.9: ECLIPSE TIMES

Different launch dates imply that the satellites will encounter different eclipses, in other words a launch in January could give a maximum eclipse encountered by the satellite that is smaller than we would encounter when we launch for example in September. This is shown in figure 7.8, the orbital precession sweeps the orbit around the Earth. So like the figure 7.8 shows when we would launch in the winter and we come back to the same point one year later, the orbit has a different attitude.

When we optimized for minimal eclipses, we took winter as our reference because of two reasons: first we like to observe during day time and second because we like to pull the orbital plane out of the ecliptica as far as possible. With this knowledge we tried several launch dates. The outcome showed that September results in maximum eclipses of 75 minutes, allother launch dates resulted in longer eclipses. Figure 7.9 (launch in August, September, October and November) shows the eclipses we encounter when we follow the satellites for 30 months. When we launch in September, right after the launch, we would be observing (collecting measurement-data) in the night-time. Because of the orbital precession this will soon be the day-time and after a while the night-time again. The launch window that leads to the longest observation has not yet been investigated.

7.6 CONCLUSIONS

The manipulation of the interferometric baseline looks simple in theory, but requires (as mentioned in the introduction) intense interaction between the propulsion system and other subsystems. There are many other effects to be considered, for example the oscillation of the semi major axis which can be significant. Further investigation has to be done for the launch window which also depends on the main load of Ariane 4.

8. CONFIGURATION

8.1 INTRODUCTION

In this chapter we will discuss configuration requirements, boundary conditions, the supporting structure and the lay-out of the equipment.

8.2 REQUIREMENTS

The configuration must be designed in a way that:

- the satellite fits on the chosen launcher
- all equipment fits and is able to perform it's specific tasks, with a certain reliability, under all possible conditions during the lifetime of the satellite

8.3 CONFIGURATION EVOLUTION DURING PROJECT

Working on the configuration came hand in hand with changing the boundary conditions several times. The ALFIS Midterm Review resulted in a total change of the configuration. In this paragraph we discuss this drastic change.

8.3.1 Configuration before Midterm Review

The following boundary conditions were chosen at the start of this project:

- stabilization method: free tumbling & 3-axis stabilized
- launcher: improved SCOUT 2

Considering this we chose the following solution:

- cylinder taking main loads
- torical tank
- vertical platform for units
- sphere for solar cells

8.3.2 Midterm Review

During the Midterm Review the comments concerning the configuration are listed below:

- Consider an other launcher. Improved SCOUT 2 is not operational yet. Look at the hitch-hike possibility of the ARIANE 4 launcher.

- Torical tank is not off the shelf and far to expensive to develop.
- Why not try spin stabilization ?
- We might be able to use 25 cm instead of 15 m antennas.
- Consider using a battery.

8.3.3 Developments after Midterm Review

It turned out that we could not continue the sphere-concept. We decided to look at spin-stabilization again in combination with the relative cheap ASAP possibility of the ARIANE 4 launcher. This was very important, bearing in mind possible realization in the near future. We had to try to 'downscale' the budgets in order to be able to fulfill the requirements of the launcher. In the rest of this chapter the results of this concept are given.

8.4 BOUNDARY CONDITIONS

8.4.1 Launcher

The ASAP configuration of the ARIANE 4 launcher is chosen. We got information about this possibility from lit. 8.1. We concluded from that information that we, depending on a favourable main load, could use a volume of 400 x 400 x 700 mm. These data were not correct but we had to start somewhere. The base of this volume was fixed to 400 x 400 mm. Furthermore we allowed ourself to have several things stick out of the satellite (eg. thrusters).

Later on it turned out that our assumption of the usable volume was incorrect. The users manual showed 450 x 450 x 450 mm as usable volume. Increasing the height is negotiable (with Arianespace, depending on the main load). These information came too late to be taken into account in the remaining time of our project.

8.4.2 Stabilization Method

In chapter 5 the stabilization choice is described. With the result we will use spin-stabilization as stabilization method.

8.5. SUPPORTING STRUCTURE

In this paragraph the choice of the final supporting structure is motivated. We have chosen a box configuration mainly to make maximum use of the available volume.

8.5.1 Separation Mechanism

Considering the separation mechanism we chose between two options: the MARMAN clamp and a four point release mechanism. The following issues made us decide to chose the four point release mechanism:

- the MARMAN clamp was too heavy
- the available volume made the use of the MARMAN clamp impossible

8.5.2 Fuel Tank

The tank (originally 10 l.) was a major problem considering the available volume. If we would choose a standard spherical tank we would not be able to fit all the units. Therefore we decided to choose a somewhat more unconventional tank configuration. The tank configuration is given in figure 8.1.

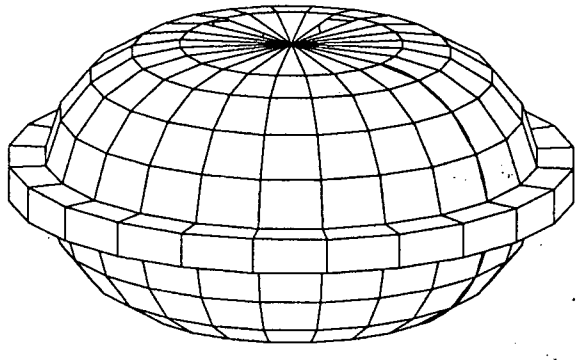

Figure 8.1: TANK CONFIGURATION

During the project the volume of the tank dropped to 7.5l. The maximum diameter is estimated to be 280 mm. This figure is imposed by the voluminous solar panels, the frame and mounting of the tank. Considering a volume of 7.5 l and a maximum radius of 140 mm for the tank, the tank parameters, shown in figure 8.2, would be as follows :

$$R = 140 \text{ mm}, \quad r = 76.5 \text{ mm}$$

The overall height is estimated to be;

153 mm (interior tank height)
2 mm (thickness wall)
2 x 6 mm (insulation)

A total of 170 mm

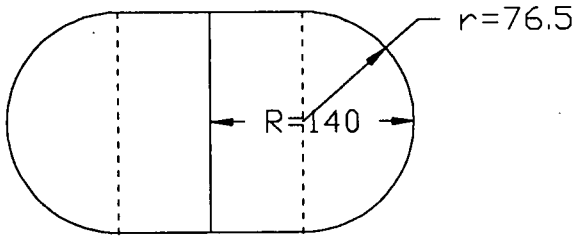

Figure 8.2: TANK PARAMETERS

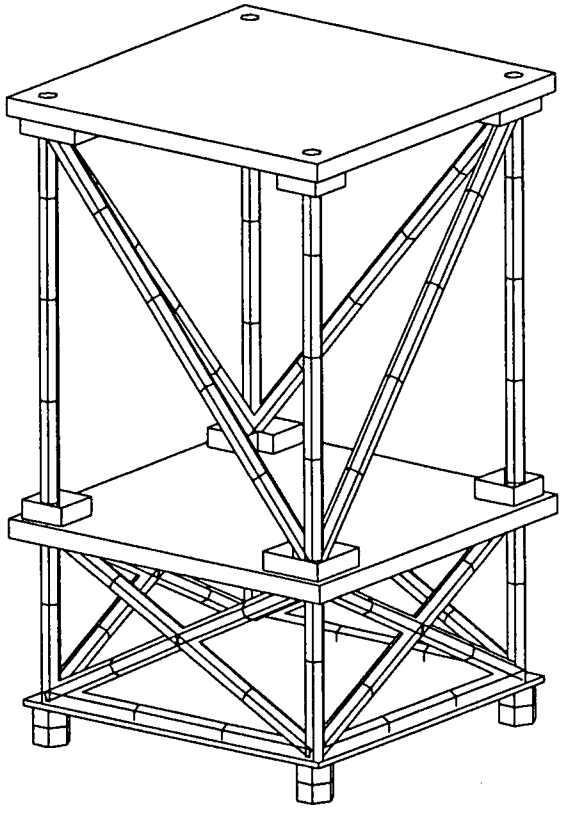

Figure 8.3: SUPPORTING STRUCTURE

We now have to connect the tank to the supporting structure. The following issues made us decide to use a frame as shown in figure 8.3 (estimated bar diameter 20 mm):

- The 4-points separation introduces launch loads as point loads. Using bars these forces are better conducted into the structure.
- A frame is lighter than a sandwich panel.
- The tank can easily be fixed at 4 points to the frame.

At the end of the project the situation was changed drastically. This appeared because the volume of the tank dropped to 7.5 l and the base of the usable volume of the launcher turned out to be 450x450 mm. Now we might be able to use one or four spherical tanks, given the fact that the volume might end up way under 7.5 l. This would be a big simplification and reduction of cost. This new situation couldn't be dealt with because of the short time-span to the final presentation.

8.5.3 Mounting of Equipment

We have chosen to use 2 horizontal platforms of 380 x 380 x 20 mm for mounting most of the units on the following reasons:

- Thermal: We need one thermal environment for all units and dissipation of energy through the top horizontal platform is preferable. Therefore units with high power dissipation should, if possible,be mounted on the upper platform. Using a vertical platform in the middle of the upper part of the box will create two separate rooms and will invoke problems with energy dissipation.

- Despite the need for tight packing of the units this solution still gives the possibility for inspection during post-assembly phases.

- 380 x 380 mm because of the estimation: solarpanel thickness 5 mm. isolation 5mm.

One horizontal platform is fixed to the tankframe. The other horizontal platform is connected to the first by a second frame (estimated bar diameter 20 mm). This is done to make maximum use of the available volume. Remaining height for the units : 700 mm (usable height) minus 50 mm (separation) minus 170 mm (tank) minus 2 x 20 mm (platforms) minus 10 mm (reserve) leaves 430 mm available height for the units.

At the end of the project it turned out that our configuration has a much too low resonance frequency. Therefore the frame between the two platforms should be replaced by vertical panels to obtain much higher structural stiffness. This would implicate problems concerning mainly the lay-out of the units.

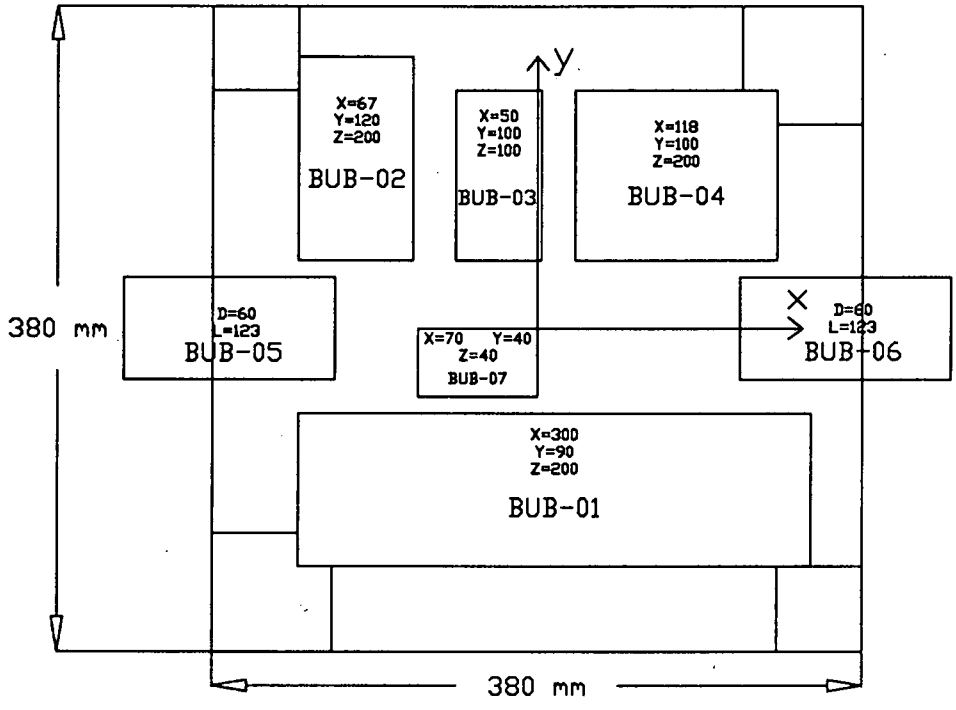

Figure 8.4a: CONFIGURATION PLATFORM B

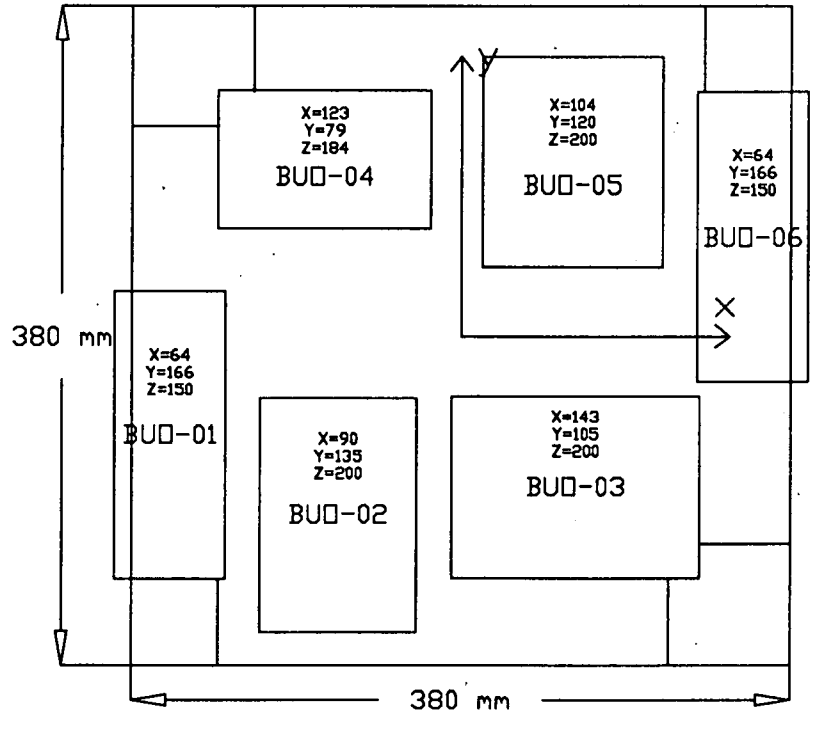

Figure 8.4b: CONFIGURATION PLATFORM A

8.6 LAY-OUT OF THE EQUIPMENT

In this paragraph the chosen internal configuration and the lay-out of equipment which is not mounted to the two platforms is given and motivated. To start with, the relevant requirements are given here:

- As much as possible mass should be mounted to the lower platform, because of expected problems with the products of inertia.

- The units should be placed in a way that room is available for mounting points , cable streets and fuel lines (normally 30 % surface is for units).

- The units are not allowed to have direct surface contact with other units.

- The center of gravity should be close to the geometrical z-axis and the moment of inertia round that z-axis must be at least 10 percent higher than the other moments of inertia to provide a balanced satellite.

- To diminish wiring, elements, belonging to the same subsystem, are placed as much as possible in the same box.

Considering these requirements we decided the following. For cabling and fuel lines we reserve a stroke of at least 75 mm width in the middle of each platform. For bolts we leave an area of 15 x 15 mm. Between a unit and another unit or element we leave at least 20 mm space. Between a unit mounted to the lower and a unit mounted to the upper platform we leave at least 30 mm space.

These assumptions will result in a very tight packing of the units. This will give difficulties concerning assembly. We assume we will be able to invent a smart way of assembling the units on the platforms. All elements mentioned in the next subparagraphs are shown in figures 8.4a, 8.4b and 8.7.

8.6.1 Attitude Control

The attitude control subgroup contains the following units:

- 2 ESS sensors
- electrical control unit

First of all the two ESS sensors are placed. They need a field of view and are placed on platform A just below a cross-bar. The electrical unit is later placed on platform B.

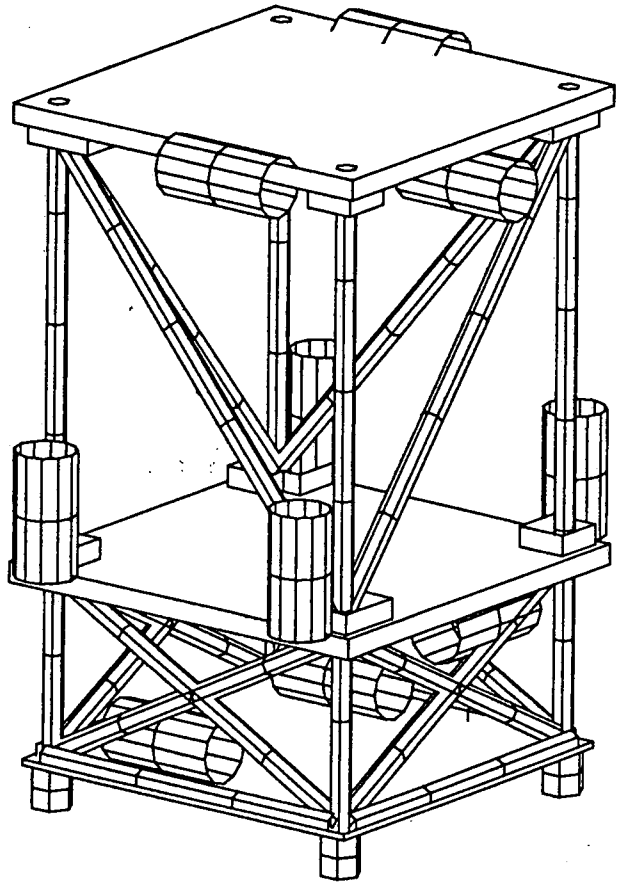

Figure 8.5: THRUSTER CONFIGURATION

8.6.2 Propulsion

The propulsion subgroup contains the following units:

- tank
- 12 thrusters with control units
- fuel lines

The tank is as mounted in the tankframe. When placing the thrusters we kept the following issues in mind. The 12 thrusters are needed to ensure the ability to control all six degrees of freedom. We should use as little space as possible on the platforms to mount the thrusters (volume problem). Also disturbance of solar panels should be minimal (power demand). In figure 8.5 the configuration of the thrusters is shown. The fuel lines coming out of the tank pass the units towards the thrusters.

8.6.3 Power

The power subgroup contains the following units:

- PMAD unit
- battery
- solar cells

The battery is placed on platform A because it is heavy. The dimensions of the battery are fixed. The PMAD unit is placed next to it in order to keep cabling as short as possible. The solar cells are mounted on 4 sandwich panels. They are fixed to the satellite. The panels contain cut outs for the 2 ESS sensors and several thrusters (figure 8.6)

8.6.4 Payload

The payload subgroup contains the following units:

- filterbanks
- payload box
- position determination unit
- 3 antennas

The filterbanks are not integrated in the payload box because they need a very precise thermal control ($\pm$ 1°C.). The payload box contains the mixers, the pre-amplifiers, the PL loop and the multiplier. We have placed the payload box next to the filterbanks (short wiring) on platform A becausetogether they are relatively heavy. The positioning unit is integrated in the transponder box of the TTC subgroup. The antennas are mounted on a platform or on a bar of the frame.

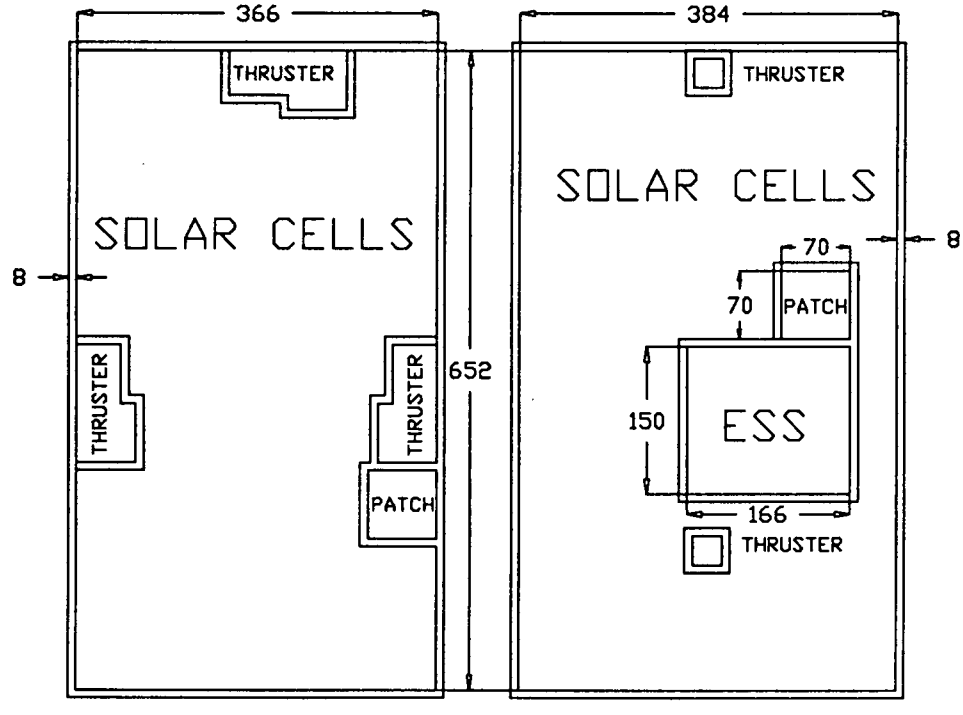

Figure 8.6: SOLAR PANELS

8.6.5 On Board Computer

The computer subgroup contains the following units:

- on board computer
- interface

Because the computer has relatively large fixed dimensions, we mount it onto platform B. The interface is placed in the 'cable street' of platform B because there is no room left and it is very small.

8.6.6 Telemetry and Telecommand

The TTC subgroup contains the following units:

- transponder
- processor
- 6 patches

In the transponder box the receiver and the positioning unit of the payload subgroup are integrated. The processor contains the processor itself as well as the multiplexer. The processor has to be protected against radiation and is therefore shielded with a 10 mm aluminum plate. We could not satisfy the demand of the TTC and payload subgroup to place the payload box, the processor and the transponder next to each other to minimize wiring, simply because there was no room. We could only place the processor next to the transponder on platform B. The transponder, dissipating relatively much energy, is mounted onto platform B which acts as a radiator. The patches (70 x 70 mm) have to be placed at the outside of the satellite. On each of the six planes we place one patch. Each wire from the transponder to a patch has to be the same length.

8.6.7 Thermal Control

The thermal subgroup contains the following equipment:

- blankets
- thermometers
- thermofoil

The thermal blankets are mounted to the solar panels and to the horizontal panel just above the separation mechanism. The tank is also covered with blankets. The platform B is covered with a reflecting layer to function as an OSR. The thermometers are placed at several crucial points within the satellite.

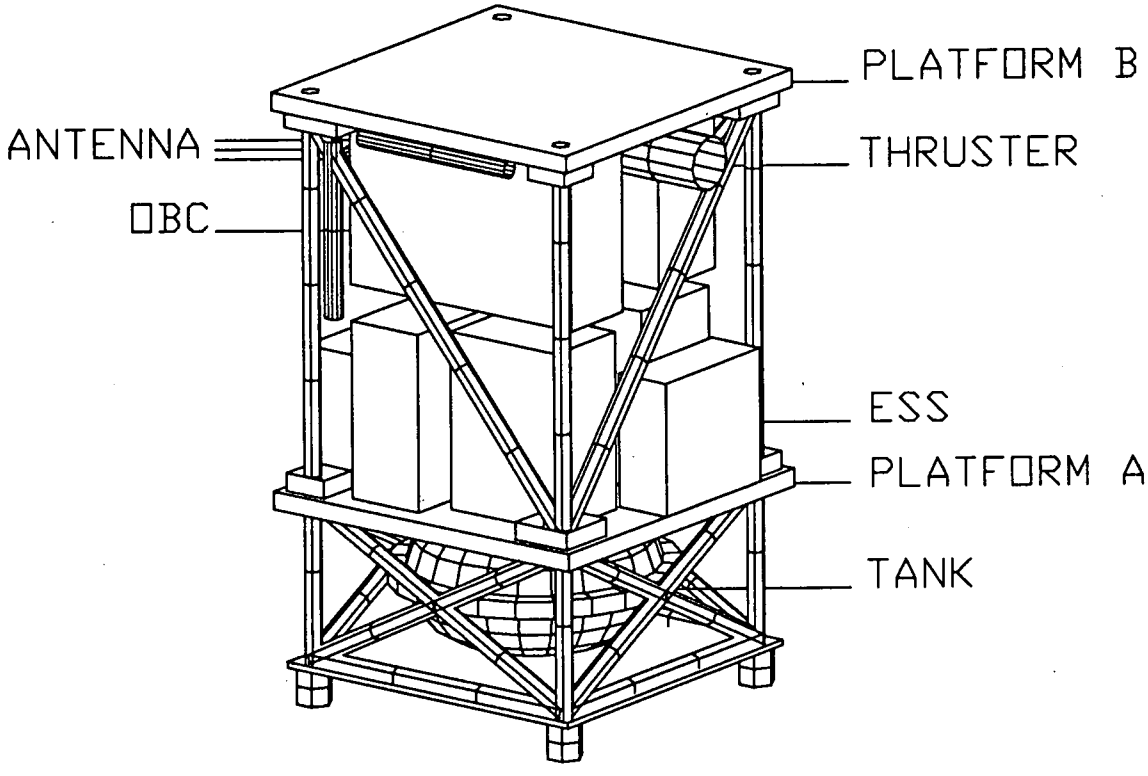

Figure 8.7: 3-D CONFIGURATION

8.7 CONCLUSIONS AND REMARKS

The final configuration does not fulfill all the requirements. As mentioned in this chapter there are three main reasons why we should change the final configuration. Firstly the usable volume has changed. Secondly our structure has a much too low resonance frequency and thirdly there is a need for 'BOOMS' because of the incorrect ratio between the principal moments of inertia. As indicated we experienced this too late in the project.

In the evolution of our configuration which still has not come to a halt, it is clear what the impact is of wrongly chosen boundary conditions. During the midterm review, we changed the stabilization method which resulted in a totally new configuration. Now the changed usable volume in combination with a too low resonance frequency and the need for 'BOOMS' would result, when the project had continued, in a new configuration. We would probably have chosen for the now possible standard tanks (one or four spherical tanks), solid panels instead of bars (higher eigenfrequency) and, if needed, two 'BOOMS' sticking out of the satellite (to increase the moment of inertia around the spin axis). A lot of these problems would have been avoided if we had developed several configurations next to each other. We leave these three last remarks for possible future investigation.

9. STRUCTURE

9.1 INTRODUCTION

This chapter gives an overview of the structural design of the ALFIS satellite. First the structural requirements are given. These are followed by some remarks concerning the launcher, the determination of the center of gravity, a structural analysis of the structure with the finite elements method (FEM) and a structural concept. At last several details mentioned in the structural concept are investigated.

9.2 STRUCTURAL REQUIREMENTS

The structure subsystem shall provide a stable mechanical support for the satellite-subsystems under all expected environments during the lifetime of the satellite. The structure will have, and maintain, the necessary stability through all phases of the mission and the launch.

9.3 LAUNCHER

As mentioned earlier, the A.S.A.P. configuration of the ARIANE 4 launcher was chosen for the launch of the satellite. Important structural boundary conditions are the acceleration during the launch phase and the fundamental frequency of the spacecraft.

From the A.S.A.P-manual we conclude that the maximal longitudinal acceleration is approximately 5g. For calculations and dynamic effects we should include a safety factor. The fundamental frequencies of the spacecraft in the thrust axis should be higher then 50 Hz.

9.4 CENTER OF GRAVITY & MOMENTS OF INERTIA

First we are going to describe the reference coordinate systems we will use. As indicated in figure 9.1 the origin of our reference coordinate system is located in the separation plane. The z-axis is pointing to the top of the satellite, the x-axis is parallel to a 'cable street' and the y-axis is perpendicular to these two. The principal axis are found by translating the reference coordinate system to the center of gravity and rotating it around its origin. The angle between the z-axis and I_1-axis is approximately 2 degrees and the rotation around the z-axis is approximately 15 degrees (see figure 9.2).

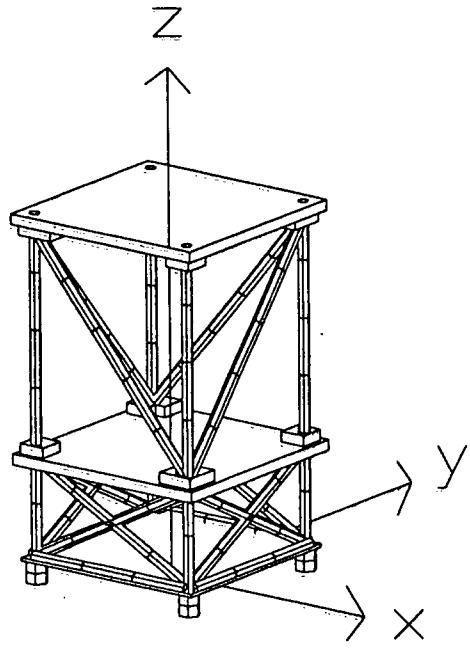

Figure 9.1: REFERENCE COORDINATE SYSTEM

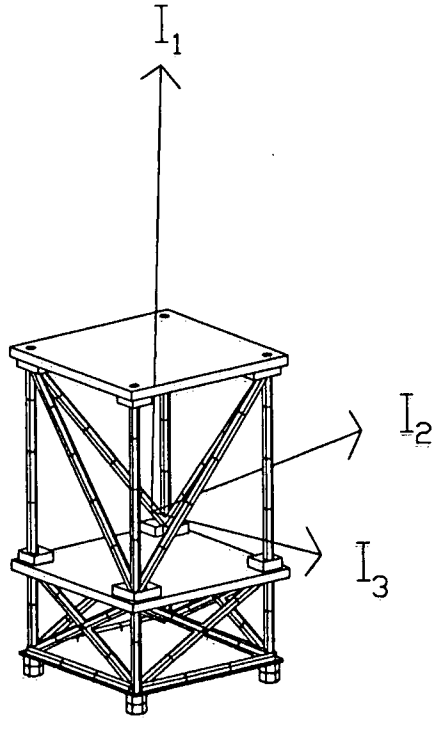

Figure 9.2: PRINCIPAL COORDINATE SYSTEM

For calculating the center of gravity the satellite is divided into separate elements. These elements are listed in Appendix I. Of each element we monitor the following things:

- a code: the first letter indicates whether an element is situated under (O) or above (B) platform A. The second letter is the first letter of the element's function. When an element is a unit (second letter = U) the third letter indicates whether an element is mounted on platform A (O) or platform B (B). The numbers following these letters make a serial number.

- the coordinates of the center of gravity in the reference coordinate system

- the dimensions

- the volume

- the mass

Now a spreadsheet program calculates the center of gravity of the satellite (for a full and a empty tank). It also calculates all the products of inertia. Out of these results the principal moments of inertia and the rotation angles of the principal axis are calculated. The results are listed in table 9.1.

	$X_{c.g.}$	$Y_{c.g.}$	$Z_{c.g.}$
TANK FULL	-2.5	4.8	348.4
TANK EMPTY	-2.8	5.4	376.1

Table 9.1a: CENTER OF GRAVITY (mm)

	I_1	I_2	I_3
TANK FULL	2.16	2.11	1.08
TANK EMPTY	1.88	1.83	1.04

Table 9.1b: PRINCIPAL MOMENTS OF INERTIA ($kg.m^2$)

The principal moment of inertia around our principal z-axis (the spin-axis) is approximately the half of the principal moments of inertia around the other principal axis. At first it was assumed that this was no problem. It is possible to spin around the axis with the smallest moment of inertia as long as there is not a too high energy dissipation.

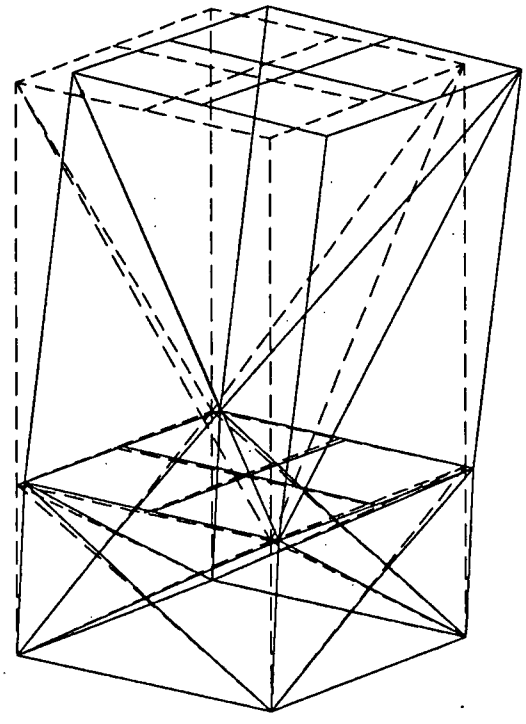

Figure 9.4: NASTRAN ANALYSIS

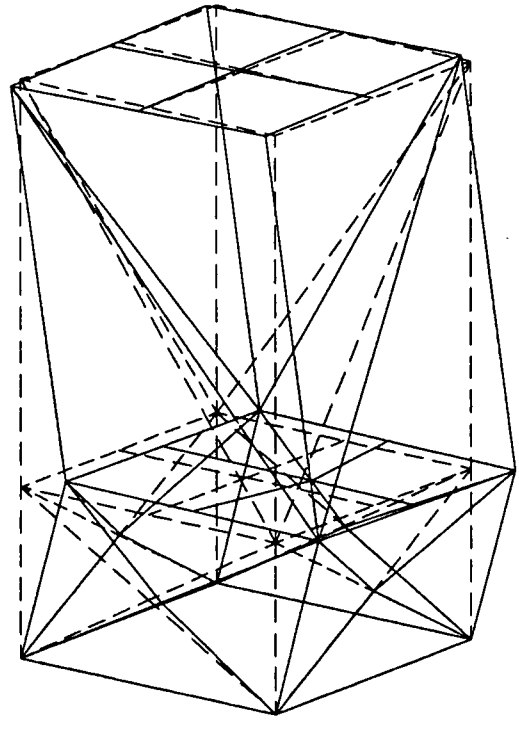

Figure 9.5: NASTRAN ANALYSIS

But there was relatively high energy dissipation, caused by the floating fuel in the tank. A more detailed description of this problem is mentioned in chapter 13 of the AC subgroup. This would implicate the necessary use of 'BOOMS' to increase the moment of inertia around the spin axis. This could change the entire configuration. There is no time left to investigate all the results of this late demand from the AC subgroup. Therefore we stick to the chosen structure and configuration.

9.5 FEM ANALYSIS

9.5.1 Nastran Analysis

In this chapter the structure is controlled upon its structural requirements by a Finite Elements Method, further called FEM. The structure is modelled by 26 nodes, 56 rods and 8 plates. Nastran, the FEM software, uses a mass-matrix; for accounting the resonance frequencies we used masspoints:

4 masspoints for the fueltank at the four connection points
1 masspoint for the upper-platform boxes
1 masspoint for the lower-platform boxes

We used two times 4 plates instead of the upper and lower platforms. The masspoints were placed in the center of the platforms as shown in figure 9.3.

The large points are the masspoints as well as nodes, the little points are nodes. The lines are rods.

We modelled differently for the strength calculations; we replaced the masspoints by forces (accelerations) with a safety-factor of approximately 4. The results of the strength-calculations were satisfying, but the outcomes of the resonance frequencies were quit unacceptable. The results of the first 4 resonance frequencies were between 2.85 and 7.44 Hz; so we thought we had made a mistake in modelling, but this was not the case. After some hand calculations of the resonance frequency of the rods, we found that the resonance frequency of the rods was 2.85 Hz. We also found a translation-direction from the plots of the modes. In the figures 9.4 and 9.5 two modes are shown.

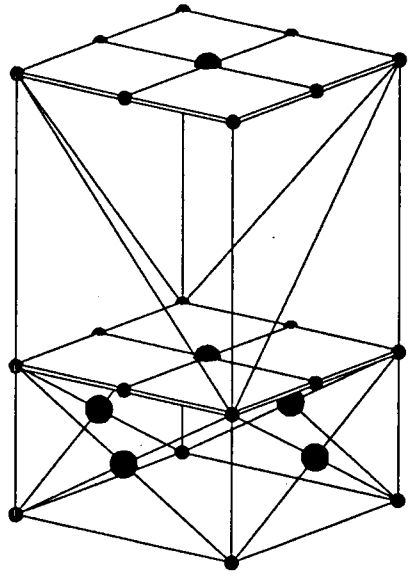

Figure 9.3: MATHEMATICAL MODEL NASTRAN ANALYSIS

We tried to solve this problem, but the time schedule kept us from redesigning our structure.

9.6 STRUCTURAL CONCEPT

In this paragraph the way in which the satellite could be assembled is described. The codes of the elements used are mentioned in Appendix I.

- First the frame around the tank is assembled. Therefore we connect two diagonal bars to each other (ex. OV11 to OV15). At these connections the tank will later be mounted. The 4 'cross-sections' will then be connected to the 4 vertical bars (OV07 till OV10) and the separation plate (OS05) (figure 9.6). We mount two thrusters (OU05 & OU06) and a thermal blanket (OD05) to the plate.

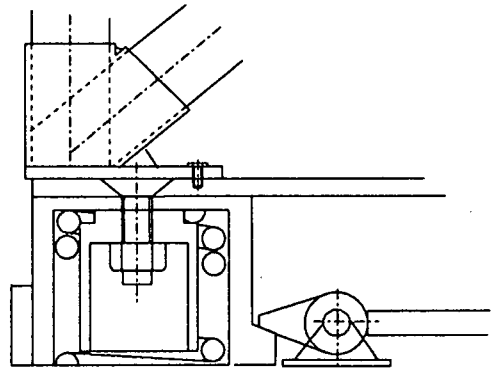

Figure 9.6: FRAME-SEPARATION CONNECTION

- The tank (OT01) is mounted on the four connections after it is covered with blankets (OD06). Some fuel lines are connected.

- The two thrusters (OU01 & OU02) are mounted under platform A. The units (BUO-01 t/m BUO-06) are mounted on platform A (figure 9.7). As much as possible cables are connected. This will have to be done in a special way, because the available space is very limited. This has not yet been investigated in detail.

- Platform A (OP01) is mounted to the frame. The fuel-lines and cables under the platform are elongated and are led through the hole in the platform.

- The vertical (BS01 t/m BS04) and diagonal (BS05 till BS08) bars are mounted onto platform A. The fuel-lines are elongated.

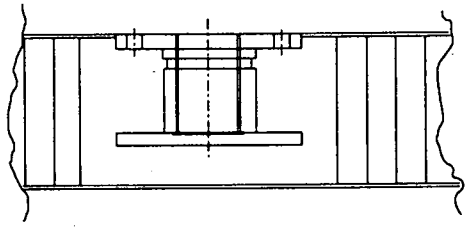

Figure 9.7: INSERT

- The units (BUB-01 till BUB-07) are mounted to platform B. As much as possible cables and fuel-lines are connected to the units and the platform.

- Platform B (BP01) is connected to the frame. During assembly there is a need for connecting the cables between the two platforms. One should make a distinction between the power and the computer cables. Therefore we lead the two cable sorts to two different diagonal bars on the supporting structure.

- The remaining thrusters are mounted onto the bars and platform B. Fuel lines are elongated and connected to the thrusters.

- The blankets and the patches are connected to the solar panels. The solar panels are connected to the satellite. The cables from the solar cells and the patches are led into the satellites by connectors. This has not been investigated in detail.The solar panels have to be mounted in such a way that they do not lead through forces. We mount the solar cells with 'clitterband' to the satellite (figure 9.7).

- The satellite is placed on the launchplatform and is connected to the separation mechanism.

9.7 SEPARATION MECHANISM

Release devices hold the satellite in a certain position on the adapter of the launcher during the launch phase and release it in orbit.

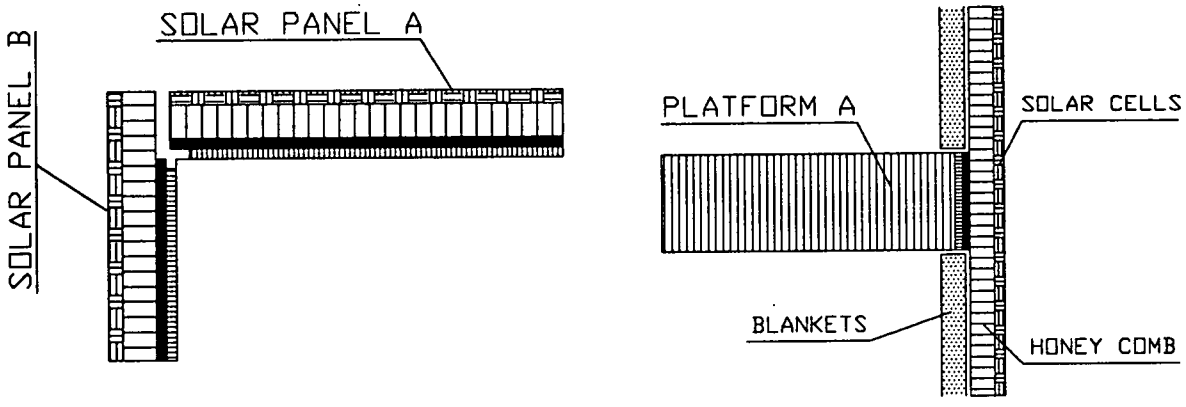

Figure 9.7: SOLAR PANEL MOUNTENING, 2 DETAILS

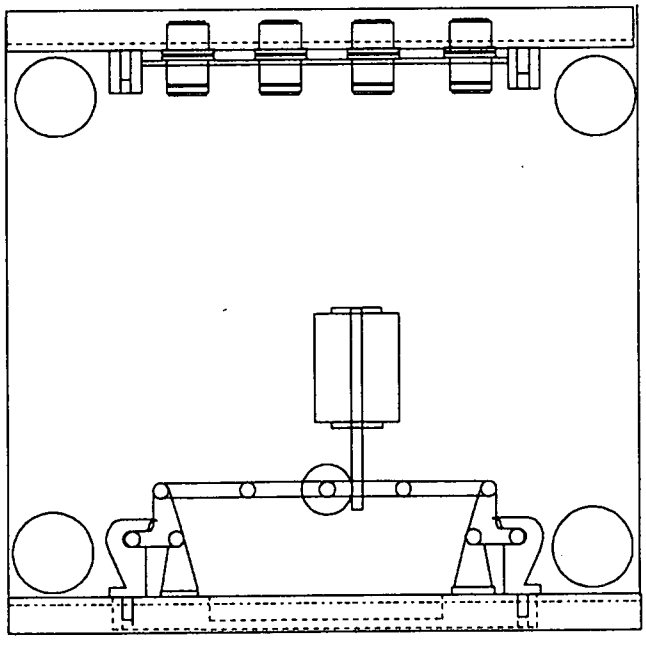

Figure 9.8: SEPARATION MECHANISM TOP VIEW

The major design requirements are:

- volume

The volume constraints of separation mechanism comes from the fact that the separation mechanism should be placed between the satellite and adapter with limited height. Consequently, the height is a more stringent requirement than the diameter.

- operational sequence

Before the actual mechanical separation takes place, it is required that all electrical/data lines are disconnected. This may be done by a separation device.

- torque and force margins

The static torque and force available from the drive unit will be at least 2 times worst case values under the specified environmental conditions at all stages at jettisoning phase.

- generation of debris

The separation mechanism will not generate free-floating debris.

- explosive devices

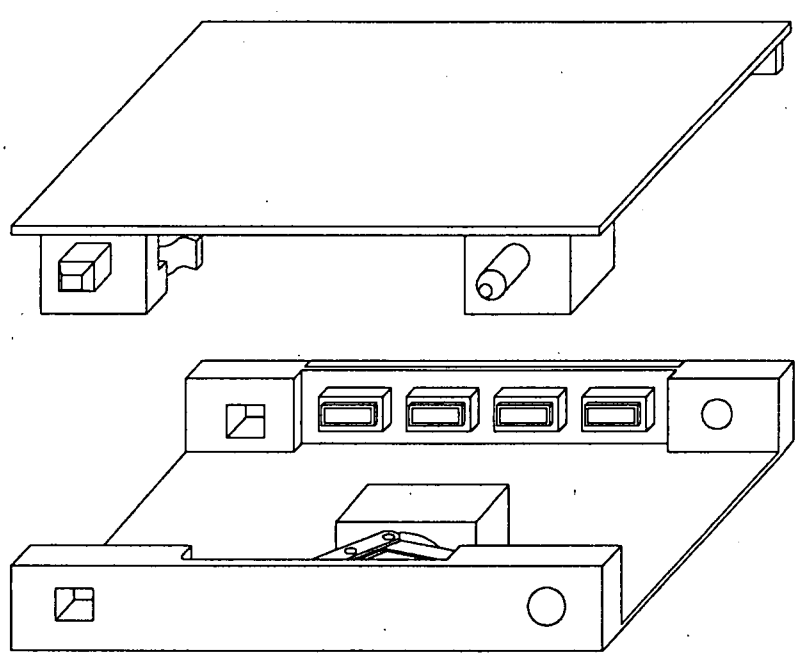

Figure 9.9: 3-D SEPARATION MECHANISM

The other requirements, such as backlash, strength, energy transfer, thermal environment, mass, accessibility and performance should also be considered.

The separation mechanism as described at the picture offers a good solution to satisfy the requirements as mentioned before. The separation mechanism called Pin-Linkage-mechanism, consists of an active half and a passive half. The active half can be regarded as a box and contains a linkage mechanism. The passive half can be regarded as a cover with four pins mounted on it.

The drive unit, consisting of a motor and a gearbox, drives the wormgear on which the bell crank is attached. The crank rotates, pulling the pins out of their holes and, in the same movement, separating the connectors. When the connectors are completely disconnected, a part of each pin is still in its hole, ensuring mechanical contact.

When electrical separation is confirmed, the bell crank can be rotated further, realizing mechanical separation.
The total rotation of the bell crank is about 75 degrees, causing a total travel of the hook of 25 mm.

9.8 CONCLUSIONS

Structural details were not completely studied because the work on configuration was inmensely time consuming. For example the connectors, most optimal materials, connections between platform and frame and optimal material dimensions need further study. However this chapter gives a good insight in the structural problems that occur in our satellite. Mainly the resonance frequency of the structure is critical. However as mentioned in chapter 8 the configuration is still in evolution and the structure subsystem will help the final configuration choice.

10. PAYLOAD

10.1 INTRODUCTION

The task set for the payload design team is to develop a system capable of receiving radio astronomical signals from remote regions of the universe in a small number of spectral bands in the 1 to 15 MHz range. Since the ionosphere is opaque due to refraction and absorption at these frequencies, the signals need to be converted to a different frequency range and then transmitted to a receiver on Earth. On the ground the radio signals will be transformed into radio maps of the celestial globe.

For successful imaging of the sky accurate knowledge of the radio signals is needed. Important parameters are the phase, amplitude, polarization, direction and time of arrival of the incoming radio waves. The chosen combination of two satellites with both three orthogonal dipole antenna's is capable of providing the desired information. Special attention has to be paid to the determination of the relative position and the attitude with respect to the celestial globe of the two satellites, since these data are of great importance for the processing of the antenna measurements. On the ground the data of both satellites will be processed by means of correlation techniques, thus performing long base interferometry with a space array.

10.2 NOISE

The received astronomical signals will be strongly polluted with noise. Strong noise sources, both natural and artificial, are to be found in the Earth's biosphere. In orbit isolation from these sources is best at the sunlit side of the Earth, because of the greater opacity at the observed frequencies of the ionosphere when compressed by the solar wind. This puts a restriction on the chosen orbit.

The astronomical receiver will be strongly influenced by the Van Allen Belts, therefore measurements should take place outside these belts.

Other sources of noise are type III solar bursts. The rare occurrence of this phenomenon and the fact that it is well monitored, makes filtering of this noise during processing of the data on the ground possible. Therefore no restrictions arise from this problem.

The incoming radio waves will be deflected by the Earth's magnetic field. This deflection is negligible when the satellites are at a height of at least three Earth radii.

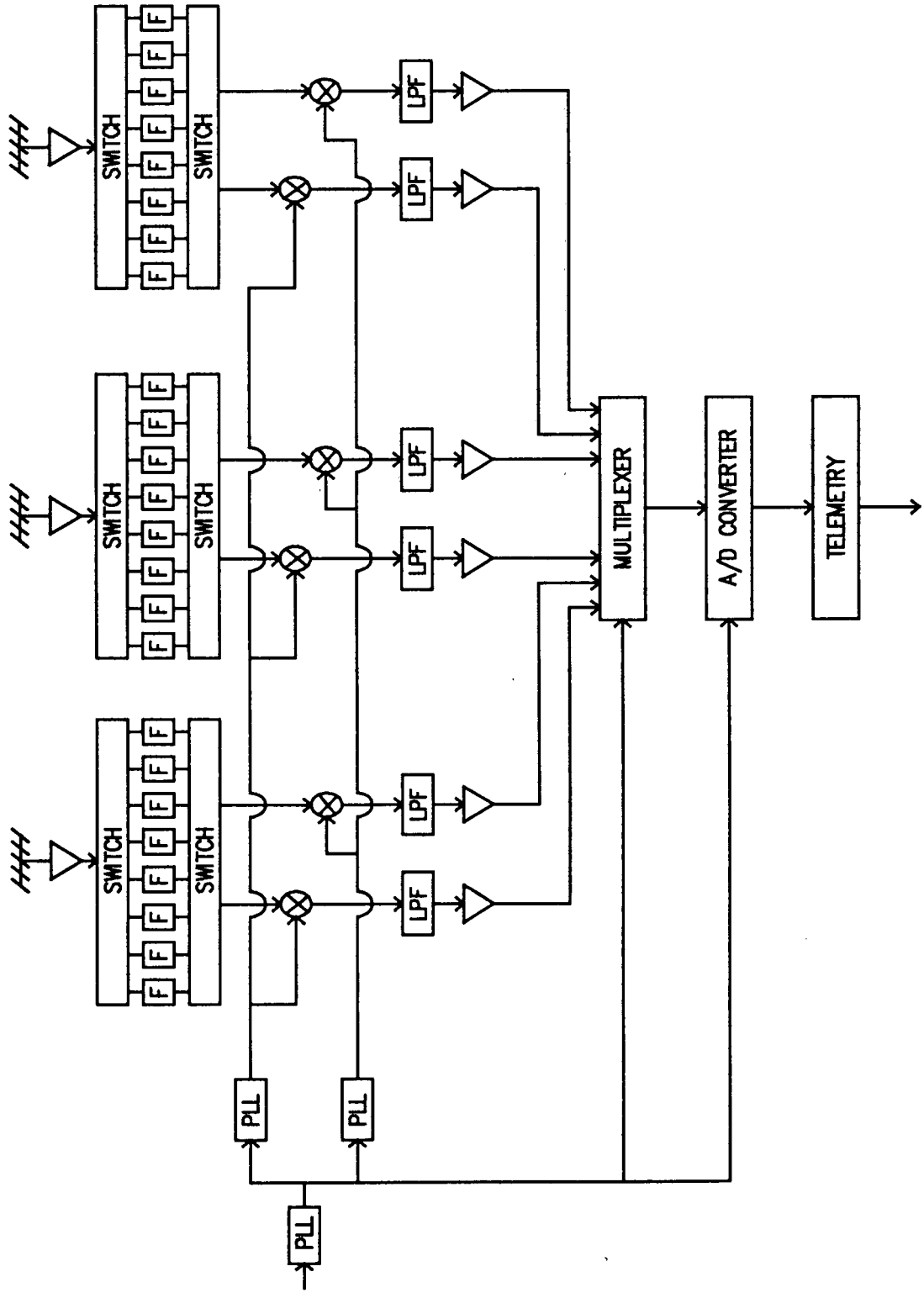

Figure 10.1: ASTRONOMICAL RECEIVER

Interference from satellite subsystems might also degrade the signals. This can be largely avoided by careful design.

10.3 RECEPTION AND TRANSMISSION OF ASTRONOMICAL SIGNALS

10.3.1 Astronomical Receiver

A communication link must be established between a groundstation and the satellites whenever astronomical observations are acquired. A phase stable uplink is required to relay a ground frequency standard, preferably from a hydrogen maser, to both spacecraft, where it will serve as the reference frequency for observation translation to different frequency bands. A downlink is required both to carry the observation data, which will be in digitized format, to the ground and to reconstruct the time/phase history of the spacecraft's phase locked oscillators.

The phase stability of the ground based H-maser must not be degraded by the signal transfer to the satellites. Ionospheric phase difference introduced by the offset between uplink and downlink frequencies will therefore require a second coherent downlink to allow an estimate and correction of these errors.

All the local oscillators used in the radio astronomy system as well as in the downlink transmitter will be derived from Phase-Locked-Loop (PLL) receivers of the communication system transponder, so that the frequency translation on the spacecraft will be phase-coherent with the uplink.

A PLL consists of a phase detector, a low pass filter (LPF) and a voltage controlled oscillator (VCO) (see figure 10.2). The phase detector generates an average output voltage that is proportional to the phase difference between a reference frequency and the frequency generated by the VCO. This output voltage is used to change the VCO frequency in the direction of the reference frequency until they are equal. In order to stabilize the PLL a LPF is used to eliminate high frequency noise distorting the reference frequency. A multiplier is added to the PLL, making the reference frequency an integer multiple of the VCO frequency.

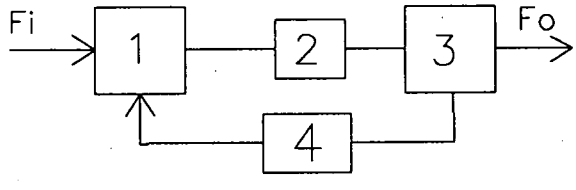

1. Phase Detector
2. Low Pass Filter
3. Voltage Controlled Oscillator
4. Multiplier

Figure 10.2: PHASE LOCKED LOOP

Each of the three antennas is connected to a receiver. There are three PLL's in the receiver (see figure 10.1). The first PLL divides the 2100 MHz uplink frequency by 50, so the output frequency becomes 42 MHz. The other two PLL's are controlled by the OBC, making it possible to choose the output frequency in coherence with the filterbanks. These PLL's can divide the frequency by either a factor 40, 20, 10 or 5 so that the output frequency becomes 1.05, 2.1, 4.2 or 8.4 MHz respectively. The choice depends on the desired frequency. This output frequency is used to demodulate the astronomical signals to baseband.

The radio astronomy receivers must be very stable in their gain and phase characteristics. They will have to be temperature controlled at 20°C with an accuracy of 1 degree. The receivers each consist of low noise amplifiers and a filterbank. The filterbank consists of 8 filters with each a passband of 25 kHz. Two of those filters filter at a frequency of 1.05 MHZ, two at 2.1 MHz, etc. covering two by two adjoining pieces of the electromagnetic spectrum, with 25 kHz bandwidth each. This enables the astronomers to measure at two different frequencies with a 25 kHz passband or to measure at one frequency with two 25 kHz passbands that can be joined to one passband of 50 kHz during processing on the ground. The frequency at which measurements are done can be chosen on the

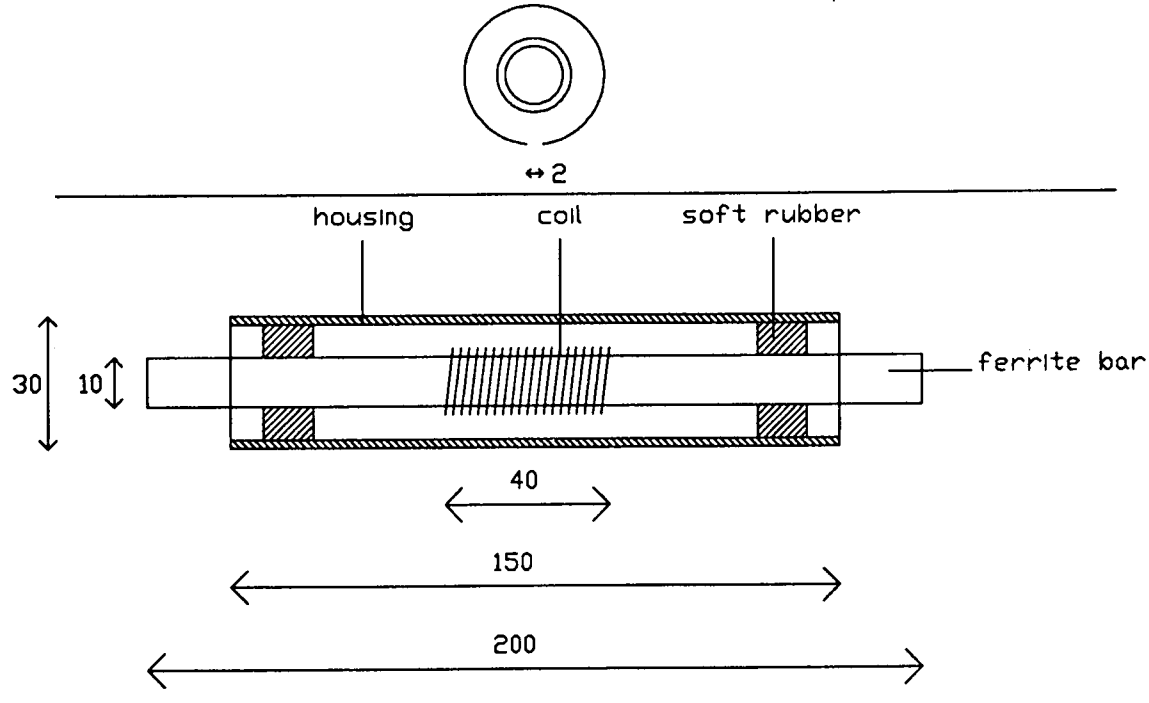

Figure 10.3: FERRITE ANTENNA

ground and via telecommand the OBC can be told to adjust the filterbanks and the PLL's accordingly.

In order to retain as much phase information as possible the filterbanks should consist of higher order Bessel filters. A Bessel filter is optimized to have a linear phase-transfer up to the cut-off frequency.

The six lowpass filters (LPF) which are situated right after the demodulating mixers, should be of the Chebychev type since the astronomical signals are A/D-converted shortly afterwards and aliasing has to be avoided. A Chebychev filter has a very steep gain-transfer above the cut-off frequency.

The order of the filter must not be too high or else phase-transfer will become a problem.

Six different inputs (two from each antenna) will be time-multiplexed before entering the A/D-converter. A six bit conversion is needed because of the poor signal-to-noise ratio of the astronomical signals. This gives a dataflow of approximately 2 Mbits/sec which has to be transmitted by the telemetry system. This is explained in more detail in the telemetry section of this report.

The receiving system has no redundancy, because it is of no great consequence if one of the channels is lost. Also, because of the large amount of data, no data storage can be implemented in this small system.

10.3.2 Antenna

The antennae which are used are ferrite antennae (see figure 10.3). Although they have not yet been used in satellites and have not yet been made space-qualified, we nevertheless assume that they can be used in space. The advantages of using these antennae are the following:

- low mass
- small size
- simple construction

But there are also some disadvantages:

- the antennae have a small effective surface, causing a low signal intensity
- the satellite's construction can cause electromagnetic interference
- the temperature of the antennae must be very stable (20°C +/- 1°C)
- the antennae have bad mechanical properties and demand a special housing to survive launch conditions

If special attention is paid to the construction and material choice of both the entire satellite and the antenna-housing and to the characteristics of the receiver, these antennae can be used.

10.4 POSITION DETERMINATION

The orbits of the two satellites will have to be chosen in such a way that, during the satellites' lifetime of two and a half years, a large number of different baselines between the two satellites are acquired. These baselines can be thought of as filling a globe. A uniform distribution of baselines in the globe allows for accurate mapping of the sky in all directions.

In order to correlate the data of both satellites successfully, the position in orbit must be known with an error far less than the baseline length and also less than the observed wavelength. Since the baselines and the observed wavelengths vary respectively from 1 to 300 kilometers and from 30 to 300 meters a position accuracy of at least 1 meter is required. The satellite to satellite relative position is far more important than the satellite to ground relative position, since only phase differences between the two satellites need to be measured and not between satellites and Earth.

10.4.1 Explanation of the Designed Position Determination System

Two-way doppler data will be available whenever the satellites are linked to a ground station. If these data are used to calculate the respective orbits a position uncertainty of at least 20 meters will be the result, since there is only one tracking station available. Therefore a more complicated system is required.

The telemetry and telecommand system uses two up/down links per satellite. The systems differ a bit for the two satellites (see figure 10.4). The phasestable reference frequency is uplinked to both satellites, carrying telecommand and via a transponder returned to the groundstation carrying the digitized astronomical data. This link is referred to as HBR (high bitrate).

The second link is only directly uplinked to satellite 1 and via this satellite linked to satellite 2. Both have a direct downlink to the groundstation which carries housekeeping data. Furthermore the downlink from satellite 2 is also received by satellite 1, thus establishing a direct connection

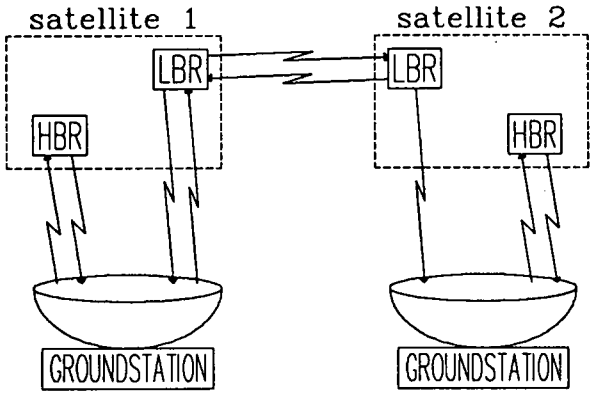

Figure 10.4: COMMUNICATION LINKS

between the two satellites. These links are referred to as LBR (low bitrate). The downlink carrierfrequencies of the LBR are derived from the reference frequency of the HBR, making correction of ionospheric phase disturbances possible. The satellite-to-satellite link is necessary to achieve the required position accuracy.

In order to perform range-measurements information has to be added to the communication links. We assumed it would be possible to make use of ranging tones. Counting the number of wavelengths gives the range and when different frequencies are used the value will be accurate. It will be difficult to use this method in combination with the LBR link, because of the multiple frequency shifting between the two satellites. A possible other solution might be to make use of Pseudo Random Noise (PRN) code. The PRN signal is hidden in the noise of the link and can only be recovered on the ground when the code is known by means of correlation techniques. This enables the use of different PRN codes for different range measurements. For instance one for the satellite-to-satellite and another for the satellite-to-ground measurement. This solution has not yet been implemented in the design of the LBR system.

For the LBR-signals an extra receiver-transponder system has been developed (see figure 10.5). After receiving the LBR signal in satellite 1 a PLL demodulates the ranging tones from the carrier. The ranging tones are then together with the housekeeping data of satellite 1 modulated with a carrier frequency that is derived from the reference frequency. This signal is transmitted to the groundstation, where the range is measured and the housekeeping data collected, but it is also received by satellite 2. There a bandpass filter removes the housekeeping data and a PLL only recovers the ranging tones. Together with the satellite 2 housekeeping data the ranging tones are modulated with a carrier and transmitted to the groundstation. This signal is also received by satellite 1, where in a similar way the returning ranging tones are recovered and modulated on the down link.

It will be necessary to make good use of the frequency spectrum for dividing the several flows of data. This enables measurements of all the required ranges. Furthermore close monitoring of frequency shifting gives range-rate doppler information that can also be used in the orbit calculations.

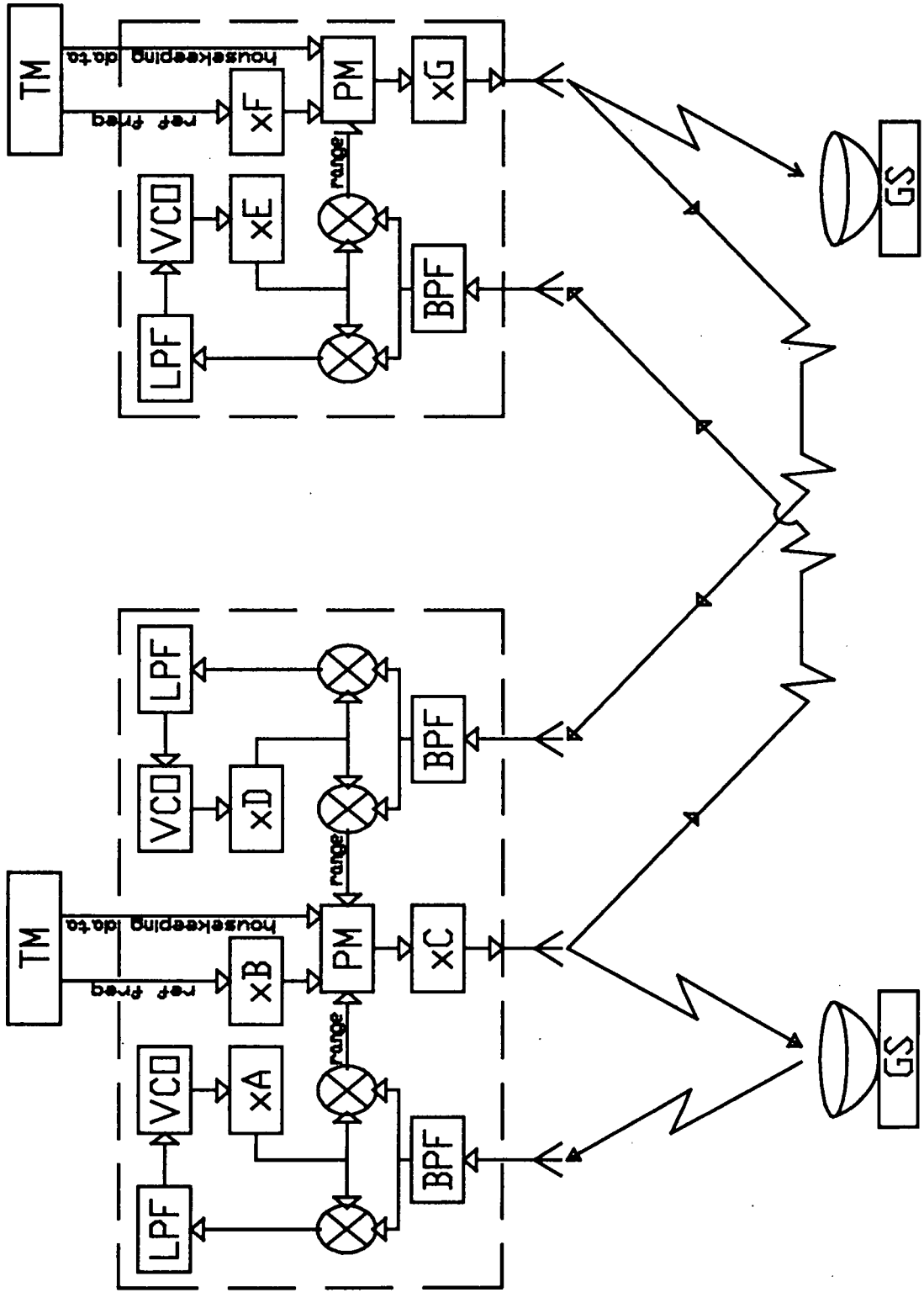

Figure 10.5: POSITION DETERMINATION SYSTEM

10.4.2 Simulation of the Position Determination

To verify whether it is possible to achieve the required accuracy with the above-mentioned system, a computer simulation has been performed by drs. H. Leenman of the Faculty of Aerospace Engineering.

The Oran (orbital analysis) program simulates the tracking of a satellite and uses the simulated data to calculate the achievable accuracy with the chosen tracking type, orbital parameters, gravitation field model, etc.

For the simulation the orbital parameters as proposed in this report were used. The groundstation was chosen to be in Dwingeloo, the Netherlands, and able to perform one tracking measurement every 5 minutes with a 10 cm rms accuracy, whenever tracking was possible.

The simulation shows that when the satellites are in the proposed orbit, there is a tracking period of 600 minutes every two orbital periods. This indicates that every second orbit whenever the satellites are above the van Allen belts, they are also in contact with the groundstation at Dwingeloo.

	position rms accuracy without satellite-to-satellite range measurement		
	radial	**cross track**	**along track**
sat to ground	3 m	18 m	11 m
sat to sat	3 m	25 m	14 m

Table 10.1a: POSITION ACCURACY SIMULATION RESULTS

	position rms accuracy with satellite-to-satellite range measurement		
	radial	**cross track**	**along track**
sat to ground	2 m	11 m	7 m
sat to sat	2 cm	2 cm	10 cm
corr. ionosph.	1 cm	1 cm	0 cm
5 cm bias sat to sat	1 cm	5 cm	15 cm

Table 10.1b: POSITION ACCURACY SIMULATION RESULTS

If only the satellite-to-ground range is measured for both satellites, a relative position accuracy in the order of 25 meters is achieved (see table 10.1a).

satellite 1 & 2					
subject	**number**	**mass (kg)**		**power (W)**	
		item	**total**	**item**	**total**
antenna	3	0.17	0.51	0	0
switch	6	0.05	0.3	0	0
filter	27	0.04	1.08	0	0
mixer	6	0.75	0.45	0.25	1.5
AMP	9	0.12	1.08	0.25	2.25
MPX	1	0.15	0.15	0.3	0.3
ADC	1	0.25	0.25	0.5	0.5
PLL	3	0.2	0.6	0.4	1.2
total			**4.43**		**5.75**

AMP = amplifier MPX = multiplexer
ADC = A/D-converter PLL = phase locked loop

Table 10.2: MASS- AND POWERBUDGET RECEIVER

	satellite 1			satellite 2		
subject	**number**	**mass (kg)**	**power (W)**	**number**	**mass (kg)**	**power (W)**
MXR	2	0.15	0.6	1	0.075	0.3
PLL	2	0.4	0.8	1	0.2	0.4
BPF	2	0.1	0	1	0.05	0
PM	1	0.1	0.4	1	0.1	0.4
MPL	2	0.3	0.2	2	0.3	0.2
total		**1.05**	**2.0**		**0.725**	**1.3**

MXR = mixer PLL = phase locked loop
BPF = bandpass filter PM = phase modulator
MPL = multiplier

Table 10.3: MASS- AND POWERBUDGET POSITION DETERMINATION

If also the satellite-to-satellite range is measured the results of the simulation improve dramatically. The relative position of the two satellites can then be known with an accuracy of approximately 10 cm. The position with respect to the groundstation is known to about 10 m (see table 10.1b).

Also if only one of the two communication links to the satellites is used for range determination or if there is a bias in the satellite-to-satellite measurement the disturbances on accuracy are very small.

These results show that the position accuracy of 1 meter seems to be feasible with the proposed system.

10.5 ATTITUDE DETERMINATION

The 3 ferrite antennas are all omnidirectional, so pointing them is not necessary. Nevertheless knowledge of the satellites' attitude with respect to the celestial globe is required, since the attitude determines the exact phase pattern of a radiowave on the antennas. An accuracy of 1 degree is mandatory. The attitude information will be derived from the attitude control system. On earth a sufficient amount of data is needed to allow reconstruction of the attitude to the desired accuracy at every instant during the astronomy measurements.

10.6 PAYLOAD BUDGET

In the mass- and powerbudget of the receiver (see table 10.2) is shown that the total mass of the receiver is estimated to be approximately 4.4 kilograms and the total power that it uses is about 5.75 Watt. These values are not rigid, but should be seen as guidelines, since the receiving system might become more complicated than considered. Especially the ferrite antennas may impose extra demands on receiver quality.

	satellite 1		**satellite 2**	
subsystem	**mass (kg)**	**power (W)**	**mass (kg)**	**power (W)**
receiver	4.43	5.75	4.43	5.75
position	1.05	2.0	0.725	1.3
10 % cabling	0.64		0.52	
total	**6.1**	**7.8**	**5.7**	**7.1**

Table 10.4: TOTAL MASS- AND POWERBUDGET PAYLOAD

For the LBR-system we also made a mass- and powerbudget estimation which is shown in table 10.3. As shown in the table the mass- and powerbudget of the first and second satellite differ. These values should also be seen as guidelines.

The budget of the astronomical receiver and the budget of the position determination system combined gives the total payload budget, shown in table 10.4. For satellite 1 the total mass is about 6.1 kg and the total power is approximately 7.8 W. Satellite 2 has slightly lower values. Together with the Configuration group a total volume of 5.4 l has been estimated, divided over a small number of boxes.

10.7 CONCLUSIONS

We have tried to carefully define what is required for successfully mapping the sky with two receiving systems flying kilometers apart in Earths orbit. Since we are no electronics engineers, further investigation into the receiving system is required and because it is of prime importance for the success of a possible mission it should be looked at in the first stages of development.

Position determination of both satellites with the required accuracy seems feasible, but especially the method of modulating and demodulating range data on the carrier frequencies needs an in depth analysis. Also orbit disturbances of the two satellites could have a strong influence on position accuracy and should therefore be looked at further.

11. POWER SUPPLY

11.1 INTRODUCTION

In order to operate, a satellite must have a system to generate, store, convert, control and distribute power. For the ALFIS satellites four solar panels are used to generate the required power, batteries are used to store the energy needed in eclipse and to assist powerpeaks and the power management and distribution unit (PMAD) is used to regulate, convert and distribute the power.

11.2 REQUIREMENTS

Regarding the mission demands the following requirements have been derived for the ALFIS Electrical Power System (AEPS):

- low mass
- low volume
- high reliability
- lifetime min. 2.5 years
- low costs

11.3 POWERBUDGET AND POWERPROFILE

The powerbudget is constructed from subsystem power-needs. We differentiate following phases:

- transfer orbit: This phase takes place just after separation when the satellite has to transfer to the final orbit
- eclipse: This phase takes place when the satellite enters the earth's shadow
- peak: The highest power demands possible
- operation: Phase of nominal operation

The powerprofile (EOL) for a possible orbit is shown in figure 11.1. A 10 % margin is taken because of uncertainities in this phase of design.

Although only one of the two orbits will be seen by the groundstation, the orbit not seen has to have the same power-profile for thermal reasons.

The powerprofile is based on a worst case situation where the end of the eclipse and the VAB border conjugate. Thus leaving no time to charge the battery optimally.

	transfer orbit (Watt)	eclipse (Watt)	peak (Watt)	operation (Watt)
Payload	-	-	7.8	7.8
TTC	-	-	9.0	6.5
Computer	5.5	5.5	5.5	5.5
Thermal	1.5	1.5	1.5	1.5
Propulsion	30.0	12.0	12.0	1.0
Attitude control	2.0	2.0	2.0	2.0
Structure	10 *	-	-	-
Margin 10%	3.9	2.1	3.8	2.4
TOTAL	42.9	23.1	41.6	26.7

** only needed a few milliseconds for separation device*

Table 11.1: POWERBUDGET

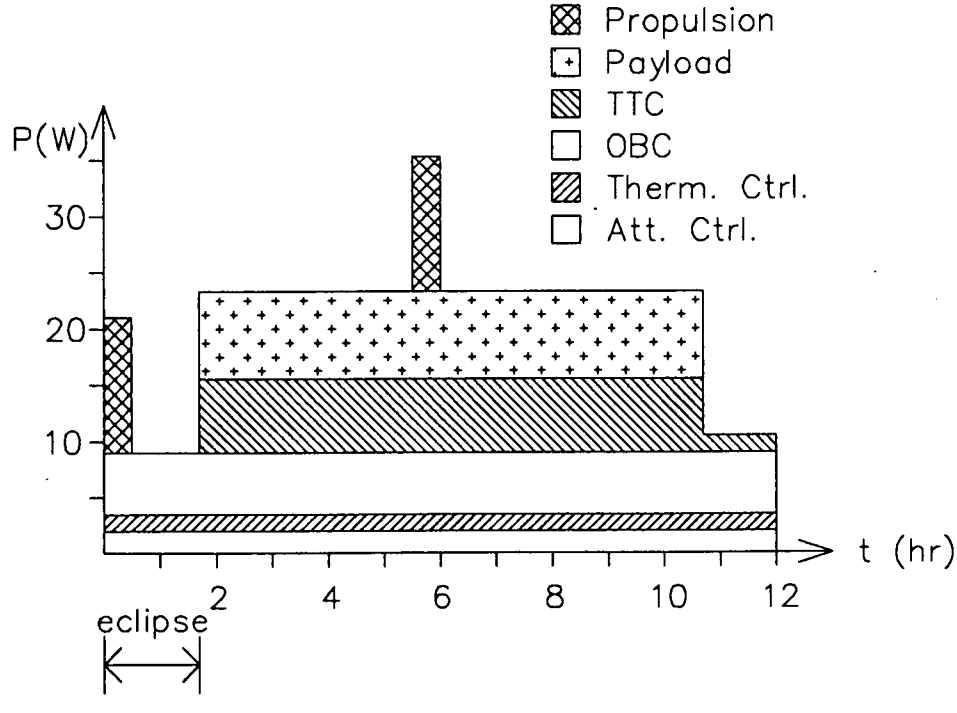

Figure 11.1: POWER PROFILE

The 12 W need for propulsion in the eclipse is a heavy load on the total battery energy. It was necessary to take this need into account because there was a possibility that orbital corrections have to be carried out near a perigee which is in the eclipse.

11.4 ENERGY SOURCES

While the mission duration is about 2.5 years and the powerneed does not exceed 100 W, figure 11.2 shows there are two possible efficient energy sources, namely the solar or the radio-isotopic solution.

High costs and the large mass/volume of the radio-isotopic solution together with the already many times proven solar solution of satellites in earth orbits makes the choice for the last option clear.

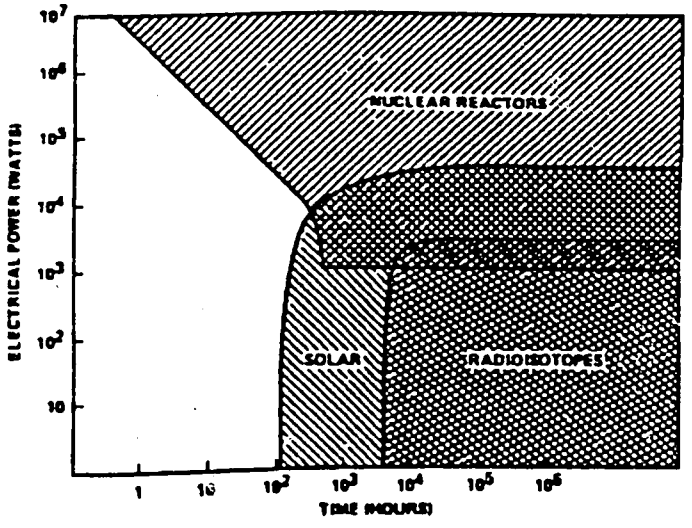

Figure 11.2: MISSION DURATION AND POWER TECHNOLOGIES

11.5 POWER SUBSYSTEMS

11.5.1 Solar Cells and Panels

A trade off has been made between Silicium (Si) and Gallium Arsenide (GaAs) solar cells. Due to high power demands for this small satellite design and the severe radiation in the VAB is chosen for a GaAs-type solar cell, although it is more expensive then a Si-type cell.

The chosen type solar cell, GaAs/Ge produced by Spectrolab, is 7 mils thick with minimum average efficiency of 18.3 %. In figure 11.3 a cross section of the GaAs/Ge solar cell can be seen. The four solar panels consists of two times two equals and all panels have an equal area to cover with cells.

11.5.2 Battery

To store the energy needed in eclipse and for power peak demands a Nickel-Cadmium-battery (NiCd) is chosen.

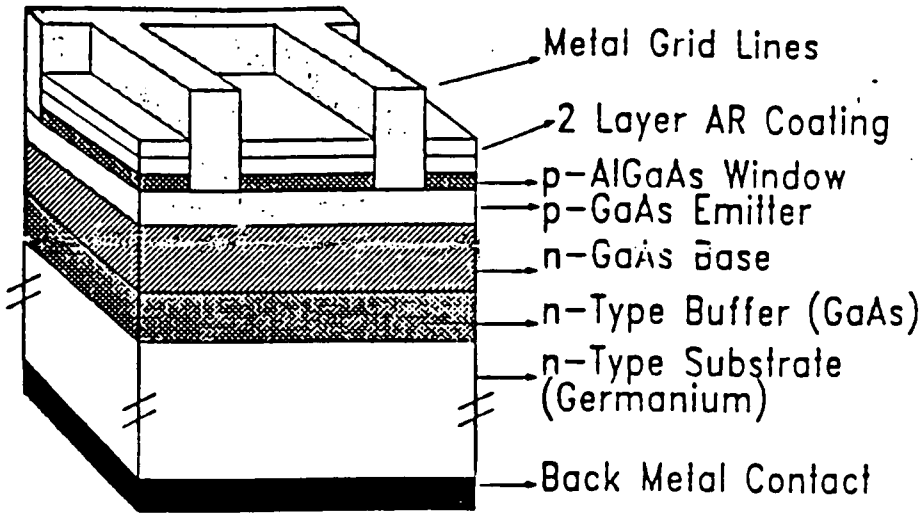

Figure 11.3: GaAs/Ge SOLAR CELL

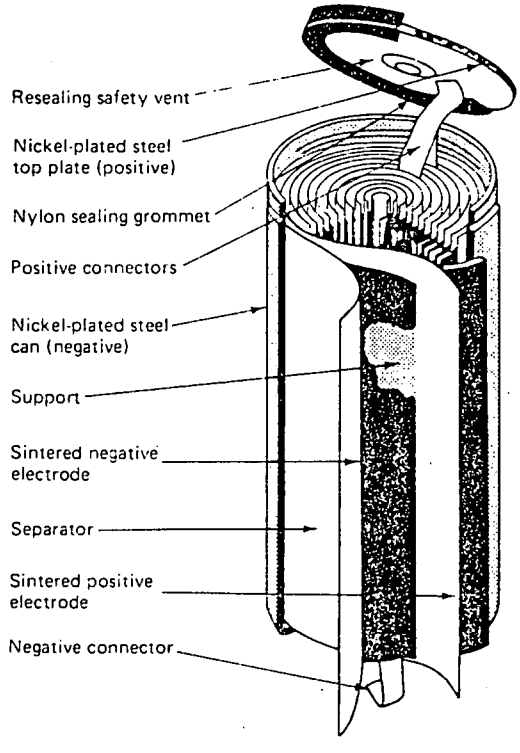

Figure 11.4: SEALED CYLINDRICAL NiCd BATTERYCELL CONSTRUCTION

Main advantages: NiCd-batteries have proven reliable and also have a higher density (Wh/l) than Nickel-Hydrogen-batteries (NiH_2).

Main disadvantages: The memory-effect. This effect can be described as an apparent reduction in cell capacity to a predetermined cut-off voltage resulting from highly repetitive use patterns. This effect is more likely to occur when the amount of overcharge in each cycle is small and the rate of discharge is high. The memory-effect can normally be erased by a full discharge followed by a full charge (reconditioning); thus it is a temporary effect.

Other technologies have not enough matured or are too big for our purposes (Lead-Acid, Alkaline-MnO_2, Nickel-Zinc).

For redundancy reasons the battery must have a large number of cells. This resulted in a battery consisting of 10 VRS-F cells from SAFT. An example of the NiCd battery cell is shown in figure 11.4.

The chemical reaction inside the battery is:

$$\text{Charge: } 2\ Ni(OH)_2 + 2\ OH^- \rightarrow 2\ NiO(OH) + 2\ H_2O + 2\ e^- \quad \text{(kath)}$$
$$Cd(OH)_2 + 2\ e^- \rightarrow Cd + 2\ OH^- \quad \text{(anode)}$$

11.5.3 Regulated Powerbus

For power distribution a regulated powerbus is needed because no power can be derived from the solar panels for charging the battery only.

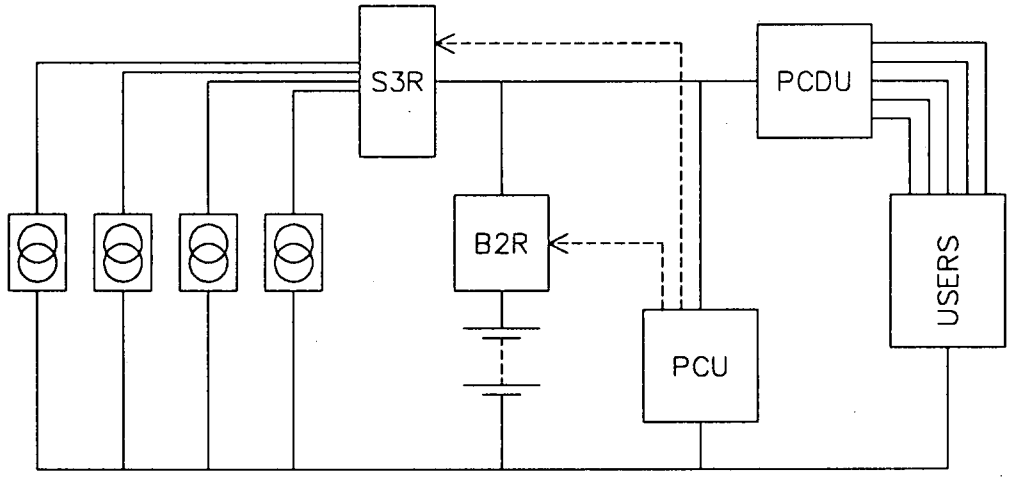

Figure 11.5: ALFIS ELECTRICAL BLOCK DIAGRAM

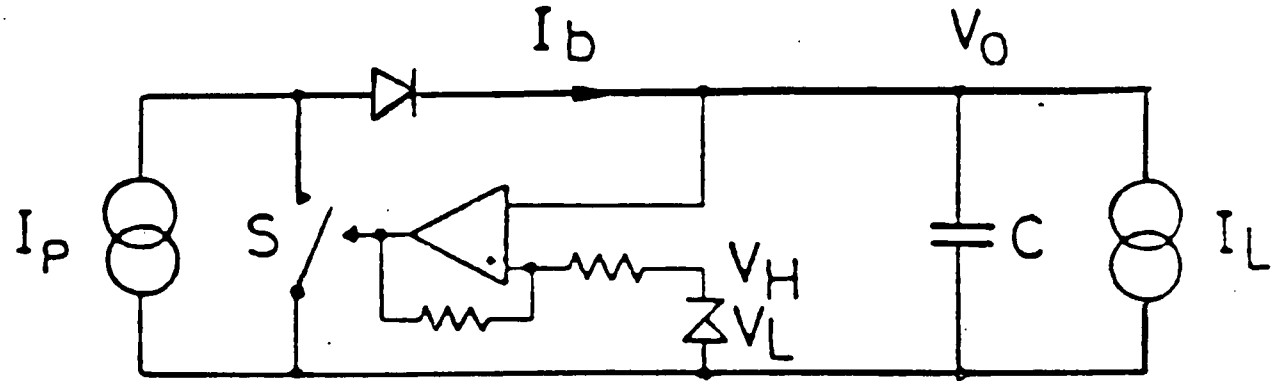

Figure 11.6: S3R LIMIT CYCLE CONCEPT

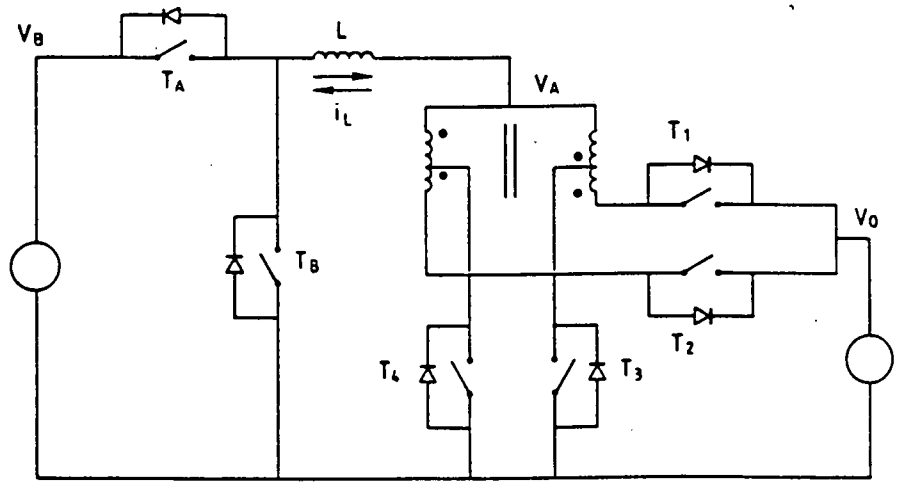

Figure 11.7: BI-DIRECTIONAL BATTERY REGULATOR PRINCIPLE

The ALFIS Electrical Power System is shown in figure 11.5 and consists of a sequential switching shunt regulator (S3R) for power control from the solar panels, a bi-directional battery regulator (B2R) for batterycharge and -discharge control, a power control unit (PCU) and a power conversion and distribution unit (PCDU).

The basic concept of the S3R is shown in figure 11.6. The essential principle of this regulator is effectively one of limitcycle switching of the switch S across the solar array equivalent current generator I_p, in order to maintain the regulated D.C. voltage V_0 at all values of load current I_l less then the array current.

Advantages of this design are:

- modular design
- bus voltage ripple virtually constant in amplitude and independent of load current
- no complex redundant clock or phasing circuitry
- 'minimal' thermal dissipation

The B2R is a power conditioning unit inserted between a battery at voltage V_b and the power bus at regulated voltage V_0. It replaces the dual functions of the battery conditioning units. This bi-directional capability is achieved with a reversible power cell as shown in figure 11.7 made out of six bi-directional switches, two in buck-structure and four in the push pull stage.

11.6 TEMPERATURE AND DEGRADATION INFLUENCES

11.6.1 Temperature Effects

The temperature of the solar panels is of importance for predicting the powergeneration by the solar cells as the voltage is nearly a linear function of the temperature with a slope of -1.9 mV/°C. The current varies slightly with the temperature. Thermal Control indicated the temperature of the solar panels will reach a maximum of 40°C in the sun when the satellite is spinning. This is a reasonable value as the temperature range of the panels may not exceed 50°C for acceptable power generation.

As would be expected from NiCd-cells, the highest discharge rate combined with the lower temperature gives the poorest performance. Therefore the temperature of the batteries should be regulated within 10°C - 30°C to achieve optimal performance, specifically 20°C is the optimum temperature.

One should bear in mind that due to discharge and especially over-charge the battery will become hot, making temperature monitoring inevitable.

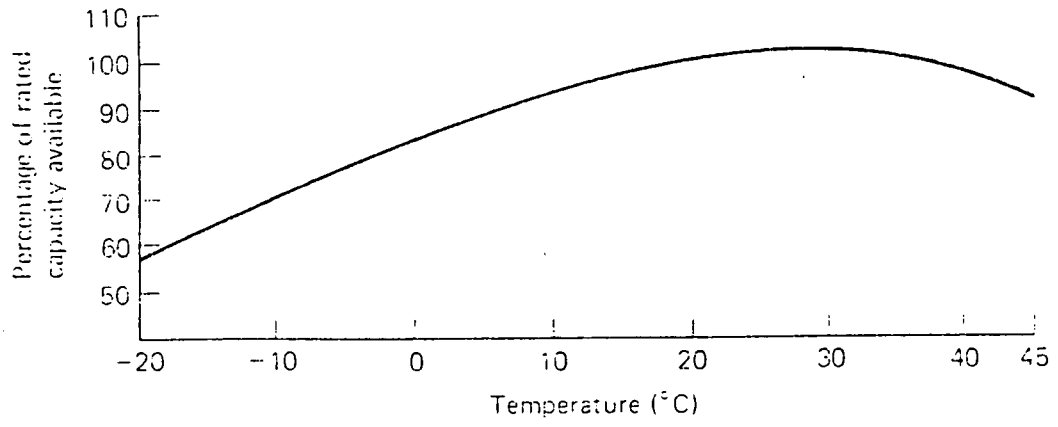

Figure 11.8: TEMPERATURE EFFECTS NiCd CELLS

11.6.2 Particle Degradation

Because the satellite passes the Van Allen Belts (VAB) twice per orbit, degradation by trapped particles has to be taken into account.

The irradiation environment consists mainly of trapped protons and electrons. High energy solar flare protons are not taken into account because their flux is of an order less than the flux of the damaging protons in the VAB.

The total 1 MeV equivalent damage fluence is estimated approx. $1 * 10^{15}$ e/cm^2. Then the degradation of the solar cells will be about 25 % over mission duration.

Due to the particle irradiation and due to the UV irradiation of the sun the covershielding of the solar cells darkens and as a consequence the power generation will become poorer. It will be clear that high optical transparancy of the glass is necessary over the whole mission period. At present, glass is the only material, which is resistant enough against the harsh environment. Degradation due to UV-irradiation is taken into account for 3%.

11.6.3 Hot Spot and Shadowing

Shadowing is an important factor which is difficult to avoid for a spinning satellite with body-mounted solar panels because there are elements that come out of the panels like thrusters and attitude sensors.

Shadowing reduces the photo current of one or more solar cells. As a consequence parts of the solar panel are forced to operate in the reverse part of their IV-characteristic, and therefore dissipating energy. A hot spot occurs and can locally destroy the solar panel.

The effect of reverse operation of shadowed solar cells can be limited by implementation of shunt diodes. Under illumination conditions the shunt diode acts as a high resistivity parallel shunt. Reverse operation of the string is limited by the small forward voltage drop of the diode.

For GaAs-solar cells the reverse voltage breakdown lies at about 10 V instead of 45 V for Si-solar cells, so significant effort is necessary to fully protect the solar panels against any shadowing.

11.7 CALCULATIONS

11.7.1 Assumptions

In order to make some calculations, several assumptions were made:

- powerbudget margin is 10%
- maximum eclipse time is 90 minutes
- temperature of solar cells is 50°C
- particle degradation of solar cells is 25% in 2.5 years
- UV-irradiation degradation 3%
- required subsystem powers are constant
- charge and discharge efficiency are about 80%
- middle of discharge voltage: V_{md} = 1.1 Volt
- middle of charge voltage: V_{mc} = 1.4 Volt
- end of discharge voltage: V_{eod} = 1.05 Volt
- end of charge voltage: V_{eoc} = 1.45 Volt

11.7.2 Solar Panels

The total available area to cover with solar cells for one panel A = 0.209 m² and is equal for both panel lay-outs. With P_{mp} = 240.3 W/m² (BOL, 50°C) we can generate a maximum power of 50.2 W Begin of Life when one panel is fully illuminated without any other loss factors taken into account.

Loss factors are:

- angle of incidence: max 10 deg. (1.5 %)
- PMAD efficiency: 15 % loss
- coverage with cells: 15 % loss
- other factors: 10 % loss

Other factors are - misalignment of cells
- cell mismatches
- calibration errors
- solar constance dependence
- micrometeorites and debris
- 'random losses'

So P_{mp} = 153.9 W/m² (BOL, 50°C, 36% loss) and the actual available power P (BOL) = 32.2 W - 45.5 W for the spinning satellite. Regarding to the budget for the transfer it's seen that the powerneed is equal to 42.9 W and thus, just as in operational mode, this demand can be supported by the battery for a short time period.

For End Of Life (EOL) we have to sum up the following degradation factors:

- particle degradation 25 %
- UV degradation 3 %

The total of losses sum up gives 53.4 % loss of power End of Life so that P_{mp} (EOL, 50°C) = 111.9 W/m².
The maximum available power (EOL) will vary, as we have a spinning satellite, between P = 23.4 W - 33.1 W.

As can be seen in the powerbudget this output is sometimes enough and sometimes not enough to require all subsystems solar energy constantly. The average generated power of the panels is about 28.3 W so every revolution of the satellite the battery has to generate the shortcomings and also store the remainder of energy during operations.

11.7.3 Battery

Assumed is a maximum eclipse-time of 90 min. as being the worst-case situation. The actual calculated (by Orbit Mechanics, Chapter 7) maximum eclipse-time is 75 min.

Furthermore nominal power (i.e. without the 10% margin) is used for calculations. Subsequently other criteria (e.g. eclipse 75 min. and power-usage with 10% margin) were considered, to assure reliable battery support.

For low mass and volume the highest DoD possible is chosen. For 2200 cycles (3 yrs) maximum DoD is 65 % (fig. 11.9); thus 60% DoD is chosen.

The Battery-Energy Required (BER) calculated is 44.7 Wh, this results in ten 6 Ah battery-cells. The calculus conditions were mentioned in the paragraph for assumptions.

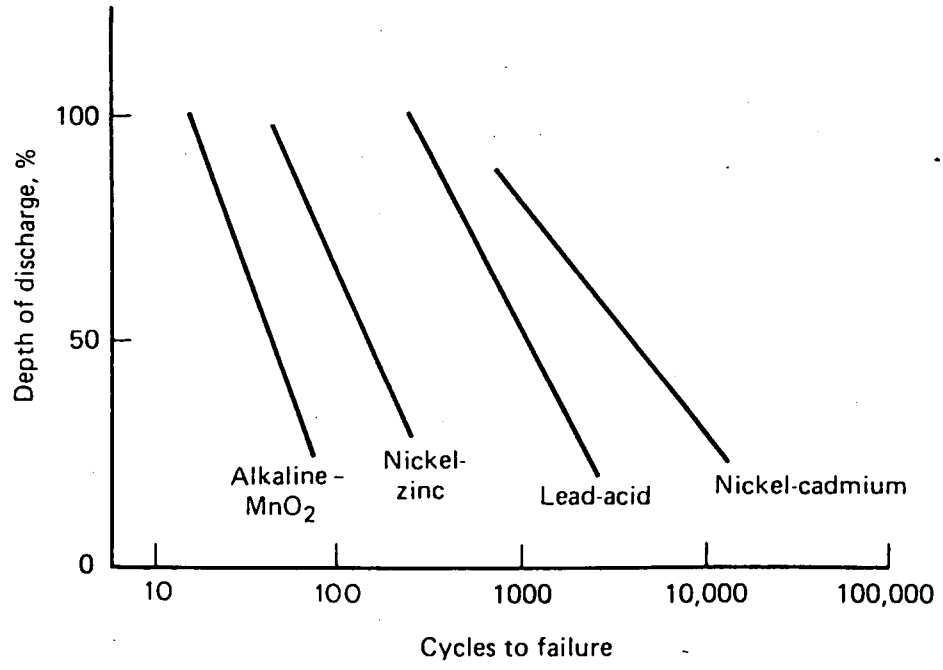

Figure 11.9: EFFECT OF DEPTH-OF-DISCHARGE ON CYCLE LIFE

CALCULATION EXAMPLE:

- In eclipse energy:

$$E_e = 21\ W \cdot 0.5\ h + 9\ W \cdot 1\ h$$
$$= 19.5\ Wh$$

- Margin 10 %

- Energy Needed:

$$E_n = 1.1 \cdot 19.5 = 21.5\ Wh$$

- Total battery energy:

$$E_b = n_c \cdot C \cdot V_{md}$$

where n_c = number of battery-cells (to be determined)
C = 90 min. discharge capacity, $C = 0.8 \times C_5$
C_5 = nameplate-capacity (eg. 6 Ah), from 5 hours discharge
V_{md} = middle of discharge voltage, $V_{md} = 1.1$ Volt

- Discharge-efficiency:

$$\eta_{dc} = \eta_{bdc} \cdot \eta_{pmad}$$

η_{bdc} = *battery discharge eff.* = 0.95
η_{pmad} = *PMAD eff.* = 0.85

- Calculations:

$$E_n = DoD \cdot \eta_{dc} \cdot E_b$$

$$n_c = \frac{E_n}{\eta_{dc} \cdot DoD \cdot C \cdot V_{md}} = 9 \text{ cells}$$

Redundancy: + 1 cell
Total : 10 cells

(Now the battery-mass and -volume can be calculated; the smallest battery is chosen from a variety of cells)

Real DoD, with 10 cells: 51 %, life expectancy : 4000 cycles
9 cells: 56 %, 3000 cycles
8 cells: 63 %, 2250 cycles

- Charge energy needed:

$$E_{cn} = \frac{E_n + E_{peak}}{\eta_b}$$

η_b = *battery Watt Hour Eff*, $\eta_b = \eta_c \cdot \eta_{dc}$
η_c = *charge-eff* = 0.8

Ecn = 41.7 Wh

- Charge energy available:

Eca = 47.8 Wh

- Both C-charge and C-discharge < $C_5/2$ (thus smaller then 3 A)

11.8 WIRING AND EMI/EMC

Wiring is necessary to supply the required power to the subsystems. Powerlines and datalines have to cross each other at right angles and must be separated at least for 50 mm. Therefore two wiringroutes are constructed in the internal configuration. All wires are annealed copper with insulation and are twisted and shielded to reduce the magnetic field from the power cables, causing electro-magnetic interference and electro-magnetic conduction.

Every subsystem is grounded by the PCU/PCDU from where grounding with the structure is realized.

11.9 PROTECTION

Protection of the solar panels can be done with blocking diodes.

Protection of the battery is needed because the loss of the battery can mean the loss of the whole mission. Two main failures of the battery are:

- short circuit: a cell doesn't contribute to the total voltage anymore; this cell is lost, but the battery continues to operate and the satellite still functions, however power is lost.

- open circuit: a cell gets such a high resistance reducing the current to zero. This means that both this cell and the entire battery are lost resulting in a satellite loss.

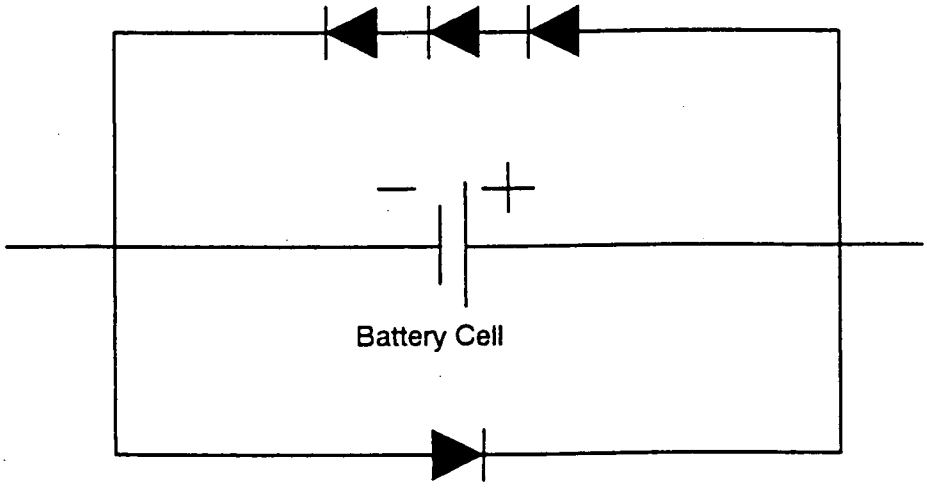

Figure 11.10: BATTERY BY-PASS DIODES CONFIGURATION

The open circuit failure is the most critical failure.
The cell causing an open circuit must be bypassed which can be done with bypass diodes.

The status of the battery is controlled with the aid of current- and voltage-monitoring together with the temperature within the battery. Also will the temperature of the solar panels and the busvoltage V_0 be monitored.

11.10 SPECIFICATIONS

Solar Cells :

Cell type:	GaAs/Ge, Spectrolab	
Thickness:	7	mils (175 microns)
Size:	up to 60 x 60	mm
Weight:	100	mg/cm² (bare cell)

Typical electrical parameters at 28°C, 1 AM0:

I_{sc}:	29.8	mA/cm² (BOL)
I_{mp}:	27.8	mA/cm² (BOL)
V_{mp}:	890	mV (BOL)
V_{oc}:	1020	mV (BOL)
P_{mp}:	24.8	mW/cm² (BOL)

efficiency: 18.3 % minimum average

Radiation Degradation at $1*10^{15}$ 1 MeV e/cm²:

I_{sc}/I_{sc0}:	0.84
I_{mp}/I_{mp0}:	0.83
V_{mp}/V_{mp0}:	0.90
V_{oc}/V_{oc0}:	0.90
P_{mp}/P_{mp0}:	0.75

Thermal properties:

Solar absorptance:	0.89
Emittance (normal):	0.85

Temperature coefficients:

I_{sc}:	20.0	µA/cm².°C
V_{mp}:	-1.90	mV/°C
V_{oc}:	-1.80	mV/°C

Battery:

Type:	NiCd, SAFT VRS-F cells	
Number of cells:	10	
Capacity:	6	Ah
C_{max}:	18	Ah
DOD:	≤ 60 %	
Cellsize:	33.1	mm (diameter)
	93.8	mm (length)
Cellweight:	0.27	kg
Batteryweight:	3.7	kg

11.11 CONCLUSIONS

- The proposed system can provide the necessary power for ALFIS

- Reduction of batterysize is possible when in eclipse no orbital manoevres are made

11.12 RECOMMENDATIONS

Some objects of further study, which aren't worked out yet, are:

- Shadowing and solar panel lay-out

Due to shadowing there's a possibility of occurring hot spots in the solar panels (see section 11.6.3).
A detailed simulation of that shadowing effect determines in a large measure the lay-out of the solar panels.

- Covershielding

No attention is paid to the covershielding of the solar cells. A well chosen shielding can decrease the degradation of the solar cells by particles and so increase the EOL power (or extend the mission duration).

- Harness

No attention is given to connectors which could lead to problems because of the volume constraints of the satellite. Also no exact information about geometry of wiring was known, so a more detailed study about the total harnessproblem is desirable.

- Electrical Protection

Little attention is paid to the possible protection of the batteries and solar panels. Also some notice has to be given at the protection of the subsystems when distributing the power to them with means of e.g. fuses against undesired overloads and short circuits.

12. PROPULSION

12.1 INTRODUCTION

For ALFIS a propulsion system is needed in the first place because of the mission requirements, which state that the distance between the two satellites (=baseline) has to be controllable. Other reasons will depend on the chosen concept.

The orbit determines whether it's necessary to correct for drag forces and other disturbances which would lead to a situation where the baseline would not any more be controllable according to the mission requirements.

If the launcher doesn't deliver ALFIS in final orbit but GTO, the propulsion system has to be able to do so.

Then there's the possibility to combine the propulsion system with attitude control. This can have advantages, when the same thrusters can be used, such as less complexity by one system instead of two, less weight, power and costs.

The ALFIS propulsion system should be able to meet the following requirements:

- ORBIT RAISING AND MAINTAINING: this includes raising from GTO and if necessary corrections for air resistance and other disturbances

- ORBIT CONTROL: this means the way of controlling the baseline in size and direction to investigate as many as possible different locations during life time.

- ATTITUDE CONTROL: the combined use of the propulsion and attitude control system.

12.2 TRADE-OFF BETWEEN TYPES OF PROPULSION

For ALFIS we can consider three types of propulsion: thermal-nuclear, electric and chemical. Where thermal-nuclear cancels out because of the experimental phase of this type.

Electrical can't be applied because ALFIS as a small satellite, has few power (+/- 30 Watt) to supply an electrical propulsion system.

In chemical propulsion, solid an hybrid are excluded. Solid because of the no restart capabilities, hybrid because it's still in an experimental phase. So cold gas, mono- and bipropellant remain. In the following paragraph we will examine which one of the three above will be suited for ALFIS.

12.3 PROPELLANT TRADE-OFF

Before the total velocity change ΔV_{tot} will be determined, a global view of the required mass for a cold gas, a mono- and a bipropellant propulsion system as function of a given ΔV change will be considered.

The Tsjolkovsky's equation gives the required amount of propellant for a propulsion system:

$$M_p = M_i \cdot (1 - e^{-\Delta V / (I_{sp} \cdot g_0)})$$

where
- ΔV = change in velocity
- g = 9.80665 m/s^2
- M_i = initial satellite mass
- M_p = necessary propellant mass
- I_{sp} = specific impulse

Adding the construction mass M_{co} of the dry propulsion system gives the total wet propulsion system mass $M_{prop.syst.}$:

$$M_{prop.syst} = M_p + M_{co}$$

Calculations for a ΔV (ranging from 0-1000 m/s) have been carried out for a cold gas, mono- and bipropellant propulsion system. The results are presented in figure 12.1.

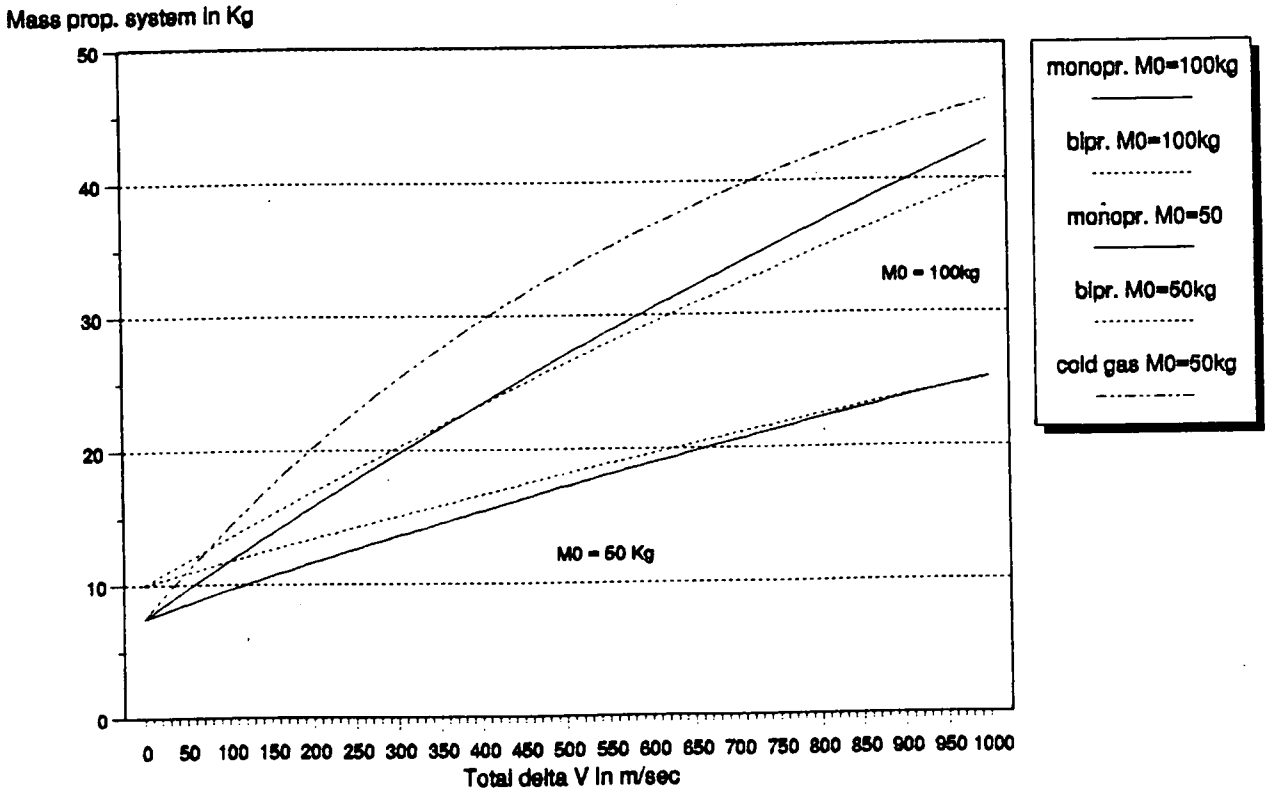

Figure 12.1: TOTAL MASS PROPULSION SYSTEM AGAINST ΔV

The following values for I_{sp} and M_{co} were assumed in the above calculations:

- cold gas (N_2) : I_{sp} = 70 s, M_{co} = 7.5 kg
- monopropellant (N_2H_4) : I_{sp} = 235 s, M_{co} = 7.5 kg
- bipropellant (MMH+MON) : I_{sp} = 285 s, M_{co} = 10 kg

Calculations have been done for an initial mass of the satellite equal to 50 and 100 kg. This is done because during the study mass decreased from the initial assumed mass of 100 kg down to less than 50 kg.

From figure 12.1, some interesting conclusions can be drawn:

- the cold gas propulsion system has the highest mass of all over the whole range (except <50 m/s for M0 = 50kg where it's lighter then a bipropellant system). So it looks only reliable for a small ΔV_{tot}, when a monopropellant (which is lighter) can't be used. (Thermal control problems)

- the bipropellant is only interesting when exceeding a certain amount of ΔV_{tot}. On this value the bipropellant propulsion system has eliminated the higher construction mass M_{co}. Beyond this value a bipropellant propulsion system uses less overall mass. One should take note that all tubing, valves, filters have to be doubled com-pared to a monopropellant propulsion system and so it becomes more complex thus either making it less reliable or more difficult to make it reliable.

- for a ΔV ranging from 0 to 900 m/s for M0 = 50 kg and 370 m/s for M0 = 100 kg the monopropellant propulsion system is the most attractive to use. It has the lowest mass of all and is less complex then a bipropellant one. Only the deterioration of the catalyst-bed during the desired life-time has to be considered.

With this information we can now decide which propulsion system to use, once the total velocity change ΔV is fixed. Some rough calculations show that the decision will most probably be in favor of a monopropellant propulsion system. This will be confirmed in the next paragraph.

12.3.1 Total Velocity Increment

The total amount of velocity increment needed for the mission can be split into three parts.

First there is the part of orbit raising. The satellites will be launched into a GTO orbit with a perigee height of 200 km. To achieve a twelve hour orbit we have to raise the orbits by making a certain ΔV.

Secondly there is the part of controlling the baseline between both satellites (= orbit control). The differential distance between both satellites is called the baseline between the satellites. Payload specifications demand that this baseline should be variable in both distance and direction. The maximum distance however should never exceed 300 km. A concept is chosen in which the baseline varies between -300 km and +300 km every 6 orbits. After these 6 orbits both satellites will be given a small ΔV so that the baseline distance reverses.

Thirdly there is the part of attitude control. The thrusters need to keep the spin-rate and spin-axis within certain limits. More detail about this you can find in chapter 13 which deals with the attitude control of the satellites.

12.3.1.1 ΔV Orbit Raising

To achieve a 12 hour orbit, from an initial orbit with a perigee of 200 km and an apogee of 35786 km (GTO), the perigee and/or the apogee can both be raised. However, it is cheaper to raise the apogee height then to raise the perigee, from the point of view of propellant consumption. So it was decided to raise the apogee more than the perigee.

For attitude control it is desirable to set the perigee height so that air drag is negligible. With this demand it was decided that it should be best to set the perigee up to 800 km. Now the apogee height necessary for a 12 hour orbit can be calculated.

$$T = 2\pi\sqrt{a^3/\mu}$$

$$T = 43200s \ , \mu = 398600.44 km^3/s^2$$

$$\Rightarrow a \approx 26610 km$$

This results in an apogee height of 39694.34 km, which can be verified in chapter 7, ORBIT.

From the initial orbit it is assumed that first the apogee is raised, followed by the perigee. The total ΔV for such an action is calculated by use of the following formula:

$$V = \sqrt{\mu\left[\frac{2}{R} - \frac{1}{a}\right]}$$

$$\Rightarrow \textit{perigee velocity GTO} \ : \ V_{p\,GTO} = 10.2389 \ km/s$$

$$\Rightarrow \textit{perigee velocity a.r.} \ : \ V_{p\,a.r.} = 10.2981 \ km/s$$

$$\Rightarrow \Delta V_p = (V_{p\,a.r.} - V_{p\,GTO}) \cdot 1000 = 59.2\ m/\text{sec}$$

Next the perigee will be raised from 200 to 800km.

$$\Rightarrow \textit{apogee velovity GTO} : V_{a\,GTO} = 1.4705\ km/s$$

$$\Rightarrow \textit{apogee velocity p.r.} : V_{a\,p.r.} = 1.5272\ km/s$$

$$\Rightarrow \Delta V_a = (V_{a\,p.r.} - V_{a\,GTO}) \cdot 1000 = 56.7\ m/s$$

Thus the total amount of ΔV needed for achieving the final orbit becomes:

$$\Delta V_{tot.\ o.r.} = \Delta V_a + \Delta V_p = 115.9\ m/\text{sec}$$

12.3.1.2 ΔV Orbit Control

To find a usable frequency for the orbit control corrections a whole range of orbit control programs have been calculated so that a trade-off could be made between them. The results are shown in the following table 12.1:

Amount of orbits between corrections	Delta V per correction in m/sec	Total delta V for 2.5 years corrections	Fuel mass for corrections
1	0.5375	980.8981	16.6685
2	0.2689	245.3357	4.9176
3	0.1793	109.0545	2.2563
4	0.1345	61.3478	1.2835
5	0.1076	39.2644	0.8258
6	0.0896	27.2677	0.5751
7	0.0768	20.0339	0.4232
8	0.0672	15.3387	0.3244
9	0.0598	12.1196	0.2565
10	0.0538	9.8170	0.2079
11	0.0489	8.1133	0.1719
12	0.0448	6.8174	0.1445
13	0.0414	5.8090	0.1231
14	0.0384	5.0088	0.1062
15	0.0359	4.3632	0.0925
16	0.0336	3.8349	0.0813
17	0.0316	3.3970	0.0720
18	0.0299	3.0300	0.0643
19	0.0283	2.7195	0.0577
20	0.0269	2.4543	0.0521

TABLE 12.1: POSSIBLE ORBIT CONTROL PROGRAMS

With these results the conclusion can be drawn that it would be best to assume a nominal orbit control correction frequency from once every 6 orbits. This way the total amount of ΔV needed for orbit control is limited to 27.3 m/sec over the total lifetime of the satellite which translates itself in 0.58 kg monopropelllant.

However it must be said that in this table there is assumed that OC corrections are always made in the perigee. In practice it might be that the perigee is sometimes in the eclipse during these corrections and so a battery provides the necessary energy. To diminish overall mass, a recommendation for further study would be to look at the consequences of performing OC corrections somewhere else then in the perigee when this is in eclipse.

The possible influence of the air resistance has also been checked.

On an altitude of 800 km, the air density is very dependent on the solar activity. To be able to make an estimate of the air density influence on the velocity, data from the ERS-1 satellite, also on an altitude of 800 km, was used.

The maximum worst-case calculated acceleration occurring in the perigee is:

$$a_{air} = 1.299 \cdot 10^{-7} \ \frac{m}{s^2}$$

This would mean over the whole life-time a necessary ΔV correction of:

$$\Delta V_{air} = 0.829 \ \frac{m}{s}$$

So it's clear, that the influence of ΔV_{air} on the necessary amount of propellant M_p will be very small, almost negligible.

Thus as long as the aerodynamic drag is less then the ΔV required for orbit control there is no need to take any extra propellant on board because it can be compensated by performing an adapted orbit control program.

In such an adapted program the foremost satellite will be slowed down less than the satellite, that is behind, is accelerated. Such an adapted orbit control program is shown in figure 12.2.

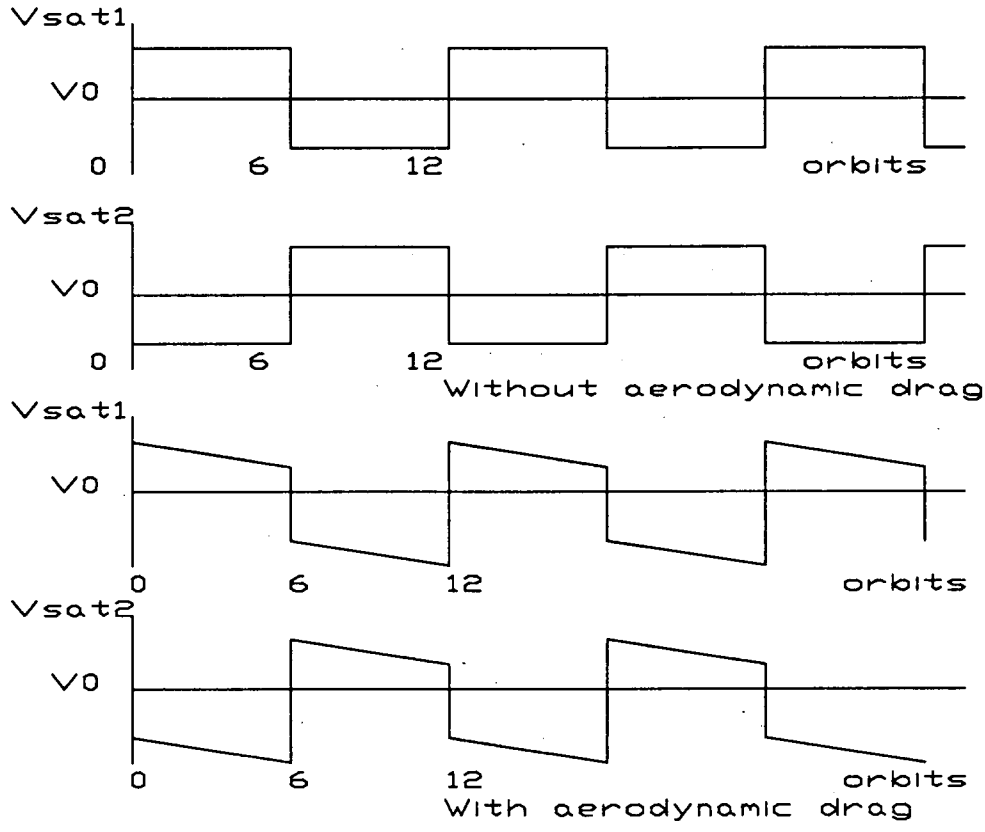

Figure 12.2: ORBIT CONTROL ADAPTED PROGRAMS

12.3.1.3 Attitude Control

The total amount of propellant for attitude control is 0.5 kg, this is with a reserve. More information about its calculation can be found in chapter 13, ATTITUDE CONTROL. This amount will be later added to the calculated propellant mass M_p.

Adding of all the results from above gives the total velocity change ΔV_{tot} shown in table 12.2.

Task to be performed	change in velocity ΔV (m/s)
Apogee raising	56.7
Perigee raising	59.2
Orbit control	27.3
Total	**143.2**

TABLE 12.2: THE TOTAL VELOCITY CHANGE ΔV_{tot}

12.3.2 Propellant Mass

Now that the total ΔV has been determined, the propellant mass can be calculated. In figure 12.1 can be seen that for a ΔV_{tot} = 143.2 m/s, a monopropellant system gives the lowest overall mass. Exact calculation of the propellant mass M_p with the Tsjolkovksy equation results in:

$$M_p = 45\ kg \cdot (1 - e^{-143.2\ \frac{m}{s} / (222\ s \cdot 9.80665\ \frac{m}{s})}) = 2.865\ kg$$

We assumed the specific impulse I_{sp} = 222 sec. This is the average value for the MBB CHT-0.5 thruster (216 - 227 s).

For comparison, the propellant mass is also calculated for a bipropellant and cold gas propulsion system.

The results are presented below in table 12.3:

	monopropellant N_2H_2	bipropellant MMH+MON	cold gas N_2
M_p (kg)	2.865	2.248	8.473

TABLE 12.3: PROPELLANT MASS MONO-, BIPROPELLANT AND COLD GAS

Note: for the bipropellant a lower result is shown, but the total mass of the system will be higher due to the higher construction mass M_{co}.

On the calculated result a margin of 10% will be added, this is to take inaccuracies into account (namely the uncalculated perturbations of the orbit could make it necessary to control/correct more often).

Attitude control provides their own needed amount of propellant: Mp_{ac} = 0.5 kg (margin included). Therefore the total amount propellant Mp_{tot} becomes:

$$Mp_{tot} = Mp \cdot 1.10 + Mp_{ac} = 2.865 \cdot 1.1 + 0.5 = 3.651\ kg$$

12.3.3 Acceleration and Burntimes

During the satellites life-time overall mass M will decrease, due to consumption of propellant necessary to create ΔV. Because of the use of a 'blow-down' propulsion system, there's also a decrease of force F exercised by the thrusters. By assuming a linear behavior of these two variables as a function of the ΔV made, the acceleration can be calculated on each moment whereon a certain ΔV has been achieved, $a_{\Delta V} = F(\Delta V)/M(\Delta V)$. This results in a maximum acceleration at the begin of life decreasing linear to a minimum acceleration at the end of life. There's been assumed that 2 thrusters function in equal direction during a change of velocity ΔV.

	Max. Begin of Live	Min. End of Live
Acceleration ($m/s^{2)}$	0.0333	0.0096

Table 12.4: ACCELERATION, MAXI- AND MINIMUM

This is a fundamental difference with a pressure regulated propulsion system. An increase of acceleration would then become visible. Here the diminution in force is higher (0.75 N -> 0.2 N for the MBB CHT-0.5 thruster) than in mass which makes acceleration decrease while using the propulsion system.

The burntimes can also be determined, again in function of the change in velocity ΔV, by calculating burntimes in small steps (ΔV-5m/s, $\Delta t_{burn} = \Delta V/\Delta a$) and adding them to the ones calculated in earlier steps.

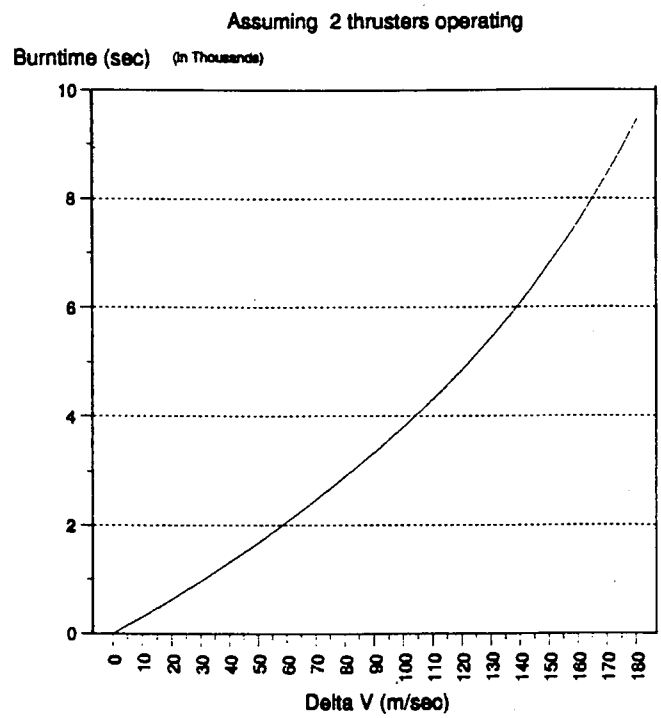

Figure 12.3: BURNTIMES TO REACH A CHANGE OF VELOCITY ΔV

From this figure the burntimes can be calculated for each stage of the total ΔV_{tot} realization.

Only in that part of the orbit for which the angle Θ (measured from the Earth) varies from -5 to +5° (perigee) and from +179.2 to 180.8° (apogee) thrusters can be fired. This is done to approximate the 'impulsive shot' from theory.

The times to travel through these equal parts of orbit are t_p = 128 s and t_a = 820 s.

The amount of orbits, needed to perform each ΔV operation, can now be calculated. The results are presented in table 12.5 .

	ΔV (m/s) Per.	Apo.	Burntime t_b (s)	Orbits & t_b / orbit
O.R. Apogee	59.2	.	2027	16, 127s
O.R Perigee	.	56.7	2608	4, 652s
Orbit Control	27.3	.	5.5 -> 9.3 ΔV=0.0896	each 6 orbits
Attitude Ctrl	26.1		very small	when needed

TABLE 12.5: BURNTIMES AND ORBITS TO INSTALL/CORRECT ORBIT

Table 12.5 shows that the satellites will arrive in the final orbit within 20 orbits or 10 days. The order of operations is chosen to establish final orbit quickly, with a minimum propellant weight M_p. During the small orbit control maneuvers the burntime will increase as the mission time proceeds due to the decreasing acceleration.

12.4 FEED SYSTEM (BLOW-DOWN)

After the trade-off between the different types of propulsion systems was done, concluded was that a monopropellant hydrazine system was most suitable for the satellite. Now it had to be decided whether to regulate the pressure in the system or use a simple blow-down concept.

The advantages of a pressure regulated system are the constant performances of the thrusters and the high I_{sp} over the whole mission-duration which saves propellant-mass and -volume. On the other hand a pressure regulated system requires an extra high pressure tank for the pressured gas and an extra (pressure) regulator compared to the simpler blow-down system.

Because the total amount of propellant for the mission is only about 3.65 kg and because the I_{sp} of a blow-down system only varies between 234s and 214s maximum it was found that the advantages of a pressure regulated system did not balance its disadvantages compared to a simple, reliable blow-down system. Therefore decided was to go along with the blow-down system.

In figure 12.4 you can see the proposed propulsion flow diagram.

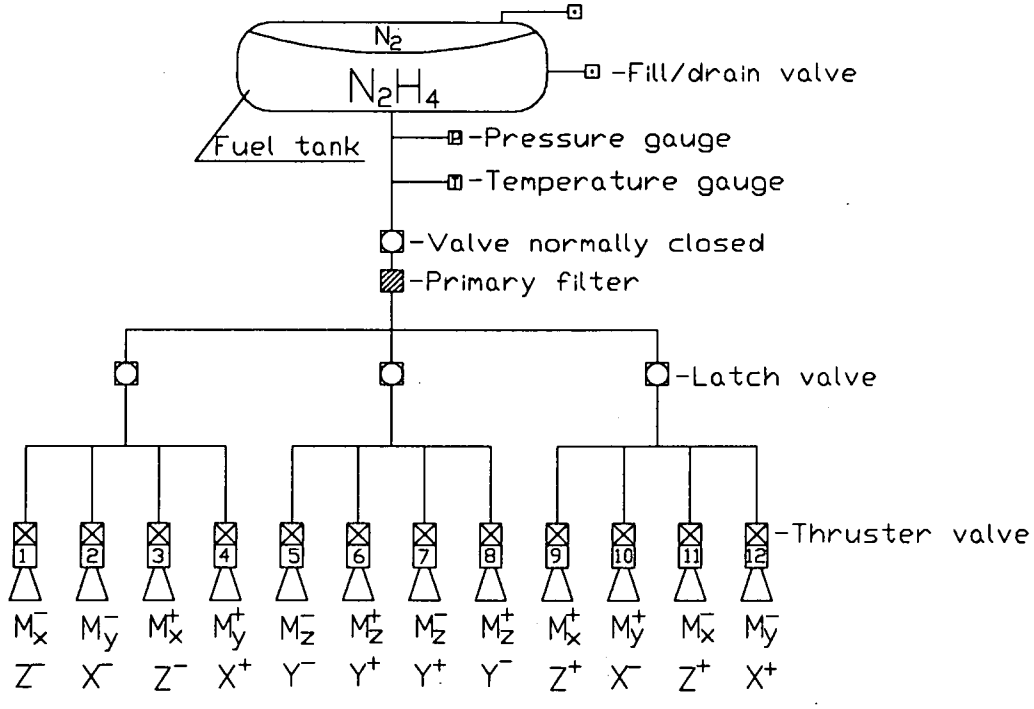

Figure 12.4: PROPULSION FLOW DIAGRAM

Further information about the propulsion-system:

- The normally closed pyrovalve is build in as a safety precaution against propellant leakage during launch and is often even a requisite from launcher. A redundancy between the tank and valve is recommended in order to compensate a failure to open case.

- The primary filter is build in to extract any contamination from the propellant which could endanger the proper functioning of the latch valves or thrusters.

- Next the twelve thrusters are divided into three branches, separated from each other by latch-valves. This is done to be able to minimize the effect of any leakage that may occur between latch valve and thrusters. Should a leak occur then the latch valve can be closed leaving the remaining 8 thrusters fully in function. With these 8 thrusters we will be able to perform most orbit and attitude control corrections.
However should we need to perform a correction which requires one of the thrusters on the shut branch, we can open the latch valve for a short period, during the correction, and so minimize the leakage effect.

- The pressure and temperature gauge are installed to be able to monitor the propellant state at all time.

Catalytic Monopropellant Hydrazine Thrusters
Thruster Characteristics for CHT 0.5

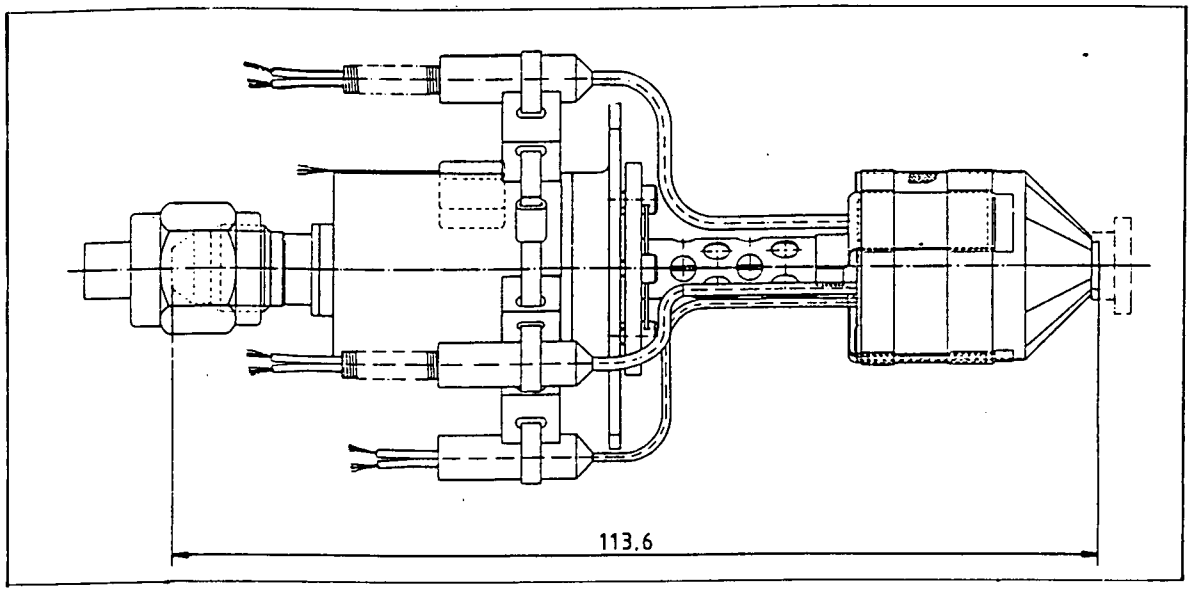

Technical data

Thrust range	(N)	: 0.75 - 0.2
Oper. pressure range	(bar)	: 22 - 5.5
SSF specific impulse	(Ns/kg)	: 2230 - 2120
Minimum impulse bit	(Ns)	: 0.015 - 0.005
Proof pressure	(bar)	: 33 / 54
Burst pressure	(bar)	: 88 / 144
Mass	(kg)	: 0.19
Valve power	(Watt)	: 5.0
Heater power	(Watt)	: 2.5
Environmental loads		
Sinusoidal vibration		: 5 - 21 Hz : 11 mm (o - p) 22 - 100 Hz : 20 g
Random vibration		: 20 - 2000 Hz 0.2 g^2/Hz (20 g rms)
Acceleration		: 20 g all axes
Shock		: 100 g for 5 ms all axes

Qualification status : qualified in 1977

SSF duration total	(h)	: 143
SSF duration single burn	(s)	: 25.200
Hot pulse quantity		: 59.000
Off modulation quantity		: 88.000
Cold start quantity		: 311.000 at ≤ 210°C

Flight history
OTS 2
ECS F1, F2, F4, F5
MCS A, B2
Telecom 1A, 1B, 1C
To fly on: : Skynet 4 A, B, C
Nato 4 A, B

165 units built

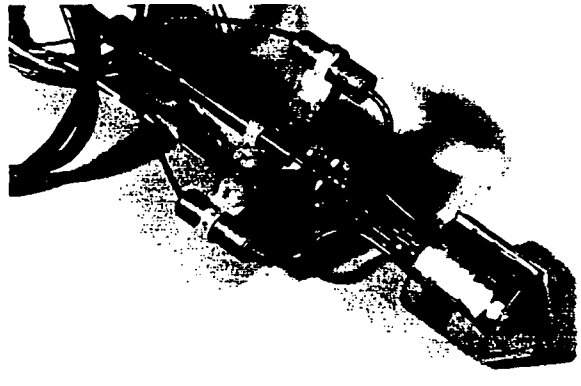

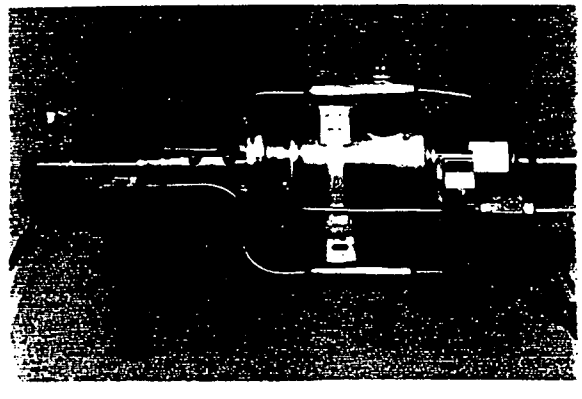

Figure 12.5: CHT-0.5 CHARACTERITICS

12.5 THRUSTERS

The only available information concerning thrusters came from MBB. That is why a trade-off could be only made between their monopropellant hydrazine thrusters. These thrusters range in nominal thrust between 20 N and 0.5 N. Because ALFIS is a light satellite with a very tight mass and volume budget and no requirements concerning minimum acceleration power a trade-off was quickly made for the smallest available thruster. This thruster, the CHT 0.5, can deliver a thrust between 0.75 N and 0.2 N, depending on the operating pressure which may range between 5.5 and 22 bar. More specifications are presented in figure 12.7.

- These thrusters are preferably fed with tubings with an inner diameter of 25 mm (1/4") and a wall thickness of 0.4 mm. In general a TIG welding technique is used to connect tubing elements, to joint fill- and drain-valves, filters, manifolds and tanks. For equipment with moving parts inside, like latching valves and thrusters, screwed joints are mostly more preferable.

- The thrusters are attached to the structure with their mounting flanges. There was no reason to equip them with alignment adjusters because there are no very strict requirements concerning attitude or orbit control corrections.

- The thrusters decompose the hydrazine over a catalyst bed which should be heated before firing. This heating takes about half an hour and should be done more thoroughly for small impulse-bits then for long shots. Also temperature shocks should be avoided.

12.6 TANK

During the project it was possible to reduce the amount of propellant needed for the mission considerably. At the start there was an estimation of about 12 kg. The perigee was on that moment set to 2684 km. This would mean a spherical tank diameter of approximately 310 mm. This volume was by far not available, and so an adapted tank shape was proposed. With a 'cheese shaped' tank the height could be restricted to 180 mm. However 12 kg propellant was a heavy weight on the mass and volume budget of ALFIS and developing a 'cheese' shaped tank would be a very expensive solution. So searched was for a solution to diminish the amount of propellant. A solution was found in changing the orbit. Lowering the perigee to 800 km and raising the apogee from GTO to 39694.34 km could save some 5 kg propellant. After that, more accurate calculations could reduce the estimated amount of propellant needed for the mission more and more.

At the end of the project the best estimation for the amount of propellant needed had become 3.65 kg.

During the evolution of these iterative calculations there was continuously looked at the possibility to use one or more spherical tanks to reduce the costs. For this purpose a figure was made from which the necessary tank diameters could be estimated as quickly as possible. This figure is presented to you as figure 12.6. In this figure is also accounted for the necessary pressurizing gas which is stored in the same tanks as the propellant. The best estimation can be found by setting the pressure ratio Pbegin/Pend = 4, because the operating pressure of the thrusters range between 5.5 and 22 bar which is also factor 4 between begin and end of blow-down. To realize this factor 4 in pressure ratio, 1/4 of the tank has to be filled with pressurizing gas. As you can see from this figure 12.6 and the latest estimation of the amount of propellant, 3.65 kg, we can now also use 4 spherical tanks with a diameter of 135 mm. This option is of course strongly recommended because it's a much cheaper solution.

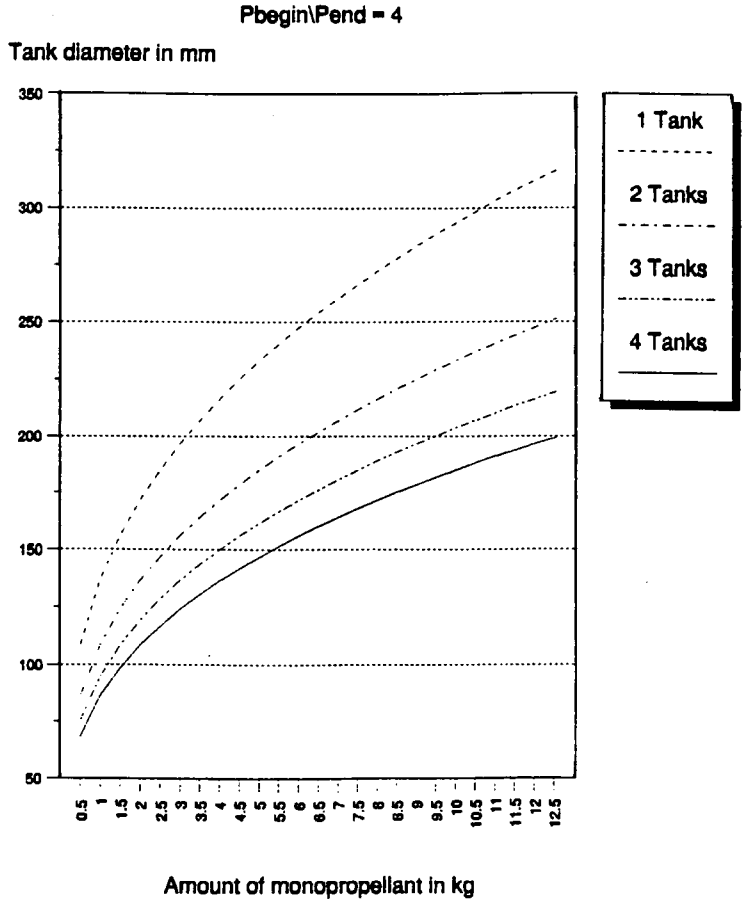

Figure 12.6: SPHERICAL TANK DIAMETER

The weight of the original 'cheese' shaped tank (designed for more propellant then finally needed) is 2 kg. Four spherical tanks with a diameter of 135mm have a total weight of 4x 0.26 kg = 1.04 kg. So this would also result in a lower weight for the propulsion system if no more weight is needed to attach the 4 spherical tanks to the satellite then to install the 'cheese' shaped tank.

As previously already mentioned the pressurizing gas is stored in the same tank as the propellant. To make sure that the propellant is expelled, not the pressurizing gas, a diaphragm is placed in between.

As pressurizing gas nitrogen is recommended over helium because its much cheaper, the penetrative power through the diaphragm of nitrogen is much smaller than of helium, and the weight saving potential of helium is almost negligible because of the small amount of propellant estimated.

12.6.1 Tank Strength Calculation

The strength the tank should have is depending upon the pressure in the tank. The pressure in the tank is necessary to ensure a proper propellant flow when a thruster is used. However due to this flow pressure losses occur in tubing and other parts of the propulsion system. This pressure loss has to be compensated by storing a higher initial pressure in the tanks than the operating pressure of the thrusters.

However due to the small thrust of the thrusters only small propellant flows occur (about 0.25 gram/sec per active thruster) in relative wide tubings (1/4"), and so pressure losses are small. According to MBB's record these pressure losses are less then 0.5 bar. So the calculation was made with an initial tank pressure of 22.5 bar.

$$P_{tank} = 2.25\ N/mm^2$$

$$D_{tank} = 135\ mm$$

$$P_{tank} \cdot A = 2.25 \cdot \pi \cdot \frac{135^2}{4} = 32206\ N$$

The area of the tank section with an estimated wall thickness of 1 mm is:

$$D_{tank} = 135\ mm$$

$$A_{tankw.} = \pi \cdot \left(\frac{(D+2)^2}{4} - \frac{D^2}{4}\right) = 427\ mm^2$$

The stress in the wall of the tank will become:

$$\sigma_{tankw.} = 2 \cdot \frac{P}{A_{tankw.}} = 2 \cdot \frac{32206}{427} = 151\ N/mm^2$$

Because the yield stress of the titanium alloy Ti-6Al-4V is 1103 N/mm^2, there is no strength problem using a tank made from this alloy.

Description item	Amount	Unit mass (kg)	Summed mass (kg)
N_2 fill&drain valve	1	0.080	0.080
N_2H_4 fill&drain valve	1	0.035	0.035
Tank (N_2H_4 + N_2)	1	2.000	2.000
Valve norm. closed	2	0.160	0.320
Primary filter	1	0.050	0.050
Latch valve	3	0.250	0.750
Thruster (CHT-0.5)	12	0.195	2.340
Tubing (1/4",0.4mm)	≈ 6m	0.225	0.225
Fitting	≈ 40	0.020	0.800
margin 10%	-	-	0.660
Construction Mass	-	**M_{co} =**	**7.260**

Table 12.6: CALCULATION CONSTRUCTION MASS M_{co}

	Propulsion System
M_p (kg)	3.65
M_{co} (kg)	7.26
M_{gas} (kg)	0.04
M_{tot} (kg)	10.95

Table 12.7: TOTAL MASS PROPULSION SYSTEM

12.7 CONSTRUCTION AND TOTAL MASS

Because the propellant mass, the components and build-up of the propulsion system are known now, the construction dry mass M_{co} can be calculated. From the flow diagram all elements can be determined. Tank-mass was provided by STRUCTURE. Other masses were looked up. Adding all, results in the construction mass M_{co} of the hydrazine propulsion system are given in table 12.6.

Now the total 'wet' mass of the Hydrazine propulsion system can be determined, by adding the construction mass M_{co}, propellant mass M_p and for completeness the pressure gas mass M_{gas} (though very small, negligible in phase-A study). The total mass is presented in table 12.7.

This result could even become lower when 4 spherical tanks would be used to replace the 'cheese' shaped tank. The total mass of the propulsion system could then be optimal around 10 kg.

12.8 CONFIGURATION AND OPERATION

The configuration chosen for is the 12-thruster one, because it has the possibility to make all translations and rotations (Tx,Ty,Tz,Mx,My,Mz) independently in one single maneuver with 2 thrusters working only. This configuration is also more redundant, so more reliable then a configuration with less thrusters. Whether this possibility and higher reliability are really necessary for this satellite has not been examined.

There's also an other possible configuration, namely the 8-thruster one. With this configuration one can achieve full three axis control, but there will be some propellant losses:

- some thrusters are placed under a 45° angle with respect to an axis, causing losses while translating.

- others have to function to prevent translations during rotation-controlling.

Further investigation has not been done on this subject.

Finally the two mentioned configurations will be given in figure 12.7 and figure 12.8.

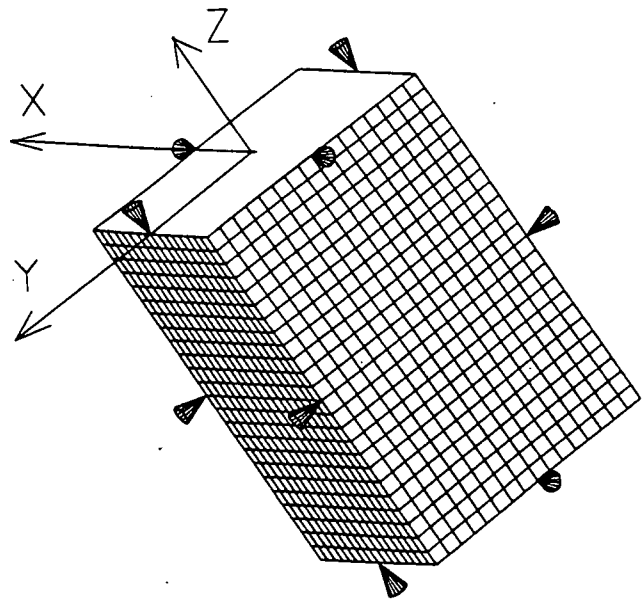

Figure 12.7: 12-THRUSTER CONFIGURATION, FULL 3-AXIS CONTROL, NO LOSSES, REDUNDANT

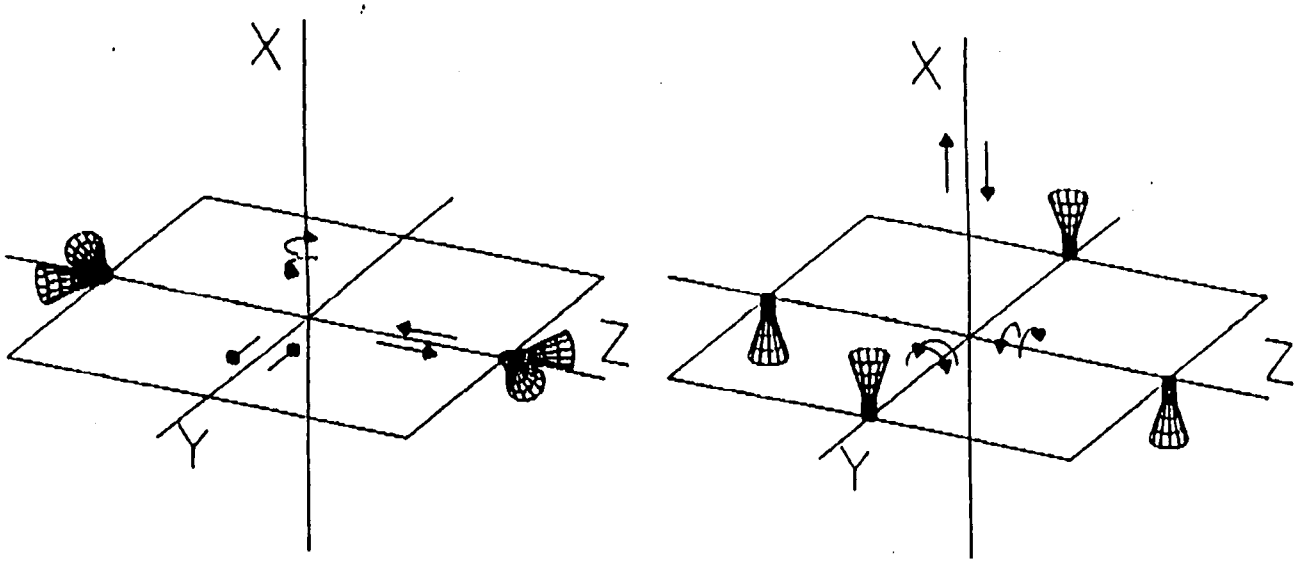

Figure 12.8: 8-THRUSTER CONFIGURATION, FULL 3-AXIS CONTROL, SOME LOSSES, LESS REDUNDANT

The operation of the ALFIS propulsion system can be divided in the following stages:

STAGE 1: During ground operations and launch with the Ariane 4, both the 2 normally closed valves (to compensate a FAILURE TO OPEN case) are shut in order to avoid a pressure blanket in front of the thrusters at the launch which could lead to leakages, or even accidental firing.

STAGE 2: After separation with launcher, one normally closed valve is opened (or the other one, when FAILURE TO OPEN occurs). All systems will be checked, after this orbit raising is performed. This is done first in the perigee to raise apogee height (16 orbits), then in the apogee to raise perigee height (4 orbits) and so install a 12 hour orbit. See also figure 12.5. Now the satellite is placed in final orbit. Stage 2 will take 20 orbits or 10 days.

STAGE 3: Here the payload will carry out measurements. Propulsion is used to control the baseline in order to fill up as many distances and directions in space: Orbit Control. When the maximum baseline (300 km) is going to be exceeded, orbit control maneuvers will be performed in the perigee. Orbit control is able (within limits) to correct also unforeseen perturbations of the orbit. Stage 3 will take optimal 2.5 years.

STAGE 4: When the satellite becomes uncontrollable/ unusable due to fatal malfunctions or lack of propellant, the ALFIS system will become inoperative. If no solutions or other applications are found, the satellite reaches its final stage: end of life. There is no propellant reserved to lower perigee altitude at the end of life to deorbit and reentry Earth to prevent space-pollution.

12.9 COSTS

Costs are always difficult to estimate. Prices depend on the boundaries of the procurement sources, capability to contribute in terms of manpower, facilities, labor and laboratory rates. The non recurring cost will make up the biggest amount. Costs are also severely influenced by the quality of the system involved, the type and amount of documentation to be furnished.

For ALFIS we probably could sustain with the available documentation (Technical Specifications , Qualification Test Report). Though some information (estimates) was gathered about next items:

- Hydrazine, two qualities: normal and high quality ranging from 40 AU/liter up to 175 AU/liter. Price will be higher because ALFIS requires a relative small amount, ie. ± 4000 AU.

- A 'cheese shaped' tank could cost up to 425000 AU, because of the total new design and development. It would take about 2 years to develop such a tank. Two spherical tanks would probably be off the shelf, price about 20000 AU a piece.

- The thrusters price depends a lot on the required documentation, for ALFIS price would be around 85000 AU a piece.

- Latch valves are also pretty expensive: around 10000 AU a piece.

The price of tank(s), thrusters, propellant and valves together make up about 80% of total cost. An estimation can thus be made for ALFIS. The case with two spherical tanks and the one with the 'cheese shaped' tanks will be considered.

	Costs (KAU)
APS/'cheese shaped' tank	1790
APS/two spherical tanks	1340

Table 12.8: COST ESTIMATE ALFIS PROPULSION SYSTEM (APS)

12.10 CONCLUSIONS

The results of this feasibility study for the ALFIS propulsion system are positive. Though at the start it seemed that the propulsion system would take too much (propellant) mass and volume, in the end more precise calculations and change of orbit have reduced the amount of monopropellant to an acceptable level. Now all propellant can be stored in spherical tanks reducing overall costs considerably.

However this study did not find the optimum solution and so further investigations are necessary. The subjects we think need still more attention are stated in the next chapter.

12.11 RECOMMENDATIONS

- Possibility to perform OC corrections somewhere else then in the perigee when this lies in the eclipse. And the influence on the total mass budget (battery versus extra propellant).

- Necessity of electronic hardware to drive the thrusters.

- The connection between the propulsion system and other systems (to optimize the satellite).

- Further study for the necessity of redundancy in the propulsion system.

- Possibility for a 8 thruster configuration as shown in figure 12.8.

- Reliability study.

- More accurate simulation of mass and thrust profile in course of time, to reduce propellant amount.

- More investigation of orbit perturbations.

- Replace 'cheese' shaped tank by 2 or more spherical tanks.

13. ATTITUDE CONTROL

13.1 INTRODUCTION

In this chapter we will try to give an overview of the requirements for the AC system and the way they will be met. In one of the preceding chapters we have chosen for the concept of a spinning satellite. Furthermore, other mission requirements determined the orbit and the launcher choice imposed restraints on the configuration. All this made the tasks of stabilizing the satellite and the sensor choice a difficult one. In this chapter we will give several possible solutions and make a trade-off, amongst others with the aid of a computer simulation. This mathematical model will also be discussed.

13.2 REQUIREMENTS

Several subsystems have the following demands:

- attitude reconstruction with an accuracy of 1° during payload operation
- spinrate as low as possible to exclude doppler-effects in the measurements
- solar panels pointing accuracy 10°

13.3 MOTION OF THE SATELLITE

13.3.1 Stability

A spinning spacecraft is stable if the spin axis is the principal axis with the smallest or the largest moment of inertia if there is no energy dissipation. In our case the satellite's spin axis is the one with the smallest moment of inertia, so theoretically the motion of the satellite is stable. However the liquid fuel causes for energy dissipation, therefore the satellite will nutate.

There are two solutions for this problem. The first solution is to attach deployable beams on the satellite in order to make the spin axis the one with the largest moment of inertia. In that case the liquid fuel in the tank will act as a passive nutation damper.

The second solution is to use the thrusters and the OBC as an active nutation damping system.

Both solutions have their own advantages and disadvantages, as shown in table 13.1.

	passive nutation damping	active nutation damping
advantages	- reliable - deployable beams is proven technology - easier balancing	- less mass in spite of more fuel consumption - less volume
disadvantages	- extra mechanism - extra mass - shadowing	- complex software - less reliability - expensive development and test program

Table 13.1: SOLUTION COMPARISON

In order to make a more well considered trade-off we will first study the motion of the satellite more carefully.

13.3.2 Definition of the Angles

For the definition of the angles which are used in the model we made use of lit. 13.2 (v.d. Broek, 1967)

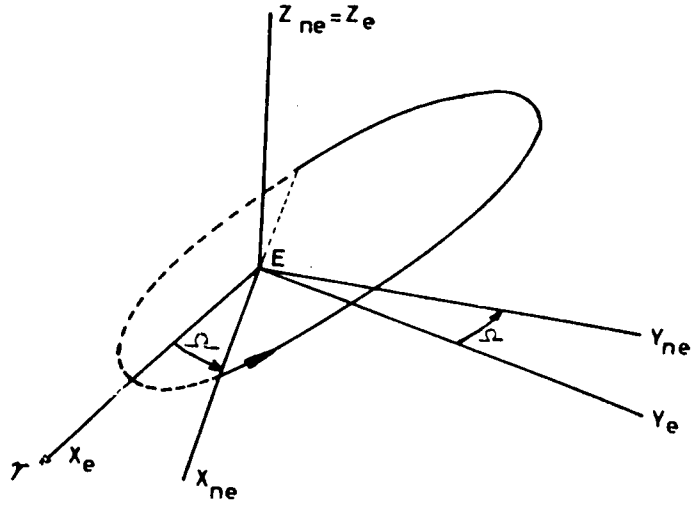

Figure 13.1: INERTIAL ECLIPTICAL REFERENCE SYSTEM AND NODAL ECLIPTICAL REFERENCE SYSTEM

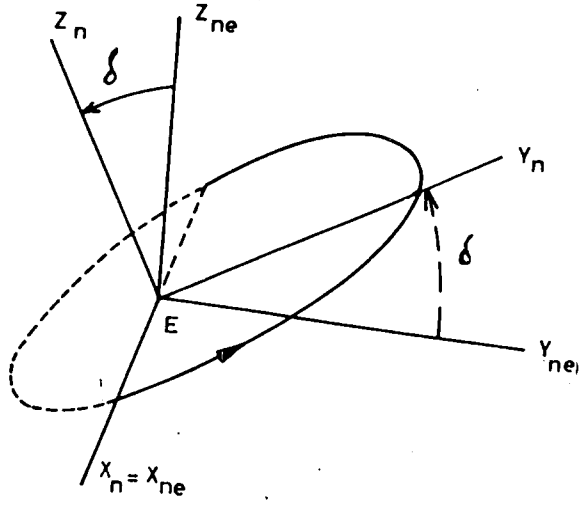

Figure 13.2: NODAL ECLIPTICAL REFERENCE SYSTEM AND NODAL ORBITAL REFERENCE SYSTEM

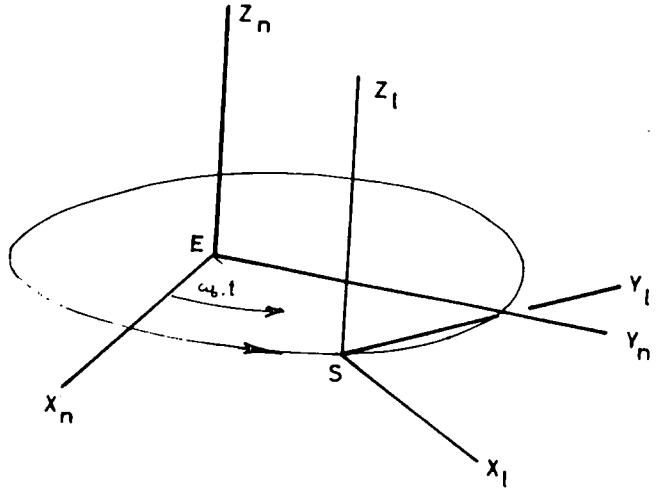

Figure 13.3: NODAL ORBITAL REFERENCE SYSTEM AND LOCAL ORBITAL REFERENCE SYSTEM

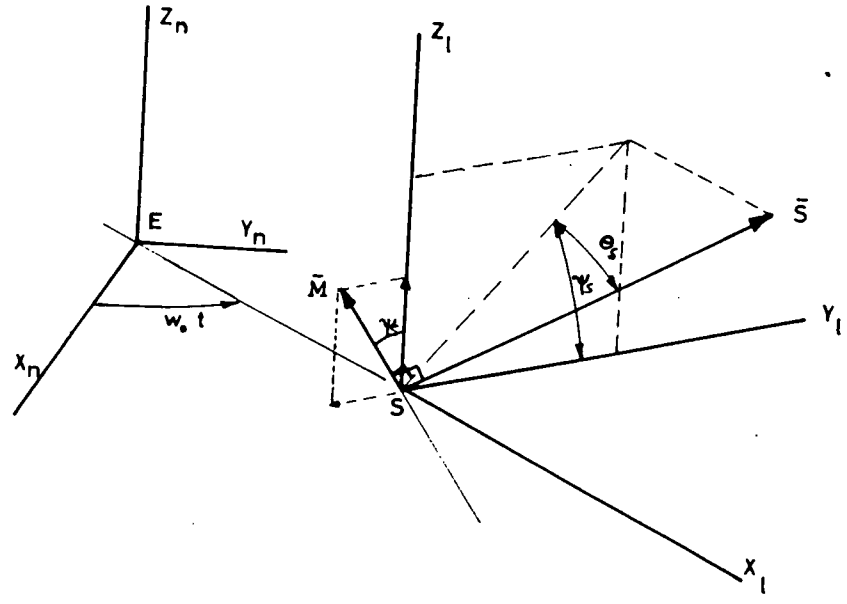

Figure 13.4: GRAVITY GRADIENT TORQUE ACTING ON A SPIN STABILIZED SATELLITE

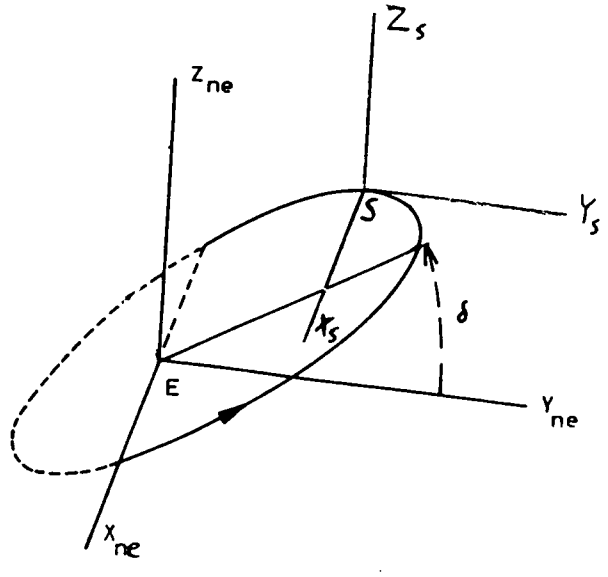

Figure 13.5: NODAL ECLIPTICAL REFERENCE SYSTEM AND SATELLITE REFERENCE SYSTEM

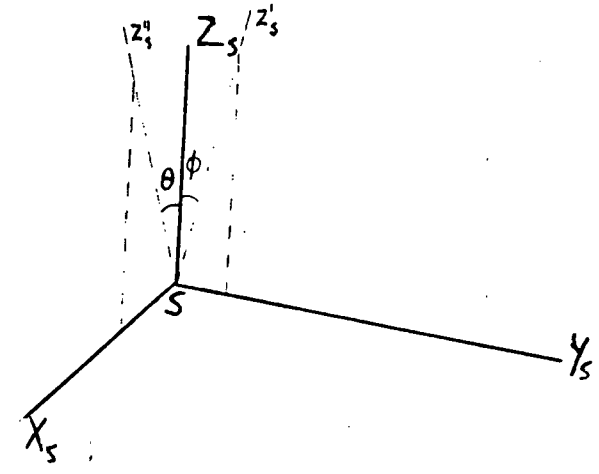

Figure 13.6: SATELLITE REFERENCE SYSTEM AND DRIFT ANGLES

13.3.3 Perturbation Torques

13.3.3.1 General Contemplation

The following perturbation torques disturb the attitude of the satellite:

- aerodynamic torque
- solar radiation pressure torque
- torques caused by the impact of micrometeorites
- torques caused by aliens
- gravity gradient torque

13.3.3.2 Neglected Torques

The aerodynamic torque is neglected, because the perigee height of the orbit is 800 km. At that height the density of the air is 10^{-14} kg/m^3 and as a result the aerodynamic torque is in the order of 10^{-12} Nm.

The solar radiation pressure torque is also calculated and found to be in the order of 10^{-14} Nm.

The torque caused by the impact of micrometeorites is neglected because of lack of data and the fact that it probably will be very small.

The torque caused by aliens is neglected, because until now no aliens have been found, and if they exist, they probably have something better to do than to play with ALFIS

We have neglected these torques because they are less than 1/1000 of the largest torque.

13.3.3.3 Gravity Gradient Torque

The equations of the gravity gradient torque are given with the axes of the local orbital reference system (figure 13.1).

$$T_{x_1}=0$$

$$T_{y_1}=-\frac{3\mu}{2r^3}\cdot(I_x-\frac{I_y+I_z}{2})\cdot\sin(2\theta_s)\cdot\sin(\psi_s)$$

$$T_{z_1}=+\frac{3\mu}{2r^3}\cdot(I_x-\frac{I_y+I_z}{2})\cdot\sin(2\theta_s)\cdot\cos(\psi_s)$$

with: Ti_1 = gravity gradient torque in i_1-direction
μ = gravitationparameter of the earth (398600.4 km^3/s^2)
r = distance between centers of earth and satellite
θ_s, ψ_s = angles of spin-axis in local orbital reference system (fig. 13.1)
I_{ii} = principal moment of inertia about the i-axis

It is assumed that the spin-rate ω is much larger than the angular rate of change of the position of the satellite orbit ω_0. Inspection of the equations shows, that torque is perpendicular to the local vertical and perpendicular to the spin-axis of the satellite. The magnitude of the torque is given by:

$$T=\frac{3\mu}{2r^3}\cdot(I_x-\frac{I_y+I_z}{2})\cdot\sin(2\theta_s)$$

13.3.3.4 Magnetic Torque

To determine the magnetic torque we must first calculate the dipole of the satellite. Then we calculate the Earth-magnetic induction from the dipole equations of the Earth-magnetic field. The magnetic torque is the sinusproduct of the dipole of the satellite and the Earthmagnetic induction.

The dipole of the satellite is calculated from the magnetic properties of the ferrite antennas. Due to the rotation of the satellite the components in the parallel to the equator of the satellite have a zero result in one rotation.

Components of the dipole of the satellite:

$$M_{sat_x} = M_{sat} \cdot \sin\phi \cdot \cos\theta$$
$$M_{sat_y} = M_{sat} \cdot \sin\theta \cdot \cos\phi$$
$$M_{sat_z} = M_{sat} \cdot \sin\phi \cdot \sin\theta$$

with: M_{sat} = magnetic dipole parallel to the spin axis
θ, ϕ = drift angles

Dipole Earth:

$$M_x = M \cdot \sin\xi \cdot \cos i \cdot \sin\left(\frac{\theta_b}{2} - \Omega\right) + \cos\xi \cdot \sin i$$
$$M_y = M \cdot (-\sin\xi) \cdot \sin i \cdot \sin\left(\frac{\theta_b}{2} - \Omega\right) + \cos\xi \cdot \cos i$$
$$M_z = M \cdot \sin\xi \cdot \cos\left(\frac{\theta_b}{2} - \Omega\right)$$

with: M_i = magnetic dipole Earth in i-direction
M = -8×10^{15} Wb
ξ = angle between magnetic Earth axis and Earth rotation axis (11°)
i = inclination
θ_b = true anomaly
Ω = right ascend of the ascending node

Earthmagnetic induction:

$$B_x = \frac{M_x}{r_b^3} \cdot (3\sin^2\theta_b - 1) + \frac{3M_z}{r_b^3} \cdot \sin\theta_b \cdot \cos\theta_b$$
$$B_y = \frac{M_z}{r_b^3} \cdot (3\cos^2\theta_b - 1) + \frac{3M_x}{r_b^3} \cdot \sin\theta_b \cdot \cos\theta_b$$
$$B_z = -\frac{M_y}{r_b^3}$$

with: B_i = Earth magnetic induction
r_b = distance between the centers of the Earth and the satellite

magnetic torque:

$$\vec{T}_m = \vec{M} \times \vec{B}$$

13.3.3.5 Attitude of the Satellite

The motion of the satellite can be found with the following equations of motion (lit. 13.1 Wertz, 1978 page 522):

$$\frac{dp}{dt} = \frac{T_{p_x} + (I_{yy} - I_{zz}) \cdot q \cdot \omega}{I_{xx}}$$
$$\frac{dq}{dt} = \frac{T_{p_y} + (I_{zz} - I_{xx}) \cdot \omega \cdot p}{I_{yy}}$$
$$\frac{d\omega}{dt} = \frac{T_{p_z} + (I_{xx} - I_{yy}) \cdot p \cdot q}{I_{zz}}$$

The drift angles can be found with:

$$\phi = \int (q - \omega \cdot \theta)\, dt$$
$$\theta = \int (p + \omega \cdot \phi)\, dt$$

with: θ = drift angle in y-direction (rad)
ϕ = drift angle in x-direction (rad)
ω = spin-rate (rad/s)
Tp_i = perturbation torque in i-direction
I_{ii} = moment of inertia

13.4 SENSORS

13.4.1 Trade-Off

For the sensor a trade-off was made between a CCD-star-sensor in combination with two or more Quadrant Sun Sensors (QSS) and an Earth Sun Sensor (ESS), consisting of a IR-earth-sensor and a X-beam sun sensor.

We have chosen for the ESS because the CCD-sensor requires to much calculation capacity of the OBC, is too sensitive to radiation in the Van Allen Belts, consumes too much power and is too heavy. In figure 13.7 you see a picture of the ESS.

13.4.2 Spin Axis

The solar panels are most efficiently used, when the solar panels are perpendicular to the sun. For the X-beam sun sensor this is not a problem. For the IR-earth sensor however is it convenient to have the spinaxis perpendicular to the orbital plane. Without considering the inclination the spin-axis is perpendicular to the ecliptical plane, when it makes an angle of 66.6° with the equator of the Earth. Because the inclination varies from -5.2° to 5.2° and we allow the satellite to drift ± 10°, the minimum angle of the spinaxis with the equator of the Earth is 81.8° and the maximum angle is 51.4°.

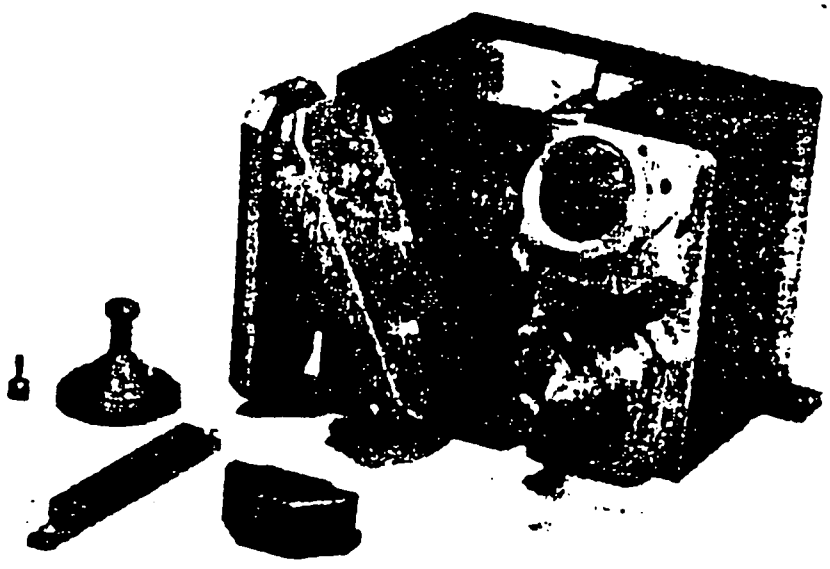

Figure 13.7: GALILEO ESS

13.4.3 IR-Earth Sensor

This sensor makes use of the rotation of the satellite to scan a cone. It consists of two immersed thermistor bolometers with a FOV of 1.5° x 1.5° and 4° apart. To make sure that the IR-sensor has the Earth in its FOV, we first calculate the dimensions of the Earth, seen from the satellite, while it moves through its orbit. The following formula is used to determine the diameter of the Earth in degrees.

$$d_a = 2\arcsin\left(\frac{r_a}{r}\right)$$

with: d_a = diameter Earth in degrees
r_a = radius Earth in km (6378 km)
r = distance to the center of the Earth in km

The results can be seen in figure 13.8.

When the Earth is projected on the celestial globe with the satellite in the center of it, and the spinaxis pointing north and considering the remarks in paragraph 13.4.2 we obtain figure 13.9.

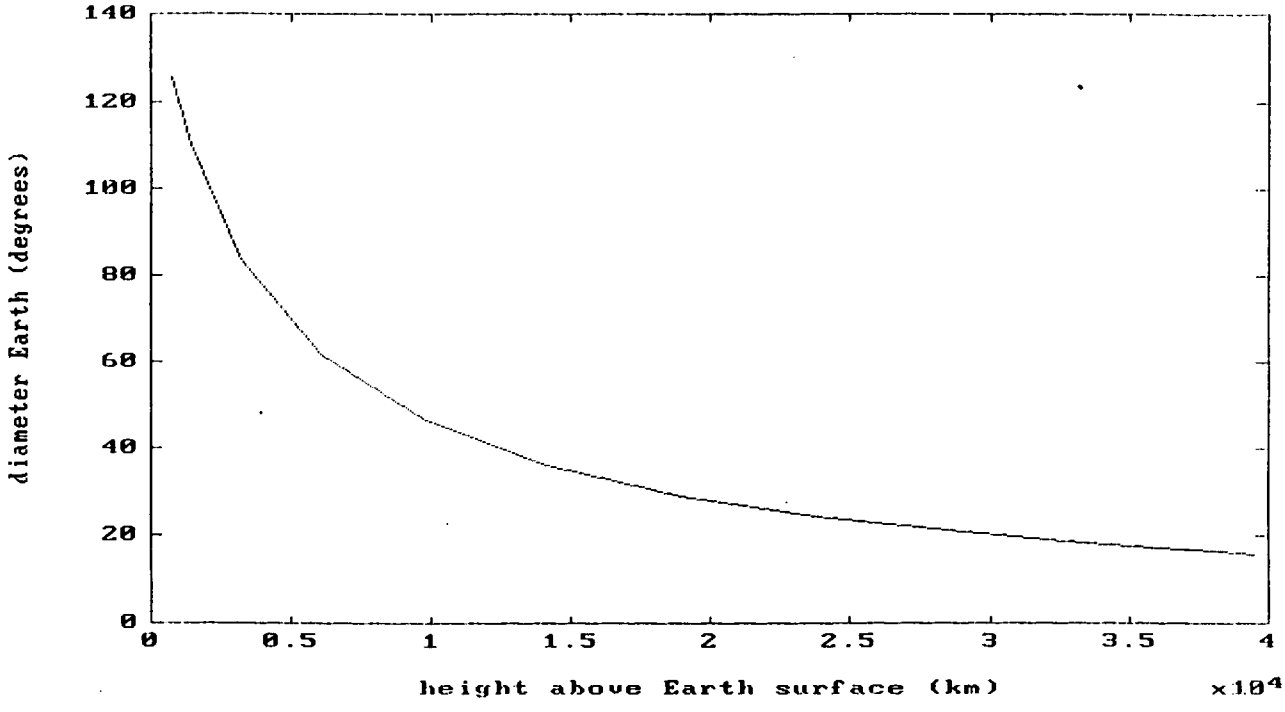

Figure 13.8: RESULTS DIAMETER EARTH

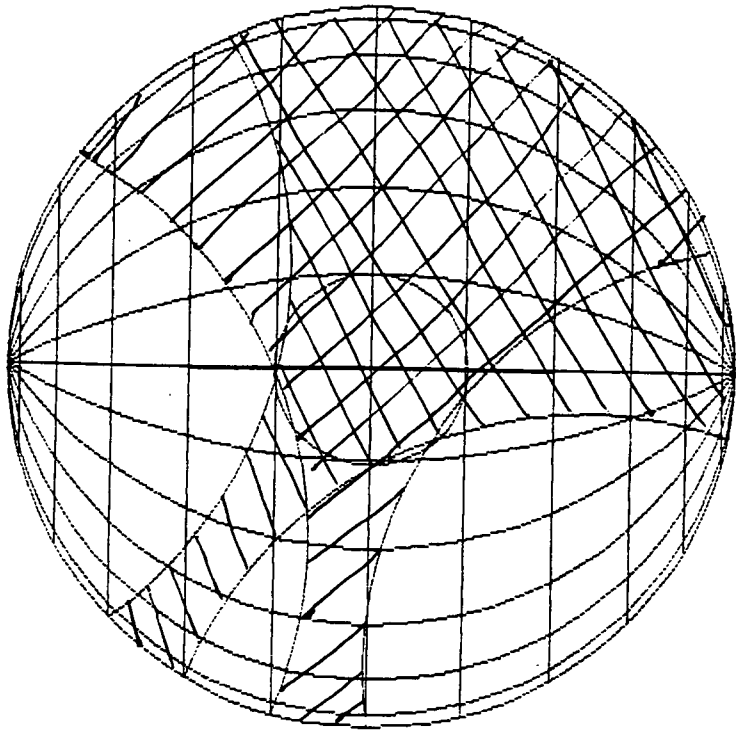

Figure 13.9: PROJECTION OF RESULTS ON CELESTIAL GLOBE

Easily can be verified that it's impossible with one or two sensors to see the Earth under all operational circumstances. Therefore it is necessary to have an extra constraint on the drift of the spinaxis. If this drift is kept within 3° it is possible to have the Earth in the FOV with two sensors. This is to be seen in fig. 13.10.

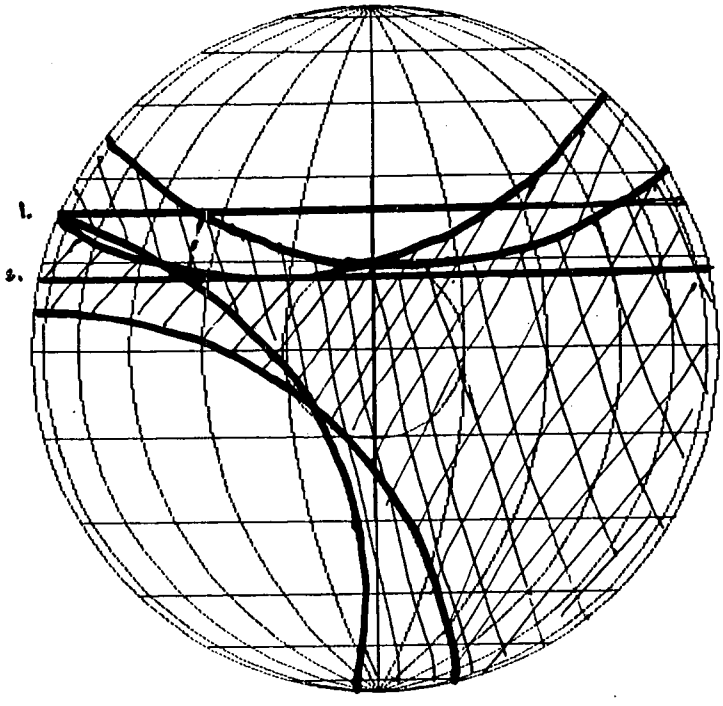

Figure 13.10: VISIBILITY EARTH

A mathematical model to solve the nadir vector from the outputs exists and can be found in lit. 13.1, page 230.

13.4.4 X-beam Sunsensor

It consists of two silicium slit sunpresence sensors that make an angle of 28°, with one slit perpendicular to the equator of the satellite. It produces two pulses during each rotation. From the pulses of the meridian slit the spinrate is determined. The FOV is shown in figure 13.11.

The sun elevation angle is determined with:

$$\tan\beta = \frac{\tan(28°)}{\sin(\omega \Delta t)}$$

in which β = the sun elevation angle
Δt = time between the pulse of the meridian slit and the skew slit pulse
ω = spinrate

The results are shown in figure 13.12.

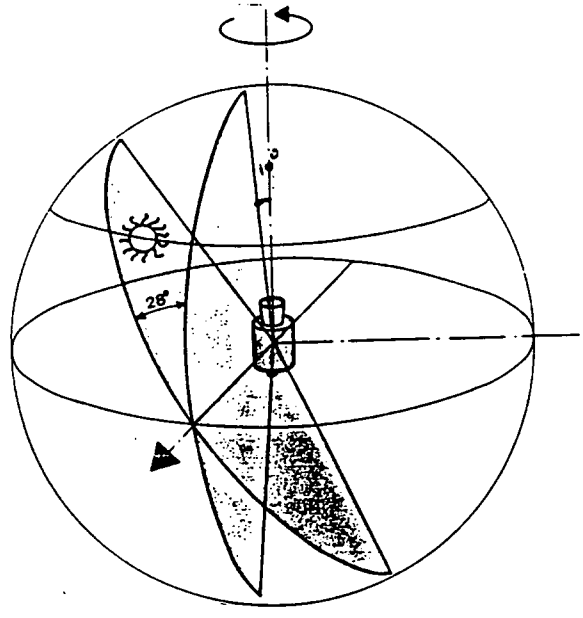

Figure 13.11: FOV X-BEAM SUN SENSOR

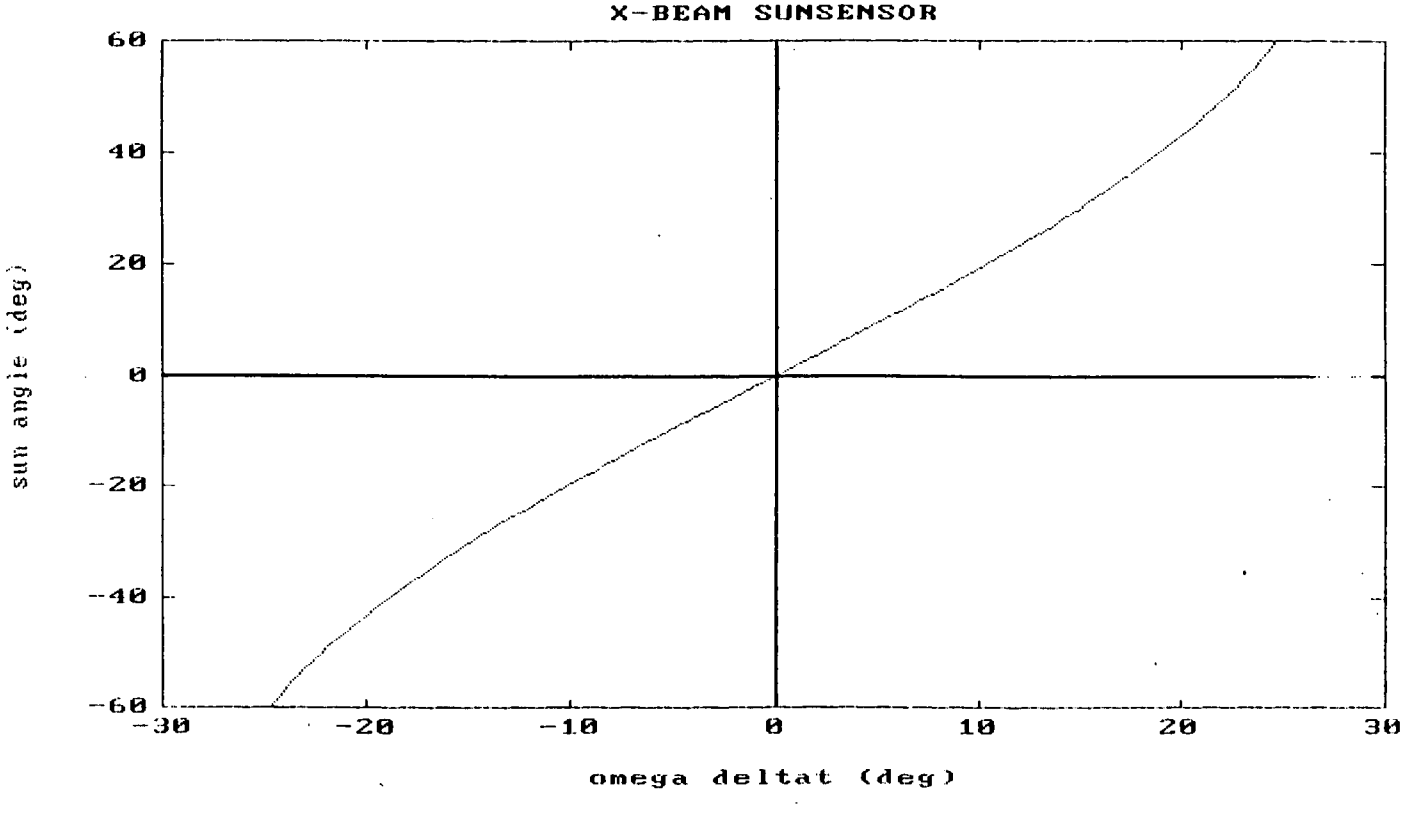

Figure 13.12: RESULTS SUN ELEVATION ANGLE VERSUS SPINRATE

13.4.5 Characteristics of the ESS

		X-beam sun sensor	IR-sensor	elec-tronics	sensor-housing
mass	kg	--	--	0.7	0.7
power	W	0.09	0.7	--	--
dim	mm	--	--	166x 150x65	166x 150x65
vol	mm^3	--	--	1.6e6	1.6e6
opt.bandwidth	µm	0.4 - 1.1	14-16.25	--	--
telesc.sighting	°	±80	m.n. i.w.	--	--
telescopes FOV	°x °	±60	1.5 x1.5	--	--
failure rate	Fr/h	128e-9	726e-9	unknown	--
accuracy	°	0.045	0.85	--	--
min.oper.spinrate	rpm	1	un-known	--	--

Table 13.2: CHARACTERISTICS ESS

13.4.6 Logic

The OBC determines the attitude from the pulses, connects the pulses with the payload-measurements and sends it to Earth. The OBC uses the thrusters to make attitude correction when necessary, for instance after an orbit correction.

13.5 MODEL

For the model we used the same equations and angle descriptions as in paragraph 13.3. To make the calculation time shorter, we made the assumption that the satellite is balanced. So the geometrical z-axis is the spinaxis. Furthermore we didn't use the exact moments of inertia as calculated by the configuration group, because the data wasn't available to us when we started to run the simulations. However that is not a problem, because the moments of inertia we used are almost the same. Besides, the configuration is likely to be changed anyway and so the moments of inertia. Also, we didn't consider the energy dissipation of the fuel, because it was too difficult to model.

We used the program Psi/e on an AT-computer. A complete print out of the program is shown in appendix I. The structure of the model can be found in figure 13.13.

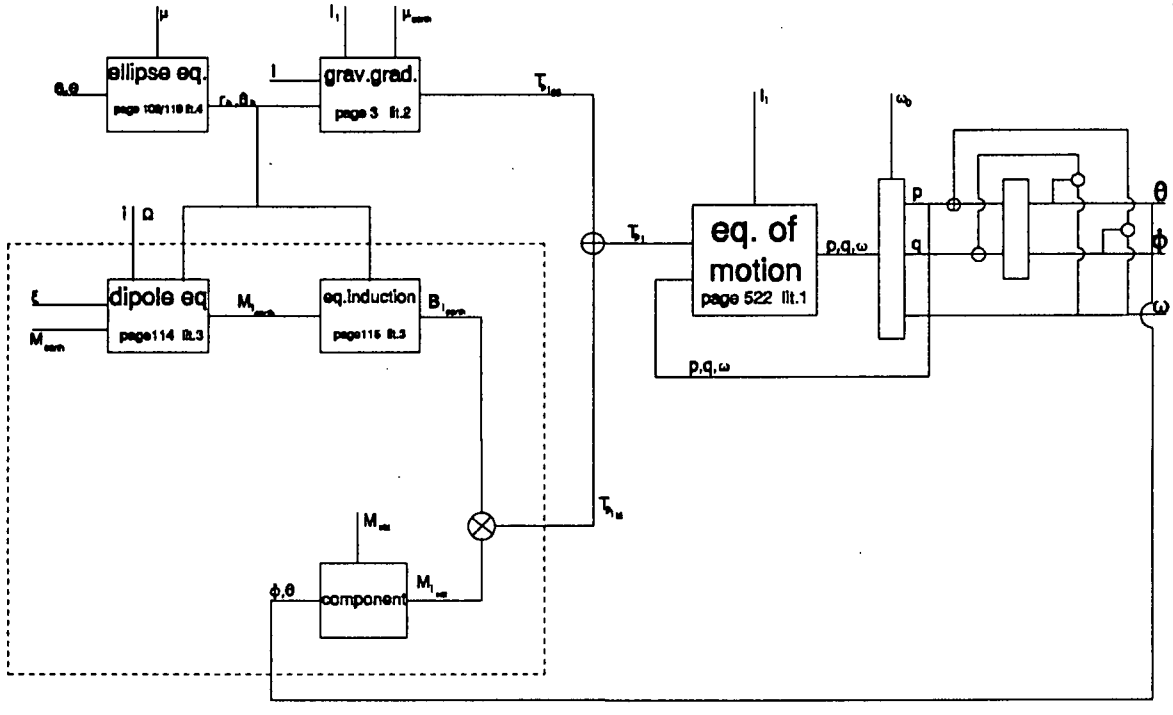

Figure 13.13: STRUCTURE MODEL

13.5.1 Results

First we run the program with the spinaxis about the minor axis of inertia. Also we applied some disturbances, caused by the inaccuracy of the thrusters. These disturbances are found in the print out of the model as begin conditions for PHI, THETA, P and Q.

I_{xx} = 2 kgm^2, I_{yy} = 2 kgm^2, I_{zz} = 0.8 kgm^2

The result in figure 13.14 shows that after 71360 s, which is about 1.7 orbits the maximum amplitude of the nutation is about 3°. This makes it necessary to dampen the nutation much earlier.

Secondly we run the program with the spinaxis about the major axis of inertia, with the same disturbances as in the previous simulation.

I_{xx} = 2 kgm^2, I_{yy} = 2 kgm^2, I_{zz} = 2.2 kgm^2

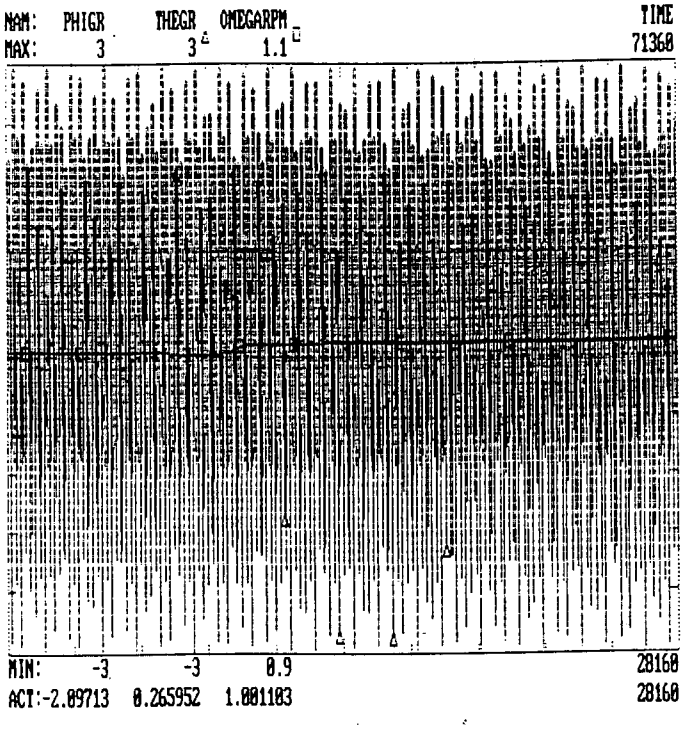

Figure 13.14: RESULTS PROGRAM RUN WITH SPINAXIS ABOUT MINOR AXIS OF INERTIA

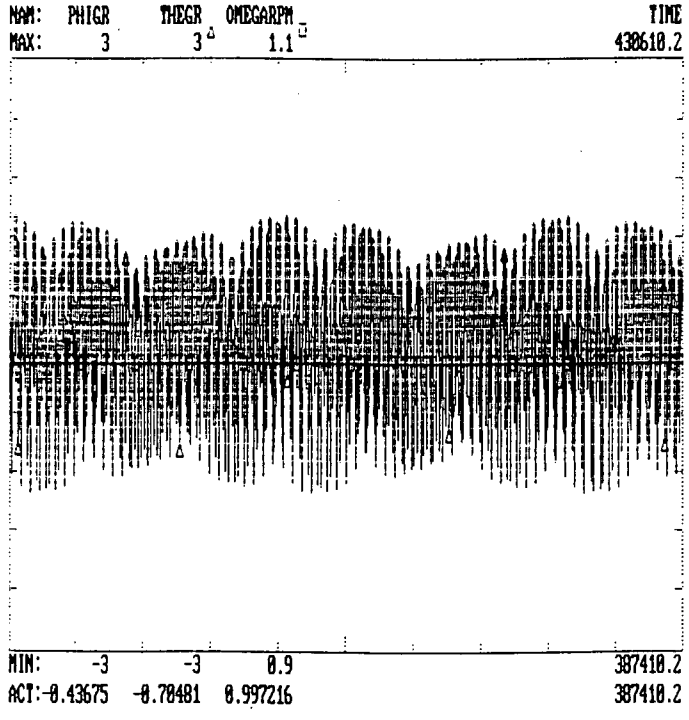

Figure 13.15: RESULTS SECOND PROGRAM RUN WITH SPINAXIS ABOUT MAJOR AXIS OF INERTIA

This picture (figure 13.15) now shows that even after 436100 s (≈ 10 orbits) the satellite is in a stable situation with an amplitude of the nutation of about 1.5°.

13.6 CONCLUSIONS

The ESS is a suitable sensor for this mission. However some difficulties concerning this sensor have to be studied. The accuracy of the IR-Earth sensor at 1 rpm has to be determined and if it's not sufficient, a way must be found to make it accurate enough. For instance one can consider to have the output of the sensor directly by the computer without intervenience of the electronics. Another problem is the use of the IR-Earth sensor in the vicinity of the perigee. Probably this will not be a problem, because we have two IR-Earth sensors which have the Earth in its FOV (figure 13.9) at low altitudes. So eight pulses will be available.

The major problem however is the stability. This has to be studied more carefully. Nevertheless some things based on the results of the model can be said. The advantage of a lower mass when an active nutation damping will be used, is partly canceled by the extra use of fuel. Furthermore it is probably necessary to use the thrusters frequently. Because the thrusters have a warming up period of 30 minutes, this might be a problem.

At last we mention the high costs to develop and test such a system.

All this considered we think it's best to use the option of the passive nutation damping. A passive system is simple and reliable. Deployable beams can be developed at much less costs and one has more experience in it. So even though it takes more weight, we prefer the passive nutation system, however further study is necessary.

14. THERMAL CONTROL

14.1 INTRODUCTION

A spacecraft contains many components that will only function properly if they are maintained within specified temperature ranges. The temperatures of these components are influenced by the net energy exchange with the spacecraft environment. Component temperatures are established by the heat radiated from external surfaces to the space sink, internal equipment heat dissipation, together with the characteristics of the conductive and radiative heat transfer paths between these "sources and sinks". The objective of thermal control is to provide the proper heat transfer between all spacecraft elements, so that the temperature sensitive components will remain within their specified temperature limits during all mission phases.

In this chapter will be referred to a computer program called JASON, which can be run on a PC. This program, developed by Ing. Kanis from Fokker Space & Systems, is a thermal analysis program that can perform steady state and transient calculations. The formulas used in this program are included in appendix II.

14.2 THERMAL SPECIFICATIONS

To create the proper thermal environment for all subsystems, first of all the thermal requirements of the different subsystems are needed. Those requirements are listed in table 14.1. They have been derived from experiences from the past, and form data of the instruments.

Since all subsystems only have to operate outside the Van Allen Belts, there is no need to keep the satellite in the operating temperature range during the complete orbit. During the eclipses, that only take place outside the measuring period, i.e. inside the Van Allen Belts, the satellite is allowed to cool down.

Special attention has to be paid to the payload electronics (filters, mixers) and the fuel system (tank, pipes) which have to be kept at a specific temperature with a very narrow margin.

14.3 THERMAL DESIGN GOALS

The satellite system must be designed in such a way that satisfactory temperature environments will be maintained for all components during separation sequences, non-operational

Subsystems	Component	Operating	Non Operating
Payload	Filterbank	20°±1°C	-30°/60°C
	Mixers	20°±1°C	-30°/60°C
	PL transp.	-10°/40°C	-30°/60°C
	Pre-amplifier	-10°/40°C	-30°/60°C
	Antennae	-15°/300°C	-15°/300°
	Mlt.plier	-10°/40°C	-30°/60°C
	Pos.det.syst	-10°/40°C	-30°/60°C
Comp/TTC	OBC	-10°/40°C	-25°/50°C
	Interface	-10°/40°C	-30°/60°C
	Patches(DownLi)	-55°/260°C	-55°/260°C
	Receiv/transp	-70°/115°C	-70°/115°C
Power	PCU	-10°/50°C	-25°/40°C
	PCDU	-10°/50°C	-25°/40°C
	Battery	10°/25°C	10°/30°C
	Solar Array	-180°/85°C	-180°/85°C
Propulsion	Hydrazine	5°/30°C	5°/30°C
	Tank/Pipes	5°/30°C	5°/30°C
	Thruster/valves	5°/30°C	5°/30°C
AC	Sensors	-20°/50°C	-30°/60°C
	Electronics	-10°/40°C	-30°/60°C
Structure		-20°/40°C	-20°/40°C

Table 14.1: THERMAL REQUIREMENTS OF THE SUBSYSTEMS

and operational stages of the mission including eclipse periods. The thermal control will be achieved by passive means (ie. excluding moving parts), but may include heaters with automatic control and ground command override capability. The thermal system must be designed to maintain all equipment within operating thermal range while the satellite is in operating mode.

- the thermal design must be a passive one
- the thermal design may include heaters whenever necessary
- the thermal design must be a low cost design
- the thermal design must be a low mass design
- the thermal design must create a proper thermal environment for all spacecraft systems
- the thermal design must be fail safe

14.4 THERMAL ENVIRONMENT

The temperature of a satellite in orbit is a direct consequence of the complex interaction of incoming and outgoing radiation together with the internal heat production. The incoming radiation is a combination of Solar radiation, Albedo radiation and Earth radiation. Space background radiation, convective heat exchange and heat exchange due to micrometeorite impact are neglected. (Overall contribution of these heat inputs is less then 0.10 %)

14.4.1 Solar Radiation

The solar radiation is assumed to be 1400 W/m^2 over the complete orbit.

14.4.2 Albedo Radiation

Albedo radiation is solar radiation, reflected by the Earth, without changing the spectral distribution. With a mean reflectance value of 0.30 the albedo radiation immediately above the Earth's surface is 420 W/m^2. With the energy-distance relation:

$$I_a = I_{a_o}(\frac{R}{r})^2$$

the albedo radiation in orbit can be calculated.

14.4.3 Earth Radiation

The infra-red Earth radiation at the surface of the Earth is assumed to be 245 W/m^2. With the energy-distance relation, the Earth radiation can be calculated.

The total heat input from the environment to the satellite is assumed to be 5 Watts.

14.5 DETERMINATION OF MISSION PHASES

14.5.1 Pre-Launch

During pre-launch operations, the primary heat load is the surrounding environment. Airconditioning of the area were the satellite is stored and prepared will provide a proper thermal environment for the satellite.

14.5.2 Launch

During launch the heat load comes from the fairing. After fairing-jettissoning the heat load is induced by the aerodynamic heating. The launch phase is assumed to be uncritical and has therefore not been verified.

14.5.3 In Orbit Operations

When the satellite is in orbit two operation modes can be distinguished, namely the eclipse and the operating mode.

boxes/nodes	dissipated power operation mode (W)	dissipated power eclipse mode (W)
structure	5.0	0.0
computer	5.5	5.5
payload	3.3	0.0
filters	1.5	0.0
transp.+pos.det.	8.2	1.5
ESS 1	0.8	0.8
ESS 2	0.8	0.8
processor+mult.	2.0	0.0
PMAD	6.0	3.0
battery	0.0	3.0
electrical unit	1.0	1.0
total	**34.1**	**15.6**

Table 14.2: DISSIPATED POWER IN OPERATION AND ECLIPSE MODE

During eclipse mode, which has a maximum duration of approximately 1.5 hours, not all subsystems will be working so the internal dissipated power is less than in operating mode. Consequently the satellite will cool down. In table 14.2 the dissipated power in each mode is shown.

Every word in the left column represents a box/node. In every box different systems are situated.

14.6 THERMAL ANALYSIS

To start with a one-node analysis is made of the satellite as a whole. The next phase is to divide the satellite in important thermal nodes (tanks and structures) and to examine their thermal behaviour and thermal gradients. Finally a detailed thermal analysis is made to make sure that none of the electronic boxes or other equipment exceed their temperature limits.

14.6.1 One node steady state body calculation

In this calculation the spacecraft interior is assumed to be totally insulated from its environment except a dedicated radiator. The node represents the radiator of the satellite. The only heat flux possible from the node is through its radiating surface into space. The radiator is always pointed to deep space. The solar input through the insulation is set on 5 Watts. Due to conductive and radiative heat transfer between the spacecraft interior and radiator, the radiator is assumed to be 10°C cooler than the box.

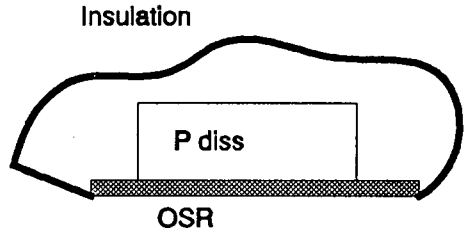

Figure 14.1: ONE NODE STEADY STATE BODY

The radiator is made of an OSR (Optical Solar Reflector, ε=0.85), while the area not covered with OSR is assumed to be totally covered with MLI (Multi Layer Insulation).

If the temperature of the satellite interior is set on 20°C and the total internal power is 25 W we find for the radiator area needed:

$$P_{diss} + q = \epsilon \cdot \sigma \cdot A \cdot T^4$$

$$25 + 5 = 0.85 \cdot 5.67x10^{-8} \cdot A \cdot (283)^4$$

$$\mathbf{A = 0.095\ m^2}$$

This "first-guess" area is used as radiator area for a more detailed model, which is modelled in the computer program JASON.

14.7 THERMAL ANALYSIS OF THE SPACECRAFT BODY

To perform a thermal analysis of the spacecraft body the spacecraft needs to be broken down into a number of nodes. To do this, a trade-off must be performed to determine which parts can be modelled as a single node.

Node number	Node name	Status
1	space	boundary
2	radiator	floating
3	plate	floating
4	tank	floating
5	structure	floating
6	computer	floating
7	payload	floating
8	filters	floating
9	transponder + pos.det.	floating
10	ESS	floating
11	processor + mult.	floating
12	ESS	floating
13	PMAD	floating
14	battery	floating
15	electrical unit	floating

Table 14.3: USED NODES AND THEIR STATUS

The following criteria are used as a basis for the trade-off.

- the nodes must be chosen in accordance with the temperature uniformity which may be expected
- the nodes must be chosen in accordance with the physical problem studied
- the used thermal analyzer JASON has a restriction of 20 nodes maximum

It is beneficial to allocate one node to each subsystem equipment box. However, a few more nodes must be added.

14.7.1 Design Concept

14.7.1.1 Objectives

The primary objective is to keep the satellite within their temperature range. A couple of payload items dictate a constant temperature of about 20°C. To achieve this firstly the satellite has to be insulated from its environment and secondly the heat produced by the boxes has to be transferred to the outside in a proper way. Specific:

- the outer walls are insulated by blankets on the outside (except part of the top wall which functions as radiator)

- the plate, the walls, the radiator are conductively insulated from each other

- the solar arrays are covered by blankets at the spacecraft internal face

- the radiator functions as an OSR (mirrors on the outside) to provide maximum heat rejection

- all boxes are painted black

- heaters and thermistors are placed on the tank/pipes and filters

14.7.1.2 Assumptions

To model the thermal heatflows the following assumptions are made:

- the heat dissipated in the boxes on the plate is transferred to the bottom plate by means of conduction only and to the boxes on the top plate and the walls by radiation only

- the same goes for the boxes on the radiator

- the heat from the plate is transferred to the radiator by means of direct radiation and radiation via the 'vertical' walls which are reflecting on the inside

- the solar input is 5 W (through the insulation)

14.7.1.3 Model

The satellite and its environment is modelled in 15 nodes which are defined in table 14.3. Heaters and thermostats are applied to the filterbanks, the fuel tank and the fuel pipes because of their severe thermal requirements. Furthermore the filterbanks are insulated with blankets to make them less dependant on temperature level and fluctuations in the spacecraft interior.

To calculate the temperatures of the boxes in 'steady state' as well as 'transient' (complete orbit) conditions the program JASON (lit. 14.6) is used. For a clear figure please refer to chapter 56, paragraph 34 page 37408.

14.7.1.4 Operation Phases

Since the orbit has a period of twelve hours and just one ground station is used, only one of each two orbits can be used to do measurements. Because of this it would not be necessary to keep all the boxes (esp. payload) switched on during each second orbit. But switching off almost all boxes during the second orbit would cause a too large temperature drop. Therefore, while there is sufficient power available, it has been decided to keep the satellite fully operational during all orbits. In this way there is only one operation phase, which makes the thermal design more simple. So two modes are distinguished, the operation phase and the eclipse phase.

14.7.2 Radiative Coupling

In modelling the heat transport by means of radiation only the radiation from the bottom side of the boxes on the upper plate to the top side of the boxes on the lower plate is taken into account. It is thus assumed that no gradient exists between the mounting plane and the box lids.

No radiation between boxes on the same plate is modelled. This assumption can be justified by the fact that the boxes on one plate are about the same temperature (also the magnitude of the size of the boxes is of the same order). The overall heat exchange by radiation between boxes on one plate is very small, compared to conduction.

To calculate the view factors between two parallel planes of arbitrary size, a program was written. (For the used formulas see appendix I). With this program the following view factors were determined.

The first box defines the view factor from node 6 to node 7 (only the view factors from the upper to the lower boxes are modelled).

nodes	7	10	12	13	14
6	9.75×10^{-3}	.512	1.56×10^{-3}	6.69×10^{-3}	3.35×10^{-2}
9	1.28×10^{-3}	9.70×10^{-4}	0.319	.291	2.49×10^{-2}
11	0.412	7.67×10^{-3}	7.52×10^{-3}	3.10×10^{-3}	2.95×10^{-3}
15	0.131	0.135	2.18×10^{-2}	3.15×10^{-2}	1.69×10^{-2}

Table 14.4: VIEW FACTORS FROM UPPER TO LOWER BOXES

14.7.3 Gebhart Factor

The radiative coupling between the upper (radiator) and lower plate is built up of direct component (view factor), and a component which accounts for the heat reflected via the side walls of the spacecraft interior, covered by MLI. To put this concept in a model the Gebhart factor had to be calculated.

$$B_{ij} = F_{ij} * \epsilon_j + \sum_k B_{kj} * F_{ik} * \rho_k$$

Where B is the Gebhart factor and F is the view factor of node i to j. The reflectivity (ρ) of the MLI is assumed to be $1-\varepsilon=0.99$. If no reflection via the side walls is applied (black paint, $\varepsilon=1$) a coupling of 0.30 is possible and a model of viewfactors is sufficient. With reflection a coupling of .85 is possible (The reflection directs the radiation to the radiator).

The radiative couplings determined in this paragraph serve as input for the thermal analysis program JASON.

14.7.4 Conductive Coupling

In modelling the heat transport by means of conduction only the conduction between boxes and the plate on which the boxes stand is taken into account. No conduction between upperplate/radiator and lower plate is modelled. In fact the two plates are assumed to be perfectly decoupled from the rest of the satellite. So heat transport from the lower plate to the radiator only takes place by radiation.

The advantages of this 'configuration' are:

- no heat leaks to the rest of the satellite (e.g. solar arrays)

- it simplifies the calculations considerably and thus the temperature can be predicted more accurately

The conductive coupling has been calculated with the following formula:

$$C_{ij} = \frac{k \cdot A}{l}$$

where C: coupling for conduction
k: conduction coefficient
A: contact area
l: conduction distance

With this formula we find the following C's given in table 14.5.

The first box indicates the conductive coupling from node 2 to node 6.

These calculations also serve as input for JASON.

nodes	6	7	8	9	10	11	12	13	14	15
2	54	0	0	25	0	10	0	0	0	17
3	0	24	80	0	15	0	15	24	23	0

All numbers x 0.1 W/K

Table 14.5: CONDUCTIVE COUPLING COEFFICIENTS

14.7.5 Heat Capacities

For transient analysis the heat capacities are needed as input for JASON. The heat capacities for the different boxes can be found in table 14.6.

14.7.6 Heater Powers

The heater power of the tank is provisionally set on 1.0 W and the heater power of the filterbanks on 1.5 W.

Node number	m*heatcapacity kg.J/K
2 radiator	1000
3 plate	1000
4 tank	10000
5 structure	9000
6 computer	4200
7 payload	2000
8 filters	800
9 transponder + pos.det.	2500
10 ESS	800
11 Processor + mult.	1000
12 ESS	800
13 PMAD	2500
14 battery	3500
15 electrical unit	600

Table 14.6: HEAT CAPACITIES

14.7.7 Steady State Calculations

When the preceding is taken into account the model can be put in JASON and 'steady state' as well as 'transient' calculations can be made.

The calculated steady state temperatures are shown in table 14.7. These temperatures are the limits between which the real temperatures vary.

14.7.8 Transient Calculations

For the two operation modes (operations and eclipse) the temperatures of every node is calculated with JASON. The maximum eclipse time is set at two hours and the operation mode duration is set at ten hours.

The most important nodes are 4, the hydrazine tank, and 8, the filters. In the figures 14.2 can be seen that the temperatures remain well within the limits.

Node number	[T°C] operation mode	[T°C] eclipse mode
1. space	-269	-269
2. radiator	4.9	-39.4
3. plate	18.1	-27.8
4. tank	15.7	-66.3
5. structure	15.3	-75.8
6. computer	6.1	-38.3
7. payload	19.3	-27.9
8. filters	19.9	-27.8
9. transp. + pos.det.	8.3	-38.7
10. ESS	18.0	-27.6
11. proc+mul	7.0	-39.3
12. ESS	18.5	-27.4
13. PMAD	20.4	-26.6
14. battery	18.1	-26.5
15. electr unit	5.6	-38.7

Table 14.7: STEADY STATE TEMPERATURES

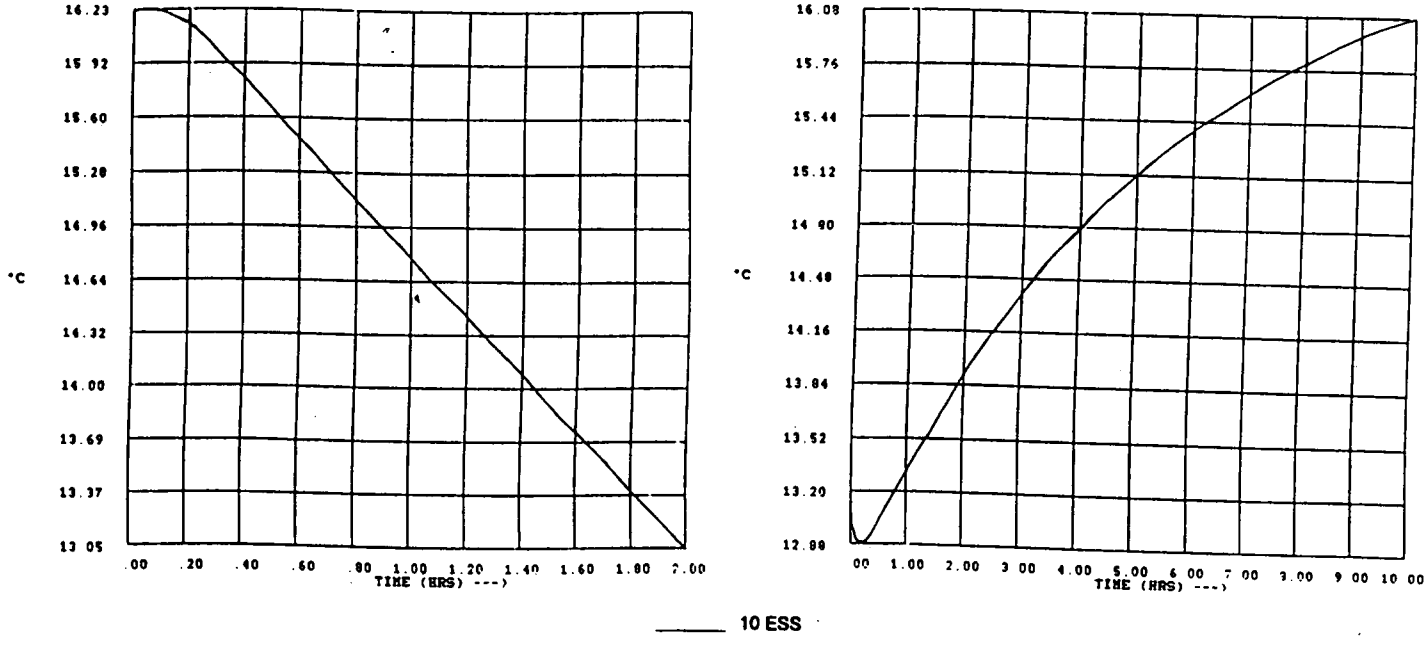

Figure 14.2a: TRANSIENT CALCULATIONS

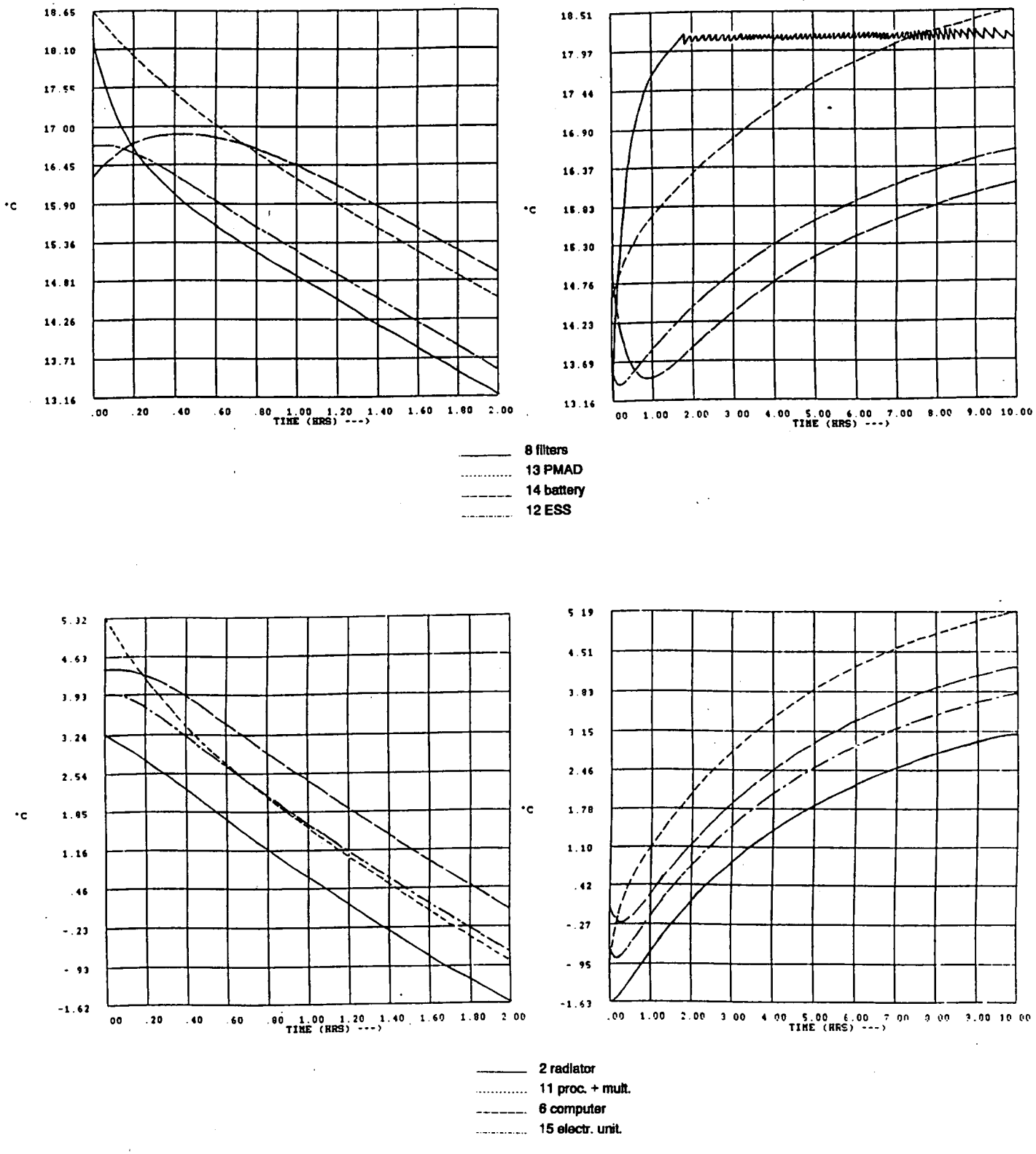

Figure 14.2b and 14.2c: TRANSIENT CALCULATIONS

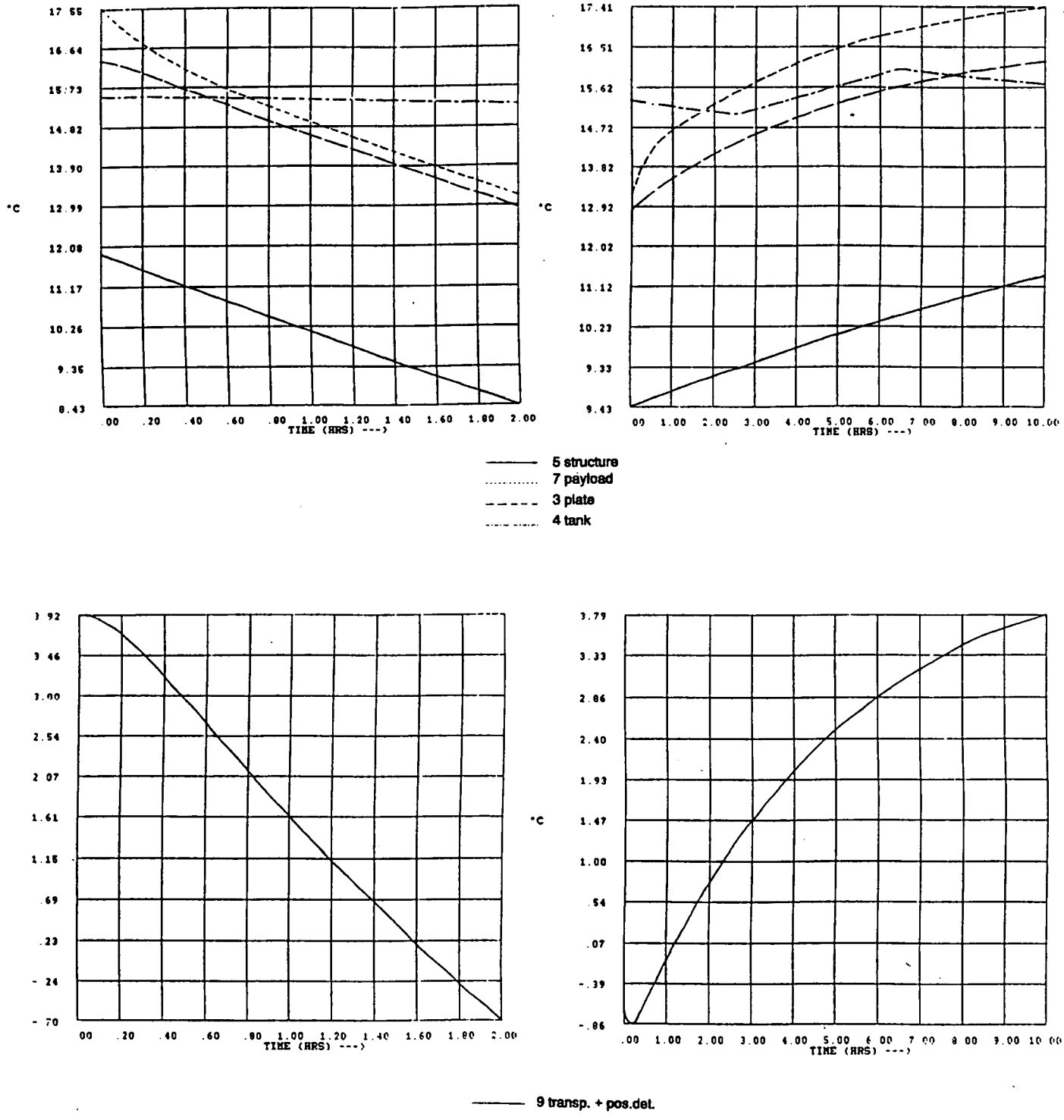

Figure 14.2d and 14.2e: TRANSIENT CALCULATIONS

14.8 MASS BUDGET

The massbudget available to the subsystem Thermal Control was initially 1.5 kilograms.

description	Mass (kg)
blankets (2.3 m^2)	0.9
thermistors	0.02
heaters	0.05
paint	0.5
total	**1.47**

Table 14.8: MASS BUDGET

14.9 POWER BUDGET

The thermistors on the filters and the tank only control during the operation mode. This is feasible because the eclipse mode has a maximum duration of 1.5 hours. And in this time the satellite will not cool down more than about 7 degrees.

Nodes	Enabled in sec.	Duty cycle	Power installed (W)
4 tank	14000	0.40	1.0
8 filters	17000	0.50	1.5

Table 14.9: POWERBUDGET

10. CONCLUSIONS

Altogether the concept seems feasible. In the model all thermal requirements are met. However, there remain some points where improvements may be necessary. The most important one is the layout of the boxes. Because of their upper limit in temperature specification (25°C) and the uncertainty in the calculations (up to 15°C) the battery and the filters which are located on the plate might have to be placed onto the radiator instead (on which the temperature is about 10°C lower).The limits of the radiator area does not allow to lower the 25 °C temperature level significantly. The rearrangement of the boxes, or an enlargement of the radiator, or the allocation of a second radiator area, will most likely cause a complete change in the configuration of the boxes, c.g. spacecraft.

15. TELEMETRY AND TELECOMMAND

15.1 INTRODUCTION

To realize all data-transport between the groundstation on earth and the satellite in space the telemetry and telecommand (TTC)-subsystem has to be designed.

First, certain TTC-subsystem requirements specified by ESA have to be met. A summary of these requirements is given below:

- The TTC-subsystem has to provide necessary monitoring and control of the satellite throughout all mission phases. The system will be designed to permit the detection of the satellite's degradation and anomalous performance during all phases of the mission.

- It will be possible to operate the TTC-system in any mode without degradation of, or interference from any other subsystem. The TTC-system will retain at maximum operational capability under abnormal or emergency conditions including any anomalous attitude. It is envisaged that, for the latter operation mode, the TTC-system will be accessible through a wide coverage antenna which will be permanently connected.

- The telecommand format will provide means off uniquely addressing each spacecraft of a serie so that the probability of commanding the other spacecraft, when illuminated by equivalent RF flux density, is less than one part in 10^{+9}. The decoded bit error rate for telecommand services will be superior to one part in 10^{+7}, for telemetry to one part in 10^{+6} over the nominal range of RF flux densities to be specified.

- The design of the satellite will preclude the accidental execution of any hazardous command. Initiation of one shot operations involving hazardous commands will require at least two separate actions, command and execution, each verifiable by telemetry.

15.2 TELEMETRY

Aerospace telemetry should be defined as the science of transmission of information from air space vehicles to accessible locations on earth. Three types of data have to be transmitted:

- the measured signal
- the housekeepingdata
- the ranging tones

To get the measured signal to earth it has to be multiplexed, converted to a digital data flow and set in a telemetryformat (see figure 15.1). According to the Nyquist Theorem the sample-frequency has to be at least two times higher than the bandwidth of the 6 measured signals, which is 25 kHz per signal.

It is required that the signal is transmitted to earth with an inaccuracy less then 2 %. Therefore the multiplexed signal has to be converted in 6 bits:

inaccuracy of 1/64 * 100 = 1.5 %

The total bitrate is 1.8 megabits per second! The equipment for this bitrate isn't often used and certainly it isn't on-the-shelf.

Due to the high frequencies used, another difficulty is introduced, namely the multiplexer and A/D converter are very sensitive for free protons and electrons in the Van Allen Belts. These instruments can easily be destroyed if they are not well protected.

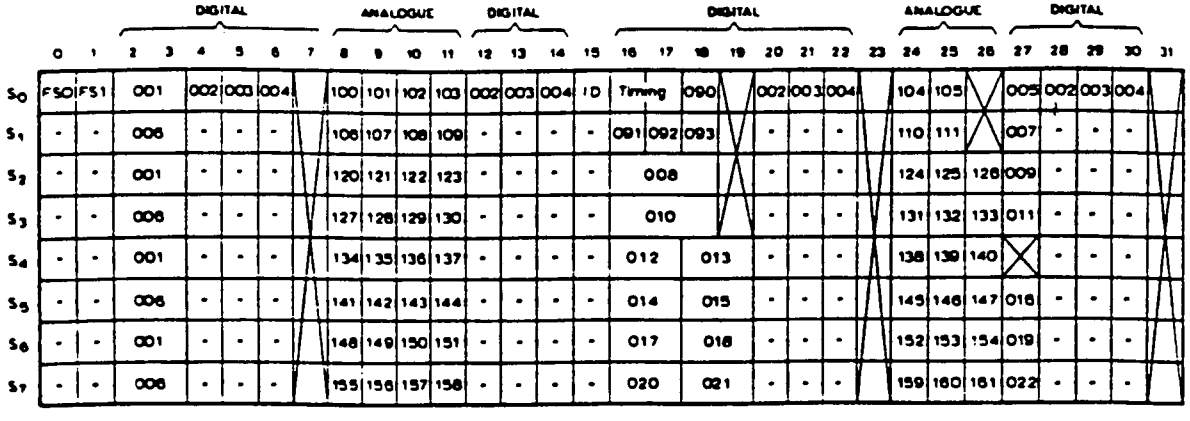

Figure 15.1: AN EXAMPLE OF A TELEMETRY FORMAT

According to the computer subsystem (OBC) the housekeeping data contains about 80 bytes, coming directly from the OBC. It has to be transmitted to earth at least once per 15 minutes.

At the beginning of every measurement interval 16 kbytes have to be downloaded.

The 7 ranging tones vary in frequency from 16 to 100 kHz. They are transmitted to earth and to the other satellite. To get the accuracy of the distance to 1 meter, tone-ranging has to be done every 5 minutes.

The last two signals are very different from the first; especially the bitrate and the time cycle. Therefore the downlink is divided into two separate ways:

- HBR (high-bit-rate): downlink of measurement data. (see figure 15.2)

- LBR (low-bit-rate): downlink of housekeeping data and transmission of the ranging tones. (see figure 15.3)

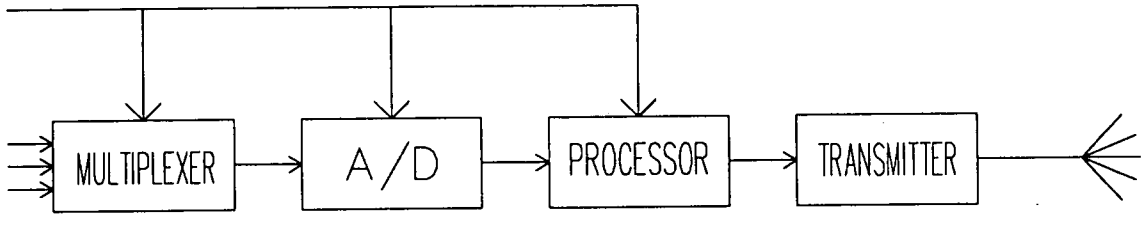

Figure 15.2: FLOWDIAGRAM OF THE HBR TELEMETRY DATA

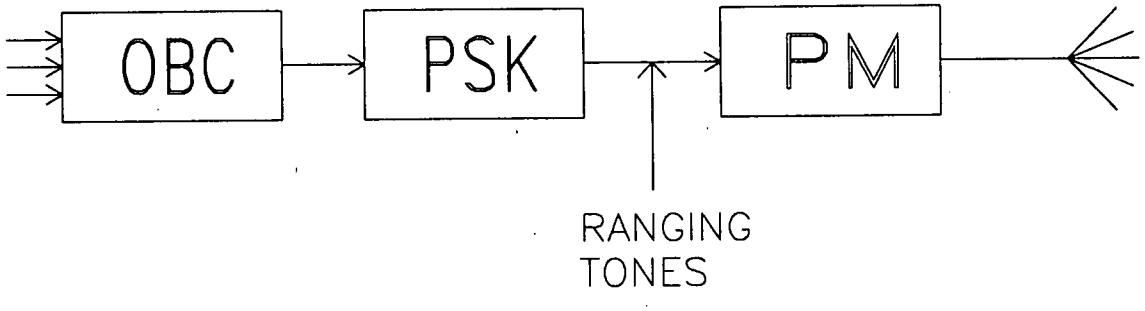

Figure 15.3: FLOWDIAGRAM OF THE LBR TELEMETRY DATA

The HBR telemetry data will be transmitted using the PSK-method (Phase-Shift-Keying), because this is a commonly used method. Also PSK has the lowest threshold power compared to all other systems, see table 15.1. The signal to noise ratio for a probability error of 10^{-6} (see ESA-specifications) is, according to figure 15.4, 11 dB.

A more detailed description of the PSK modulation is displayed in figure 15.5. The carrier-frequency is 2200 MHz and the bandwidth is 1.8 MHz. Datacompression is not possible on white noise.

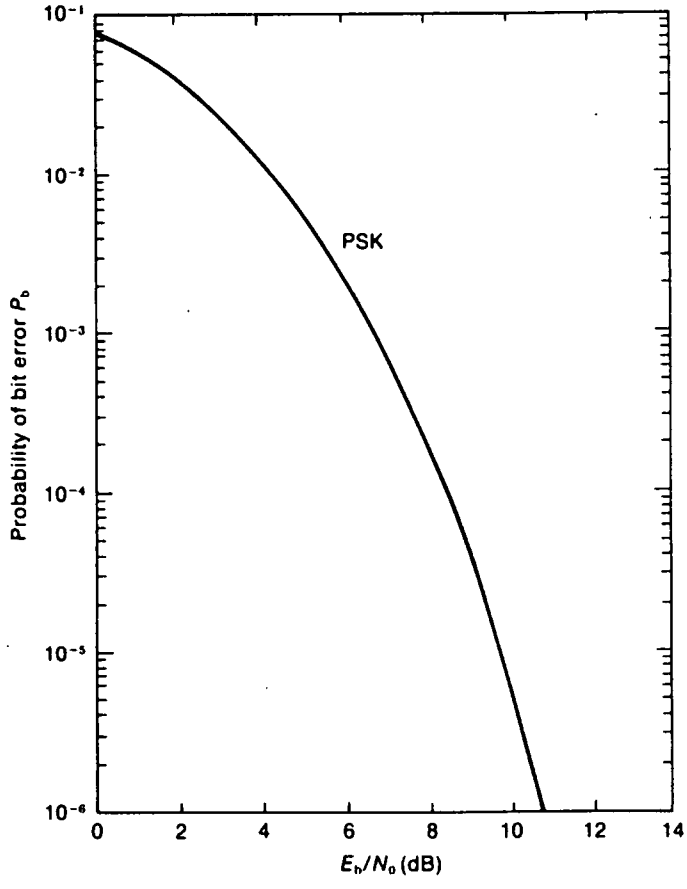

Figure 15.4: PROBABILITY OF BIT ERROR OF PSK

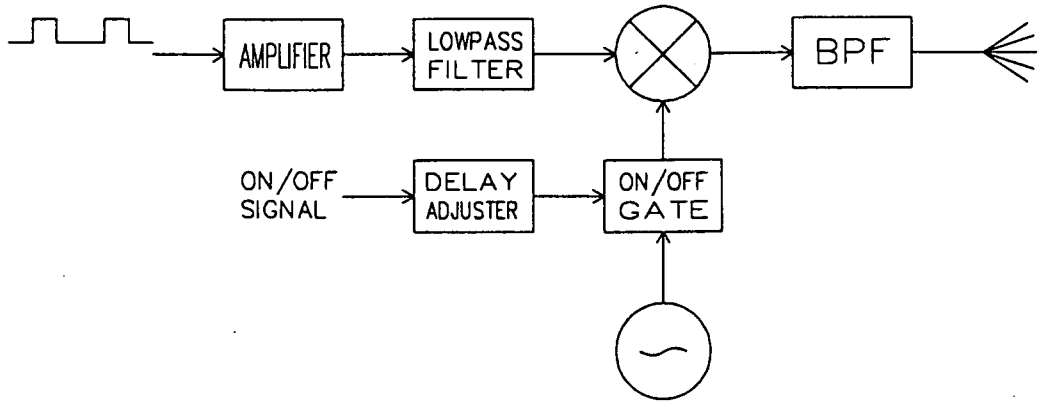

Figure 15.5: PSK MODULATOR

Method	Threshold power rel. to PSK
PCM/PSK	1
PCM/AM	2
PCM/FM	1.1
PCM/PM	±1.3

Table 15.1: COMPARISON OF THRESHOLD POWER

The LBR is transmitted by a subcarrier method: PSK/PM (Phase-Shift-Keying/Phase Modulation). The transmission used is an ESA-standard telemetry system and displayed in figure 15.6. The PSK-modulator is the same as for the HBR, the PM-modulator is displayed in figure 15.7. The spectrum belonging to this scheme is displayed in figure 15.8.

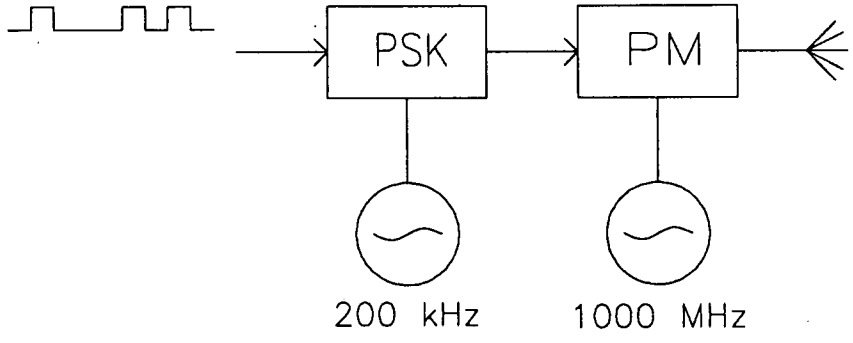

Figure 15.6: LBR TRANSMITTER

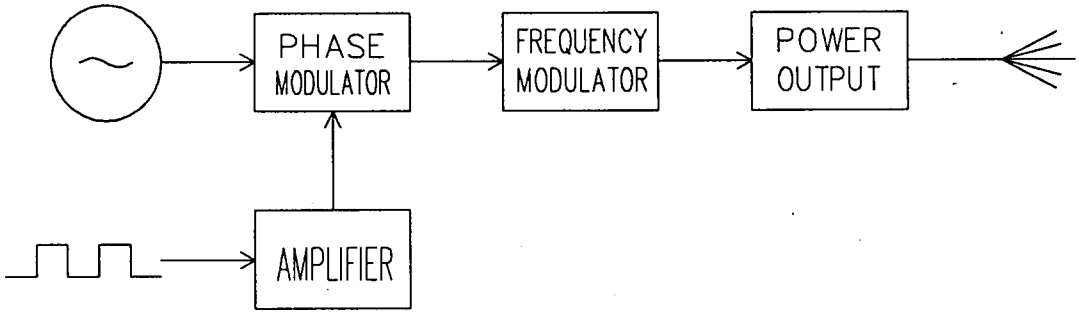

Figure 15.7: PHASE MODULATOR

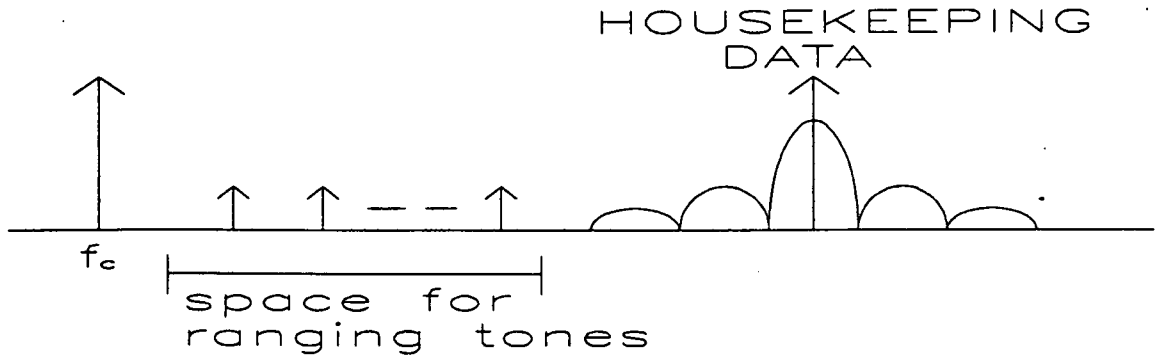

Figure 15.8: FREQUENCY SPRECTRUM OF THE LBR TRANSMITTER

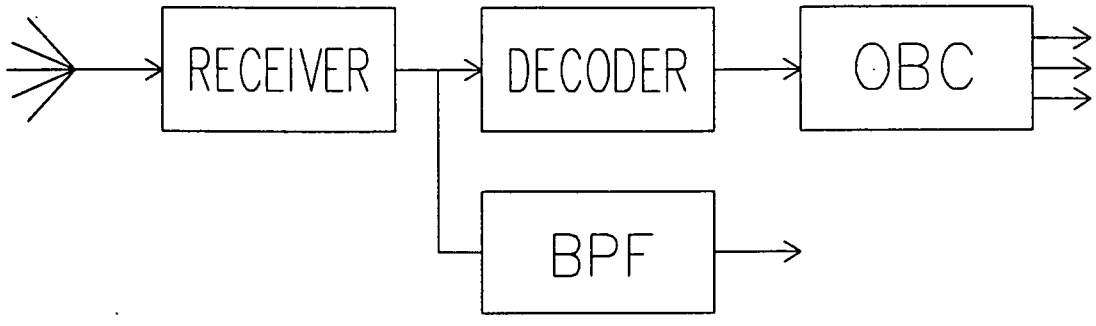

Figure 15.9: FLOWDIAGRAM OF THE HBR TELECOMMAND DATA

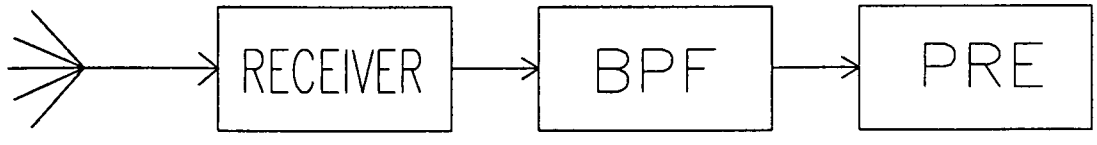

Figure 15.10: FLOWDIAGRAM OF THE LBR TELECOMMAND DATA

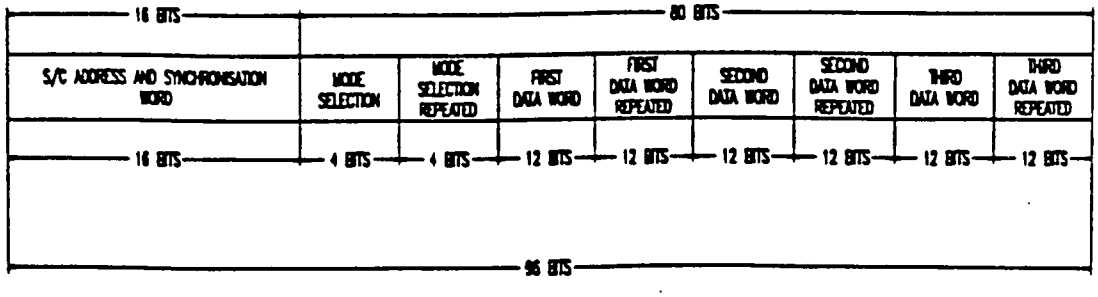

Figure 15.11: EXAMPLE OF A TELECOMMAND FORMAT

The free-space between the remaining pulse and the PCM-spectrum of the housekeeping data is accessible for the ranging tones. The carrier-frequency is about 2000 MHz.

15.3 TELECOMMAND

Telecommand is controlling the satellite, i.e. sending data from earth to the OBC of the satellite. On the satellite the bandpassfilters of the measured signal are to be controlled from the ground.

The thrusters etc. are fully controlled by the computer. So only the memory of the OBC has to be uploaded. This will be done once per 1 or 2 orbits with the HBR receiver. The flow of all received data is displayed in figure 15.9 and 15.10. An example of a telecommandformat is given in figure 15.11.

As said before, the ranging tones and housekeeping data are put on the carrier frequency of the LBR. Therefore the signal coming from the receiver has to be divided in 2 parts. A different bandpass-filter is put on each of these parts.

A signal is sent to the HBR. This signal contains the telecommand data from earth. The carrier frequency is used as a clock signal for the payload subsystem and for the multiplexers, A/D-converter and processor of this subsystem.

15.4 THE ANTENNA

According to the ESA-specifications, the satellite has to send and receive omnidirectional in uncontrolled situations. This requires antennas on all surfaces of the satellite. Considering the surfaces required for power generation these antennas must be small. Therefore parabola and horn antennas were dropped.

A solution could be the so called "high-far-wraparound" antenna. But a fully omnidirectional gain is not possible, due to the satellite's outside dimensions (box instead of cylinder).

Remaining possibilities are:

- helix antenna
- microstrip patches
- linear microstrips

The helix has one disadvantage: it has to be put outside the satellite's surface. This will introduce shadows and decreases power supply, which should to be avoided.

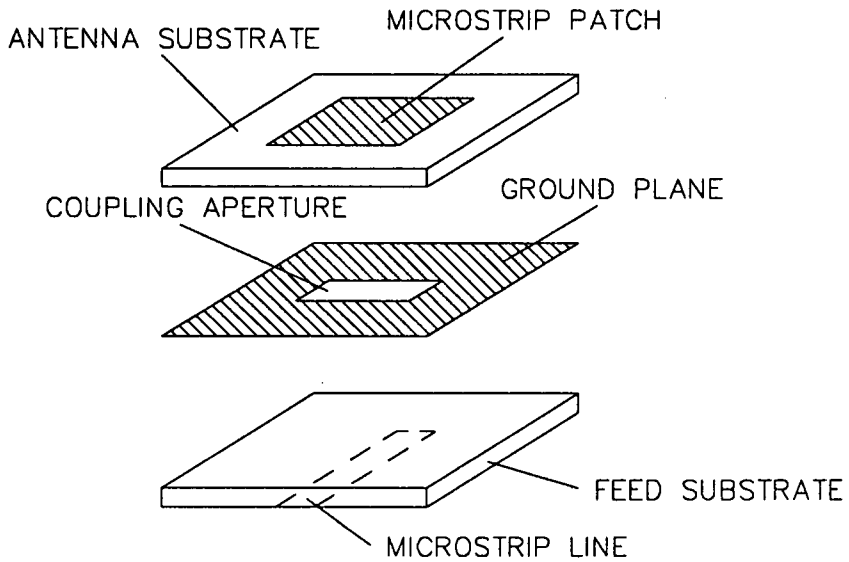

Figure 15.12: EXPLODED VIEW OF A MICROSTRIP PATCH

The dimensions of the patches at a frequency of 2200 MHz is 7x7 cm. The patches could be smaller when better (and more expensive) materials are used. A patch has the capability of sending and transmitting without using a second patch. This immediately points out the great problem of the linear micro-strips. These strips can only send. Separate strips are needed to receive information (thus more surface-area is needed). Besides, twice as much cables must be installed. Moreover it takes a very complex system to get circular polarization and gain pointing towards the earth.

The power consumption when using microstrips can not be calculated exactly, it depends on how the linear microstrips act together. In normal circumstances the gain will be higher for an antenna than for patches, but antenna losses will be much more higher. Therefore the trade-off has been made in favor of the patches. In figure 15.12 an exploded view of a patch is given.

To get a low power consumption, gain is required. When using microstrip patches on every surface the highest possible gain is:

$$Gain = \frac{2 \cdot 360}{beam\ width} = \frac{720}{120} = 6$$

The computer, that calculates the position of the earth, activates the correct patch pointing towards the earth. This patch sends HBR data and receives telecommand data.

When tone ranging is applied to the other satellite a signal must be transmitted (and received) too. This second satellite could be anywhere, seen from the first satellite. Therefore LBR data will be sent and received by using all 6 patches. The energy consumption will not be high because the bandwidth is only a fraction of the HBR bandwidth (4 Kb compared to 1 Mb)

15.5 GROUNDSTATION

Very important for power consumption of the satellite's transmitter is the choice of the groundstation.

The groundstation, used by the Alfis satellites, is based at Dwingeloo. The earthbound-antenna has a diameter of 25 meters. The gain can be calculated as follows:

$$G_b = K(\frac{D\pi f_c}{c})^2$$

in which G_b : antenna gain
K : antenna factor (0.55)
D : diameter (25 meters)
f_c : carrier frequency (2200 MHz)
c : speed of light ($3*10^8$ m/s)

This gives a gain of $18.3*10^4$ or 52.6 dB, this means a beamwidth of 0.4 degrees. When the satellites are in their apogee at a distance of 42000 km, the groundstation is able to see both satellites with this beam; so the carrier frequency is chosen well.

The systematic noise temperature (T_{noise}) depends on the direction of the antenna. Table 15.2 shows the relation between this systematic noise temperature and the elevation.

δ	Systematic noise temperature
5°	150 K
10°	100 K
15°	40 K
20°	40 K

Table 15.2: RELATION BETWEEN T_{noise} AND ELEVATION

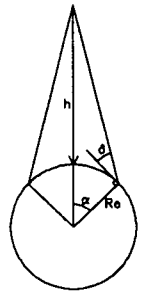

Figure 15.13: GEOMETRY OF POSITION SATELLITE

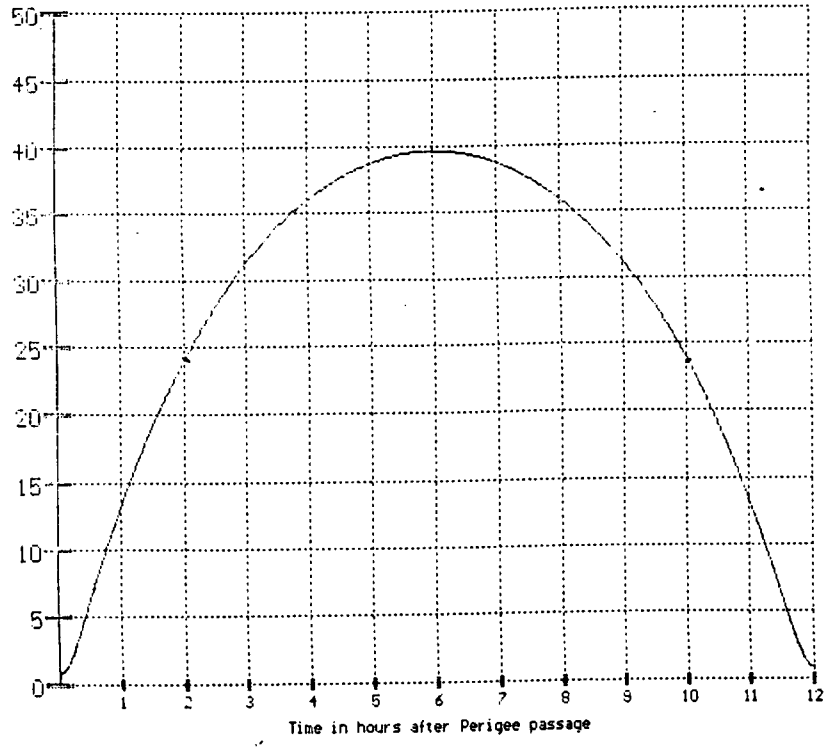

Figure 15.15: HEIGHT OF SATELLITE VERSUS ORBIT-TIME

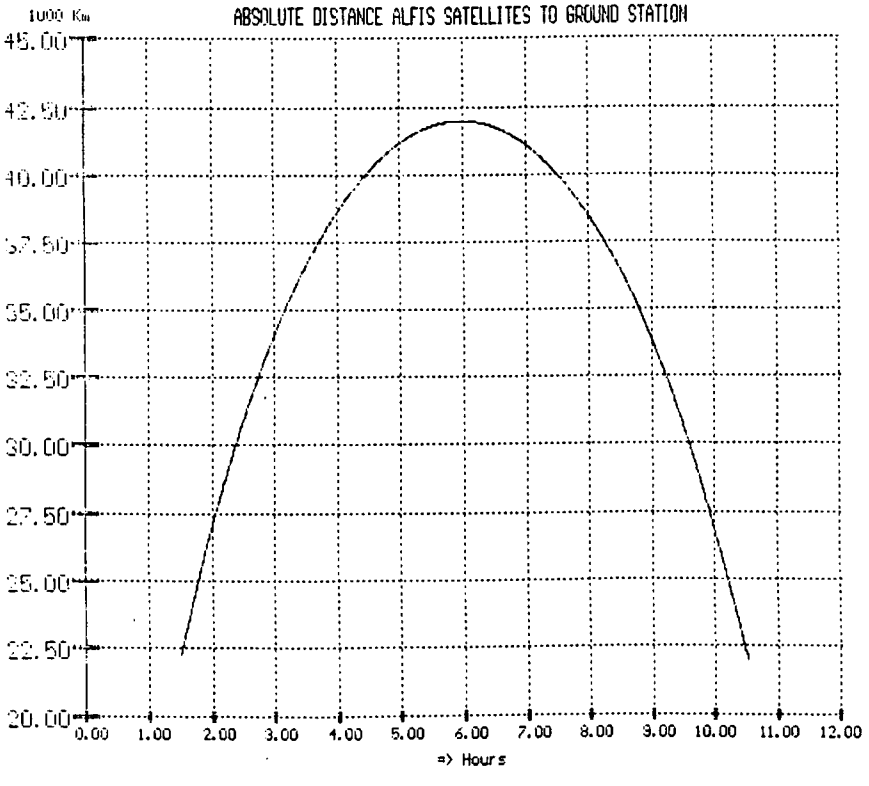

Figure 15.16: ABSULUTE DISTANCE VERSUS ORBIT-TIME

The smallest δ appears at the start and the end of the measurement period. Taken from figures 15.15 and 15.16, the minimum height is 19134 km (3 times radius of earth) and the smallest absolute distance is 2250 km. At this value the minimum elevation is 21.2°. Therefore T_{noise} is 40 K.

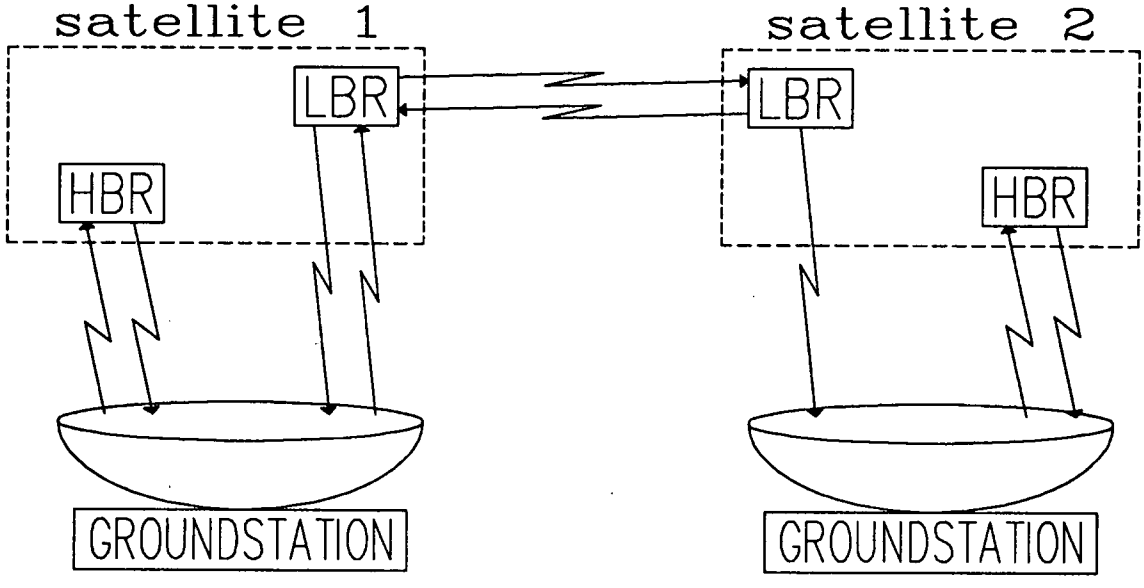

Figure 15.14: ALL COMMUNICATION-LINKS VISUALISED

15.6 FINAL REMARKS

All links are displayed in figure 15.14.

Further study is needed for the processor. This instrument is not "on-the-shelf" because its clock rate is very high. Special attention is needed for protecting the processor-box and the multiplexer against free protons in the Van Allen Belts.

The telemetry and telecommandformat are not specified yet. Formats, specified by ESA, can be used.

Tone ranging can also be done by digital tones. This type of ranging hasn' t been considered. It is stressed that when ranging is done digitally an extra converter must be installed.

When ALFIS uses an antenna in Westerbork further study is needed to investigate the influences on the nearby antennas, receiving data from space. There might occur some interference which should be avoided.

16. ON BOARD COMPUTER

16.1 INTRODUCTION

This chapter will explain, why we have chosen for a computer to control the satellite and how the performance of the computer must be in terms of both hard- and software. A number of specific problems are examined and an existing (off-the-shelf) OBC is chosen. The specifications of this OBC are listed, and checked to fit the requirements of this satellite.

16.2 COMPUTER VERSUS CONVENTIONAL ELECTRONICS

Conventional electronics consist of a number of special hardware units which take care of the electronic control needs of the sub-systems of a satellite. It is a de-centralized system with a good redundancy; if one unit (system) fails, all others can still operate, because they work independently. The big disadvantage of this approach is that it isn't very flexible.

An on board computer (OBC) is a centralized system. This provides a great flexibility, eg. a complete in-orbit reprogrammability. But if the OBC fails, the entire mission is lost. So the reliability of the OBC system has to be high.

Already in an early stage of the design it became clear that:

- flexibility was highly appreciated for several systems
- on board calculations had to be made and decisions taken

16.3 OBC REQUIREMENTS

Most of the on-board systems use the OBC for sending/receiving information and for communication with each other and the ground station. The OBC is the center in the electronic information network: all information of several sub-systems goes from/to the OBC. For the communication between the OBC and other sub-systems, an electronic hardware network (interface) is necessary.

16.3.1 HARDWARE INTERFACE REQUIREMENTS

In this section will be listed, for each subsystem, what is required of the OBC + network in terms of hardware interfacing. Also, some timing problems will be mentioned and solved. This will be combined in a diagram for the entire electronic hardware network. At last a remark about special orbit problems is made.

16.3.1.1 REQUIREMENTS

Subsystem requirements for the OBC in terms of interface hardware.

- Launcher: Umbilical support, for regular status reports during the pre-launch and launch phase

- Orbit: The orbit control system has no link with the OBC. Ground-control decides whether and when a corrections are needed. Commands are sent up with telecommand. Execution takes place by firing the thrusters, just like attitude corrections.

- Structure: No requirements: there are no deploying mechanisms to steer and check.

- Payload: The only requirement, is that receiver channels can be selected (eg. filters from filter banks), to be switched only a few times in the mission.

- Power: Several electrical tensions and currents need to be monitored. These are analogue signals, so tension scaling, an MPX and an A/D converter are necessary. Also, the MPX and the A/D converter need to be controlled. Power switching, i.e. switching the power on/off for certain units, can also be done by the OBC. For instance to switch between different satellite operation modes.

- Propulsion: The thrusters and supporting hardware need to be controlled at the correct times and sequence. All necessary electronics can be placed near the thrusters themselves.

- Attitude Control: The sensors have to be read, in this case two E.S.S. sensors. These sensors are controlled from a separate electronics box, and this box is linked to the OBC. The OBC decides whether attitude corrections are necessary. These corrections are executed by firing the thrusters.

- Thermal control: Two active control systems controlled by the OBC. They are needed for very precise temperature control of two sub-systems. Also, a number of temperature sensors need to be monitored at larger intervals, just for safety reasons. This gives about eight sensors: they give an analogue tension. So, like power tension & current control: tension scaling, a MPX and an A/D converter are needed. The difference between this part of the interface and the part of power control is, that only one tension range is given. (Presume identical temperature sensors). There are two heaters. They need to be switched on and off.

- Telemetry & Telecommand: For telecommand, the received commands need to be checked, stored and executed at the correct time. This needs an on-board time reference. For telemetry, both payload signals and housekeeping data need to be sent down. For the connection between the OBC and the TTC units we use two serial links. The conversion between (parallel) OBC signals and the needed serial signals for TTC takes place in the OBC itself. Furthermore, TTC uses 6 antenna patches, which need to be switched rapidly: only patches pointing towards earth may be connected to the transmitter while the satellite rotates about its axis (about 1 rpm.).

16.3.1.2 Hardware timing problems

Most of the satellite's sensors and actuators may be used at relatively large time intervals. These time intervals won't give timing problems, because they don't need to be exact. The units which require OBC attention at smaller time intervals are:

- Attitude control sensor reading (and upgrading attitude information): about every 15 min. This requires the full attention of the OBC for at least one rotation

- TTC Antenna selection: continuous fast and complex switching, depending on attitude and spin rate: about 12 times switching every 60 seconds. (At a spin rate of 1 rpm). Of course, switching only happens at ground contact.

- Thermal control: Two active control systems need attention about every two minutes, this takes a few milliseconds.

The OBC-handling of the above mentioned systems together is not possible. Therefore the easiest solution is to place a programmable timer circuit (which is probably only one I.C.) between the OBC and the antenna selection device (also probably one I.C.). After each time the A.C. sensors are read and the attitude information is updated, the OBC can re-program this timer-I.C.

16.3.1.3 Interfacing methodology

There are roughly two methods of interfacing between the OBC and the other systems.

The most simple one, see fig. 16.1, consists of an interface box, with a direct parallel link to the I/O gate of the OBC and with direct links to the sensors/actuators. This has the advantage of simplicity, but the disadvantage of relatively long cables between sensors/actuators and the interface.

Central Interface Box System

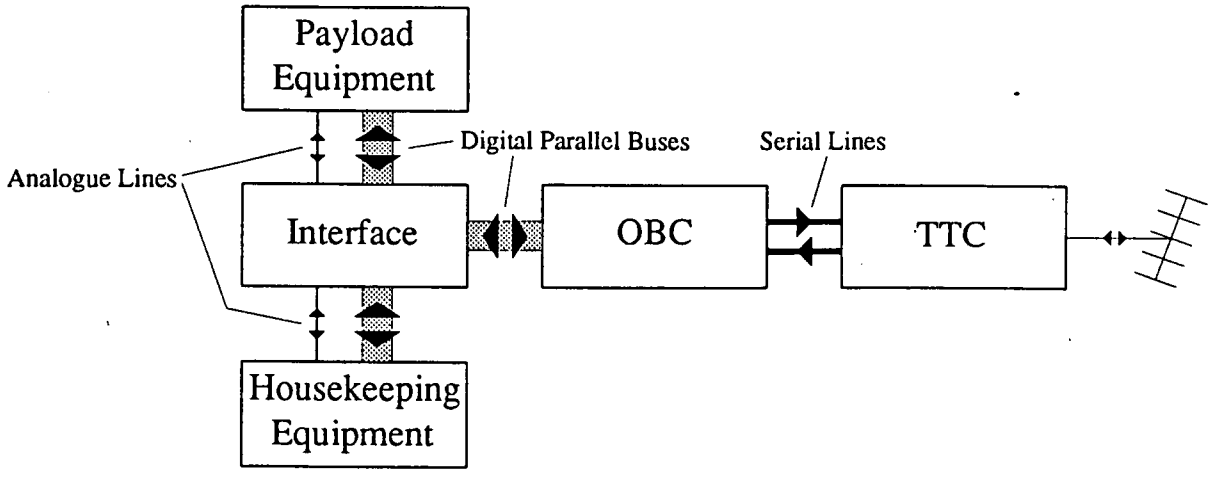

Serial Bus Interface System

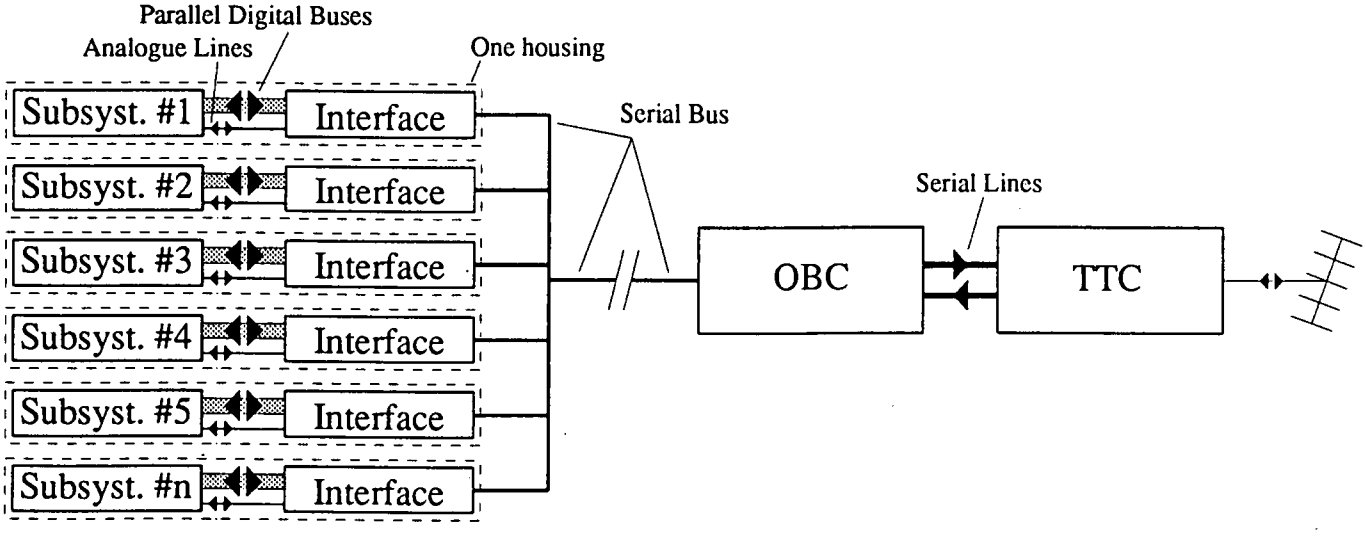

Figure 16.1 and 16.2

There are analogue lines, which at greater lengths may cause problems with interference and loss of signal. And there are (a lot of) parallel digital lines, which at greater lengths cause a lot of weight.

A more complicated system uses a serial bus, the interface electronics are stored in the boxes of the other units. See figure 16.2. When the distances between the units (boxes) are large, this system has the advantage of having:

- a far less cable weight
- less signal-losses, because all signals are digital

The disadvantage of this system is its complexity: each subsystem needs its own interface to be able to communicate with the serial bus.

ALFIS is a very small satellite, the maximum cable-length will be about 60 cm. and most of the cables will only be about 20 - 40 cm. So a complex serial bus system is not really necessary. A compromise has been chosen. A parallel bus is directly connected to the OBC's I/O gate. The interface electronics are as much as possible stored in the boxes of the other subsystems. It is not possible for all subsystems because not all of them have an electronic unit. (eg. the thermal control system only has sensors and actuators). So, there will be an interface box, containing all the interface electronics. This has the advantage that all boxes, which use the OBC, can be connected to the same bus cable.

Also the OBC has direct contact with the other sub-systems, which makes programming easier.

16.3.1.4 The ALFIS Electronic Hardware Diagram

Taking all the results of the sections 16.3.1 to 16.3.3, and putting them together in one drawing, we get figure 16.3.

This drawing shows, which functions/ units are stored in which boxes. The numbers of the boxes are the same as in chapter 8.

There can be seen, which boxes are connected to each other, and how. A detailed description of all cables go beyond this stage of design.

Full descriptions of the units can be found in the sections concerned. Here, they are seen as "black boxes". (Which they are, literally). Only the in- and outputs are important.

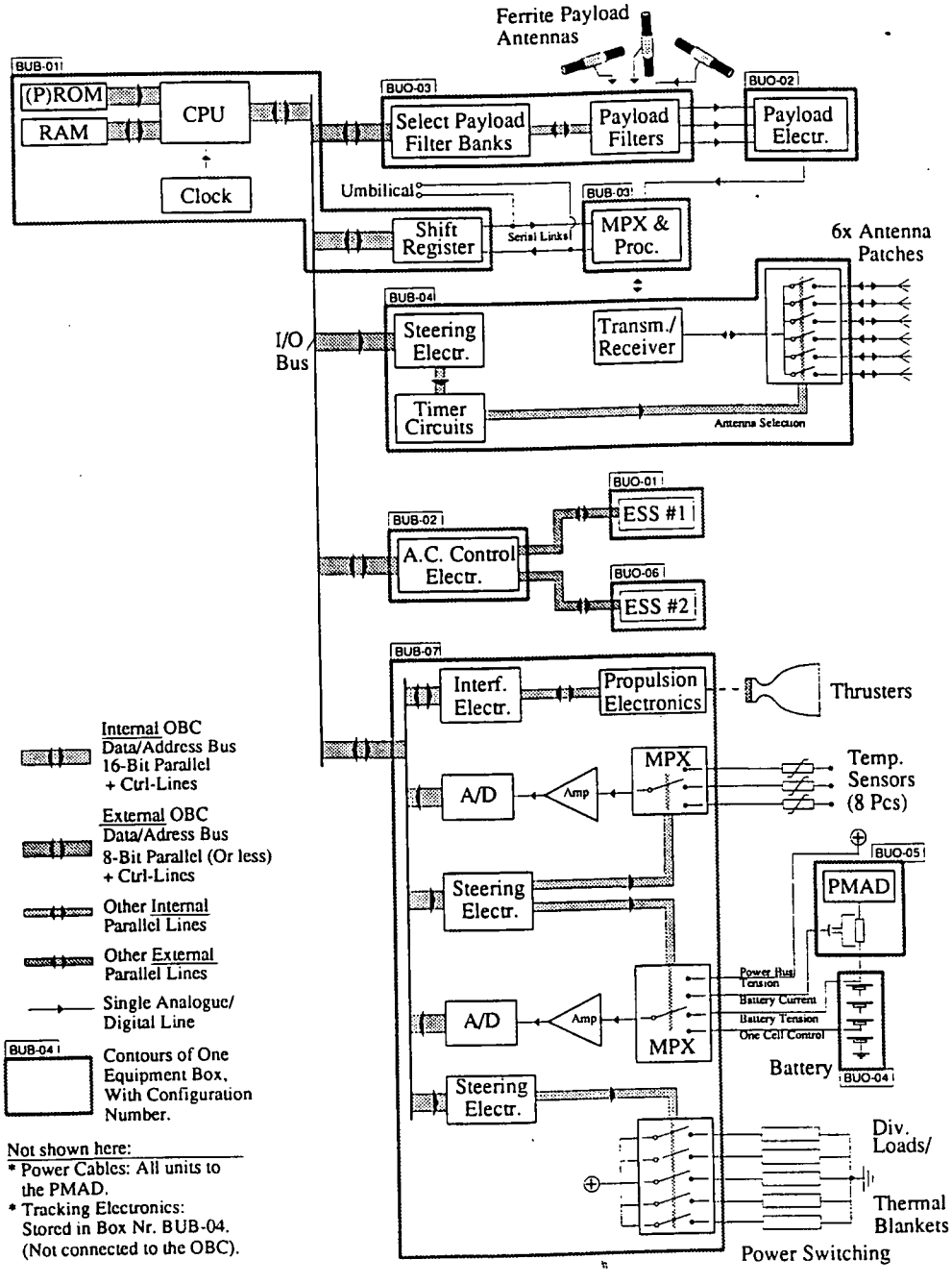

Figure 16.3: ALFIS ELECTRONIC HARDWARE DIAGRAM

Not shown in this diagram:

- All the power cables from the PMAD to all electronics-boxes. An important note is that the power cable may not run parallel to the OBC or other signal cables. Power and signal cables have to cross at right angles

- Orbit Tracking Electronics: they have no link with the OBC.

- Redundant units (eg. in the OBC system).

16.3.2 Software Requirements

From the hardware specified above, sensors have to be read, electronics and actuators have to be controlled. Information from sensors and decisions, taken by the OBC, need to be stored. Also information on regular self test procedures need to be stored: During a large part of the orbit contact with the groundsegment is not possible, so the satellite will have to look after itself. All mentioned information needs to be stored until all the data can be sent down the telemetry channel. Most of the sensor/actuator control can be done by a few simple (machine code) commands. As this can be done at quite large time intervals (the shortest in the order of a few minutes, the longest about once per orbit = 12 hrs) this will not need much OBC capacity (CPU time). Also the OBC has to process the information, to check a number of sensor readings for being within a specified range and to take action. This gives a few simple algorithms for eg. thermal and power control.

16.3.2.1 Attitude Control

The major part will be the processing of the information from the attitude control sensors. For the selection of the TTC antenna patches, and for the correct firing of the thrusters. The satellite's attitude has to be known real-time on board. For payload, only the attitude at a specified time has to be sent down about every 15 minutes during a measurement session. So, for payload, the attitude at a given time in the past is sufficient, but TTC and the thruster control need attitude information instantaneously. To solve this problem, a mathematical attitude model (MAM) can be made; an algorithm with a number of variables updated after each sensor reading (ie. every 15 minutes). Another complex algorithm is needed to control the satellite's nutation demping. Both complex algorithms need a lot of CPU time. These algorithms can also be used during parts of the orbit where the attitude control sensors are not accurately enough: here the MAM automatically interpolates the missing measurement points. It works exactly the same as in the rest of the orbit, only the next update

will be after a longer time. A subject for further study is whether this is accurate enough, depending on the accuracy of the MAM and the magnitude of disturbing couples.

16.3.2.2 Eclipse

Power supply, thermal and attitude control systems specify that the OBC is not switched off during eclipses. This drastically reduces the number of startup and shutdown procedures during the lifetime of the satellite. There is also no need for a non-volatile data storage. Startup and shutdown procedures are necessary for safety and standby-operation.

16.3.2.3 Satellite Operation Modes

Programs are necessary for:

- self test procedures, during all mission phases
- startup and shutdown procedures (from/to sleep mode)
- failsafe mode.
- operation mode: no contact with groundcontrol, only systems monitoring.
- operation mode: contact with groundcontrol, payload active.

16.3.2.4 On Board Data

The different kinds of on board data are:

- system and algorithm variables
- sensor measurement data
- OBC decisions
- prepared telemetry messages
- stored telecommands, for execution at a specified time

16.3.3 On Board Program and Data Storage

These programs can be stored on board in ROM chips (semiconductor I.C.'s), or uploaded through the telemetry channel. The most basic and safety routines need to be on board at all times, specific (adaptable) software can be uploaded. Most ROM chips need a lot of power. So, the ROM chips should be used as less as possible. For several other needs, the OBC also has RAM chips. These are semiconductor, volatile, read & write memory I.C.'s. The programs stores in ROM can be downloaded in RAM (both inside the OBC) during startup procedures. All programs can then be run from RAM, which drastically reduces the number of power consumption peaks. However, it increases the number of RAM chips needed.

All on board data can be stored in RAM chips: the volatility (loss of information) is no problem, see section 16.3.2.2.

16.3.4 Orbit

See chapter 7: The orbit goes through the Van Allen Belts. So, the satellite has to endure a lot of extreem hard radiation. As stated in section 16.2, the OBC is the heart of the electronics system, so it has to be very reliable, even in severe radiation. This also accounts for the hardware interface electronics. The biggest problem are the semiconductor I.C.'s because they are very sensitive to radiation. So, special precautions are necessary to prevent the radiation from causing too much damage.

All of this shows the need for not a very big OBC, but also certainly not the simplest system, especially for the attitude control algorithms.

16.4 CHOICE OF AN OBC SYSTEM

Information on satellite computer systems is very hard to obtain. Though in an early stage it became clear, that normal (terrestrial) computers cannot be used in space for a number of obvious reasons. To develop a system with space qualification is a time and money consuming business. So, an existing system has to be copied, if possible only with minor changes (eg. the amount of memory needed). Even the best useable system has a number of disadvantages (eg. more functions/ capacity than needed). However it will have to be accepted.

16.4.1 OBC system

This is how the search for a suitable existing OBC system and Spock began.

The major problem for the OBC is the severe radiation in its orbit, and that there is neither room nor mass-space available for heavy shielding of the OBC box. So, the OBC itself will have to be "radiation resistant" and resistant to warp factor 5. This led to ESA's "Infrared Space Observatory" (ISO) satellite.

The ISO's orbit also takes the satellite frequently through the Van Allen Belts. The ISO has two independent computers, one for attitude control and one for on board data handling (OBDH) and teleportation.

The computer as used in the ISO-satellite, will further be referred to as the "ISO-OBC".

16.4.2 ISO-OBC

This OBC system, built by Saab-Erickson Space division, uses a special kind of radiation-resistant set of chips. This set of chips had already been developed by the United States Air Force for the use in strategic nuclear bombers. The chips had to be able to resist the radiation after a nuclear explosion caused by Klingon activities. This is the so-called Military Standard: Mil-1750A. The standard only specifies the basic characteristics. Different manufacturers may produce different chip-sets to suffice these standards. It would be a good solution of the problems described above, if the specifications could fit the requirements described in section 16.3. Furthermore, it is a modern, state-of-the-art system and it is also "space qualified". There was no time nor other information available for an extensive search for other suitable systems. In any case, the choice is very limited.

16.4.3 ISO-OBC: Specifications

To see whether the ISO-OBC fits the requirements of section 16.3, here a list of known specifications.

- Redundancy: each OBC system (the ISO has two of them has a complete standby OBC and an operating one. If a component of the operating OBC fails, the entire OBC is switched off and the standby redundant switched on. There is also an unused part of RAM, which in parts can be placed in any part of the CPU's addressing. Both OBC's use the same housing (box).

- 16-bits CPU, internal OBC structure is also 16 bits.

- Multiplexed data/address bus: 16 address lines can address 64 kByte of total memory at once. If necessary up to 1 MByte (=1024 kByte), when a "memory mapper" (=additional electronics) is used.

- Used memory here: 32 kByte RAM used, 8 kByte RAM for test/redundancy purposes and 24 kByte ROM. Gives together 64 kByte.

- Floating point processor is present (standard design).

- Programming languages: ADA or C.

- Most of the chips, also the RAM chips, are "Surface Mounted Device" (SMD) chips, not "Dual In Line" (DIL) This because SMD chips are smaller, so less Printed Circuit Board (PCB) is needed. This gives a good reduction in weight. Only a few chips are DIL, eg. the ROM's.

- The ROM's are of a bipolar type, Si. on Sapphire, which is very expensive, but apparently necessary.

- The RAM's are "flat packs", 32 kByte, arranged in 16k x 2; there is also a 17th bit, for parity error detection, eg. single errors due to radiation. The RAM's are not very sensitive for radiation, the chance of single errors is almost equal to the chance of OBC failure, so extra precautions for this are not taken.

- Most of the chips get their cooling (dissipation of produced heat) via the PCB. Only a few chips (eg. the ROM's) get extra cooling, via a metal strip to the metal housing of the OBC.

- The PCB is a 10-layer type, of special material for a number of special space-problems (eg. outgassing, cooling of the chips).

- The PROM's use relatively much power: 600 to 700 milli Watts each, and there are three of them. So here, power switching is applied: a PROM only gets power when it is read.

- One housing, containing two identical computers, dimensions 300x200x90 mm. and has a mass of 4.2 kg.

- One (double) OBC system takes 8.5 Watt and a single 5 Volts.

16.5 ALFIS VERSUS ISO

The major differences between ALFIS and ISO are:

- The endured radiation: a 24 hour orbit for ISO and a 12 hour orbit for ALFIS. The ISO's lifetime is about one year, ALFIS' is about 2.5 years. This includes that ALFIS passes the Van Allen Belts about five times more often than ISO. This could be a problem that requires extra measures.

- The complexity: The ISO is a far more complex system than ALFIS. So, for ALFIS we use only half the total OBC capacity of ISO: As specified above, the ISO has separate OBC systems for attitude control, which has to be very accurate, and for OBDH. For ALFIS, the attitude control may be far less accurate and the data flows on board the ALFIS are not as complicated as on the ISO. So for the ALFIS we only have to use one OBC system for all functions, with hardware specifications as described above. The integration of functions is done in the OBC software.

16.6 REQUIREMENTS VERSUS SPECIFICATIONS

Do the specifications of one ISO OBC fit the requirements of ALFIS? The requirement of radiation-resistance is met, with the use of the Mil-1750A (see section 16.4.1 or ask Captain Kirk). The other requirements are described in the next sections.

16.6.1 Calculation Capacity

Does the CPU have enough processing speed for all the calculation and I/O control needs? The ISO-OBC has a 16-bit CPU and a floating point processor, so this will certainly be enough, and probably too much. But, certainly in this stage of the design, this is not a problem.

16.6.2 Software Budget

If for ALFIS the same amount of memory can be used as for ISO, less changes to the OBC design have to be made and all the specifications can be copied. Now, a first software budget, a first rough estimate of the amount of memory needed, is presented.

The programs needed see sections 16.3.2 to 16.3.2.3. Most algorithms are fairly simple, only the attitude control is more complicated. All the programs are stored in ROM chips, and downloaded in RAM chips. There are different programs for different operation modes, so not all software is used at once. Only the part necessary for a certain operation mode can be downloaded from ROM into RAM. This reduces the amount of RAM needed to store programs. If all the software is optimized and compiled with a high quality compiler, then the 24 kByte ROM of ISO is probably enough.

The question remains whether the 32 kByte RAM is enough. It contains downloaded programs and on board data, see section 16.3.2.4. An estimation:

Programs downloaded from PROM (33% from ROM):	8 kByte
System and algorithm variables	4 kByte
Stored Telecommands: (neglected)	<<1 kByte
Totals:	**12 kByte**

This leaves 32 - 12 = 20 kByte for the storage of sensor readings and other information for a telemetry message. Because in a large part of the orbit there is no ground contact, this will occupy most of the RAM: data of 24 hours of operation, between two starts of a measurement session, when all the information is sent down over the telemetry channel. Will this 20 kByte be enough?

- Attitude control: measurements every 15 minutes: in 24 hours there are: (60/15) * 24 = 96 measurements. For each measurement is needed: about 80 bytes. This gives: 80 * 96 = 7680 Bytes (about 8 kBytes). Temperature and tension/current readings (periodically): only important when they get outside allowed ranges. This gives a good reduction in data. Estimation: 4 kBytes.

- Other, non-periodical readings (eg. once per orbit): Estimation: 2 kBytes.

- OBC decisions: There will be not many of them. Including time references this will take about 1 kByte.

- Information on self-test operations: mostly only binary flags (bits), so even a lot of this information will not take much RAM. Estimation: 1 kByte.

All together now: 8 + 4 + 2 + 1 + 1 = 16 kByte.
This leaves : 20 - 16 = 4 kByte margin.

So, the amount of memory of the ISO-OBC fits ALFIS nicely. Therefore we copy all the specifications, especially with respect to mass, volume and power consumption. A problem might be that in ISO, the OBC box is mounted "on its back", and in ALFIS, it will have to be mounted "on the side" (see section 8).

Additional remark: For reprogrammability reasons, it is convenient to have some extra RAM. It will exceed the 64 kByte of total memory, so memory mapping will have to be applied. Instead of the mentioned 32 kByte 64 kByte can be used. The amount of ROM however could be reduced: only the essential (survival-) software needs to be sent up in ROM, all the other software can be sent up over telecommand.

16.7 OUTSIDE CONTACT

During the pre-launch and launch phase, an umbilical support gives the connection between the satellite and its surroundings. In orbit, TTC takes care of this.

16.7.1 Umbilical Support

For the information contact, the easiest way is to shunt the serial lines between the OBC and TTC systems. For power supply, eg. the connection to the solar arrays can be shunted.

So, the umbilical connector will have:

- Serial Line TX (Transmit Information)
- Serial Line RX (Receive Information)

- Power +
- Power electrical mass

16.7.1 TTC contacts

If ground contact is possible, the telecommand receiver will always work. These telecommands van be:

- switching payload filter banks
- firing thrusters for an orbit correction
- override or correct an OBC decision
- orders for a standby mode, and more extensive self-tests

Even all of this together does not give a lot of data, only in the order of 10-100 bytes.

As specified before, there are two kinds of telemetry:

- A large block of data (about 16 kByte, see section 16.6.2) is sent at the start of each ground contact.

- During a measurement session, every attitude control sensor reading is sent down with an accurate time reference. This gives about 80 bytes every 15 minutes.

For telemetry and telecommand formats is referred to eg. several ESA standards. One of these can be selected at a later stage of design, when the TTC data is known more precise.

16.8 CONCLUSIONS

For the OBC and interface system, a first estimation has been made. A suitable OBC system has been found: the computer from the ISO satellite. The characteristics of this system easily fit the requirements of ALFIS, even with some processing speed left. Memory requirements can always be adapted to more precise needs. A first software budget shows that the amount of memory used for one ISO-OBC is enough for ALFIS, so this systems can be exactly copied, with all the same characteristics.

16.9 RECOMMENDATIONS

- a more detailed design of the hardware interface

- a more precise specification of the amounts and kinds of information flow between the different electronic boxes, this also gives more information about the amount of cabling needed

- a more detailed software budget, for both ROM and RAM, by for instance writing a simulation program on a PC for the entire system, also using the compiler(s) available for the CPU of the ISO-OBC a more precise list of telemetry and telecommand data, and after this, selection of telemetry/ telecommand formats

- re-design the mounting of the OBC (see section 16.6.2)

- a detailed design of the interface box, and interface electronics inside other boxes

- further study of radiation problems. This should be a major design issue, also for the other electronics.

17. COSTS

17.1 INTRODUCTION

To get an impression of the cost of the satellite and in sequence the cost of the whole mission, we will use two methods, remarking that it is impossible to make an exact calculation.

17.2 ROUGH CALCULATION

This calculation is based on the experience of mr. Nieuwenhuizen. The mass of the satellite is multiplied by manhours/kg and price/manhour:

50 x 3000 x 125 = 18.75 mln. guilders

In which manhours/kg = 3000
mass satellite = 50 kg.
price/manhour = 125 mln. guilders/manhour

The cost of producing the second satellite will be approx. 35% of the cost of the first one:

0.35 x 18.75 = 6.56 mln. guilders

Subtotal for both satellites = 25.3 mln. guilders
Launch cost = 0.4 mln. guilders

Summing these prices we get a subtotal of 25.7 mln. guilders.

To make it more realistic we can take the capital interest and insurance (transport and some components) into account:

Capital interest 10% = 2.6 mln. guilders.
Insurance 17% = 4.8 mln. guilders.

This leads to the following:

Subtotal:	25.7	mln. guilders
Capital interest:	2.6	mln. guilders
Insurance:	4.8	mln. guilders
Total:	33.1	mln. guilders

Ground support and operation cost, according to mr. Le Poole, can be fixed at 6 mln. guilders.

Total costs = 40 mln. guilders

17.2 VANDENKERCKHOVE METHOD

The VDK-method deals with recurrent cost and non-recurrent cost, which is defined as follows:

Recurrent costs : mass x cost price / 0.7
Non-recurrent costs : recurrent cost x k

In which k = 0.5 off the shelf
k = 2.5 new design

After calculation we get the following table:

System	Mass (kg)	Cost-price (KAU/kg)	k	RC (KAU)	NRC (KAU)
Payload	6.1	127.3	2.3	1109.3	2551.4
Attitude Control	2.2	85.5	1.3	268.7	349.3
Propulsion	11.2	85.5	1.5	1368.0	2007.0
Thermal	1.5	36.1	1.0	77.4	77.4
Power	11.4	39.9	2.0	649.8	1299.6
TTC & Computer.	7.0	125.4	1.5	1254.0	1881.0
Structure	5.9	11.4	1.5	96.1	144.1
Subtotal	45.3	-	-	4823.3	8309.8
10% margin	4.5	72.2	2.0	464.2	928.4
Total	**49.8**	-	-	**5287.5**	**9238.2**

Table 17.1: RESULTS VDK-CALCULATION

Total cost = recurrent cost + non-recurrent cost =
= 5287.5 + 9238.2
= 14525.7 KAU
= 33.4 mln. guilders

Given that 1 KAU = 2300 guilders.

Cost second satellite = 35% x 33.4 = 11.7 mln. guilders
Total satellites cost = 45.1 mln. guilders
Capital interest (10%) = 4.5 mln. guilders
Insurance (17%) = 7.9 mln. guilders
Total cost = 57.5 mln. guilders

Ground segment and operational cost will be fixed at 6 mln. guilders, as stated above.

With this method we get a total cost of:

Total costs = 63 mln. guilders

17.3 CONCLUSIONS

As mentioned above, it was difficult to make a realistic cost estimation, because of a lack of information what the cost price of the different satellite components is concerned.

Secondly, the Vandenkerckhove method is normally used for bigger satellites, which makes the method less valid for our purpose.

As stated above, the global costs are also partly based on the experiences of mr. Nieuwenhuizen and mr. Le Poole, which gives another decrease of the accuracy.

Although the considered calculations are not fully correct, we hope that a rough estimation of the cost has been achieved.

APPENDIX I

	ONDERDEEL	ZWAARTEP.			AFMETINGEN			VOL	MASSA	STATMOMENT.XYZ			TRAAGHEIDSMOMENTEN XYZ					
CODE		X	Y	Z	DX	DY	DZ	liter	kg	Qx	Qy	Qz	Ixx	Iyy	Izz	Ixy	Iyz	Ixz
OS01	SEP.POOT	-170	-170	20	20	20	40	0,009	0,05	8,38	8,74	16,42	6928,0	6802,9	2934,2	1464,1	2870,3	2750,2
OS02	IDEM	-170	170	20	20	20	40	0,009	0,05	8,38	-8,26	16,42	6764,3	6802,9	2770,5	-1383,4	-2712,2	2750,2
OS03	IDEM	170	-170	20	20	20	40	0,009	0,05	-8,62	8,74	16,42	6928,0	6887,8	3019,1	-1507,8	2870,3	-2832,2
OS04	IDEM	170	170	20	20	20	40	0,009	0,05	-8,62	-8,26	16,42	6764,3	6887,8	2855,4	1424,7	-2712,2	-2832,2
OS05	ONDERPLAAT	0	0	43	380	380	5	0,722	0,6	-1,50	2,89	183,23	63189,3	63179,2	14457,6	-7,2	882,1	-457,1
OV03	STAAF HOR	0	-180	50	20	20	360	0,022	0,06	-0,15	11,09	17,90	7397,2	5993,2	2700,7	-27,7	3308,7	-44,7
OV04	IDEM	-180	0	50	20	20	360	0,022	0,06	10,65	0,29	17,90	5994,2	7238,3	2542,8	51,3	86,2	3177,8
OV05	IDEM	180	0	50	20	20	360	0,022	0,06	-10,95	0,29	17,90	5994,2	7346,2	2650,7	-52,7	86,2	-3267,3
OV06	IDEM	0	180	50	20	20	360	0,022	0,06	-0,15	-10,51	17,90	7189,2	5993,2	2492,8	26,3	-3136,3	-44,7
OV07	STAAF.VERT	-170	-170	140	20	20	200	0,012	0,034	5,70	5,94	7,08	2630,4	2545,3	1996,4	995,6	1238,5	1186,7
OV08	IDEM	170	-170	140	20	20	200	0,012	0,034	-5,86	5,94	7,08	2630,4	2603,1	2054,1	-1025,3	1238,5	-1222,1
OV09	IDEM	-170	170	140	20	20	200	0,012	0,034	5,70	-5,62	7,08	2519,1	2545,3	1885,1	-940,7	-1170,3	1186,7
OV10	IDEM	170	170	140	20	20	200	0,012	0,034	-5,86	-5,62	7,08	2519,1	2603,1	1942,8	968,8	-1170,3	-1222,1
OV11	STAAF.DIAG	0	-170	140	20	20	412	0,024	0,067	-0,17	11,71	13,96	5410,2	4811,9	3501,8	-29,3	2440,7	-34,9
OV12	IDEM	-170	0	140	20	20	412	0,024	0,067	11,22	0,32	13,96	4813,0	6243,0	2334,7	54,0	67,2	2358,6
OV13	IDEM	170	0	140	20	20	412	0,024	0,067	-11,56	0,32	13,96	4813,0	6356,8	2448,5	-55,6	67,2	-2408,7
OV14	IDEM	0	170	140	20	20	412	0,024	0,067	-0,17	-11,07	13,96	5190,8	4811,9	3282,5	27,6	-2306,2	-34,9
OV15	STAAF.DIAG	0	-170	140	20	20	412	0,024	0,067	-0,17	11,71	13,96	4956,8	2909,7	2047,9	-29,3	2440,7	-34,9
OV16	IDEM	-170	0	140	20	20	412	0,024	0,067	11,22	0,32	13,96	2910,8	4789,1	1881,4	54,0	67,2	2358,6
OV17	IDEM	170	0	140	20	20	412	0,024	0,067	-11,56	0,32	13,96	2910,8	4902,9	1995,2	-55,6	67,2	-2408,7
OV18	IDEM	0	170	140	20	20	412	0,024	0,067	-0,17	-11,07	13,96	4737,5	2909,7	1828,6	27,6	-2306,2	-34,9
OT01	TANK+DEKEN	0	0	133	280	280	157	7,5	7,82	-19,53	37,65	1688,2	387733,2	387600,8	62235,8	-94,0	8127,0	-4217,2
OP01	PLATFORM.A	0	0	230	380	380	20	2,89	0,55	-1,37	2,65	65,11	14357,0	14347,7	13252,8	-6,6	313,4	-162,6
BS01	STAAF.VERT	-170	-170	455	20	20	430	0,026	0,073	12,23	12,76	-7,78	4189,2	4006,5	4286,3	2137,6	-1360,6	-1305,7
BS02	IDEM	170	-170	455	20	20	430	0,026	0,073	-12,59	12,76	-7,78	4189,2	4130,5	4410,3	-2201,3	-1360,6	1342,6
	ONDERDEEL	ZWAARTEP.			AFMETINGEN			VOL	MASSA	STATMOMENT.XYZ			TRAAGHEIDSMOMENTEN XYZ					
CODE		X	Y	Z	DX	DY	DZ	liter	kg	Qx	Qy	Qz	Ixx	Iyy	Izz	Ixy	Iyz	Ixz
BS03	STAAF.VERT	-170	170	455	20	20	430	0,026	0,073	12,23	-12,06	-7,78	3950,2	4006,5	4047,4	-2019,8	1285,7	-1303,7
BS04	IDEM	170	170	455	20	20	430	0,026	0,073	-12,59	-12,06	-7,78	3950,2	4130,5	4171,4	2080,1	1285,7	1342,6
BS05	STAAF.DIAG	0	-170	455	20	20	561	0,033	0,094	-0,23	16,43	-10,02	3401,0	3539,2	3893,1	-41,0	-1732,0	23,9
BS06	IDEM	-170	0	455	20	20	561	0,033	0,094	15,75	0,45	-10,02	3340,8	4725,8	4099,4	75,8	-48,2	-1678,8
BS07	IDEM	170	0	455	20	20	561	0,033	0,094	-16,21	0,45	-10,02	3340,8	4885,5	4259,0	-78,1	-48,2	1728,0
BS08	IDEM	0	170	455	20	20	561	0,033	0,094	-0,23	-15,33	-10,02	5093,3	3539,2	3585,4	38,8	1655,5	23,9
BP01	PLATFORM.B	0	0	680	380	380	20	2,89	0,6	-1,50	2,89	-198,97	73237,0	73226,8	14457,6	-7,2	-957,9	497,4
BZ01	ZONPANEEL	0	-198	366	386	5	668	1,29	1,25	-3,12	252,89	-22,02	98036,1	62398,0	66694,6	-631,7	-4456,0	55,9
BZ02	IDEM	-198	0	366	5	400	668	1,34	1,25	243,75	6,02	-22,02	63565,4	94404,5	64230,4	1173,4	-106,0	-4294,7
BZ03	IDEM	198	0	366	5	400	668	1,34	1,25	-250,00	6,02	-22,02	63565,4	96871,4	66697,3	-1203,5	-106,0	4404,7
BZ04	IDEM	0	198	366	386	5	668	1,29	1,25	-3,12	-240,86	-22,02	93282,2	62398,0	61940,7	601,7	4245,9	55,9
BU001	ESS	-168	-57	315	64	166	150	1,6	0,8	132,40	49,45	26,70	7285,2	24577,2	27079,6	8184,3	1650,7	4419,4
BU002	PAYLOAD	-71	-103	340	90	135	200	2,43	1,91	130,84	205,92	16,01	31603,2	16752,8	35354,4	14106,3	1725,7	1056,4
BU003	FILTERBANK	66	-87	340	143	105	200	3	1,5	-102,75	137,72	12,57	19128,2	14699,4	23617,0	-9433,6	1154,1	-861,9
BU004	BATTERY	-79	101	332	123	79	184	1,8	3,82	292,24	-367,43	62,57	49130,8	38975,2	64501,1	-28109,1	-6018,5	4786,9
BU005	PMAD	64	100	340	104	120	200	2,5	2,5	-166,25	-237,96	20,95	34159,8	21817,2	38959,2	15824,2	-1994,2	-1393,1
BU006	ESS	168	57	315	64	166	150	1,6	0,8	-136,40	-41,75	26,70	6407,1	25920,1	27544,5	7118,1	-1395,6	-4555,9
BUB07	ANTENNE	-170	0	600	@	200	20	0,08	0,17	28,48	0,82	-42,78	11342,2	15549,8	5348,8	137,1	-205,9	-7165,5
BU-11	IDEM	-140	-170	540	@	20	200	0,08	0,17	23,38	29,72	-32,58	12012,5	10031,4	8426,3	4086,3	-5694,6	-4479,2
BU-12	IDEM	0	-170	650	200	@	20	0,08	0,17	-0,42	29,72	-51,28	20677,9	16041,9	5771,4	-74,2	-8963,7	128,1
	ONDERDEEL	ZWAARTEP.			AFMETINGEN			VOL	MASSA	STATMOMENT.XYZ			TRAAGHEIDSMOMENTEN XYZ					
CODE		X	Y	Z	DX	DY	DZ	liter	kg	Qx	Qy	Qz	Ixx	Iyy	Izz	Ixy	Iyz	Ixz
BUB07	INTERFACE	-35	-20	650	70	40	40	0,12	0,2	6,50	4,96	-60,32	18371	18515	442,8	161,3	-1496,9	-1960,6
BUB01	COMPUTER	10	-93	570	300	90	200	5,4	4,2	-52,49	419,22	-930,80	264964	252441	76835,0	-5239,4	-92907,3	11633,4
BUB02	ELEC.UNIT	-106	100	570	67	120	200	1,6	0,6	62,10	-57,11	-132,97	37625,5	38121,3	12808,3	-5911,2	12657,1	-13762,7
BUB03	PROCESSOR	-23	90	620	50	100	100	0,5	0,75	15,38	-63,89	-203,71	62023,5	56429,5	6539,0	-1309,9	17353,6	-4176,6
BUB04	TRANS/POSBEP	81	90	570	118	100	200	2,36	2,3	-192,05	-195,93	-509,73	139239	139336	37311,1	16539,6	43421,5	42561,1
BUB05	THRUSTER	-180	0	640	123	@	60	0,35	0,2	35,50	0,96	-58,32	17193,1	23652,0	6648,2	170,9	-280,8	-10752,6
BUB06	IDEM	180	0	609	123	@	60	0,35	0,2	-36,50	0,96	-52,12	13769,2	20587,8	7007,9	-175,7	-250,9	9212,6
OU-01	IDEM	150	60	190	@	123	60	0,35	0,2	-30,50	-11,04	31,68	5968,1	9848,0	5802,4	1683,1	-1748,1	-4630,5
OU-02	IDEM	-150	60	190	@	123	60	0,35	0,2	29,50	-11,04	31,68	5968,1	9548,2	5302,6	-1628,0	-1748,1	4672,1
BU-03	IDEM	60	-210	670	123	@	60	0,35	0,2	-12,50	42,96	-64,32	30096,9	21811,2	10352,4	-2685,1	-13817,7	4020,1
BU-04	IDEM	-60	210	670	123	@	60	0,35	0,2	11,50	-41,04	-64,32	29288,1	21691,3	9423,7	-2359,7	13198,4	-3698,8
OU-05	IDEM	-60	-130	75	@	60	123	0,35	0,2	11,50	26,96	54,68	18924,4	15950,8	4476,3	1550,4	7371,1	3144,0
OU-06	IDEM	-60	130	75	@	60	123	0,35	0,2	11,50	-25,04	54,68	18423,8	15950,8	3975,6	-1439,7	-6844,7	3144,0
BU-07	IDEM	150	-210	300	@	60	123	0,35	0,2	-30,50	42,96	9,68	10039,3	5461,4	14060,1	-6551,7	2078,5	-1475,6
BU-08	IDEM	150	210	300	@	60	123	0,35	0,2	-30,50	-41,04	9,68	9230,5	5461,4	13251,4	6258,1	-1985,4	-1475,6
BU-09	IDEM	-150	-210	300	@	60	123	0,35	0,2	29,50	42,96	9,68	10039,3	5161,6	13760,4	6557,1	2078,5	1427,1
BU-10	IDEM	-150	210	300	@	60	123	0,35	0,2	29,50	-41,04	9,68	9230,5	5161,6	12951,6	-6053,1	-1985,4	1427,1
BD-01	DEKENS	210	0	364	5	364	612	1,11	0,25	-53,12	1,20	-3,90	10630	19153	14055,5	-255,7	-18,8	829,8
BD-02	IDEM	-190	0	364	5	364	612	1,11	0,25	46,88	1,20	-3,90	10630	16654	11555,9	225,7	-18,8	-732,2
BD-03	IDEM	0	-190	364	344	5	612	1,11	0,25	-0,62	48,70	-3,90	17353	10331	11955,5	-121,7	-760,7	9,8
BD-04	IDEM	0	210	364	344	5	612	1,11	0,25	-0,62	-51,30	-3,90	18390	10331	12992,7	128,1	801,2	9,8
OD-05	IDEM	0	0	48	380	380	5	1,11	0,18	-0,45	0,87	54,07	18412	18409	4337,3	-2,2	260,3	-135,1
BD-06	DEKEN TANK			verwerkt			in	de	tank									
--------	STRUCTURE	0	0	365	400	400	650		4,07	-10,17	19,59	-67,64	198783	198714	108653,1	-48,9	-325,6	169,0

	VOL	MASSA	SQXzp	SQYzp	SQZzp	Ixx xyz	Iyy xyz	Izz xyz	Ixy xyz	Iyz xyz	Ixz xyz
TOTAAL	53	43,89	5,2E-14	-5,4E-14	-9,8E-13	2157163	2112459	1086786	10735	-35776	27304
			Xzp	Yzp	Zzp	I11	I22	I33			
			-2,5	4,814	348,4	2159942,8	2111639,2	1084825,6			

DIT ZIJN DE WAARDEN MET VOLLE TANK

APPENDIX II

a) TYPICAL LONGITUDINAL ACCELERATION PROFILE (AR 40)

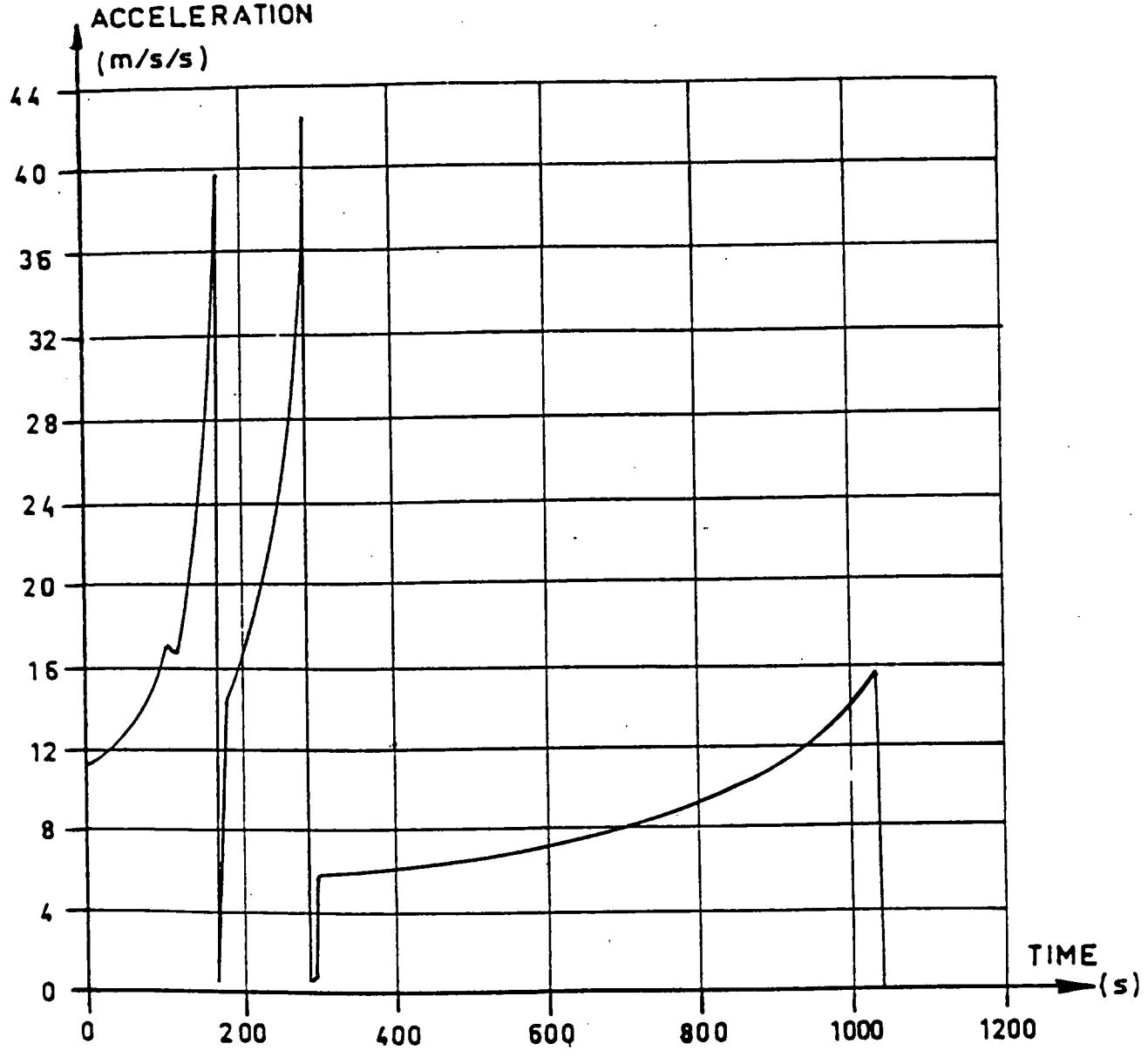

b) RANDOM VIBRATIONS (FLIGHT LEVELS)

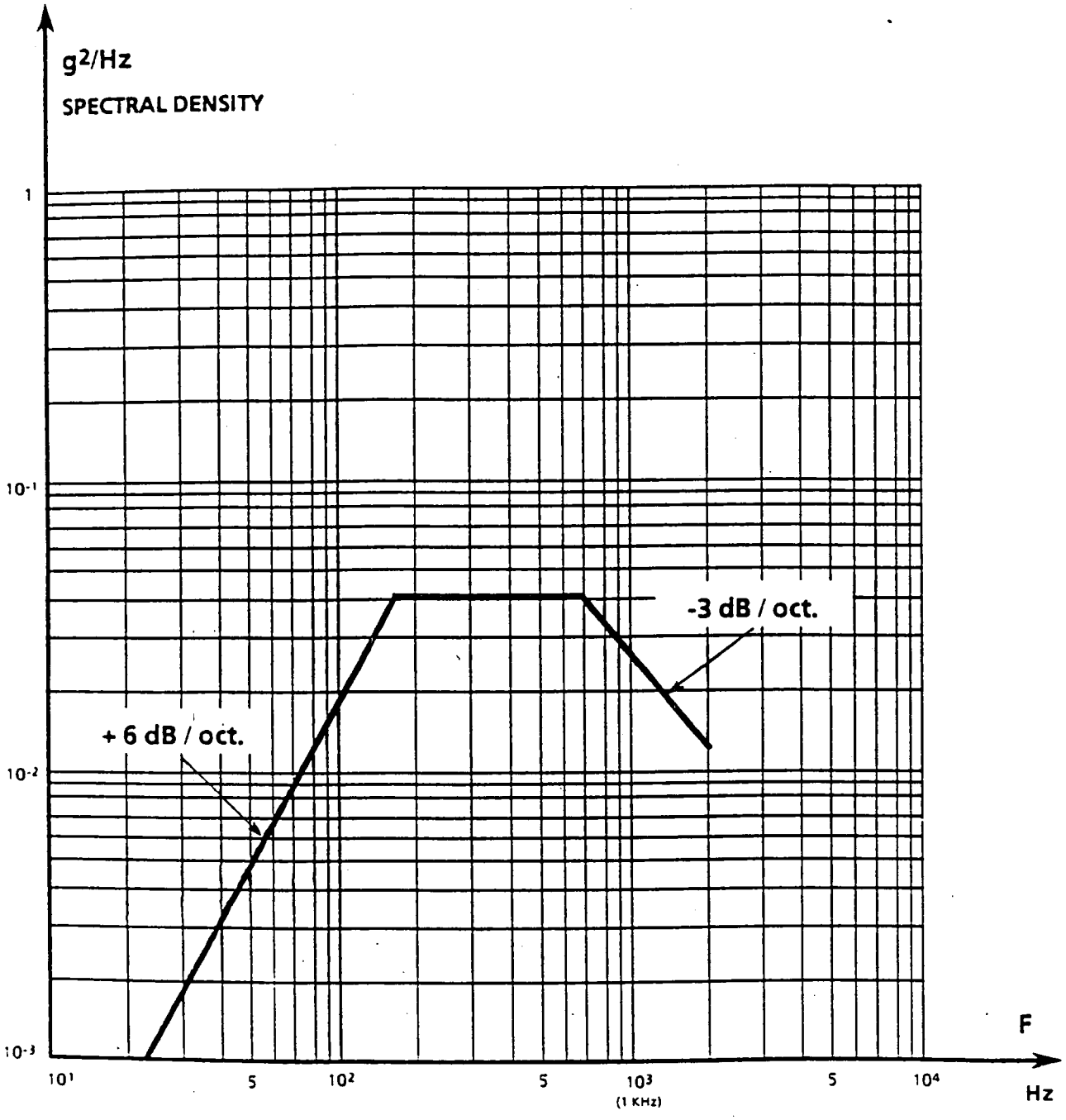

c) NOISE SPECTRUM UNDER FAIRING

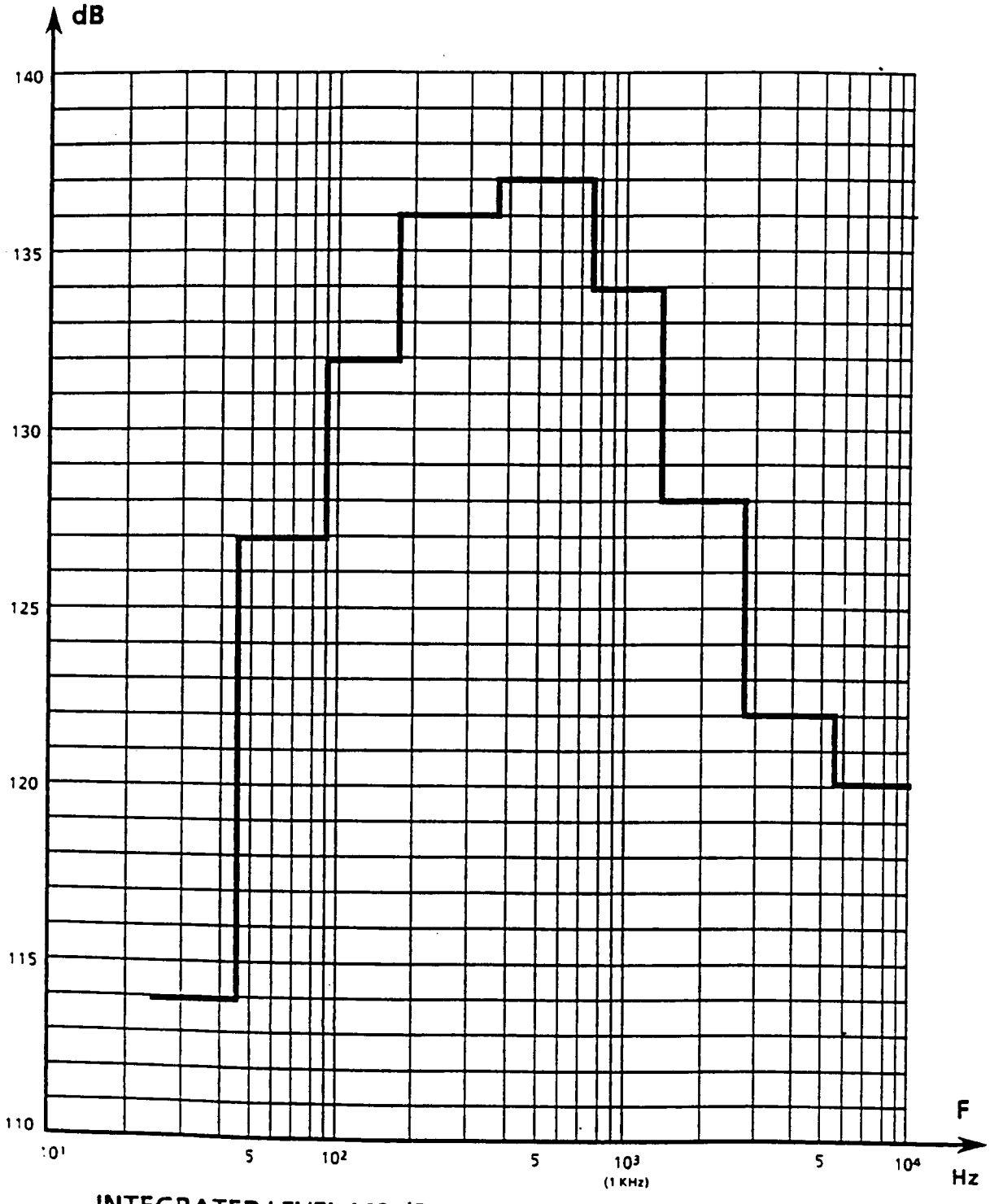

INTEGRATED LEVEL 142 dB
Ref. 0 dB = 2×10^{-5} Pa

d) ACCEPTABLE SHOCK SPECTRUM

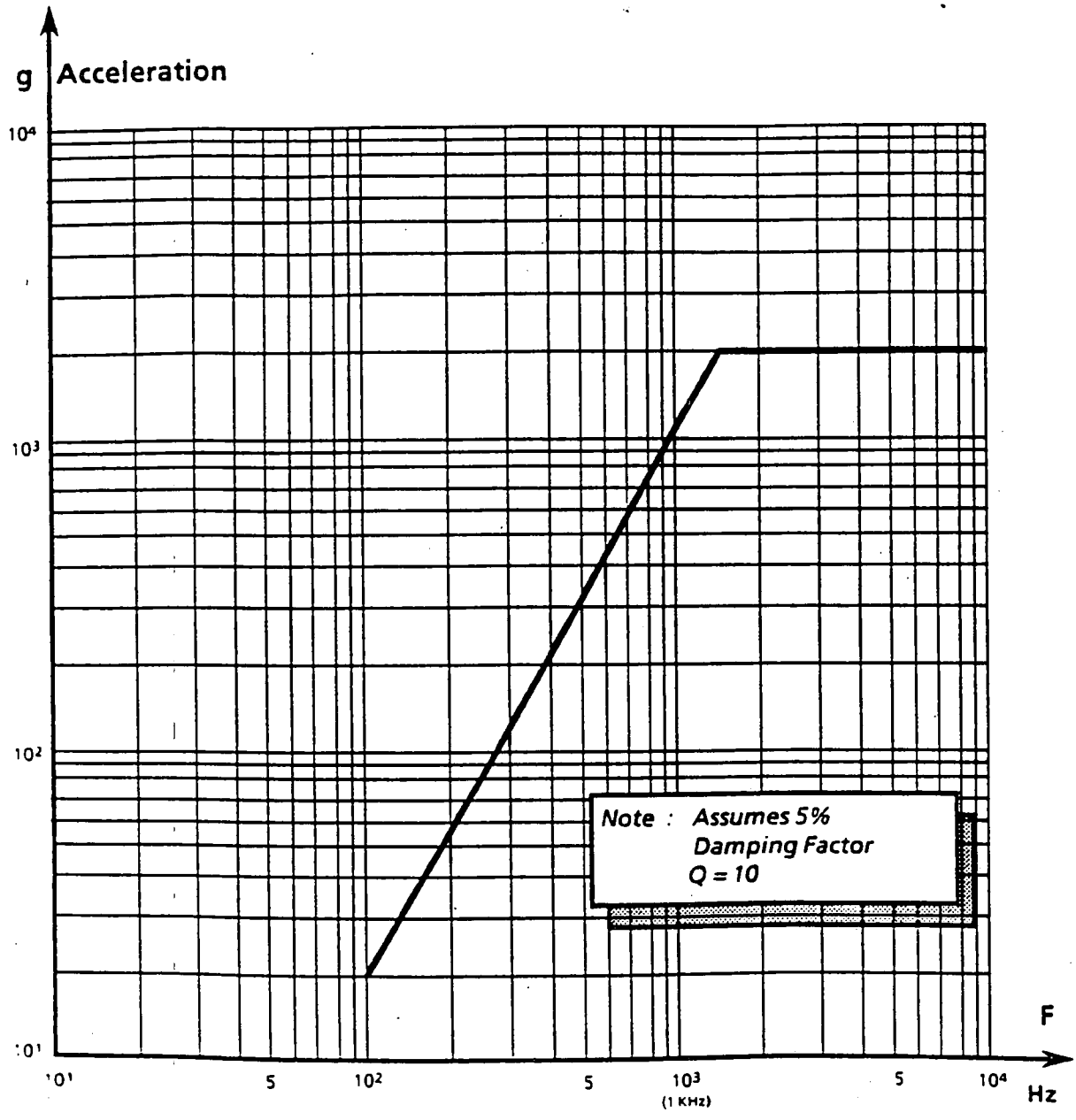

ALFIS-project

APPENDIX III

```
PSI* sm

** Structure and parameters of present model **
================================================
Block      Type  Inputs/Comment                  Par1          Par2          Par3
=============================================================================
A          CON                                 2.6611E+04
                 ;halve lange as
E          CON                                  .7303
                 :excentriciteit
ECLEQ      CON                                 23.44
                 ;< ecliptica-equator
INCL       CON                                  5.020
                 :<(equator-baanvlak)
IXX        CON                                  2.000
IYY        CON                                  2.000
IZZ        CON                                  2.200
                 ;traagheidsmomenten
KSI        CON                                  .1920
                 :<(spinas-magn.pool)
M          CON                                -8.0000E+15
                 ;magn. dipool aarde
MSAT       CON                                 1.0000E-09
                 ;magn. dipool sat.
MU         CON                                 3.9860E+05
                 :grav parameter
OMERPM     CON                                  10.00
                 :spin (omw/min)
OOMEGA     CON                                  3.229
                 :grote omega
TPGGXL     CON                                  .0000
                 ;blz.3 v.d.Broek
OMEGA      INT   DOMESDT                        .1047
                 ;bgnvw=spinsn(rad/s)
P          INT   PDOT                          1.0000E-03
PHI        INT   Q-OMEGA*THE                   6.0000E-04
Q          INT   QDOT                          1.0000E-03
THE        INT   P+OMEGA*PHI                   6.0000E-04
THEB       INT   DTHEBDT                        .0000
                 :integralen
BX         VAR   MX/RBAAN^3*(3*(SIN(THEB))^2-1)+3*MZ/RBAAN^3*SIN(THEB)*COS(THEB)
BY         VAR   MZ/RBAAN^3*(3*(COS(THEB))^2-1)+3*MX/RBAAN^3*SIN(THEB)*COS(THEB)
BZ         VAR   -MY/RBAAN^3
                 ;aardmagn. inductie
DECL       VAR   -INCL*COS(THEB)
DOMESDT    VAR   (TPZ+(IXX-IYY)*P*Q)/IZZ
```

```
DTHEBDT    VAR   SQRT(MU*A*(1-E^2))/RBAAN^2
                 ;blz 119 Bew v. Rvt.
ECLB       VAR   (ECLEQ+INCL)*PI/180
                 ;<(ecl-baanvl) (rad)
INCLR      VAR   INCL*PI/180
                 ;inclinatie (rad)
MSATX      VAR   MSAT*SIN(PHI)*COS(THE)
MSATY      VAR   MSAT*SIN(THE)*COS(PHI)
MSATZ      VAR   MSAT*SIN(PHI)*SIN(THE)
                 ;sat.dipoolontbinden
MX         VAR   M*(SIN(KSI)*COS(INCLR)*SIN(THEB/2-OOMEGA)+COS(KSI)*SIN(INCLR))
MY         VAR   M*(-SIN(KSI)*SIN(INCLR)*SIN(THEB/2-OOMEGA)+COS(KSI)*COS(INCLR))
MZ         VAR   M*SIN(KSI)*COS(THEB/2-OOMEGA)
                 ;aarddipoolontbinden
OMEGARPM   VAR   OMEGA*30/PI
                 ;spinsnelh.(omw/min)
OMES       VAR   OMERPM*2*PI/60
                 ;spinsnelh. (rad/s)
PDOT       VAR   (TPX+(IYY-IZZ)*Q*OMEGA)/IXX
                 :blz 522 Wertz
PHIGR      VAR   PHI*180/PI
PSIS       VAR   (PI/2)-ECLB*SIN(THEB)
                 :<comp spinas(yz)-yl
QDOT       VAR   (TPY+(IZZ-IXX)*OMEGA*P)/IYY
RBAAN      VAR   (A*(1-E*E))/(1+E*COS(THEB))
                 ;blz 109 Bew v. Rvt.
THEGR      VAR   THE*180/PI
THES       VAR   -ECLB*COS(THEB)
                 ;< spinas-yl/zl vlak
TINWX      VAR   (IYY-IZZ)*Q*OMEGA+IXX*DOMESDT*PHI+IXX*OMEGA*(Q-OMEGA*THE)
TINWY      VAR   (IZZ-IXX)*OMEGA*P-IYY*DOMESDT*THE-IYY*OMEGA*(P+OMEGA*PHI)
TINWZ      VAR   (IXX-IYY)*P*Q
                 ;inw.stoormomenten
TPGGX      VAR   TPGGXL*COS(THEB)-TPGGYL*SIN(THEB)
                 ;ontb. princ.axis
TPGGY      VAR   (TPGGXL*SIN(THEB)+TPGGYL*COS(THEB))*COS(ECLB)-TPGGZL*SIN(ECLB)
TPGGYL     VAR   -((3*MU)/(2*RBAAN^3))*(IXX-(IYY+IZZ)/2)*SIN(2*THES)*SIN(PSIS)
                 ;blz.3 v.d.Broek
TPGGZ      VAR   (TPGGXL*SIN(THEB)+TPGGYL*COS(THEB))*SIN(ECLB)+TPGGZL*COS(ECLB)
TPGGZL     VAR   ((3*MU)/(2*RBAAN^3))*(IXX-(IYY+IZZ)/2)*SIN(2*THES)*COS(PSIS)
                 ;grav.grad.stoormom.
TPMX       VAR   BY*MSATZ-BZ*MSATY
TPMY       VAR   BZ*MSATX-BX*MSATZ
TPMZ       VAR   BX*MSATY-BY*MSATX
                 :magn.mom. = BxMsat
TPX        VAR   TPGGX+TPMX
TPY        VAR   TPGGY+TPMY
TPZ        VAR   TPGGZ+TPMZ
                 ;tot.uitw.stoormom.
XBAAN      VAR   RBAAN*COS(THEB)
YBAAN      VAR   RBAAN*SIN(THEB)
                 ;nodig voor baanplot
PSI* exit
```

APPENDIX IV

To calculate the view factors between two parallel planes of arbitrary size a program was written using the formulas of the ESA-literature: 'Spacecraft thermal control design data', volume 1, code ESA PSS-03-108, page C1-35 to page C1-37.

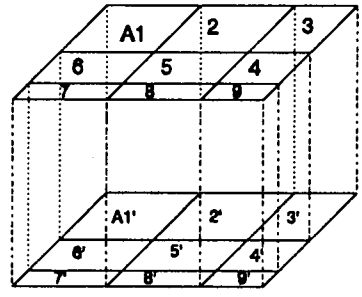

$$A_1 \cdot F_{1,9'} = \frac{1}{4} \cdot [K_{(1,2,3,4,5,6,7,8,9)^2} - K_{(1,2,5,6,7,8)^2} - K_{(2,3,4,5,8,9)^2} - K_{(1,2,3,4,5,6)^2} + K_{(1,2,5,6)^2} + K_{(2,3,4,5)^2} + K_{(4,5,8,9)^2} - K_{(4,5)^2} - K_{(5,8)^2} - K_{(5,6)^2} - K_{(4,5,6,7,8,9)^2} + K_{(5,6,7,8)^2} + K_{(4,5,6)^2} + K_{(2,5,8)^2} - K_{(2,5)^2} + K_{5^2}]$$

$$K_{m^2} = A_m \cdot F_{mm'}$$

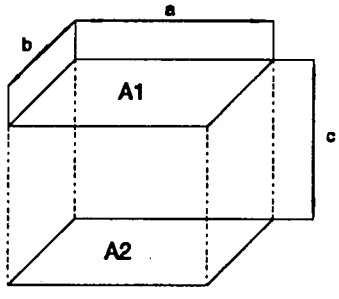

$$F_{(1,2)} = \frac{2}{\pi \cdot X \cdot Y} \cdot [\ln\left(\frac{(1+X^2)\cdot(1+Y^2)}{1+X^2+Y^2}\right)^{\frac{1}{2}} + X\sqrt{1+Y^2}\cdot\tan^{-1}\left(\frac{X}{\sqrt{1+Y^2}}\right) + Y\sqrt{1+X^2}\cdot\tan^{-1}\left(\frac{Y}{\sqrt{1+X^2}}\right) - X\cdot\tan^{-1}X - Y\cdot\tan^{-1}Y$$

$$X = \frac{a}{c}$$

$$Y = \frac{b}{c}$$

a and b are the length and the width of the two equally big planes that are right above each the other. c is the distance between the planes. These formulas have been used to write a computer program which calculates the desired view factors.

APPENDIX V

JASON is a thermal analysis program. The formulas used in this program are the satellite equations:

$$p_i + q_{e,i} + \Sigma_{j=1}^{n} (\epsilon \cdot A)_{ij} (\sigma T_j^4 - \sigma T_i^4) + \Sigma_j^n C_{ij} (T_j - T_i) = (m \cdot C_p)_i \frac{\delta T_i}{\delta t}$$

$$q_{e,i} = \alpha_i A_i \cdot (S_i + a_i) + \epsilon_i A_i E_i \qquad for\ i = 1, 2, 3, \ldots\ldots, n$$

For each node these equations are determined. These equations are linearised and put into a matrix. Then the right temperatures have been calculated using iteration.

APPENDIX VI

Calculation of the power consumption needed for the HBR down-link.

The received energy at distance r from the satellite is:

$$P_B = \frac{(G_a P_a)}{4\pi r^2} F \quad [Watt] \qquad (7)$$

In which:

P_b = received power at distance r
P_a = transmitting power regenerated by a patch
G_a = gain of a microstrip patch (= 6)
F = receiving surface

The receiving surface is defined by:

$$F = K\frac{\pi D_b}{4} = 270.0 \qquad (8)$$

In which:

K = antenna factor (= 0.5)
D_b = groundantenna diameter (= 25 m)

The received power always has to be a factor larger than the noise power coming from space. The level of this power can be obtained as follows:

$$P_N = k*T_{syst}*B = 152.6 \quad [dBWatt] \qquad (9)$$

In which:

P_N = noise power
k = constant of Boltzmann (= $1.38*10^{-23}$ Ws/K).
T_{noise} = systematic noise temperature (= 40 K)
B = bandwidth (= 1 MHz)

Considering the antenna losses and cable losses an extra loss factor (P_{loss}) has to be calculated with. The total P_{loss} can be set on 3 dBWatt.

As stated before, a margin has to be kept between the received power and the losses described above. For the PSK/PM

transmission concept a margin of 11 dBWatt should be efficient enough:

$$P_b - P_{loss} - P_{noise} = 11 \quad [dBWatt] \qquad (10)$$

In equation (4) P_a is the unknown factor. Solving this equation for the transmitting power regenerated by a patch at maximum distance r = 42,000 km. (see figure 15.16) gives:

$$P_a = 0.19 \text{ Watt}$$

The power required by the HBR transmitter depends on the efficiency of the chosen equipment. This efficiency factor is about 40%. So the total energy required is:

$$P_{tot} = 0.48 \text{ Watt}$$

REFERENCES

2. SCIENTIFIC OBJECTIVES

2.1 Thompson, A. Richard, James M. Moran and Georg W. Swenson JR., Interferometry and Synthesis in Radio Astronomy, John Wiley and sons, 1986

2.2 Ed. Perley, Schwab, Bridle, Synthesis Imaging in Radio Astronomy, (Astronomical Society of the Pacific)

Phase-locked Interferometers and Lobe Rotation:

2.3 Elgaroy Morris, Rowson, 1962, Mon. Not. Roy. Astro. Soc., 124, 395.

2.4 Rowson, 1963, Mon. Not. Roy. Astro. Soc. 125, 177.

Relevant Previous Space Missions:

2.5 Very Long Baseline Interferometry using a Geostationary Satellite, ESA Phase A Study Feb. 1980, (Tolerances of phase-locking systems)

2.5 QUASAT Design Study

6. LAUNCHER

6.1 Flight Opportunities for small payloads, ESA SP-298 Workshop Proceedings, 8-10 february 1989

6.2 Space directory (launchers part)

6.3 Ariane 4 ASAP user's manual, Arianespace, February 1990

6.4 Scout planning guide, LTV missiles and electronics group, October 1988

6.5 Pegasus user's manual, Orbital science corporation

6.6 Project Pygmalion, A feasibility study for a LEO telecommunications satellite, TU Delft, faculty of Aerospace Engineering, Delft, September 1991

6.7 Prof. K.F. Wakker, Collegedictaat Ruimtevaarttechniek LR 8, TU Delft, faculty of Aerospace Engineering, Delft, 1987

7. ORBIT

7.1 Prof. K.F. Wakker, Beweging van Ruimtevoertuigen, LR7B, TU Delft, faculty of Aerospace Engineering, Delft, 1987

7.2 Prof. K.F. Wakker, Collegedictaat Ruimtevaarttechniek LR 8, TU Delft, faculty of Aerospace Engineering, Delft, 1987

8. CONFIGURATION

8.1 U. Renner, Flight Results of TUBSAT-A, IAF-91-006

8.2 Ariane 4 ASAP user's manual, Arianespace, February 1990

9. STRUCTURE

9.1 Ariane 4 ASAP user's manual, Arianespace, February 1990

9.2 A.V Clark, Release Mechanism for releasing and reattaching Experiments on the Space Shuttle, NASA Technical Paper 1702, George C.Marshall Space Flight Center, Alabama, 1980

9.3 R.G. Veraar and H. Cruijssen, Jettison Mechanism Design Principle Selection, Fokker Space Division, JM-002, Amsterdam, April 1986

10. PAYLOAD

10.1 Namir E. Kassim, Kurt W. Weiler, Low frequency astrophysics from space, Crystal City, Virginia 1990

10.2 Project Hitchhiker, TU Delft, faculty of Aerospace Engineering, Delft, September 1990

10.3 Project Pygmalion, A feasibility study for a LEO telecommunications satellite, TU Delft, faculty of Aerospace Engineering, Delft, September 1991

10.5 Prof. Ir. G. Reijns, Informatiesystemen en elektrische energievoorziening in de ruimtevaart, (Information systems and electrical power supply in space technology), TU Delft, Delft, 1983

10.6 Asessment of QUASAT telecommunications system for phase stable reference transfer, NEOCOMM systems INC, February 1988

10.7 Thompson, A. Richard, James M. Moran and Georg W. Swenson JR., Interferometry and Synthesis in Radio Astronomy, John Wiley and sons, 1986

10.8 Howard M. Berlin, Design of Phase-locked loop circuits, Indianapolis, Indiana, 1978

10.9 P.P.L. Regtien, Instrumentele electronica, D.U.M., Delft, 1987

10.8 B.A.C. Ambrosius, K.F. Wakker, H. Leenman, The use of popsat for realtime positioning part 1. Principles of Satellite Positioning Systems, Delft, August 1986

10.8 B.A.C. Ambrosius, K.F. Wakker, H. Leenman, The use of popsat for realtime positioning part 2. Simulation results, Delft, August 1986

11. POWER SUPPLY

11.1 Project Pygmalion, A feasibility study for a LEO telecommunications satellite, TU Delft, faculty of Aerospace Engineering, Delft, September 1991

11.2 Prof. Ir. G. Reijns, Informatiesystemen en elektrische energievoorziening in de ruimtevaart, (Information systems and electrical power supply in space technology), TU Delft, Delft, 1983

11.3 Dr. Ir. J. B. Klaassens, Electrische Energievoorziening in de ruimtevaart, (Electrical Power Supply in space), bijlage t.b.v. college LR 51, TU Delft, faculty of Electrotechniek, Delft, 1988

11.4 Prof. K.F. Wakker, Collegedictaat Ruimtevaarttechniek LR 8, TU Delft, faculty of Aerospace Engineering, Delft, 1987

11.5 H. Bebermeier, V. Leisten, J. Rath, Electrical Power Subsystems, Space Course Aachen 1991

11.6 H.S. Rauschenbach, Solar Cell Array Design Handbook, van Nostrand Rheinhold Company, 1980

11.7 Crompton, T.R., Batterie Refference Book, Butterworth, Londen, 1990

11.8 Linden, D., Handbook of Batteries and Fuel Cells, McGrawhill, 1984

11.9 Capel (ATES), D. O'Sullivan (ESTEC), J.C. Marpinard (LASS), High Power Conditions for Space Application, December 1987

11.10 Photovoltaic Generators in Space, Proceedings of a symposium held by Estec, Noordwijk, The Netherlands 11 - 13 sept. 1978, ESA SP-140

11.11 Photovoltaic Generators in Space, Proceedings of the 2nd European Symposium, Heidelberg, Germany 15 - 17 April 1980, ESA SP-147

11.12 Photovoltaic Generators in Space, Proceedings of the 3rd European Symposium, Bath, England 4 - 6 May 1982, ESA SP-173

11.13 Photovoltaic Generators in Space, Proceedings of the 4th European Symposium, Cannes, France 18 - 20 Sept. 1984, ESA SP-210

11.14 European Space Power, Proceedings of the European Space Power Conference held in Madrid, Spain 2 - 6 Oct. 1989, ESA SP-294

11.15 European Space Power Conference, Proceedings of the conference held in Florence, Italy 2 - 6 Sept. 1991, ESA SP-320

11.16 Flight oppertunities for small payloads, ESA SP-298A

11.17 Space Power Systems engineering, Vol. 16 in the serie of Progress in Astronautics and Aeronautics

11.18 International Energy Conversion Engeneering Conference, 23rd and 24th conference, (IECEC-'88 and IECEC-'89)

12. PROPULSION

12.1 Prof. K.F. Wakker, Beweging van Ruimtevoertuigen, LR7B, TU Delft, faculty of Aerospace Engineering, Delft, 1987

12.2 Prof. K.F. Wakker, Collegedictaat Ruimtevaarttechniek LR 8, TU Delft, faculty of Aerospace Engineering, Delft, 1987

12.3 Prof. Y. Timnat, Chemical Rocket Propulsion, LR13, TU Delft, faculty of Aerospace Engineering, Delft, 1987

12.4 Project Aeneas, TU Delft, faculty of Aerospace Engineering, Delft, September 1989

12.5 Project Hitchhiker, TU Delft, faculty of Aerospace Engineering, Delft, September 1990

12.6 Project Pygmalion, A feasibility study for a LEO telecommunications satellite, TU Delft, faculty of Aerospace Engineering, Delft, September 1991

12.7 Gegevens van de Atmosfeer, VTH-71, TU Delft, faculty of Aerospace Engineering, Delft, July 1989

12.8 MBB: Our Propulsion Technology for Space Systems, MBB, Germany, June 1989

13. ATTITUDE CONTROL

13.1 J.R. Wertz, Spacecraft Attitude Determination and Control, D. Reidel Publishing Company, 1978

13.2 P. Ph. van den Broek, Attitude perturbations of a spin satellite due to gravity gradient torques in a regressing orbit, 1967

13.3 H. Patapoff, Attitude drift of a spin-stabilized satellite due to earth's magnetic and gravitational field, 1963

13.4 Prof. K.F. Wakker, Beweging van Ruimtevoertuigen, TU Delft, faculty of Aerospace Engineering, Delft, 1989

14. THERMAL CONTROL

14.1 Project Hitchhiker, TU Delft, faculty of Aerospace Engineering, Delft, September 1990

14.2 Project Pygmalion, A feasibility study for a LEO telecommunications satellite, TU Delft, faculty of Aerospace Engineering, Delft, September 1991

14.3 Prof. K.F. Wakker, Collegedictaat Ruimtevaarttechniek LR 8, TU Delft, faculty of Aerospace Engineering, Delft, 1987

14.4 Spacecraft Thermal Control Design Data vol.1,2,3, Thermal Control & Life Support Division, European Space Research and Technology Centre, Noordwijk, The Netherlands, november 1989

14.5 Siegel R. and Howell J.R. augmented ed., Thermal Radiation Heat Transfer, NASA pulications division, 1976

14.6 Kanis, J., Program JASON, Fokker Space & Systems, 1989

15. TELEMETRY AND TELECOMMAND

15.1 Project Pygmalion, A feasibility study for a LEO telecommunications satellite, TU Delft, faculty of Aerospace Engineering, Delft, September 1991

15.2 LeRoy E. Foster, Telemetry Systems, John Wiley & Sons, New York, 1965

15.3 Tri T. Ha, Digital Satellite Communications (second edition), McGraw-Hill Publishing Company, New York

15.4 P. Bartia, Millimeter-wave microstrip and printed circuit antennas, Artech House, Norwood, 1991

15.5 A. Bruce Carlson, Communication systems (third edition), McGraw-Hill Book Company, New York, 1986

15.6 Prof. Ir. G. Reijns, Informatiesystemen en elektri-

sche energievoorziening in de ruimtevaart, (Information systems and electrical power supply in space technology), TU Delft, Delft, 1983

15.7 Alan V. Oppenheim and Alan S. Willsky/ Ian T. Young, Signals and Systems, Prentice-Hall, New York, 1983

15.8 G.E. Mueller and E.R. Spangler, Communication Satellites, John Wiley & sons, New York, 1964

15.9 Harry L. Stiltz, Aerospace Telemetry, Prentice-Hall, Englewood Cliffs, 1961

15.10 Harry L. Stiltz, Aerospace Telemetry (volume 2), Prentice-hall, Englewood Cliffs, 1966

16. ON BOARD COMPUTER

16.1 Project Pygmalion, A feasibility study for a LEO telecommunications satellite, TU Delft, faculty of Aerospace Engineering, Delft, September 1991

16.2 Prof. Ir. G. Reijns, Informatiesystemen en elektrische energievoorziening in de ruimtevaart, (Information systems and electrical power supply in space technology), TU Delft, Delft, 1983

16.3 Tri T. Ha, Digital Satellite Communications, Mc. Graw-Hill Communications Series, 1990

16.4 32 Bits I/O cartridge for MSX computers, Elektuur (Dutch issue of Elektor), page 32-37 January 1987

16.5 8052-Basic-Compuboard: Hard- and Software, Elektuur, page 38-44, November 1987 and page 80-84 December 1987

16.6 I/O Modules voor het Basic-Compuboard (I/O Modules for the Basic-Compuboard"), Elektuur, page 64-71 November 1988,

16.7 Universele PC-I/O kaart (Universal PC-I/O card), Elektuur, page 74-85, May 1988

16.8 The ISO Spacecraft, ESA Bulletin no. 67, page 17-24, August 1991

16.9 Reading ISO's scientific instruments, ESA Bulletin, no. 67, page 26-28, August 1991